

Steel Edition

RHI

2015
METEC
EDITION

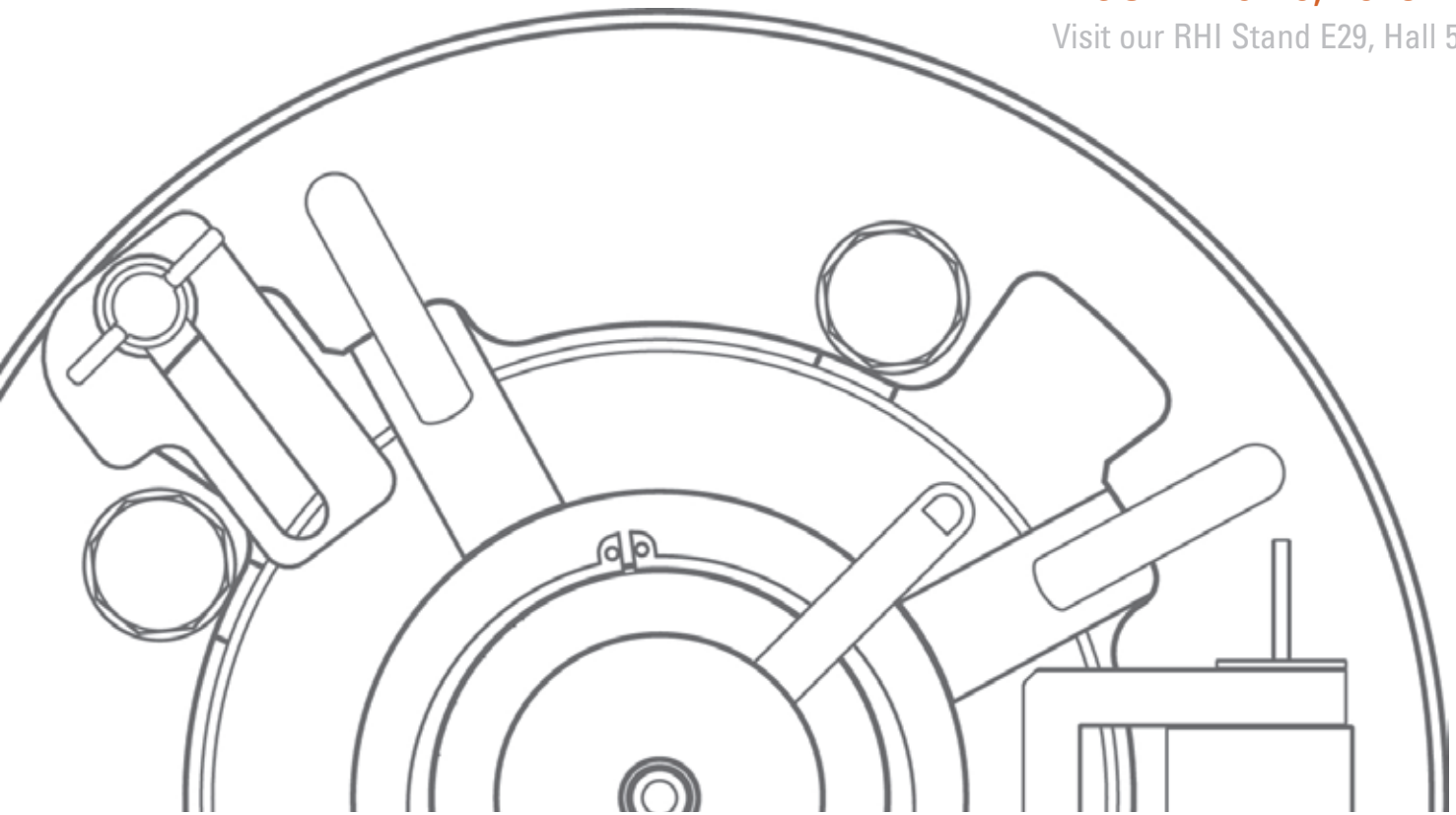
RHI Bulletin >1> 2015

The Journal of Refractory Innovations

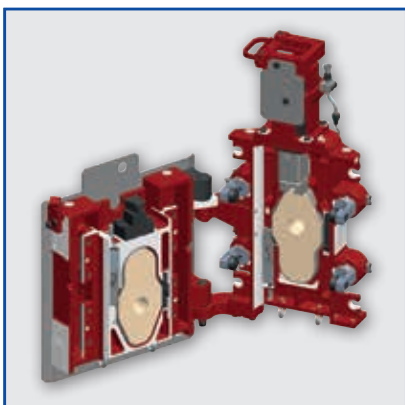
BE AHEAD
WITH INNOVATIVE TECHNOLOGY

RHI at METEC 2015
JUNE 16-20, 2015

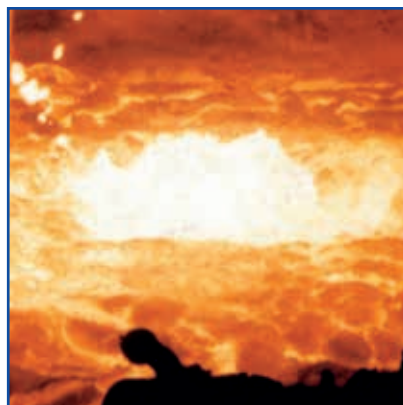
Visit our RHI Stand E29, Hall 5



INTERSTOP Ladle Gate Type S
Improves Refractory Utilization



Gas Purging in an Electric
Arc Furnace



GYRO Nozzle for Bloom and
Billet Casting



RHI Bulletin >1>2015

The Journal of Refractory Innovations

RHI Bulletin 1/2015
Steel Edition

Published by: RHI AG, Vienna, Austria
Chief Editor: Stefan Schriebl
Executive Editors: Alexander Maranitsch and Marcos Tomás Casado
Raw Materials Expert: Gerald Gelbmann
Technical Writer: Clare McFarlane
Proofreader: Clare McFarlane
Project Manager: Ulla Kuttner
Photography, Graphics
and Production: Markus Kohlbacher, Christoph Brandner
Design and Typesetting: Universal Druckerei GmbH, Leoben, Austria
Printers: Universal Druckerei GmbH, Leoben, Austria

Contact: Ulla Kuttner
RHI AG, Technology Center
Magnesitstrasse 2
8700 Leoben, Austria

E-mail: ulla.kuttner@rhi-ag.com
Tel: +43 50213-5323
Fax: +43 50213-5237
www.rhi-ag.com

The products, processes, technologies, or tradenames in the RHI Bulletin may be the subject of intellectual property rights held by RHI AG or other companies.

RHI worldwide

New TUNFLOW Production Line Operational in North America

Canada >> Within only a few years, RHI has established a strong market presence in the US and Canada with TUNFLOW, the tundish antiturbulence box. RHI can now optimally take advantage of further growth opportunities on the North American market with a new production line in Burlington (Canada). The facility went online at the beginning of 2015 and doubles the manufacturing capacity of this product series.

Currently, RHI sells around 20 different TUNFLOW designs in the US.

Cavity-Free Sidewall Blocks for Glass Melting Furnaces Now Available From RHI Podolsk Refractories

Russia >> Glass melting tanks should be constructed with the fewest possible joints between the refractory blocks as they are areas of weakness. The joints can facilitate attack, providing a site for molten glass penetration that can initiate corrosion at the block interface. In this regard horizontal joints are the most detrimental as molten glass attack proceeds preferentially at these positions. When molten glass is in contact with a horizontal joint it can cause a type of corrosion termed upward drilling. To avoid having any vulnerable horizontal joints in a melting furnace, blocks with a length of 1500–1600 mm are used, resulting in a palisade arrangement with continuous vertical joints.

Previously, RHI Podolsk Refractories was unable to produce such sidewall blocks of sufficient length due to technical limitations regarding the casting equipment. However, due to the development of a horizontal casting method, full-length vertical sidewall blocks (type BK-37 FC) for glass melting tank construction can now be produced. These cavity-free sidewall blocks are currently available in sizes up to 1600 x 400 x 250 mm³.

Successful Implementation of the First CLP Type Ladle Gas Purging System at AHMSA

Mexico >> Altos Hornos De Mexico (AHMSA) is the largest integrated steel plant in Mexico. Located in Monclova, the entire operation produces 3.5 million tonnes of liquid steel annually. AHMSA uses a fleet of 150-tonne ladles to transport and treat liquid steel heats. The products include plate, hot and cold rolled, tin plate, tin-free, and structural steels.

Due to the requirement for a more accurate and consistent stirring operation at the secondary metallurgy stations, AHMSA requested an offer from RHI to provide a state of the art ladle stirring system for producing higher quality steels. The customer identified improvement potentials concerning the installed ladle purging system and a team from RHI and INTERSTOP presented the new in-house developed Controlled Ladle Purging (CLP) system in a package that included long wearing, segment purging plugs, which had already been supplied by RHI for some time.

RHI successfully quoted and won a contract to provide and commission the first, newly designed, modular gas flow controls for ladle stirring. The new gas flow controls were designed, built, and successfully commissioned by INTERSTOP. The customer began stirring operations at the end of 2014 and is pleased with the results achieved.

AHMSA was convinced by the multiple system advantages that include easy operator handling, smooth flow rate controllability at both high and low flow rates, high purging system availability, process data availability, high component lifetime, and minimum service effort.

The customer has reported various improvements since the CLP system was installed such as decreased electrode consumption, improved melt stirring, less electric power consumption, and reduced melt cooling due to the reduced argon consumption. In addition, there is now a much better overall process control and improved slag management.

Tundish Water Model Study for Stahlwerk Thüringen—Optimization Through Simulation

Germany >> For more than 15 years, there has been a Full Line Supply project between Stahlwerk Thüringen GmbH in Unterwellenborn (Germany) and RHI Refractories Site Services GmbH. Approximately 95% of the refractory requirements for the steel liquid phase are covered by RHI products and services. The success of this long-term partnership is due in part to continuously optimizing and implementing new technologies.

In line with RHI's commitment to provide process improvements, a scaled model of their tundish geometry was constructed and used to perform extensive flow analysis at the Competence Center for Simulation in Leoben (Austria). The aim of the water modelling study was to achieve a sustainable improvement in the flow behaviour using the RHI patented TUNFLOW (impact pot) product series. The physical flow analysis convinced the customer that beneficial results can be achieved with this approach and the entire water modelling facility left a lasting impression.

As a result of this study RHI was awarded 100% of the TUNFLOW delivery requirements.

RHI worldwide

RHI's New Plant for Gunning and Tundish Mixes Under Construction in Eskişehir

Turkey >> The demand for high-quality, low-iron basic mixes like those RHI produces in Eskişehir (Turkey) is increasing. In order to exploit the site's logistical advantage, a second mix plant is currently being built at this location. The foundations were started in November 2014, and the new plant for gunning and tundish mixes is expected to be completed by the end of 2015. This will increase the site's mix capacity to 150000 tonnes and optimize global transport costs.

Occupational Health and Safety—RHI Implements OHSAS 18001 Globally

RHI is striving to make everyday working conditions as safe as possible. With the goal to be accident-free by 2017, implementing the Occupational Health and Safety Assessment Series (OHSAS) 18001 puts the necessary framework in place to achieve this target. OHSAS is a British Standard that defines requirements for the management of health protection and safety at work. The specification enables RHI to monitor, measure, and improve safety and health in the workplace.

In total, 24 RHI locations around the world have been certified, including the recently audited isostatically pressed product plant in Clydebank as well as sites at Mainzlar, Aken, Trieben, Radenthein, Lugones, Bayuquan, and Dashiqao.

RHI's Bayuquan Plant Celebrates 20 Years

China >> On February 4, 2015, approximately 560 guests celebrated the 20-year anniversary of RHI's Bayuquan plant in China. They were officially welcomed by the management and during his speech Franz Buxbaum, Chief Operations Officer, described the historical development of the site and emphasized that RHI Refractories Liaoning is a true success story and the most successful joint venture within the RHI Group.

Successful Implementation of GEKKO Gunning for Ladle Maintenance at ArcelorMittal

Germany >> After several successful trials at customer sites (Europe and the Near East), RHI installed the first GEKKO ladle maintenance machine at ArcelorMittal Eisenhüttenstadt (Germany) as a permanent gunning solution. The GEKKO device for ladle gunning is a modular development of the GEKKO for BOF gunning, with seven manipulators of the latter type already in operation and a further two in production. The machine is famous for its high manoeuvrability, simplicity, cost-effectiveness, and low maintenance requirement.

After a short training period for plant personnel, a 4-week autonomous testing period was successfully concluded and the machine was approved by the customer. The realization of planned goals like an optimized gunning image, selective and economical material gunning, and an impressive low material rebound was positively confirmed by the customer.

The customer was impressed by the simple handling and low maintenance. The level of safety during gunning for staff has also increased. Further trials are planned in the near future at various sites and two additional manipulators have already been sold to customers in India.

Partnership Contract With JSW Increases Converter Lifetime and Decreases Maintenance

India >> JSW Steel Ltd., the fastest growing steel producer in India, has an installed capacity of 14 million tonnes per year with steel plants in Toranagallu, Dolvi, and Salem. In Toranagallu, JSW has two integrated steel plants (SMS1 with 3 x 130-tonne LD converters and SMS2 with 4 x 170-tonne LD converters) as well as an EAF shop (SMS3 with a 1 x 160-tonne furnace).

Last year JSW signed a partnership contract for Total Converter Management with RHI for SMS2, incorporating targets to increase converter availability and enhance gas purging conditions. The contract covers 15000 tonnes of refractory materials, comprising 24 converter linings, including tapholes, purging plugs, and maintenance mixes.

In the first 11 converter campaigns of this partnership, RHI was able to increase the BOF lifetime by 39% from 2389 heats to an average of 3315 heats whilst the refractory maintenance frequency and consumption decreased during this period by 36%. The BOF bottom purging has improved significantly by 83%, from 1783 heats to 3262 heats on average. The purging efficiency has improved and the [C] x [O] levels decreased from 32×10^{-4} to 22×10^{-4} , which provides remarkable cost savings for JSW regarding deoxidation and alloying agents.

RHI India was also awarded a 3-year EAF maintenance contract for SMS3 at the same plant. Within 6 months of commissioning the EAF operation has been stabilized and average refractory consumption is currently around 7.5 kg/tonne, with further improvements in progress.

To achieve all these results an expert Austrian service team and the local RHI Indian personnel have worked closely together with the customer and changed the operating conditions successfully by implementing new standard operating procedures for slag maintenance work, flux additions, gunning, and patch repairs. Furthermore, gas purging patterns have been introduced in order to optimize the gas flow as well as the plug wear to achieve the best metallurgical results. Ongoing training sessions are in place as well as steady monitoring of the operation conditions to maintain and improve this level of modern furnace management.

Editorial

RHI is very enthusiastic to be part of METEC 2015 and the 2nd European Steel and Technology Application Day. Billed as the exhibition event for the metallurgical technology of tomorrow, we have taken this opportunity to publish a special edition of the RHI Bulletin and completely update the majority of steel, flow control, INTERSTOP, and nonferrous brochures to include recent advances. RHI considers innovative power a prerequisite for remaining globally competitive. This includes addressing ideas systematically and turning them into marketable products, processes, and services. In this RHI Bulletin a range of innovations for the steel industry are described that will support metallurgical advances to be realized in the future.

The articles include a review of excellence in inert gas control systems for the steel industry, improved lining concepts for current EAF processes, and a pre-assembled EAF slag door that has improved furnace availability by reducing installation time and maintenance requirements. Furthermore, taphole developments for both BOF and EAF applications are described as well as benefits that can be realized through gas purging in the converter regarding material efficiency and CO₂ emission reductions.

A controversial topic for both RHI and many of its customers is the current European emissions trading system. In the sixth paper examining the impact of current legislation, necessary areas for future reform are highlighted in terms of safeguarding value creation and jobs in Europe.

As a result of numerical modelling, a ladle bottom design concept, termed IBOS, has been developed that enables steel yield to be maximized in combination with reducing slag carryover into the tundish. This is followed by a paper describing doloma refractory slag corrosion, as a comprehensive understanding of the wear mechanisms occurring can contribute to improving the durability of this highly cost-effective solution for ladle linings.

In the area of flow control many exciting novel technologies are presented including the INTERSTOP Ladle Gate Type S System, which encompasses a maintenance-friendly design, safety, and refractories that allow a larger range of mass flows to be covered with the same mechanical system. This is followed by two papers detailing multiple isostatically pressed product advances for the continuous casting process that improve steel cleanliness and productivity. RHI's New Tundish Roadmap is also introduced, focusing on further approaches to improve clean steel production by minimizing hydrogen, nitrogen, and carbon pick-up.

RHI's historical and extended partnership with the Libyan Iron and Steel Company is described in the final paper. Through a strong commitment to refractory supply and services, even immediately after the civil war, RHI has remained integral in this customer's expansion and optimization programmes to increase steel production over the last decades.

I joined RHI as Head of Corporate Research and Development in February and it is a great pleasure to be the new Chief Editor of the RHI Bulletin. In my view it is unique—the only journal published by a refractory company—and I am committed to retaining its diverse and informative content. In closing, I would like to wholeheartedly thank all the authors who contributed to this edition and the editorial team who worked diligently for many months to realize such a substantial publication.

Yours sincerely

Stefan Schriebl
Corporate Research and Development
RHI AG

Contents

- 7 Excellence in Inert Gas Control Systems for the Steel Industry
- 17 Modern Electric Arc Furnace Processes and Their Requirements for Improved Lining Concepts
- 25 Installation and Practical Experience With Preassembled EAF Slag Door Blocks at Arcelor Mittal Point Lisas
- 30 Taphole Developments for Specific Steel Industry Demands
- 37 Gas Purging Benefits in the BOF: A Focus on Material Efficiency and CO₂ Emission Reduction
- 44 Is the Current European Emissions Trading System a Suitable Means for Achieving Climate Protection Goals?
- 51 IBOS—Improved Bottom Optimized Solution for Enhanced High-Quality Steel Yields
- 57 Slag Corrosion of Doloma Refractories
- 61 INTERSTOP Ladle Gate Type S—A New Milestone in Ladle Gate Technology
- 68 Tundish Technology and Processes: A New Roadmap
- 78 Novel Isostatically Pressed Products for the Continuous Casting Process
- 84 Anticlogging Solutions for Isostatically Pressed Submerged Nozzles

Subscription Service and Contributions

We encourage you, our customers and interested readers, to relay your comments, feedback, and suggestions to improve the publication quality. Furthermore, to receive the RHI Bulletin free of charge or contribute to future editions please e-mail or fax your details (name, position, company name, and address) to the Subscription Service:

E-mail: ulla.kuttner@rhi-ag.com
Phone: +43 50213-5323
Fax: +43 50213-5237

RHI – BE AHEAD
with Excellence in Refractories

BE AHEAD

June 16-20, 2015 Düsseldorf 
Hall 05, Stand E29

TAKE THE LEAD IN THE METALS INDUSTRIES.

Discover how RHI – the industry's leader – has changed the pace of the market again and again through innovative TECHNOLOGY, unmatched RELIABILITY and SERVICE that truly supports your success. A combination that results in key advantages for our customers in a competitive industry environment.

BE AHEAD with Excellence in Refractories.

RHI AG, Wienerbergstrasse 9, 1100 Vienna, e-mail: metec@rhi-ag.com, www.rhi-ag.com


RHI

Reinhard Ehrenguber

Excellence in Inert Gas Control Systems for the Steel Industry

Steelmakers are continually improving their process technology to meet market requirements in terms of both steel quality and price. At first glance it can appear that the application of inert gas has a minor impact on overall costs across the entire steel production process, and therefore it is normally a topic where little focus is placed. However, steelmaking requires inert gas introduction at some of the most critical process steps. While it is established that sufficient inert gas benefits the process, too much can degrade the product. If improper purging systems are installed, not only significant amounts of alloying elements are wasted, but process time and energy are lost since the steel has to be downgraded when specifications are not met. It is also costly to reproduce downgraded steel and considerable logistic effort is incurred, especially at the continuous caster. Therefore, accurate and reliable inert gas control is essential. This article describes the holistic approach RHI and INTERSTOP offer regarding this area and the new designs of their inert gas control systems used in basic oxygen furnaces, electric arc furnaces, ladles, and at the continuous casting machine.

Introduction

Today, inert gas is applied at various different process stages in steel plants, starting in the primary metallurgical units like BOFs and EAFs. Further down the steel production route, inert gas enhances several processes during secondary metallurgy and also provides an essential contribution at the caster. The two main purposes of inert gas application during the entire steel production process can be subdivided into purging and shielding. When discussing excellence in inert gas applications, the three main factors shown in Figure 1 must be considered.

Metallurgical and Process Know-How

For each steel grade, an individual gas purging program drives the process as close as possible to equilibrium. Modern purging systems allow parameters to be preset, thereby controlling the most important parameters like switching the gas (e.g., argon and nitrogen) at a precise point in a defined process step and regulating the gas flow rate during a defined process step.

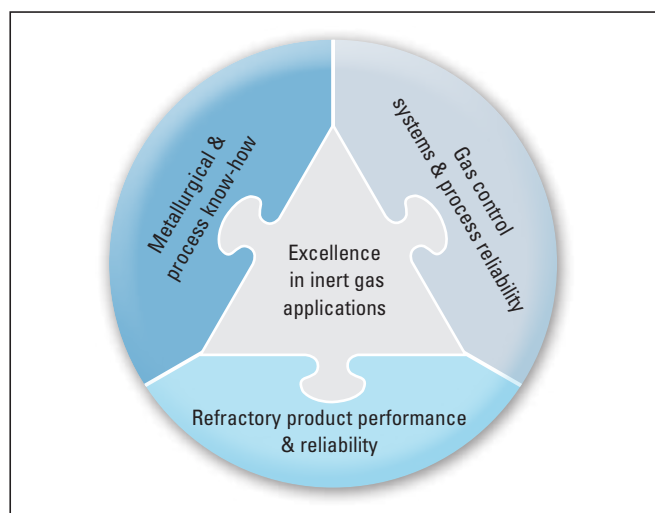


Figure 1. Factors required for excellence in inert gas applications.

Performance and Reliability of Functional Refractory Products

For all applications, an optimized functional refractory product has to be selected in order to generate for example the desired throughput and bubble characteristics. It is important that the products are capable of maintaining the required characteristics not only at the beginning of a vessel's operating lifetime (e.g., purging plugs for BOFs, EAFs, and ladles) or sequence (e.g., purging or shielding at the continuous casting machine (CCM)), but over the entire service life.

Gas Control Systems and Purging Process Reliability

INTERSTOP gas control systems are designed to fully support the process and operator. In cases where the functional purging product changes its flow characteristics to negatively impact on the purging result, the systems are capable of alerting the operator and automatically readjusting the flow to provide the desired rate.

An important point to highlight is that the focus should not be on an individual production step, but on the entire process. For example, a frequent approach to solve nozzle clogging in the tundish is intensifying the inert gas supply for the stopper control system or tundish slide gate. In contrast, the total system approach solves nozzle clogging by checking the effectiveness of gas purging in the BOF or EAF, as well as the situation in the ladle from the tapping stage, via the secondary metallurgy, through to when the ladle is put into the ladle turret at the CCM for casting. In this example of nozzle clogging, attention is on the overall process and the parameters determined provide tools for holistic problem solving.

Key Elements for Reliable Gas Purging Systems

Steel plants and refractory suppliers mainly focus on refractory purging products such as plugs and their characteristics in terms of bubble generation, flow, pressure,

and lifetime. Whilst the importance of these factors is undisputed, the same attention must also be paid to the gas regulation, piping, and system maintenance.

Mass Flow Controller

A centrepiece of modern purging systems is the mass flow controller (MFC). In older installations these are manually controlled mass flow meters, whereas the latest state of the art MFC (Figure 2) has the following features:

- >> Based on a caloric measuring system.
- >> Enables precision of +/- 1.5%.
- >> Flow regulation using a proportional directional valve.
- >> Depending on the application, regulation ranges are for example:
 - > 0.5 NI/min up to 20 NI/min.
 - > 2 NI/min up to 100 NI/min.
 - > 6 NI/min up to 300 NI/min.
 - > 12 NI/min up to 600 NI/min.
 - > 24 NI/min up to 1200 NI/min.
 - > 30 l/min up to 1500 NI/min.
- >> Setting time < 500 ms.

The compact arrangement of a gas control box based on a standard block and the complete gas control unit are shown in Figures 3 and 4.

General Advantages of State of the Art Gas Purging Systems

The benefits of RHI/INTERSTOP's gas purging systems include:

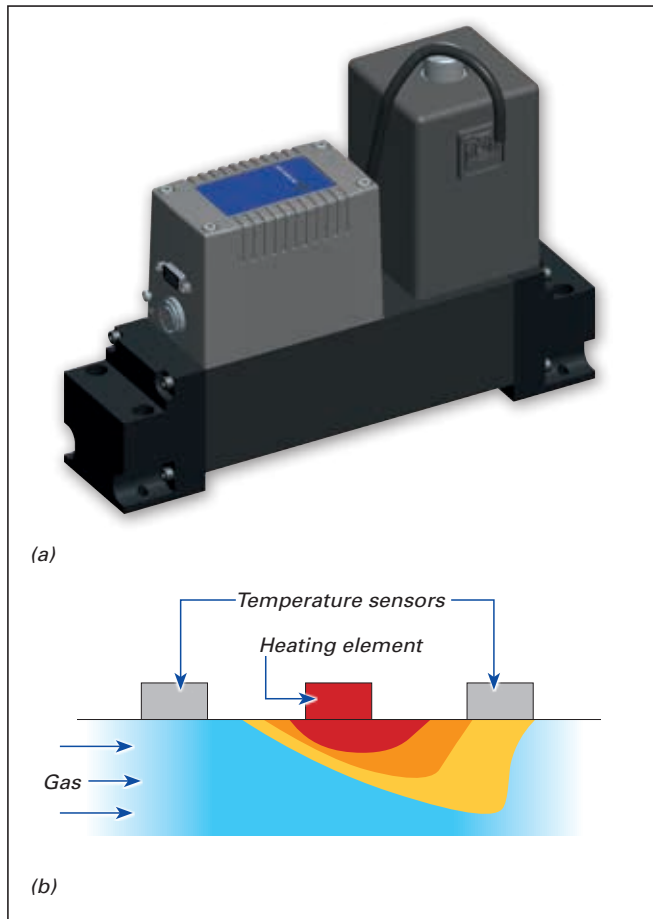


Figure 2. Mass flow controller. (a) system layout and (b) measuring principle.

- >> Modular, maintenance-friendly design.
- >> 100% leak-free system due to O-ring sealed standard blocks instead of pipes.
- >> Opportunities to control the stirring efficiency.
- >> Visualization of all input and output signals on customer demand.
- >> Error report with failure detection.
- >> Program language: Siemens Step 7/WinCC flexible or TIA Portal.
- >> Accurate and individual flow control for multiplug purging systems (e.g., BOF).

The typical guaranteed parameters of a RHI/INTERSTOP system are:

- >> 100% leak-free system.
- >> Accuracy of +/-3%.
- >> Setting time < 500 ms.

System Availability and Maintenance

The more a holistic system approach is adopted, the more it becomes apparent that the function of all single system items—including the piping and coupling—must be ensured. It is recommended that there is clear ownership of the gas purging process across all units in a steel plant to avoid a single unit receiving more focus compared to others.

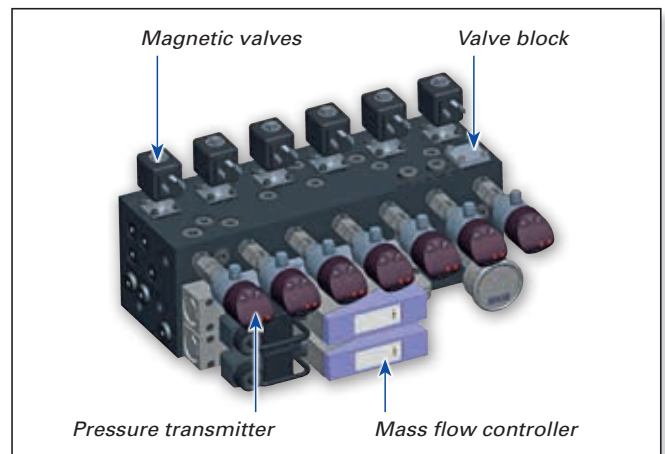


Figure 3. Compact arrangement of the gas control block.



Figure 4. Gas control box containing units based on a standard block.

During the design of INTERSTOP system parts, a uniform spare part concept was introduced. Hence, the same basic components can be used for EAF, BOF, and ladle purging stations. This supports easy and rapid maintenance because one specialist in the steel plant can maintain all purging stations. An example of the modular design is shown in Figure 5.

It is also essential that increased care is taken for example at the ladle preparation stand to check the function of the ladle purging plug after each heat and guarantee correct function over the entire purging plug lifetime. The principle of such a system is shown in Figure 6 and the typical flow rates are listed in Table I. In addition, data recording is supported to guarantee the purging plug provides the correct purging characteristics and the piping has no leaks.

Gas	Nitrogen or compressed air (emergency gas)
Number of outlet lines	1–3
System pressure	5–16 bar
Flow range	12–600 NI/min

Table I. Typical specifications and flow rates at a purging plug test stand.

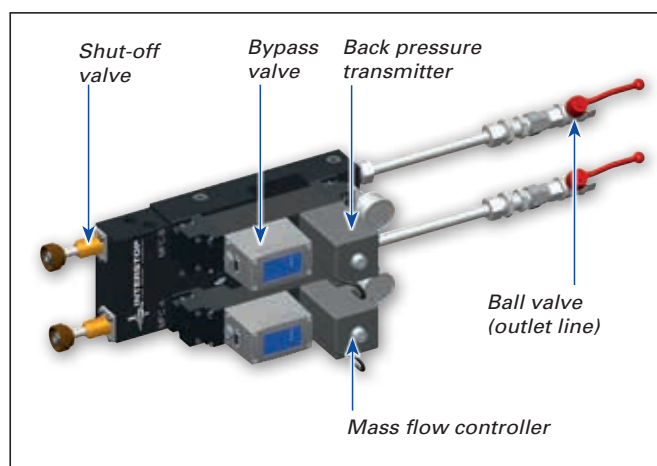


Figure 5. Modular design provides rapid maintenance and fewer parts are required in stock.

In the following sections an overview of the new gas purging systems available from the EAF/BOF to the ladle to the mould, their support in the process, and the resulting advantages are provided.

EAF Direct Purging Plug Gas Purging System

The EAF process benefits realized using direct gas purging systems are related to an overall increased steel bath movement as well as increased mixing between the lower and upper steel melt volumes. The specific reported benefits of direct purging plug (DPP) bottom gas purging systems can be subdivided into three main areas.

Increased thermal and temperature homogeneity in the steel melt, which results in:

- >> Decreased melting time of scrap and direct reduced iron (DRI).
- >> Increased heat transfer during the superheating period.
- >> Increased power transfer.
- >> Decreased specific electrical energy demand.
- >> Decreased deviation between the measured steel temperature in the EAF and the ladle furnace.
- >> Avoidance of skull formation or debris in the EAF hearth after tapping (clean furnace).

Increased chemical homogeneity in the steel melt, which provides:

- >> Increased metal yield.
- >> Increased use of secondary ferrous raw materials.
- >> Decreased deviation between the measured carbon content in the EAF and the ladle furnace.
- >> Increased yield from alloy addition.
- >> Increased rate of carbon oxidation, in particular from hot metal charges.
- >> [C] x [O] levels closer to equilibrium conditions, resulting in less alloy addition, better alloy prediction, and more stable ladle furnace operations.
- >> Increased dephosphorization (decreased rephosphorization).
- >> Decreased oxygen consumption.

Generation of gas bubble columns in the steel melt and thereby:

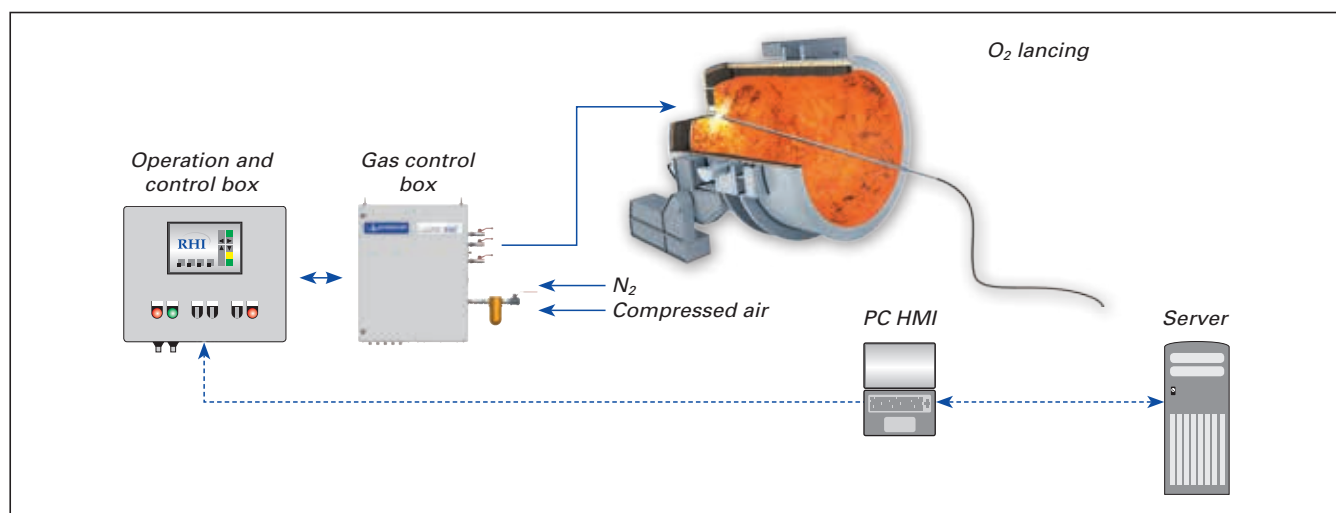


Figure 6. Schematic of ladle purging plug test. Abbreviations include human machine interface (HMI).

>> Avoidance of instantaneous or retarded CO boiling in the steel melt [1].

An overview of various aspects of a gas purging system are provided in Figures 7–9, where the holistic approach provided by RHI and INTERSTOP for gas purging is illustrated using the example of an EAF. Typical DPP gas system parameters are shown in Table II, including the distinction between small and large EAFs.

Converter Inert Gas Purging System

The basic layout of a converter inert gas purging (CIP) system for BOFs is provided in Figure 10.

The typical findings of on-site surveys examining other types of purging systems include too high flow oscillation, which results from:

- >> Imbalanced flow controller for the required flow rate—over dimensioned or under dimensioned.
- >> Insufficiently precise to control the flow.
- >> Existing process valves work too slowly and are dependent on temperature and other factors.

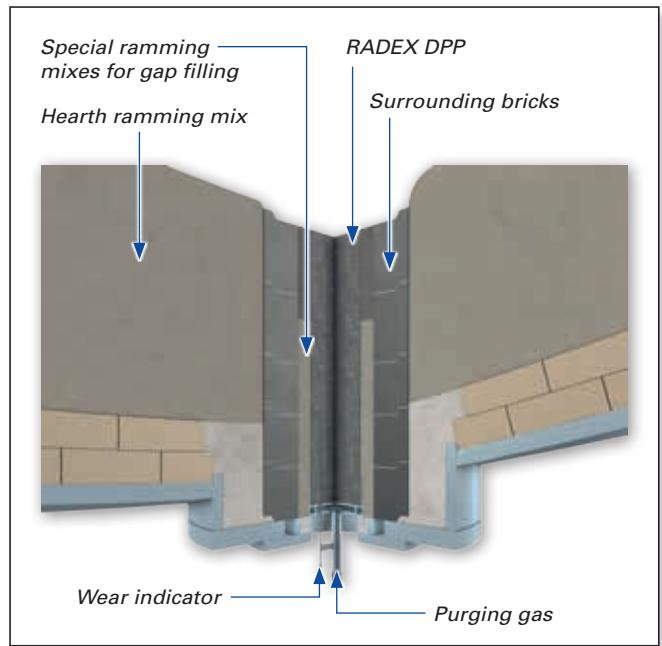


Figure 8. Schematic of a direct system purging plug installed in an EAF.

Technical data and performance characteristics	Gas control box DPP	Gas control box DPP small
Number of lines	3–6	1–2
Gas flow rate per plug	10–300 l/min	1–20 l/min
Speciality	Modular setup of gas control system	Redundant gas control for maximum system availability
Stirring medium	Nitrogen and/or argon	
Pressure range of supply	Up to 25 bars	
System pressure	6-16 bars or higher	
Gas purging brick supervision	Wear indication lines	
Standard control system	Siemens S7 PLC	
Visualization panel	Touch panel (12")	
Customer-specified connection to furnace control system		
Data logger and storage		
Options	Continuous temperature monitoring of each DPP plug Level 2 communication (e.g., ProfiNet, Ethernet, and ProfiBus)	

Table II. Typical performance characteristics of DPP systems.

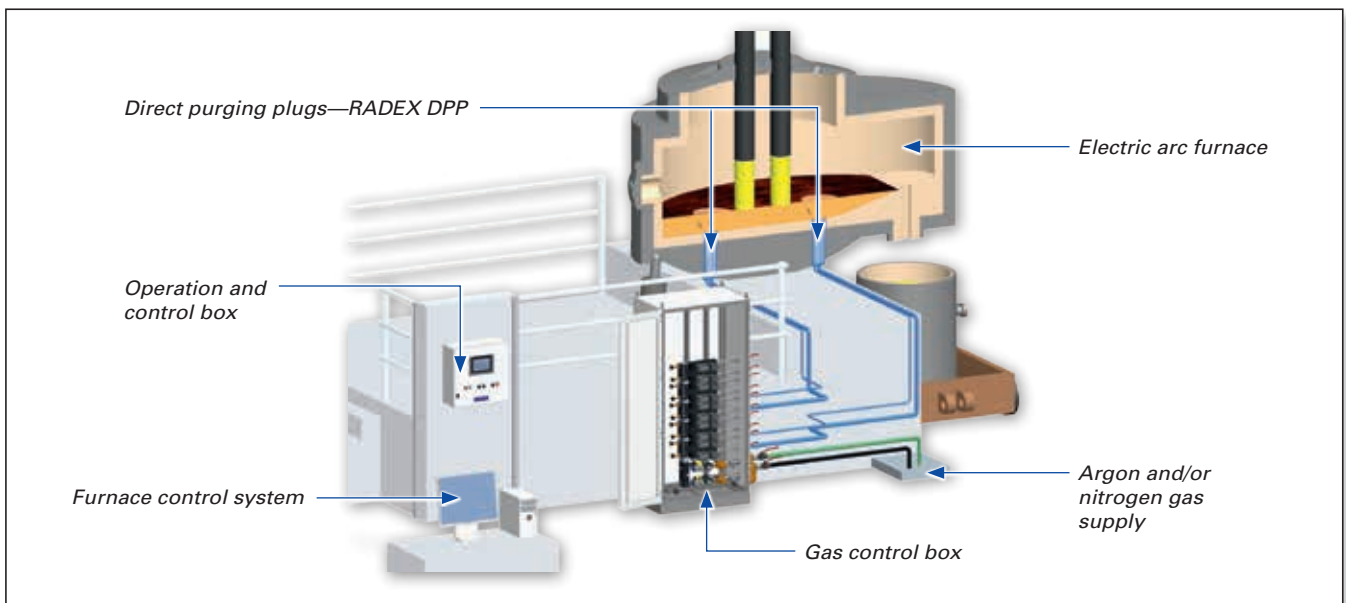


Figure 7. Overview of gas control in an EAF.

The RHI and INTERSTOP BOF CIP system offers the following advantages:

- >> Modular design.
- >> O-ring sealed blocks instead of pipes.
- >> Duplex filters.
- >> Nitrogen release when using argon (to ensure that no nitrogen can penetrate into the argon supply line).
- >> Monitored 3/2-way ball valves on each outlet line.

Also excludes any inert gas flow during relining of the converter for safety reasons.

- >> Check line with a mass flow meter that enables the performance of each MFC to be verified by the MFC analysis program at the control computer.

The general benefits of the described package comprising the gas control system and refractory purging plugs are listed in Table III.

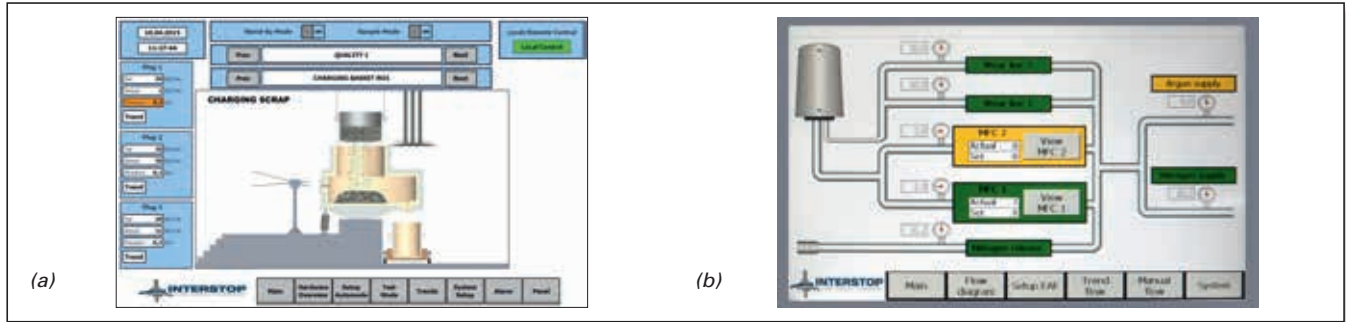


Figure 9. Visualization of the purging process. (a) actual purging gas values in a plug and (b) MFC measurements.

Benefits	Benefits in detail
High-quality and economical steel production	Minimization of the tap-to-tap time
	Reduction of the reblow rate numbers
	Lower (FeO), [P] levels, and [Mn] oxidation loss
	Higher yield
	More stable metallurgical results during the entire campaign
Realization of lower [C] x [O] levels/ P_{co} values	Lower [O] levels for the same aimed [C] levels after end of blowing are obtained
	Less deoxidation alloys (e.g., Al) are required
Improved steel bath homogenization/kinetic and temperature distribution	Shorter and quicker reaction pathways between the slag and steel bath (better conditions for scrap/flux additive melting and higher scrap/hot metal ratio)
	Improved process control (higher accuracy of the tapping temperature and element levels)
	Improved steel yield and flux additive levels (reduced slag volume and slopping material)

Table III. Benefits of the gas purging system package [2].

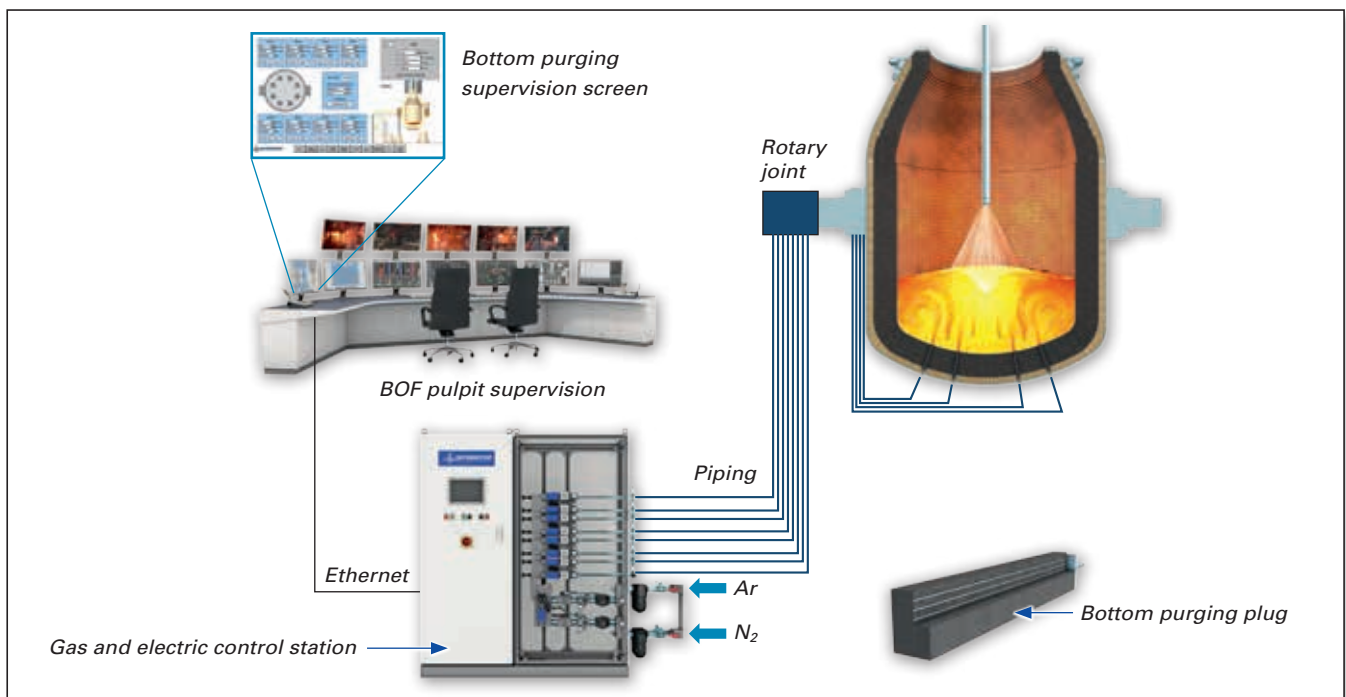


Figure 10. Layout of the BOF CIP system.

Gas Purging System for Ladles

Besides temperature and composition homogenization, ladle stirring is also essential for inclusion removal. In principal, inclusions can be removed successfully at all steelmaking process stages by directing them towards a metal/gas, metal/slag, or metal/refractory interface. However, at the same time sufficient precautions must be taken to avoid reoxidation, slag entrainment, and reassimilation of inclusions back into the liquid steel, or the rate at which the inclusions are generated could be even greater than their removal rate.

In general, the small size range of primary deoxidation inclusions precludes most of them from floating up in the ladle (or tundish or mould) through buoyancy forces alone, as determined by Stock's law, because there is generally insufficient processing time available. For example, 100 µm diameter alumina inclusions will take 4.8 minutes to float up from a position 2.5 m below the steel surface while for a 20 µm diameter particle the flotation time increases to 119 minutes. Consequently, natural floatation is not very efficient for removing small particles. Stirring the liquid steel bath, by applying gas or electromagnetic stirring, increases the number of collisions taking place between inclusions. This encourages agglomeration of solid particles and coalescence of liquid inclusions into larger clusters, with the prospect of increasing the inclusion removal rate. Stirring the liquid steel bath is therefore a basic feature of all clean steel operations [3]. A schematic of the Controlled Ladle Purging (CLP) system is shown in Figure 11 and Table IV details the flow rates and specifications.

Excellent ladle gas purging systems feature the following:

- >> Easy handling for operators: Reduces possible mistakes and prevents accidents.

- >> Achievement of divergent process aims through a smooth flow rate controllability (e.g., homogenization at high flow rates and soft bubbling at very low flow rates).
- >> High purging system availability (avoids no stirring being possible) supports ladle logistics and reduces costs (no downgrading steel grades and no reworking necessary).
- >> Process data availability through embedding into existing IT infrastructure for data transfer and processing.
- >> High component lifetime reduces costs.
- >> Minimum service effort and high availability of trained service technicians (optimum would be 24/7) reduce costs and enable optimum production logistics.

One of the latest innovations on the market that supports the aforementioned ladle gas purging features is the SOC-H (Safety Operating Closing system with Hinged door) purging system. It consists of purging ceramics, a safety closing system, a gas connection with internal check valve, plug setting and extraction devices, with additional tools and equipment necessary for a safe, reliable, and easy to handle ladle gas purging system. SOC-H has proven its efficiency during tests in several steel plants [4]. The SOC-H closing system for ladle purging plugs is shown in Figure 12.

Gas	Nitrogen and argon
Number of outlet lines	1–4
System pressure	16–25 bar
Flow range	0–1200 NI/m

Table IV. Typical specifications and flow rates of ladle gas purging.

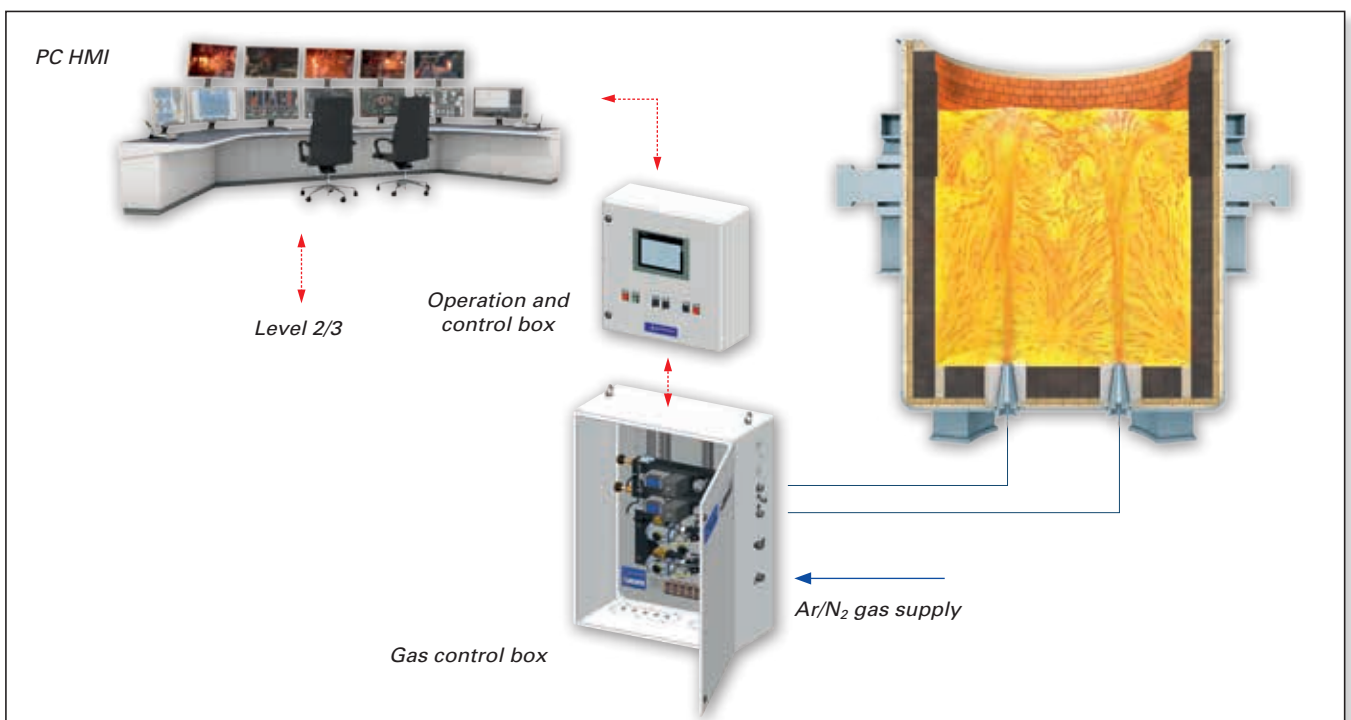


Figure 11. Typical layout of the CLP ladle gas purging system. Abbreviations include human machine interface (HMI).

Once the refining process is finished in the ladle, where balanced purging enables the elimination of macroinclusions, in the final liquid steel treatment step—the CCM process—the highest focus is placed on avoiding formation of new inclusions caused by reoxidation.

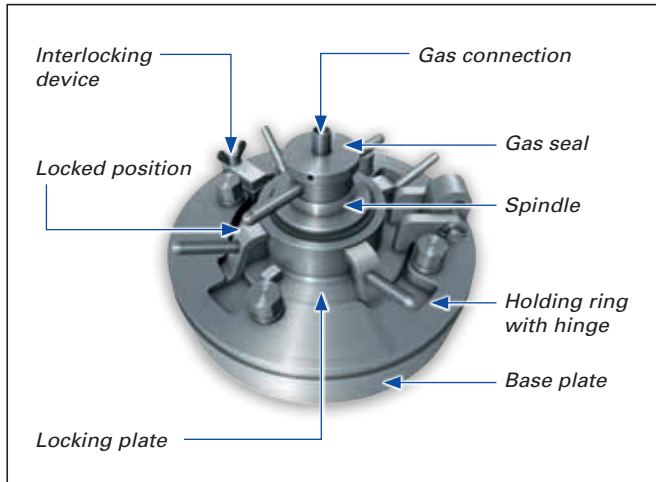


Figure 12. SOC-H closing system for ladle purging plugs.

Inertization From the Ladle to the Tundish

The main driver for air ingress at the ladle slide gate and the joint between the collector nozzle and ladle shroud is the negative pressure created during steel flow throttling. The first measure is to minimize this negative pressure by optimizing the casting diameter to the actual caster demand. For very sensitive steel grades, inert gas purging between the plates is performed to generate a 100% oxygen-free atmosphere around the throttling position, as shown in Figure 13.

The INTERSTOP control system (Figure 14) provides inert gas to a specially designed gasket between the ladle gate lower nozzle and the ladle shroud. The inert gas is monitored for flow and backpressure and these feedback signals determine the quality of the gasket seal. Data is sent to the steel plant's level 2 historical data system and the control box also has local warning lights and an alarm to notify the operator of any problems.

The benefit of an effective inertization system is a very low nitrogen pick-up as shown in Figure 15.

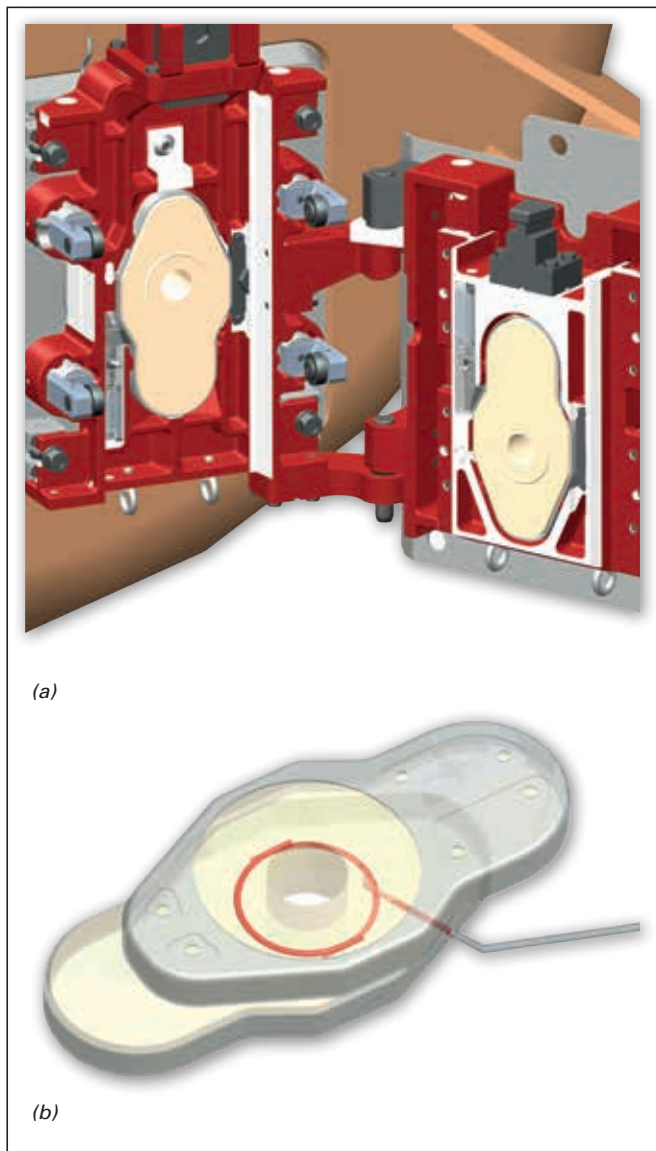


Figure 13. (a) INTERSTOP Ladle Gate Type S configuration and (b) inert gas purging between the plates provides a 100% oxygen-free atmosphere.

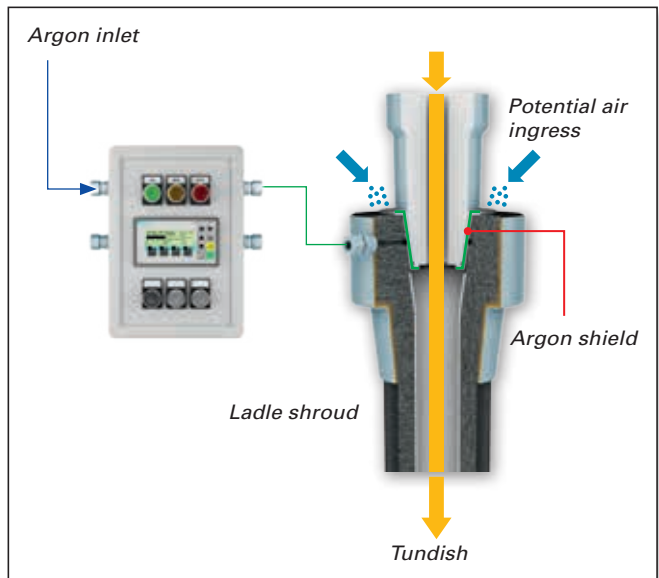


Figure 14. INTERSTOP gas control system for ladle shroud inertization.

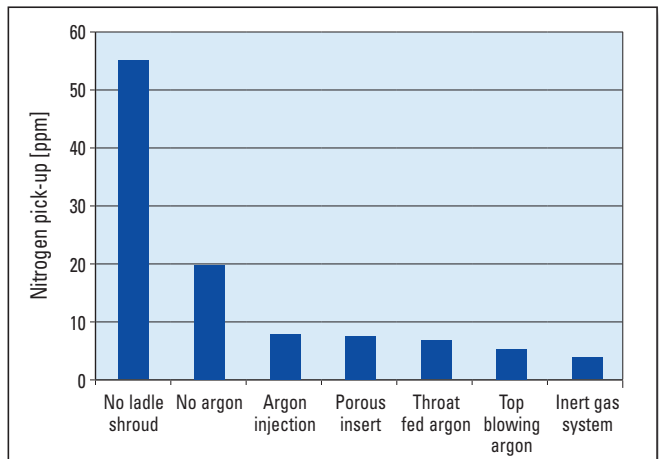


Figure 15. Effectiveness of ladle shroud inertization measured by nitrogen pick-up (ppm).

Gas Purging System for Tundish Beams

Besides fully shielding the steel surfaces from air contact, the tundish also offers the opportunity for effective segregation of nonmetallic inclusions by argon rinsing in the tundish bath, as shown in Figure 16. The general advantages of a purging beam in the tundish regarding clean steel production are:

- >> Removal of nonmetallic inclusions—less downgrades.
- >> Reduction of nitrogen content and oxygen pick-up.
- >> Less clogging—increased sequence length.

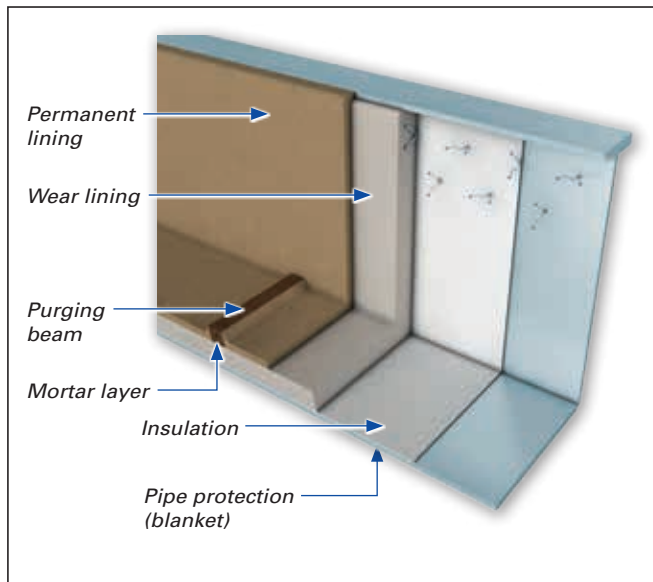


Figure 16. Inert gas purging beam in the tundish.

A state of the art purging beam system guarantees that purging will not stop during the sequence because once stopped the beam will be infiltrated and nonoperational for the rest of the sequence. It also provides an easy interface to facilitate gas flow rate control by the operator as well as comprises easy and fast connections that ensure no time is lost at the caster platform.

Tundish to Mould Inertization/Gas Purging System

Steel flow regulation between the tundish and mould can either be performed with a tundish slide gate or by means of stopper control. In both cases argon injection is required to limit the under pressure inside the refractory parts and consequently air ingress due to refractory porosity and through the joints between refractory parts. With regard to clogging, it has been determined that a minimum argon flow rate is required to avoid air suction. Nevertheless, it is necessary not to inject a too high argon flow rate into the continuous casting nozzle in order to avoid disturbances in the mould and the occurrence of blister defects in steel products [5]. At this sensitive point close to the end of the phase where steel is still liquid, a very accurate and sensitive argon control system is required because at this application stage very small changes in argon flow will have significant consequences: A too low flow rate will support nozzle clogging, while a too high flow rate will negatively influence the conditions in the mould by introducing too many bubbles. Therefore, very sensitive flow controlled and/or back pressure controlled systems are offered. Figure 17 shows the general control box layout and the typical argon flow values involved.

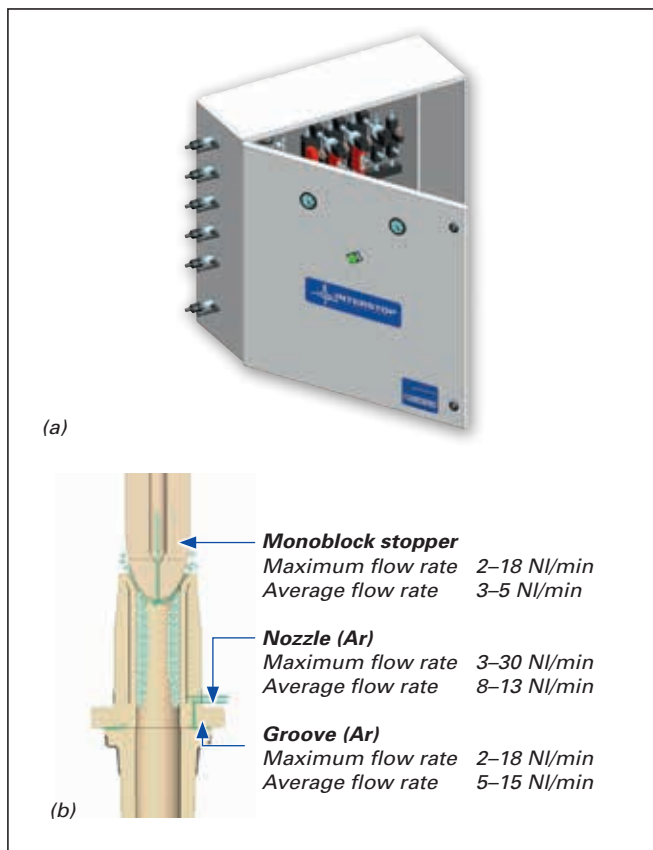


Figure 17. (a) argon control box for tundish slide gate or stopper control and (b) typical flow rates at various positions from the stopper to the casting nozzle.

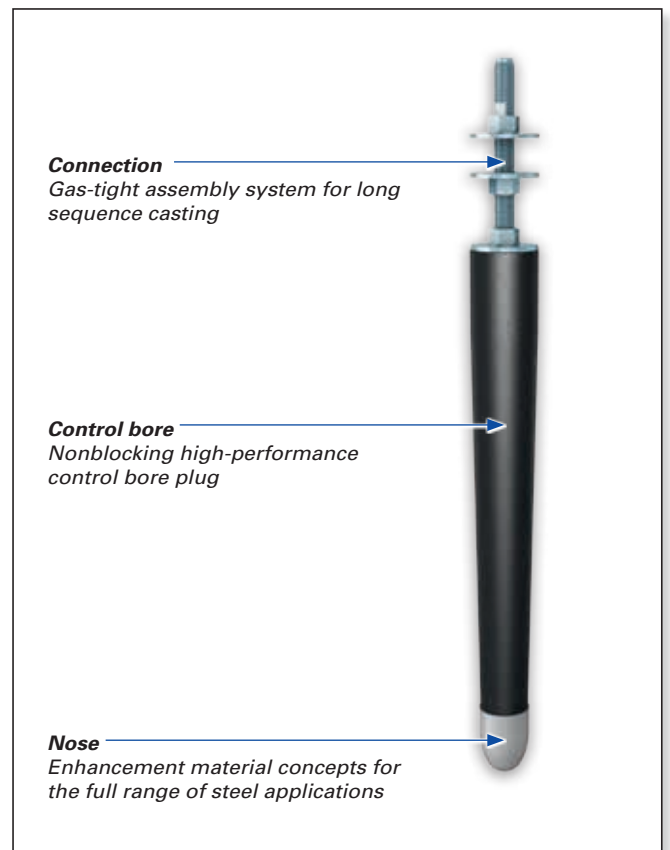


Figure 18. RHI stopper to ensure uniform argon flow over the entire sequence length.

For stopper control, besides the argon control box, an important factor is that the argon flow rate through the stopper can be maintained continuously over the entire sequence length. For this application the latest RHI innovation shown in Figure 18 ensures a gas-tight connection, a nonblocking control plug, and a long-life stopper nose.

Summary

Inert gas systems have become crucial tools as the quality requirements for steel production have increased. These systems not only offer simple gas flow control, but are also capable of complex operations and provide a high-level operator interface when improved controllers, programmable logic controllers (PLCs), and human machine interfaces (HMIs) are added. In addition, a consolidated system approach is key to achieve the desired metallurgical results with advantageous cost savings due to the highest degree of process control. It is also very important not to separate the gas regulation system and the functional refractory purging products, but to consider the gas purging system, refractory purging elements, and maintenance concept holistically. The approach offered by RHI and INTERSTOP results in an improved overall process control and cost savings due to the multiple advantages described.

References

- [1] Kirschen, M., Hanna, A. and Zettl, K.M. Benefits of EAF Bottom Gas Purging Systems. *2013 AISTech Proceedings*, Pittsburgh, USA, 6–9 May, 2013; pp. 761–767.
- [2] Kollmann, T., Jandl, C., Schenk, J., Mizelli, H., Höfer, W., Viertauer, A. and Hiebler, M. Comparison of Basic Oxygen Furnace Bottom Gas Purging Options. *RHI Bulletin*. 2012, No. 1, 8–15.
- [3] Millham, S. *IISI Study on Clean Steel: State of the Art and Process Technology in Clean Steelmaking*; International Iron and Steel Institute: Brussels, 2004; pp 64–65.
- [4] Trummer, B., Kneis, L., Pellegrino, M., Klikovich, M. and Kresaldo, M. SOC-H System—The New Standard Solution for Ladle Gas Purging. *RHI Bulletin*. 2013, No. 1, 45–50.
- [5] Nadif, M., Burt, M., Soulard, H., Boher, M., Pusse, C., Lehmann, J., Ruby-Meyer, F. and Guiban, M.A. *IISI Study on Clean Steel: State of the Art and Process Technology in Clean Steelmaking*; International Iron and Steel Institute: Brussels, 2004; p. 110.

Originally presented at the 8th European Continuous Casting Conference. Reprinted with permission from the Austrian Society for Metallurgy and Materials.

Author

Reinhard Ehrenguber, Stopinc AG, Hünenberg, Switzerland.

Corresponding author: Reinhard Ehrenguber, reinhard.ehrenguber@rhi-ag.com



RHI – BE AHEAD
with Excellence in Refractories

BE AHEAD

June 16-20, 2015 Düsseldorf
Hall 05, Stand E29

METEC



TAKE THE LEAD IN THE METALS INDUSTRIES.

Discover how RHI – the industry's leader – has changed the pace of the market again and again through innovative TECHNOLOGY, unmatched RELIABILITY and SERVICE that truly supports your success. A combination that results in key advantages for our customers in a competitive industry environment.

BE AHEAD with Excellence in Refractories.

RHI AG, Wienerbergstrasse 9, 1100 Vienna, e-mail: metec@rhi-ag.com, www.rhi-ag.com

RHI

Ashraf Hanna and Karl-Michael Zettl

Modern Electric Arc Furnace Processes and Their Requirements for Improved Lining Concepts

Introduction

Since the early 1980s, EAF processes have been continuously improving and have achieved spectacular performances in terms of productivity and specific electrical energy consumption. Several approaches have been introduced to optimize EAF operations, including those relating to energy savings, energy recycling, and the use of more chemical energy in combination with good slag foaming practice. A general trend observed worldwide is an increase in oxygen and carbon injection and multifunctional tools for oxygen injection have become standard for new EAFs and revamped old EAFs. Additionally, the decreased natural gas price in North America will lead to an increased use of direct-reduced iron (DRI) as a pure iron resource for EAFs. With the introduction of such tools, materials, and processes, it has been necessary to develop and review furnace refractory lining concepts that can withstand the new high oxygen-containing environment and slag with high FeO levels, combined with significant thermal stress and mechanical lining wear. In this paper the impact of recent EAF process improvements and the use of DRI on EAF lining concepts are discussed and refractory advances are described that have been developed for the demanding conditions.

EAF Process Improvements

The most highly perfected steelmaking units are EAFs in which electrical energy is converted by various methods into thermal energy for heating and melting the metal. EAF steelmaking processes have many advantages in comparison to other steelmaking methods. It is the only process that can achieve very high temperatures (up to 2000 °C) and operate with highly basic slag [1].

The main feature that distinguishes EAFs from other steel-making units is that heat is generated by electrical power rather than from fuel combustion [2]. As electrical energy became more competitive, the use of EAFs expanded to include the production of routine carbon steel grades. This change occurred in the late 1940s, when steel producers who had rapidly expanded their capacity during the war searched for ways to use the idle equipment. Gradually the EAF began producing grades that had been predominantly made in open hearth furnaces. In 1983, 73.4% of all the EAF steel produced was carbon steel while 19.6% was alloy and 6.9% was stainless. As the open hearth process was gradually replaced by EAFs and BOFs, the annual production increased and in 2013 more than 58% of crude steel was made in the USA using the EAF process.

With the recent natural gas price drop in the USA, steelmakers are planning to use more natural gas for steel production and operate most EAFs in a manner that uses more chemical energy and less electrical energy. Therefore, it is becoming more common for EAFs to be equipped with burners and injectors. In addition, the reduced natural gas price has resulted in the production and use of DRI being more economical and the new trend in the USA steel industry is to use more DRI.

Burners and Injectors

Current EAF technology is oriented towards an ever more efficient use of electrical and alternative energy sources. The increasing need for furnace flexibility and efficiency is directing research towards simple and reliable devices able to guarantee high-performance standards [3]. The system is composed of injectors and burners distributed in the EAF (Figure 1). Each injector unit includes the following:

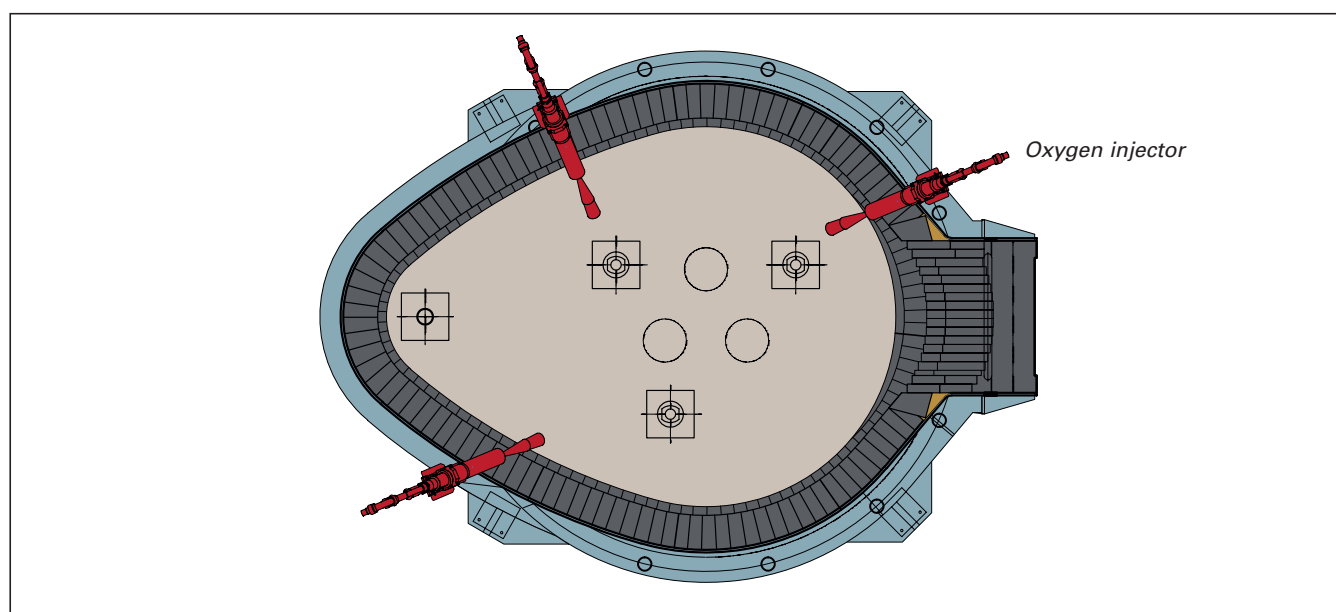


Figure 1. Oxygen injectors positioned inside an EAF.

- >> An oxygen injector with an oxygen and natural gas burner function installed on a water-cooled tile box and equipped with nonreturn valves on the oxygen and natural gas lines; flexible water, oxygen (lance and burner), and natural gas connections; and on-off valves for all the fluids (Figures 2 and 3).
- >> A carbon injector with an oxygen and natural gas burner function installed on a water-cooled tile box and equipped with nonreturn valves on the oxygen and natural gas lines; flexible water, oxygen (lance and burner), and natural gas connections; and on-off valves for all the fluids (Figures 2 and 3).

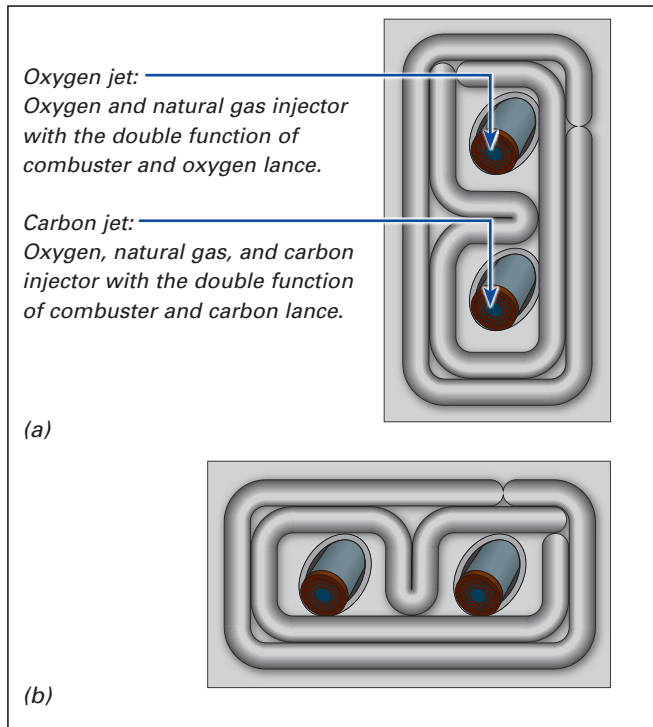


Figure 2. Carbon and oxygen jet configurations. (a) vertical and (b) horizontal orientation.

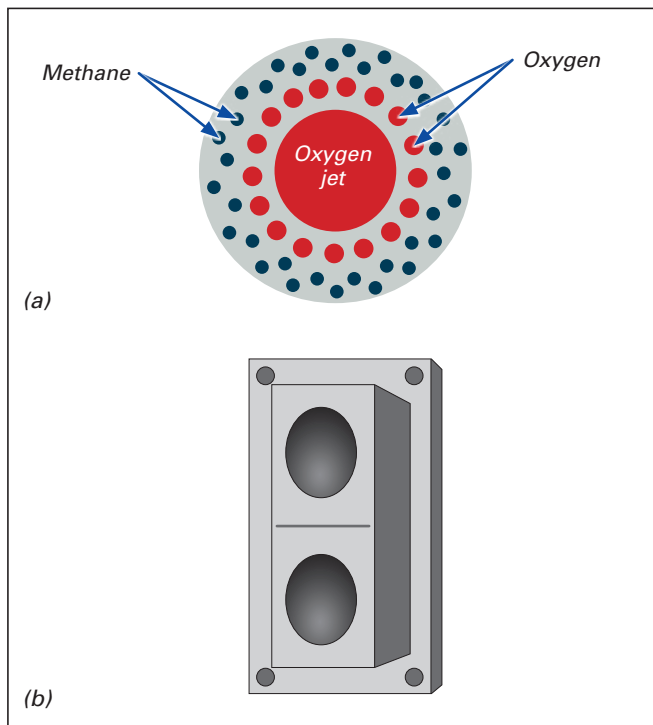


Figure 3. (a) oxygen jet with the holes for oxygen and methane and (b) water-cooled box.

- and natural gas connections; and on-off valves for all the fluids. A flexible carbon lancing system connection is also necessary.
- >> A water-cooled protection panel comprised of a copper water-cooled shield, which must be fixed to the furnace wall shield as well as a tile box for the oxygen injector, which must be fixed in the copper shield. The oxygen injector is assembled in the tile box.

The injectors must be installed externally on the EAF and positioned so that the oxygen supersonic flow (injected via the oxygen jet) intersects with the carbon flow (injected via the carbon jet) at a preestablished angle a certain distance across the liquid bath.

The injectors shown in Figure 2a are orientated vertically while the injectors in Figure 2b are installed horizontally, namely the carbon and oxygen jets are beside each other. This is the configuration used for injectors near the tapping area because the molten metal reaches higher up the wall when the furnace is tilted to tap the molten metal; therefore, refractories are installed to cover the large surface area in contact with the molten metal during this time (Figure 4). Since the injectors have to be fixed into the water panels and not the refractories, the injectors must be fitted horizontally [2].

Correctly setting the injector angles is important for their effective operation and the aim is to control the intersection point of the oxygen and coal and avoid slag splashing and/or refractory wear. The optimum or desired point is in the slag layer about 200 mm above the steel bath level. The slag layer is almost 400 mm thick, making the intersection point in the middle of the slag. If the intersection point is too low it becomes closer to the steel bath and there is a possibility of higher metal oxidation. The reaction between iron and oxygen results in iron oxide (FeO) formation that

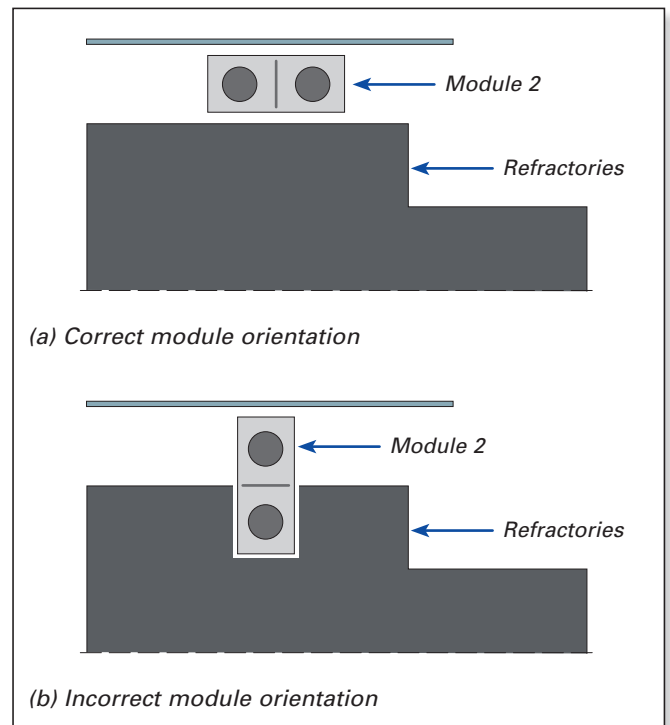


Figure 4. (a) correct horizontal position of injectors near the tapping area and (b) vertical installation in the refractory lining is not possible.

will increase the steel yield as well as increase the aggressiveness of the molten slag, thereby causing a higher corrosion rate of the wall refractories. If the intersection point is too high it results in splashing on the walls and roof, which will cause excessive refractory corrosion. Figure 5 shows the optimal angles for the injectors. However, these angles are normally modified many times to prevent splashing and reduce corrosion and mechanical refractory wear.

Refractory Attack Under the Oxygen Jet

The refractory area under the oxygen jet is subject to a very aggressive environment and the following wear mechanisms can occur:

- >> Mechanical wear or washing due to the supersonic oxygen speed.
- >> High thermal stress as a result of the exothermic oxidation reactions.
- >> Decarburization and oxidation of carbon in the MgO-C bricks under the injectors.
- >> Chemical attack by aggressive slag containing a high FeO content that has a low viscosity and is very active.

Use of Direct-Reduced Iron in EAFs

The use of DRI or hot-briquetted iron (HBI) can have specific effects on the melting process. For example, the energy consumption, productivity, and yield are affected by the DRI chemistry, percentage of DRI used in the scrap mix, and operating practices [4]. DRI is used as a scrap replacement and to dilute the residual elements contained in the scrap. However, not only the residual element levels drop as the DRI percentage increases, of equal importance is that the nitrogen levels show a reduction while appropriate slag foaming is retained.

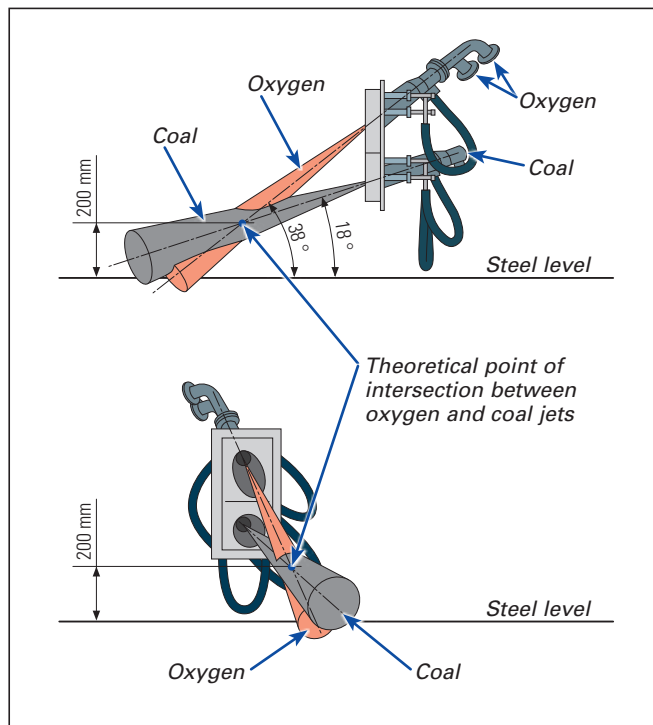


Figure 5. EAF carbon and oxygen jet angles relative to the steel bath level.

This nitrogen decrease enables EAF-based melt shops producing slabs for hot strip mills or billets for wire rod applications to effectively compete with blast furnace/basic oxygen furnace shops for many product applications.

The level of DRI metallization affects refractory consumption. The lower the metallization, the higher the FeO level. Furthermore, since increasing levels of SiO₂ in the DRI increase basic MgO-C refractory attack, the addition of lime is required to maintain the basicity ratio. However, both SiO₂ in the DRI and calcined lime consume energy during the melting process. In addition, the phosphorous and sulphur content can have a negative effect on refractory consumption due to a refining treatment process that requires in some cases a higher temperature and more oxygen injection. Charging the DRI above 20–35% of the total metallic charge in the EAF generally has a negative effect on the productivity, refractory lifetime, consumables, power-on time, and energy consumption.

DRI can cause the following EAF refractory damage:

- >> DRI can increase the percentage of FeO in the slag resulting in corrosion reactions with the working lining and bottom ramming mix.
- >> DRI has a high bulk density compared to scrap and this leads to arcing in an open bath. The arc creates splashing along with very high temperature plasma being directed to the EAF wall that causes heat stress and mechanical wear (Figure 6).
- >> Acidic oxides in the DRI (e.g., SiO₂ and P₂O₅) can increase chemical attack of the basic MgO-C bricks.
- >> Accumulation of skulls and icebergs in the EAF may lead to additional spalling.
- >> Long tap-to-tap times reduce the overall refractory lifetime.

The following sections describe available solutions to minimize refractory wear associated with the various operating conditions.

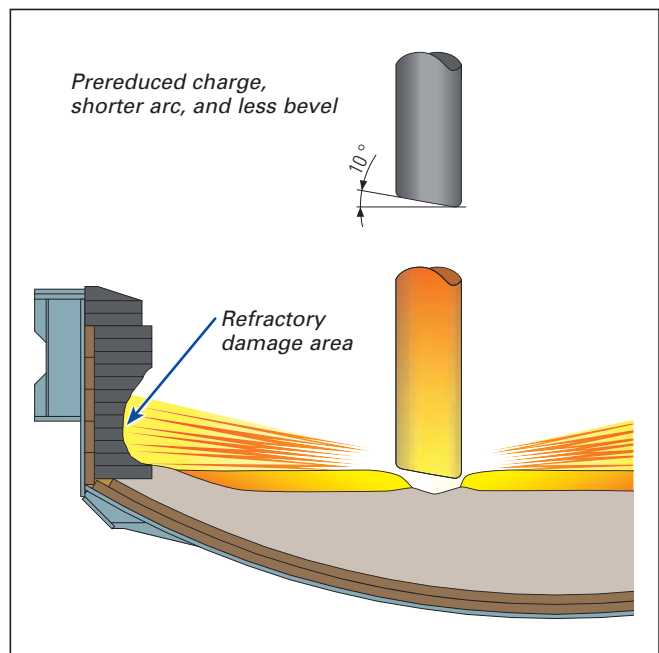


Figure 6. Refractory damage during DRI charging in an EAF.

Carbon-Bonded EAF Sidewall Bricks

As a result of the aggressive feed mix and varying percentages of fines, gangue, and FeO, it has been necessary to optimize EAF refractory lining design. Since the new oxygen injection technology has resulted in furnace operations that resemble the BOF process, RHI redesigned the refractory lining for EAF furnaces using carbon-bonded bricks that are normally used in BOF applications, instead of resin-bonded bricks. A general comparison of carbon- and resin-bonded brick properties is given in Table I. Typically, the thermal conductivity of carbon-bonded bricks is lower than resin-bonded bricks and this reduces thermal stress on the EAF shell [5].

A comparison of the actual wear in relation to the specific EAF zone recorded for carbon- and resin-bonded brands at

ArcelorMittal Point Lisas (AMPL) is provided in Table II. From this table it is evident that a reduction in the wear rate can be achieved with carbon-bonded bricks, which increases the furnace lining performance.

Area	Resin-bonded brand	Carbon-bonded brand
	Wear (mm/heat)	
CoJet area	1.4–2.3	1.0–1.7
EBT	1.3	1.0
Hot spots	1.52–2.16	1.0–1.7
Slag line	1.15–1.7	0.9–1.3

Table II. Wear rate comparison of carbon- and resin-bonded brands in various EAF zones at AMPL.

Brick properties	Carbon-bonded	Resin-bonded
Thermal conductivity	++	+++
Thermal expansion	++	++ (without metallic additives) +++ (with metallic additives)
Cold crushing strength	+++	++++
Crushing strength at high temperature (1000 °C)	++++	+++
Corrosion resistance	++++ (without the requirement for high carbon content or metallic additives)	++++ (without metallic additives) ++ (with metallic additives) (requirement for higher carbon content)
Thermal stress resistance	++++	++
Oxidation resistance	++++	++ (without metallic additives) +++ (with metallic additives)

Table I. General comparison of carbon- and resin-bonded bricks.

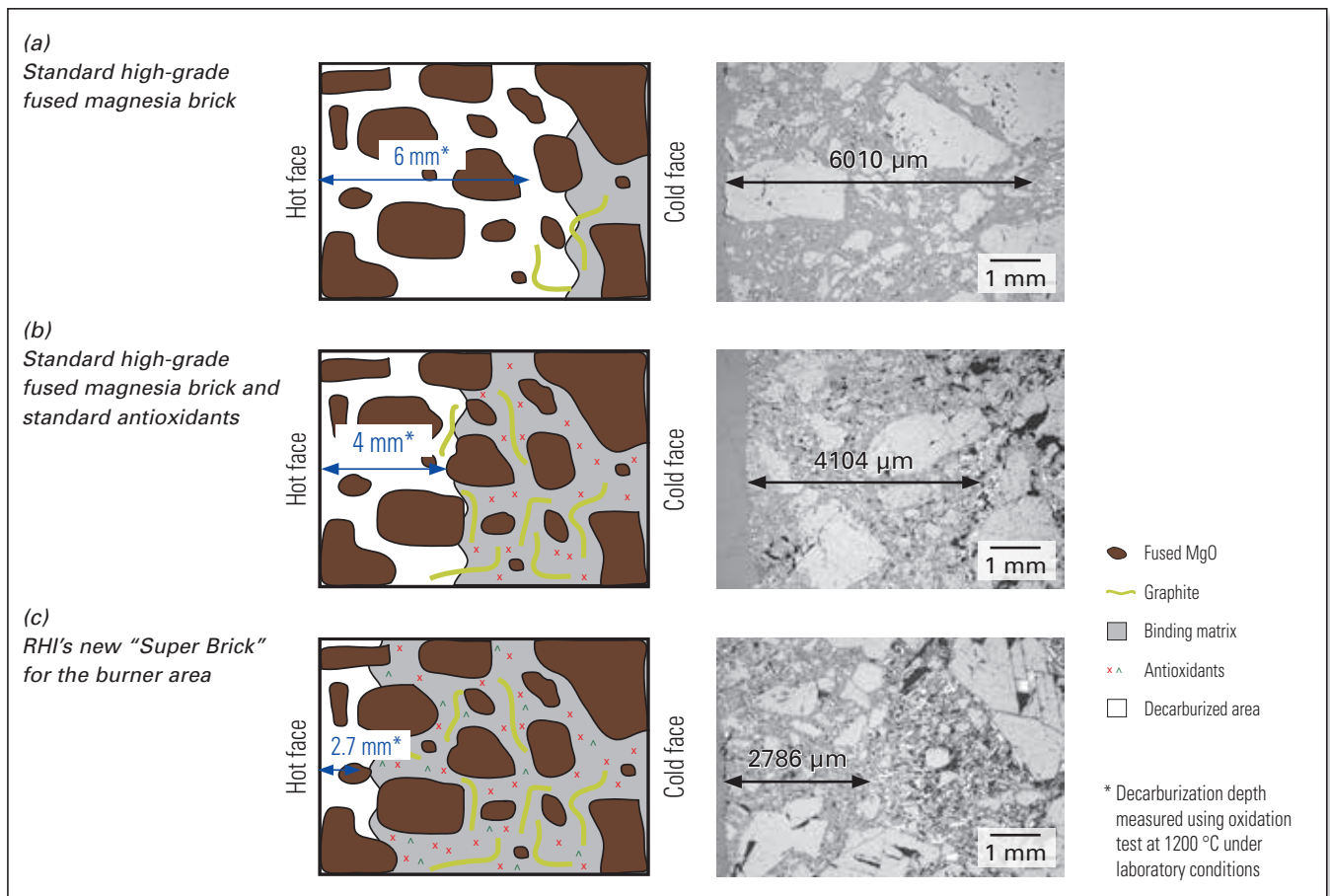


Figure 7. Comparison of the oxidation depth in MgO-C bricks. Oxidation of carbonaceous components results in increased matrix porosity at the hot face. The decarburization depth is indicated (arrows). (a) without antioxidants, (b) with standard antioxidants, and (c) B₄C addition in combination with Al and Mg.

Special Designed Bricks for the EAF Burner Area and Oxygen Jet Area

The refractory bricks under the oxygen injector are subjected to high mechanical wear from oxygen injected at supersonic speed as well as additional wear factors due to oxidation of carbon in the bricks, chemical attack from the slag, and high heat stress following exothermal reactions arising from oxidation. This results in the necessity for patch repairs in the damaged area, normally requiring personnel to enter a hot furnace to conduct the maintenance and causing costly downtime. Therefore, it was necessary to develop bricks with a very well adjusted composition of several antioxidants combined with a rather high carbon content to withstand the thermomechanical load. The RHI Technology Center Leoben (Austria) developed MgO-C bricks, called "Super Bricks", for the burner area. Boron carbide was introduced as an antioxidant in this brick type that contains high-quality fused magnesia. Both resin-bonded and carbon-bonded versions of the brick are available. The boron carbide provides very good application results due to the excellent antioxidation behaviour in combination with commonly used Al and Mg metal powders (Figure 7). The boron carbide reacts with fine oxide components in the matrix to generate viscous, low temperature melting phases with melting points between 1000–1300 °C. These phases form a protective film that covers the pore walls and carbon components, thereby reducing oxygen attack [6].

The performance of different EAF burner brick grades listed in Table III was tested and proven at more than 40 EAF steel plants around the world.

Special Designed Bricks for EAF Hot Spot Areas

Although carbon-bonded bricks without antioxidants demonstrate good resistance to slag and chemical attack, RHI has conducted many studies to examine the performance of these bricks in a very aggressive environment. Based on a series of laboratory tests and field trials, a special high-performance carbon-bonded grade based on very high-quality fused magnesia, 15 wt.% carbon, and a special metallic system was developed. To achieve the maximum temperatures as well as hot corrosion and hot erosion resistance, the brand has a carbon-enriched matrix due to post-impregnation with a special polymer (Figure 8). While typically it is not easy to add antioxidants to carbon-bonded bricks, once this brick was produced it showed very good performance especially in the EAF hot spot areas. The brick grade termed SYNCARBON C F1T15SX, produced in Europe, has been trialled in more than 10 EAF steel plants worldwide; among others, in EAFs that use up to 90% DRI where in some cases the FeO content in the slag reached 65 wt.%.

Grade	Bonding system	Production location
SYNCARBON C F1T10MBD	Carbon, additionally dense pressed	Europe
SYNCARBON C F1T10MB	Carbon	Europe
SYNCARBON R F1T10MB	Resin	Europe
ANCARBON F1T10MB	Resin	China

Table III. Overview of available special EAF burner bricks.

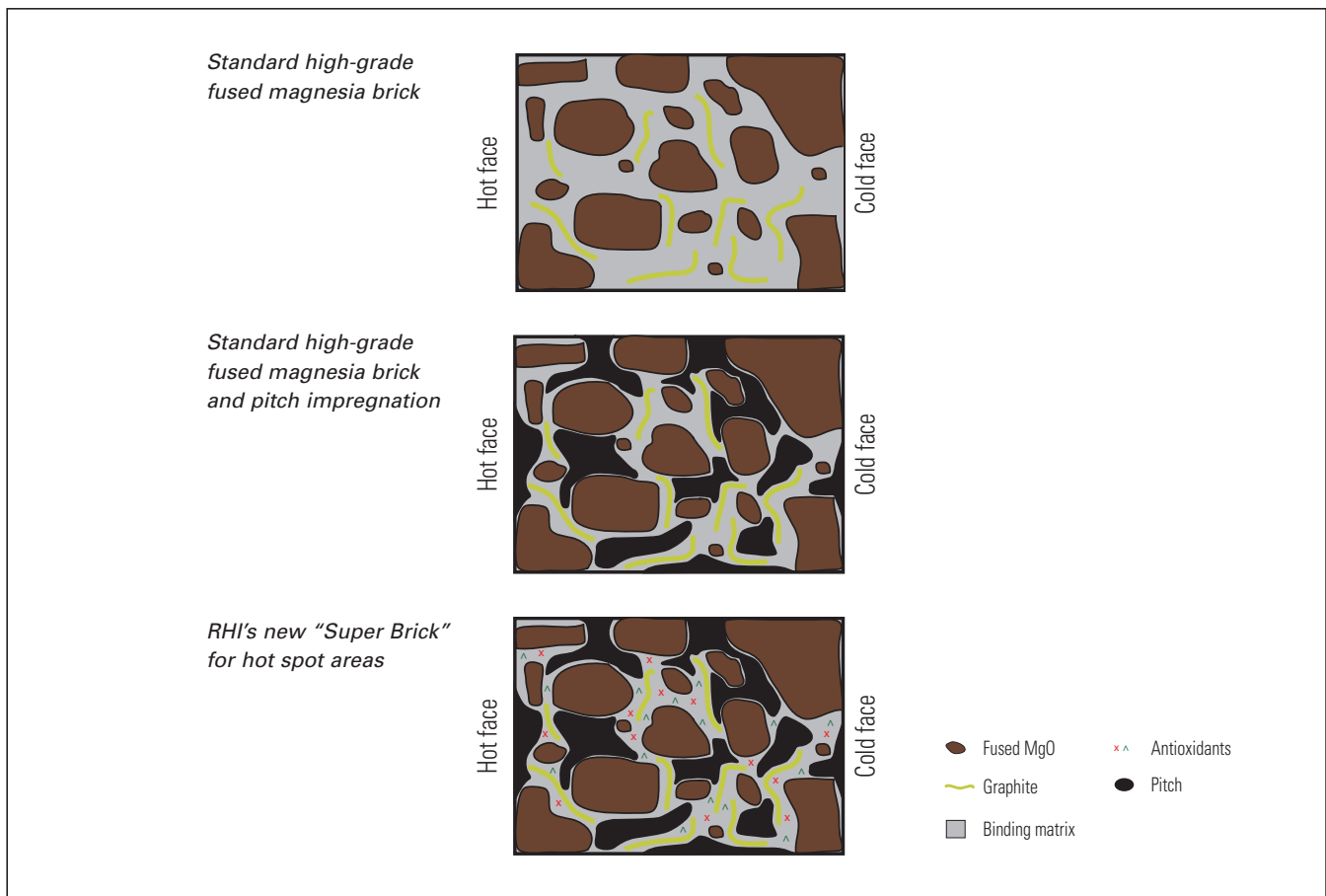


Figure 8. Comparison of standard EAF hot spot bricks with SYNCARBON C F1T15SX.

SYNCARBON C F1T15SX has demonstrated significantly improved performance compared to the standard bricks used for this application. Comparing EAF hot spot bricks, produced in China, ANCARBON F1T14D is the preferred grade showing the highest performance. It contains top-grade fused magnesia, 14 wt.% carbon, and is manufactured using the dense brick technology.

EAF Bottom Design

The use of DRI and intense operations with a long arc in the furnace bottom result in increased bottom temperatures. Therefore, the bottom insulation properties have become a more and more important topic, combined with the aim to reduce electric energy consumption by avoiding heat losses. There are various different bottom designs used worldwide. Figure 9 shows three selected designs for an initial hearth thickness of 800 mm from the upper surface of the steel shell to the upper surface of the hearth ramming material.

Heat transfer calculations were performed for the cases in Figure 9, taking into account wear progression of the EAF

bottom. The different calculated steel shell temperatures, as well as the minimum possible hearth thicknesses, are provided in Figure 10. The results showed increased thermal stress in the EAF shell when more safety lining was installed. Depending on the chosen hearth design, different consequences regarding operational impact, energy efficiency, material efficiency lining effort, and safety have to be considered. Table IV summarizes the various factors.

With the increasing use of DRI in addition to high-power EAF operations and a long arc there is a need to use a ramming mix that has a lower sintering behaviour combined with the formation of a thin sintered material layer at the hot face. Figure 11 illustrates the sintering behaviour of different RHI hearth ramming mixes [7]. The main influence on sintered layer thickness is the Fe₂O₃ content, followed by the amount of impurities that form low melting phases during operation (e.g., SiO₂ and Al₂O₃). Furthermore, an appropriately high CaO content in the hearth ramming mix is necessary to neutralize the infiltrating SiO₂

	Historical design	Standard design	ANKERHARTH-only design
Operational aspects	<ul style="list-style-type: none"> >> Only short campaigns without hearth repair possible (restricted by low maximum wear depth) >> Increased maintenance effort and reduced maintenance interval lead to high downtimes >> Only low hot heel operation possible, therefore reduced productivity and long tap-to-tap times 	<ul style="list-style-type: none"> >> Long campaigns without hearth repair possible (high maximum wear depth) >> Reduced maintenance effort and increased maintenance interval lead to low downtimes >> High hot heel operation; leads to high productivity and short tap-to-tap times 	<ul style="list-style-type: none"> >> Very long campaigns without hearth repair possible (very high maximum wear depth) >> Low maintenance effort and long maintenance interval lead to very low downtimes >> Very high hot heel operation possible; leads to very high productivity and very short tap-to-tap times
Energy efficiency	>> High thermal conductivity of MgO-C bricks leads to low insulation and high energy losses	>> Low thermal conductivity of ANKERHARTH leads to high insulation and low energy losses	>> Low thermal conductivity of ANKERHARTH leads to high insulation and low energy losses
Material efficiency	<ul style="list-style-type: none"> >> High ANKERHARTH material losses due to low repair interval. Entire layer of ANKERHARTH (200 mm) must be renewed after only 200 mm wear. >> Material efficiency ratio = 50% >> Risk of having to renew the MgO-C layer in the case it is glued together with a sintered ANKERHARTH layer 	<ul style="list-style-type: none"> >> Low material losses due to increased repair interval. Sintered ANKERHARTH layer (200 mm). Renew after ~ 400 mm wear. >> Material efficiency ratio = 67% 	<ul style="list-style-type: none"> >> Very low material losses due to high repair interval. Sintered ANKERHARTH layer (200 mm). Renew after < 550 mm wear. >> Material efficiency ratio = 73%
Lining effort	>> Very high effort necessary to line the MgO-C layer and the permanent lining layer	>> Only approximately once a year maintenance effort necessary to renew the permanent lining	>> No special lining effort necessary
Safety	>> Disproportional safety (not necessary)	>> Very high and well-proven safety level	<ul style="list-style-type: none"> >> Stable process conditions necessary >> Hearth to be monitored and EAF to be shut down in time >> Highest reliability and highest quality hearth ramming mix required

Table IV. Various factors that arise depending on the chosen EAF hearth design.

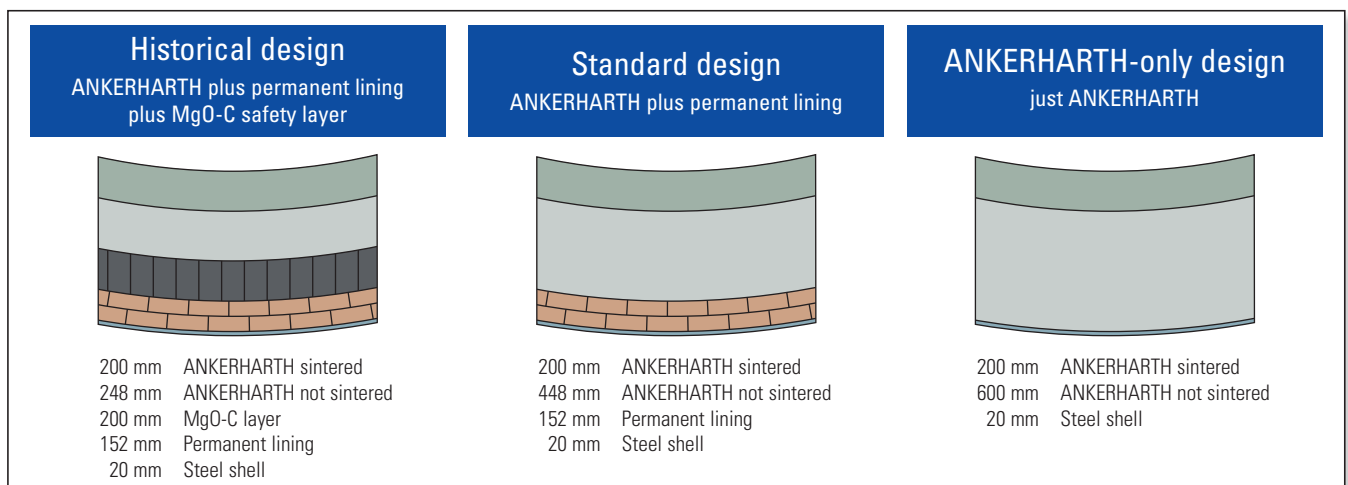


Figure 9. Comparison of different hearth lining designs, shortly after start up of an EAF campaign.

present, especially for the case of process slag forming in EAFs charged with DRI. The correct CaO content helps to stiffen the infiltrated slag already present in the upper ANKERHARTH layer and inhibits further infiltration. Thereby, corrosive slag attack can be reduced to a minimum. A further indication of slag resistance is the hearth ramming mix CaO/SiO₂ ratio: The higher this value, the better the mix is suited for aggressive slag resulting from DRI charging.

ANKERROCS–Refractory Observing Control System for EAF Sidewalls

Due to the high lining wear rate resulting from the negative impact of DRI and oxygen injectors there is a requirement for accurate methods to measure the actual lining thickness without the huge investment costs associated with laser scanning. Therefore, RHI developed ANKERROCS (Refractory Observing Control System), an easy to install, simple,

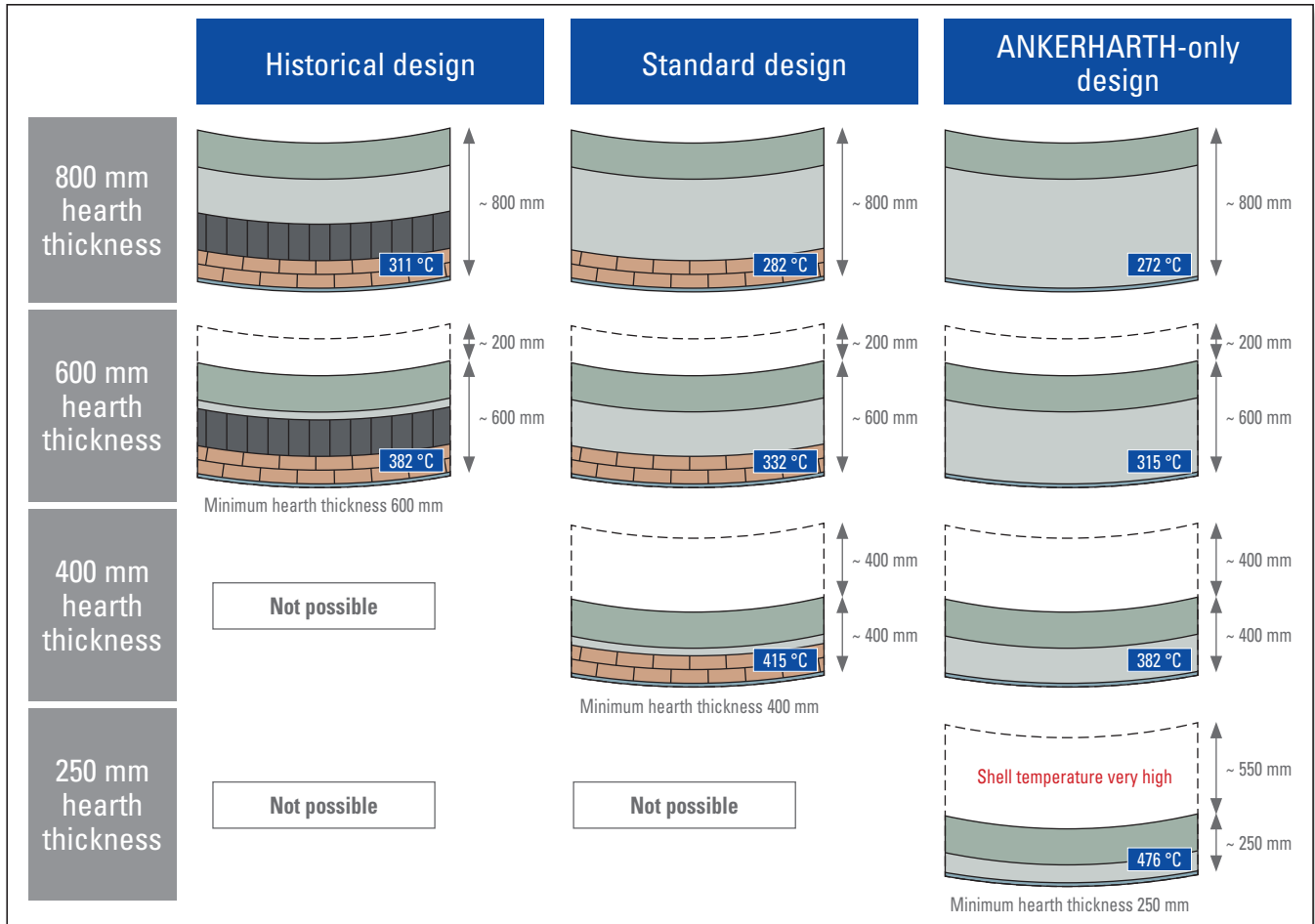


Figure 10. Calculated steel shell temperatures, considering a steel bath temperature of 1650 °C, for various hearth designs and minimum hearth thicknesses.

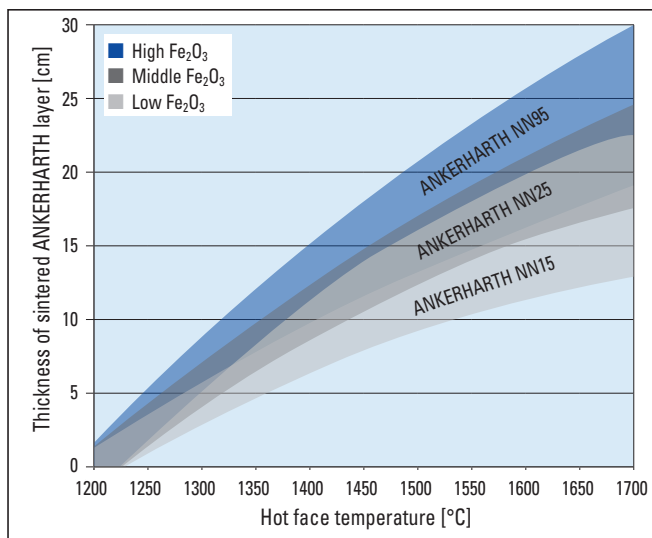


Figure 11. Hot face temperature influence on the sintered layer thickness of various ANKERHARTH mixes containing different levels of Fe₂O₃ [7].

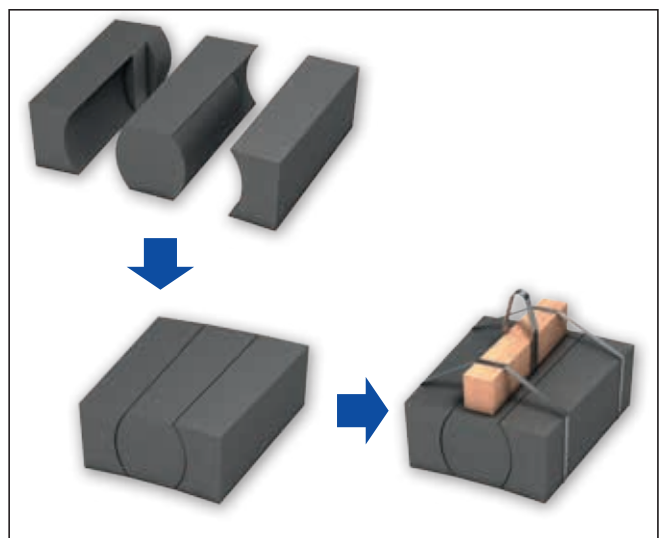


Figure 12. ANKERROCS (Refractory Observing Control System). (a) individual brick shapes, (b) assembled brick set, and (c) user-friendly lifting aids for installation.

residual thickness indicator that is directly implemented in the vessel lining (Figure 12).

ANKERROCS can be manipulated as every other brick, but due to its special design it changes the profile of its cross section depending on the level of wear (Figure 13). The gradual slimming down of the middle segment provides reasonable information concerning the residual thickness of the wear lining. During operation the joints of ANKERROCS gleam and as a result the individual cross sections can be detected during the wear process (Figure 14).

Summary

As a result of modern EAF practices and charging with DRI, the lifetimes of both magnesia-carbon bricks and bottom ramming mixes are affected. Concerning the wear lining, a new generation of carbon-bonded magnesia-carbon bricks with significantly reduced open porosity and an excellent resistance to high temperatures has been developed for high wear areas. In addition, special brands for high oxygen attack and aggressive slag conditions have been developed and trials have shown very positive results during application. The new brands, based on European-sourced magnesia raw materials, are characterized by an excellent

resistance to high temperatures and slag attack due to their large periclase crystal size and low silica content and the addition of special antioxidants. Further solutions to optimize furnace bottom design as well as a simple, easy to implement lining wear indicator have also been developed to improve EAF operations.



Figure 14. ANKERROCS in operation.

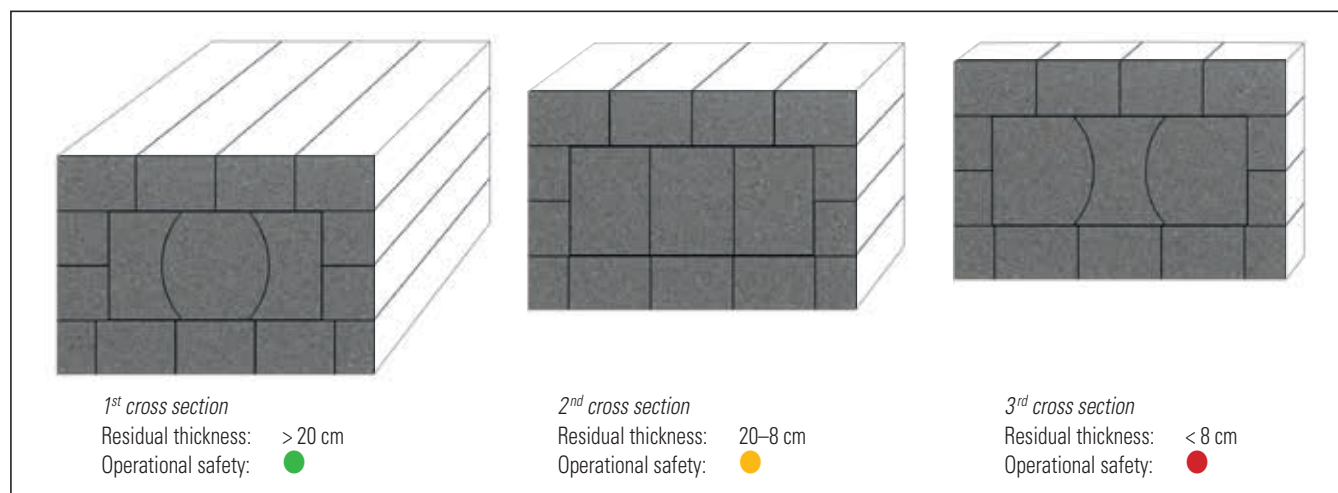


Figure 13. Change in the ANKER ROCS cross section during wear.

References

- [1] Polukhin, P., Grinberg, B., Kantenik, S., Zhadan, V. and Vasilyev, D. *Metal Process Engineering*; Mir Publishers: Moscow, 1970.
- [2] Hanna, A. *Electric Energy Saving in Electric Arc Furnace Steelmaking*, Master's Thesis, Mansora University, Egypt, 2001.
- [3] Michielan, A. and Fior, A. The Danieli DANARC Plus M² Furnace at ABS Meltshop. Presented at 6th European Electric Steelmaking Conference, Düsseldorf, Germany, June 13–15, 1999.
- [4] Dressel, G.L. Direct Reduced Iron Process Effects and Applications, Pawleys Island, USA. <http://www.dresseltech.com/dripart4.pdf>
- [5] Buchebner, G., Hanna, A. and Zettl, K-M. Latest Developments in Magnesia-Carbon Bricks For Modern Electric Arc Furnaces. Presented at AISTech 2013, Pittsburgh, USA, May 6–9, 2013.
- [6] Rief, A., Heid, S. and Höck, M. Effects of Metal Powder Additives on MgO-C Brick Performance. *RHI Bulletin*. 2013, No. 1, 33–37.
- [7] Eckstein, W., Zettl, K-M. and Wappel, D. ANKERHARTH—50th Anniversary of Electric Arc Furnace Bottom Ramming Mixes. *RHI Bulletin*. 2013, No. 1, 8–13.

Originally presented at AISTech 2014 and published in the AISTech 2014 Conference Proceedings. Reprinted with permission from the Association for Iron and Steel Technology (AIST).

Authors

Ashraf Hanna, RHI Canada Inc., Steel Division, Burlington, Canada.
Karl-Michael Zettl, RHI AG, Steel Division, Vienna, Austria.

Corresponding author: Ashraf Hanna, ashraf.hanna@rhi-ag.com

Kerry Servos, Matthias Madey, Ashraf Hanna, Markus Hochegger and Ritchie Debisarran

Installation and Practical Experience With Preassembled EAF Slag Door Blocks at Arcelor Mittal Point Lisas

Introduction

In a joint effort with Arcelor Mittal Point Lisas (AMPL), located in Trinidad, the challenge was to find solutions to overcome premature wear at the slag door area and improve the furnace relining time as well as reduce the gunning mix consumption. The plant operates with 90–100% direct-reduced iron (DRI) that generates a very aggressive slag containing high amounts of iron oxide. In addition, the oxygen jet directly attacks the slag door, slag movement results in mechanical wear, and there is physical damage caused by the cleaning process.

Towards the end of 2013, RHI provided AMPL with two pre-assembled slag door blocks. The concept evolved from the precast EAF slag door blocks (breast blocks) RHI currently supplies to some customers in the United States. Underpinning the decision to design a preassembled (preglued) slag door block were the benefits of using RHI’s excellent quality magnesia-carbon bricks combined with the ability to zone the blocks and target specific grades to the wear areas and optimize costs. Additionally, the large P-shapes that RHI can produce and their use in these assemblies provide a design advantage especially in high wear areas that are exposed to mechanical damage.

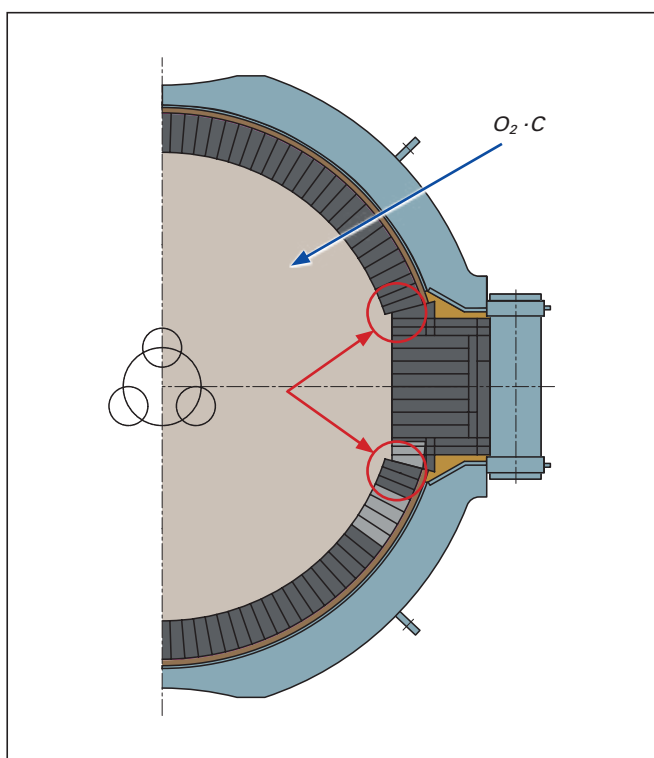


Figure 1. Position of early erosion at the slag door. The gunning consumption in these areas is increased and in certain situations the furnace is stopped early for patching.

Current Situation at AMPL

The plant at AMPL is equipped with two 150-tonne AC EBT electric arc furnaces. The mill produces rebar for the local market. Typically, the furnaces are charged with up to 90–100% DRI along with scrap steel. DRI can cause refractory damage due to multiple factors (see page 19) such as increased FeO levels in the slag, a high bulk density that causes arcing in an open and flat bath, and the presence of acidic oxides (e.g., SiO₂ and P₂O₅). Therefore, considerable effort has been made over the years to improve the EAF refractory design. Furthermore, with an aggressive DRI feed mix containing varying percentages of fines, gangue, and FeO, an optimum EAF slag door refractory design was required due to excessive erosion at an early stage in the campaign on the door jambs (from approximately 60 heats onwards) caused by the CoJet lance and phase # 1 electrode (Figure 1). Normally the slag door is replaced during furnace relining approximately every 400–450 heats, with one patch after an average of 250 heats. As a result of the early erosion on the slag door the gunning consumption in this area is increased and in some situations the furnace is stopped early for patching.

Installation of the Preassembled Slag Door Block

The standard slag door lining is shown in Figure 2. Normally the slag door area is bricked using SYNCARBON C F6T14, a carbon-bonded grade based on medium-quality fused magnesia with a carbon content of 14 wt.%. The first preassembled slag door block was constructed using only one grade—SYNCARBON C F6T14. For easy and above all safe lifting the preassembled slag door block (unit weigh



Figure 2. Standard slag door lining. Normally the slag door area is bricked using SYNCARBON C F6T14, a carbon-bonded grade based on medium-quality fused magnesia with a carbon content of 14 wt.%.

3.376 tonnes) was supported by wooden slats, which include four 30 mm x 5 mm clamps (Figure 3). An overhead crane was used to bring the block into its final position. A 10-mm ANKERFIX NS60 (mortar) layer was applied to the bottom to ensure correct installation regarding the levelling

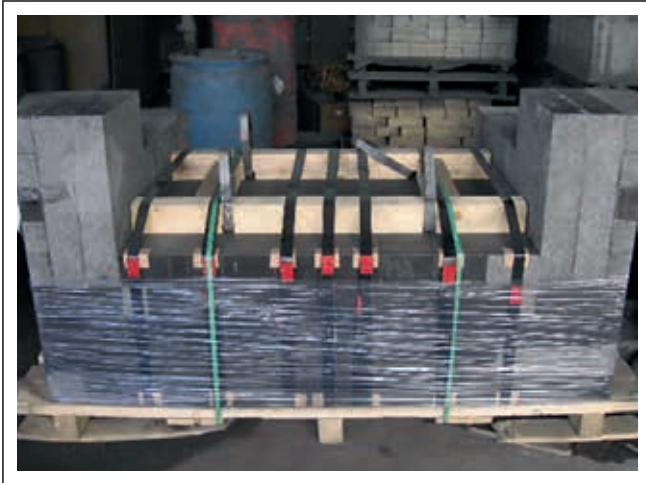


Figure 3. The first preassembled slag door block was constructed using SYNCARBON C F6T14. For easy and safe lifting the preassembled slag door block (unit weight 3.376 tonnes) was supported by wooden slats, which included four 30 mm x 5 mm clamps.

(Figures 4 and 5). Slight modifications in the geometry had to be made for the cooling panel to fit after positioning the upper split shell. The remaining gaps towards the breast electrode and steel shell were rammed with ANKERMIX NP13 (Figure 6).



Figure 6. The remaining gaps towards the breast electrode and steel shell were rammed with ANKERMIX NP13.



Figure 4. An overhead crane was used to maneuver the block into its final position. A 10-mm ANKERFIX NS60 (mortar) layer was applied to ensure correct installation regarding levelling.



Figure 7. Intact preassembled slag door after 346 heats.



Figure 5. Final placement of the preassembled slag door. Slight modifications to the geometry were required so the cooling panel fitted after positioning the upper split shell.



Figure 8. Brick patch to the working hot face of the slag door.

Operational Advantages of the Preassembled Slag Door

The main benefits that have been achieved with the preassembled slag door block are:

- >> Reduction of the bricking time by 90–120 minutes during relining.
- >> Block remains intact after patching and runs for a full campaign. The patch was carried out after 346 heats (Figures 7 and 8).
- >> Significantly reduced refractory maintenance (gunning and fettling) during the campaign and no heat stress hazard while gunning.
- >> Reduced turnaround time/downtime.

The first trial showed that the preassembled slag door block had an inhomogeneous wear pattern (Figure 9) in some areas that were in contact with very aggressive slag containing a high percentage of FeO (up to 60 wt.%). The red coloured areas indicate chemical attack by high FeO-containing slag in addition to mechanical wear (erosion) resulting from slag movement and the physical damage by the slag door cleaning machine. Therefore, it was necessary to redesign the preassembled slag door block using several grades and adapt it to these conditions. It was also found that the oxygen lance beside the slag door was incorrectly angled, which led to direct oxygen contact with the slag door shoulder. Oxygen causes aggressive attack due to brick

decarburization and the energy generated by oxygen-mediated exothermic reactions increases thermal stress in the bricks and at the same time the supersonic oxygen speed leads to mechanical wear.

Modification of the Preassembled Slag Door

SYNCARBON C F1T15SX is a high-performance carbon-bonded grade based on very high-quality fused magnesia (FMN98 TOP fused) with a large periclase size of up to 2000 µm and low silica content, produced at RHI's plant in Norway. The grade also contains 15 wt.% carbon and a special metallic system (see page 21). To achieve maximum hot corrosion and hot erosion resistance it has a carbon-enriched matrix due to postimpregnation with a special polymer. SYNCARBON C F1T15SX has been trialled in EAFs that use up to 100% DRI, where in some cases the FeO content in the slag reached 65 wt.%, and has shown excellent slag resistance.

SYNCARBON C F3T14 is a carbon-bonded grade based on FMN98 TOP fused magnesia and contains 14 wt.% carbon. The high carbon content reduces slag wettability and increases resistance to slag attack.

Based on the wear pattern observed with the first two slag door assemblies, RHI will now zone the block using SYNCARBON C F1T15SX in the most demanding areas and the remainder will comprise SYNCARBON C F3T14 (Figure 10).

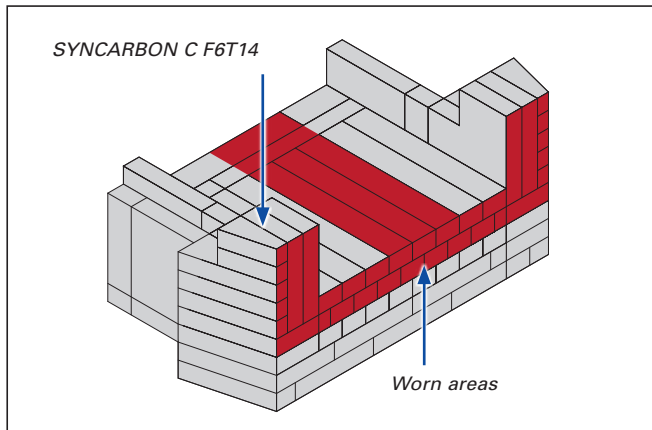


Figure 9. Wear pattern of the SYNCARBON C F6T14 slag door when in contact with slags containing high levels of FeO.

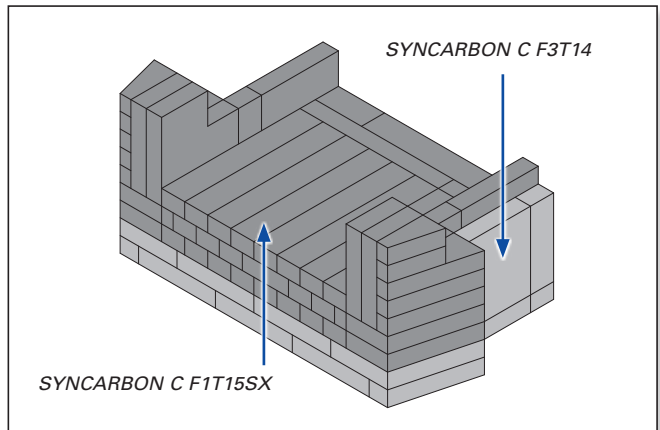


Figure 10. Zoning of the slag door assembly using SYNCARBON C F1T15SX in the high wear areas and SYNCARBON C F3T14 in the remaining sections.

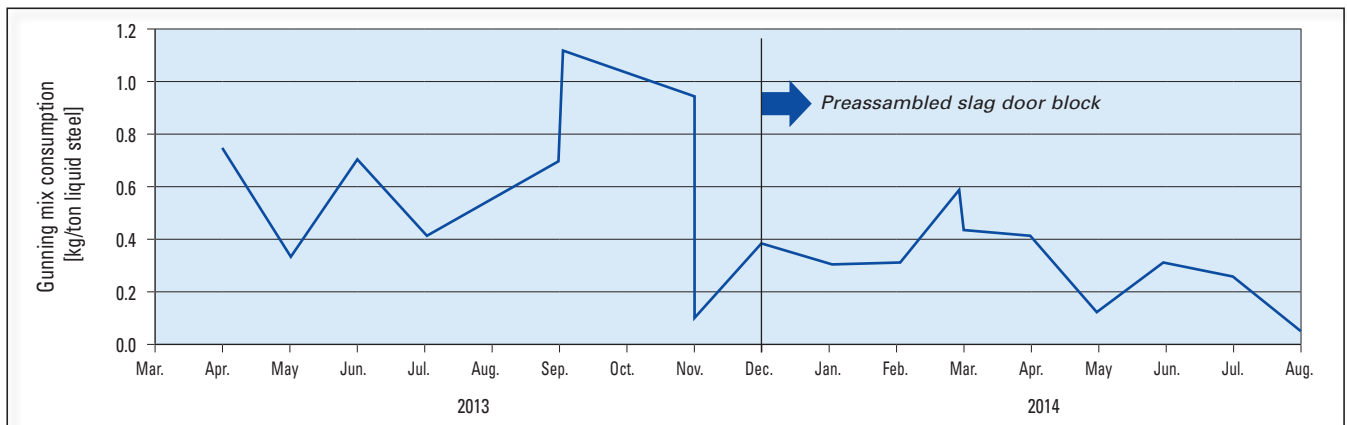


Figure 11. Gunning material consumption per tonne of liquid steel before and after installation of the preassembled slag door block in January 2014.

Conclusion

Following the successful running of the first two preassembled slag door blocks (Figure 11 and Table I), AMPL ordered four more assemblies with the new zoned design to reduce wear and increase service life. Since implementing the RHI preassembled slag door block, AMPL have been able to achieve a 10% reduction of the installation time but more importantly they have reduced downtime for gunning and patching and improved the campaign life of the furnace, thereby improving furnace availability.

Key performance indicator	Performance prior to improvement action	Performance after improvement action
Delay due to gunning (min/heat)	2.08	1.56
Gunning mix consumption (kg/ton of net billet)	0.70	0.37

Table I. Performance improvements realized with the preassembled slag door block.

Acknowledgement

The authors would like to thank AMPL Refractory Management for their support during the course of this work.

Authors

Kerry Servos, RHI Canada Inc., Steel Division, Burlington, Canada.

Matthias Madey, RHI Refractories Andino CA, Point Lisas, Trinidad.

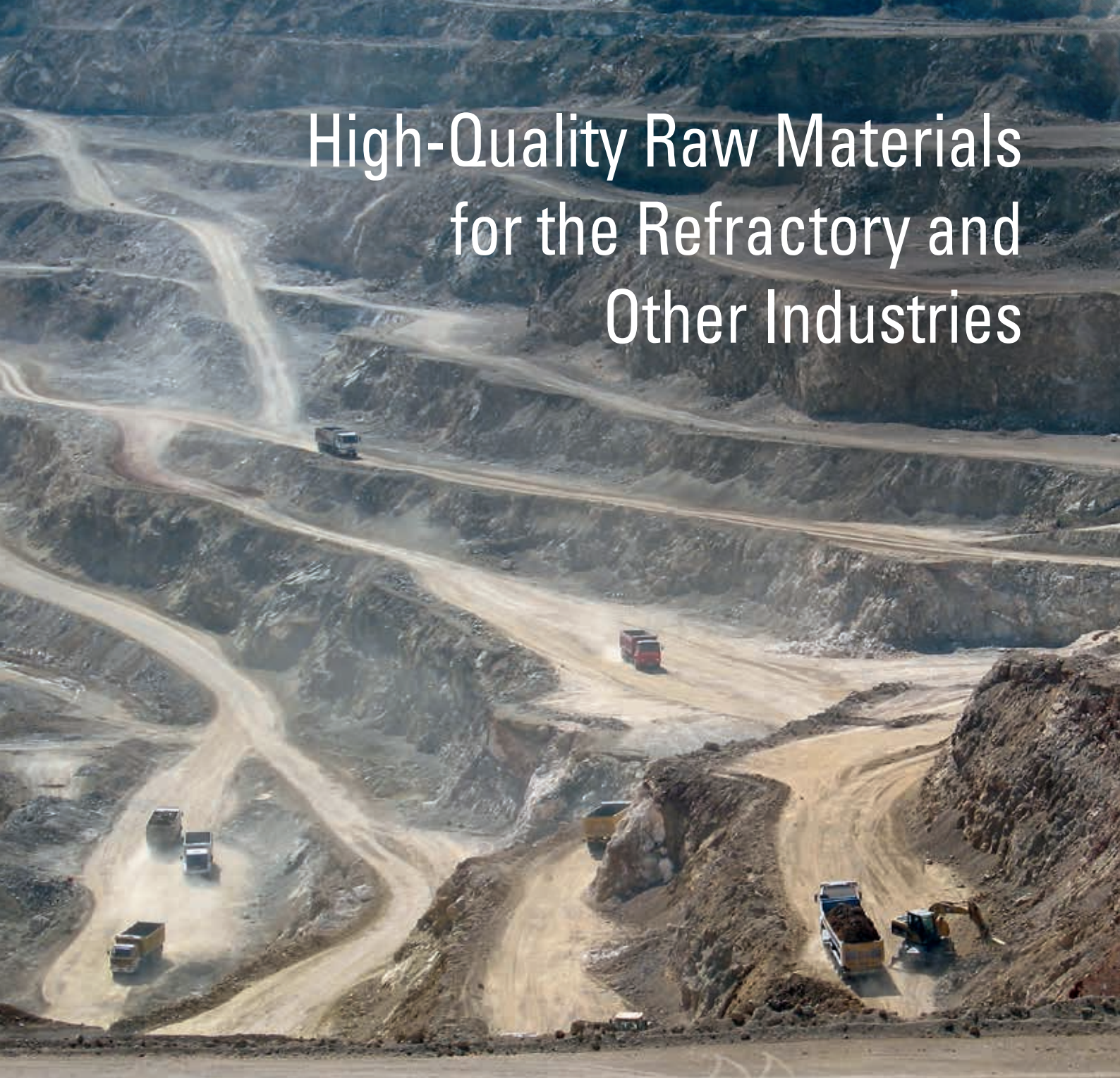
Ashraf Hanna, RHI Canada Inc., Steel Division, Burlington, Canada.

Markus Hochegger, RHI AG, Steel Division, Vienna, Austria.

Ritchie Debisarran, ArcelorMittal Point Lisas, Trinidad.

Corresponding author: Matthias Madey, matthias.madey@rhi-ag.com

High-Quality Raw Materials for the Refractory and Other Industries



RHI supplies high-quality raw materials for the pulp and paper, refractory, construction, chemical, and animal feed industries.

Approximately 900000 tonnes of magnesia and doloma, from mining and seawater origins, are currently produced at eight raw material sites in Europe as well as Asia and processed into high-grade fused, sintered, and caustic products.

Top quality and supply security—RHI is your reliable partner in the raw material sector.

www.rhi-ag.com EXCELLENCE
IN REFRACTORIES

RHI

Birgit Bellgardt, Sarah Köhler, Bernd Neubauer and Roland Pungerssek

Taphole Developments for Specific Steel Industry Demands

The taphole is an important part of each BOF and EAF, having an influence on both vessel availability and secondary metallurgy. To reduce taphole repair and maintenance, constant further developments of high-performance taphole brands with respect to the raw material composition and production technologies are necessary and have been undertaken for both segmented and isostatically pressed sleeves. At steel plants focused on clean steel technology, the effective separation of steel and slag during tapping is a critical step to achieve the least possible slag carryover in the ladle after tapping while at the same time maximizing steel yield. Therefore, computational fluid dynamics (CFD) modelling was performed to examine the influence of different channel designs on the amount of slag carryover and residual steel at the end of tapping. The results showed that a reduction in slag carryover and residual steel can be achieved with the CFD-optimized HYFLO channel geometry.

Introduction

Converter and EAF tapholes comprise segmented or single piece inner sleeves, surrounding elements, and an annular gap filled with refractory mix (Figures 1 and 2). For many years RHI has offered customers high-performance tapholes as well as various machines that enable rapid and precise repair [1–3]. To address current and future steel industry demands, a project was initiated for both BOF and EAF taphole developments with the target to improve performance and provide very competitive products tailor made for specific applications. This included extending the product portfolio to include isostatically pressed sleeves in addition to segmented tapholes.

The main customer demand is to reduce taphole maintenance and repair time with the goal of increasing steel production efficiency. Based on the results of postmortem investigations, new grades have been created and evaluated in different field trials. A performance improvement was recorded in all cases, as determined from the steel flow rate during tapping. Additionally, different channel geometries were examined using computational fluid dynamics (CFD) modelling with regards to slag carryover at the end of tapping because of the impact on clean steel production.

The amount of residual steel was also quantified and showed that steel yield as well as the cleanliness can be enhanced using a CFD-optimized HYFLO channel design.

Postmortem Analyses of Segmented Taphole Sleeves

Several postmortem investigations of RHI’s high-performance segmented sleeve grades were conducted and provided the basis for both BOF and EAF taphole material developments. The main wear mechanisms observed were hot erosion, oxidation, and corrosion due to FeO attack, which resulted in the formation of magnesio-wustite.

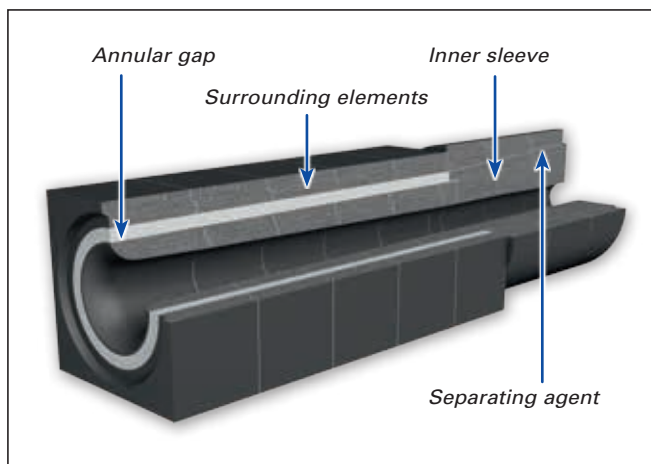


Figure 1. BOF HYFLO C taphole.

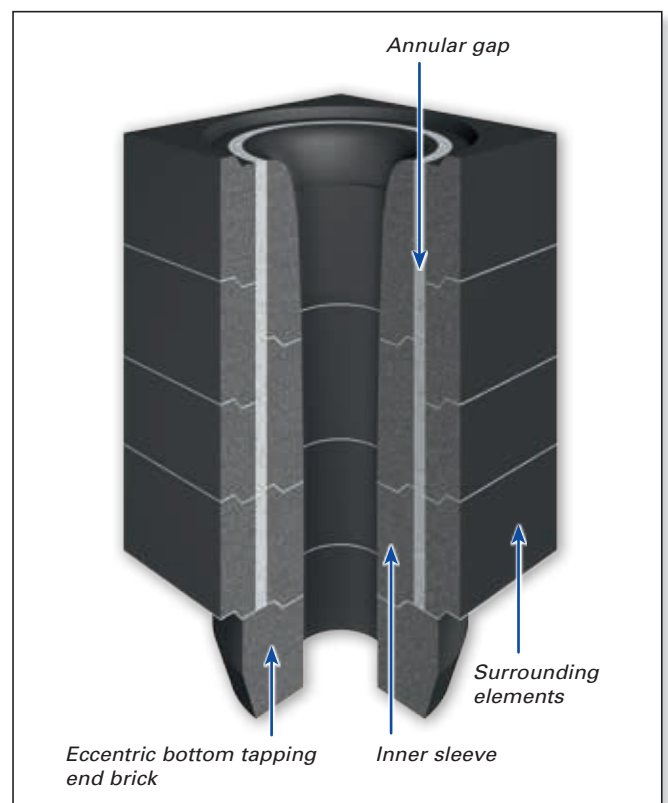


Figure 2. EAF EBT taphole.

In addition, carryover of calcium silicate slag was found to increase corrosion. Slag coating at the hot face, a wide iron oxide rich reaction zone mainly comprising magnesio-wustite ((Mg,Fe)O), and a second reaction zone below where calcium silicate phases were dominating can be seen in Figure 3. Immediately below the second reaction zone, the carbon was mainly oxidized and the fine fraction was

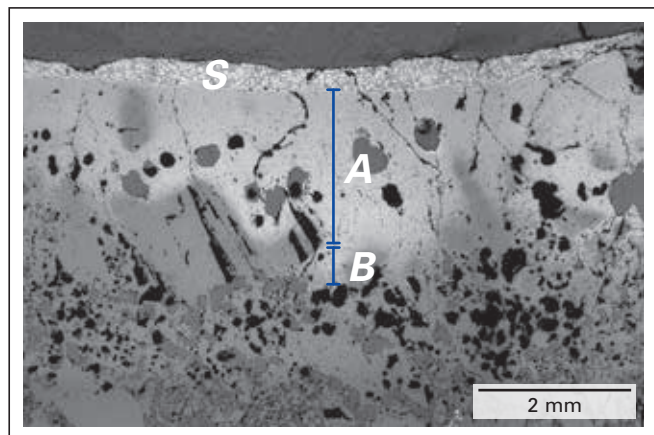


Figure 3. Microstructure of a used MgO-C taphole sleeve brick showing slag coating at the hot face (S), a zone mainly containing magnesio-wustite (A), and a second reaction zone containing calcium silicate phases (B). Immediately below zone B, the carbon was mainly oxidized and the fine fraction was completely dissolved.

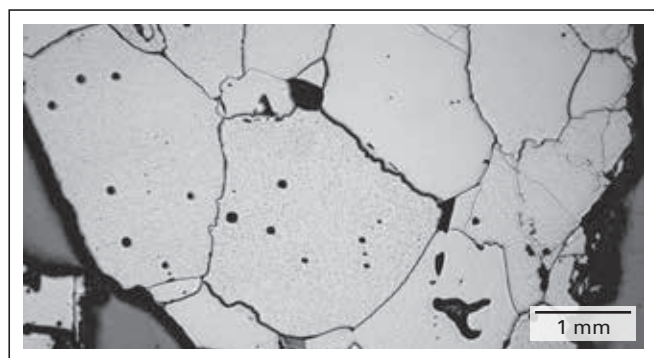


Figure 4. RHI's high-purity FMN98 TOP fused magnesia produced in Norway.

completely dissolved; however, the coarse magnesia grains with large crystals remained.

Based on these and additional results various development targets were identified to optimize the material properties. They were application-specific and included achieving a dense microstructure with low porosity, high hot strength, and precisely balancing the carbon content.

Segmented Taphole Sleeve Grade Developments

A wide range of measures concerning the raw material composition as well as optimizing production technology were taken to achieve the targeted taphole properties. These included the use of RHI's Norwegian-produced high-purity fused magnesia (FMN98 TOP fused) with a very large periclase crystal size of up to 2000 μm (Figure 4); incorporating high-purity graphite with a low ash content and thicker lamella, where the impurities are present on the surface and not in the basal plane for more oxidation and corrosion resistance (Figure 5); and a precise composition of the metallic-ceramic bonding system. In addition, significantly improving the pressing process and a brand-new high-pressure vacuum impregnation facility at the Radenthein plant (Austria) have been key factors in the developments.

A combination of these approaches resulted in three new taphole brands with significantly improved properties (Table I).

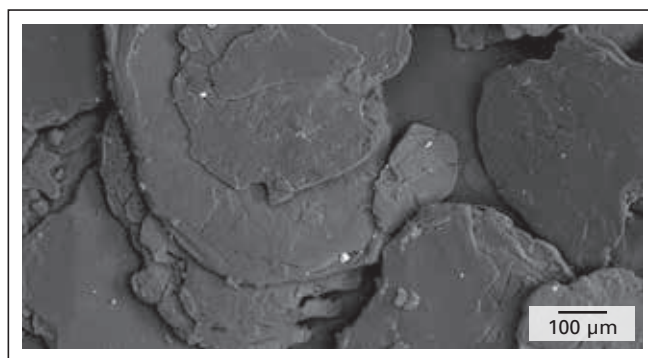


Figure 5. High-purity graphite with thick lamella.

	Standard BOF grade	ANKERTAP HMC269X	ANKERTAP HMC287X	Standard EAF grade	ANKERTAP TB077
Physical properties					
BD (g/cm ³)	3.19	3.23	3.30	3.01	3.00
AP (vol.%)	1.0	1.0	1.0	1.0	1.0
CCS (N/mm ²)	90	90	80	50	50
After coking at 1000 °C					
BD (g/cm ³)	3.14	3.18	3.23	2.97	2.97
AP (vol.%)	6.5	6.0	6.0	8.0	7.0
CCS (N/mm ²)	80	80	70	50	50
After coking at 1500 °C					
BD (g/cm ³)	3.04	3.07	3.20	n.a.	n.a.
AP (vol.%)	10	9	7	n.a.	n.a.
HMOR at 1400 °C (reduced conditions) (N/mm ²)	3	6	9	25	29
Chemical composition					
MgO (wt.%)	98.0	98.0	98.5	88.1	88.5
C (wt.%)	6	6	4	16	16

Table I. Physical properties and chemical composition of various taphole grades for BOF and EAF segmented sleeves. Abbreviations include bulk density (BD), apparent porosity (AP), cold crushing strength (CCS), hot modulus of rupture (HMOR), and not available (n.a.).

For BOF applications, ANKERTAP HMC269X has an increased microstructure density compared to the standard grade. The high degree of matrix filling and homogenous distribution of the fine and ultrafine magnesia as well as carbon-containing components are visible in the detailed micrograph (Figure 6). ANKERTAP HMC287X is characterized by a significant increase in the bulk density and a reduced content of minor phases. High corrosion and oxidation resistance can be expected from these material properties. At increased temperatures the improvement in the physical properties becomes more significant (see values at 1500 °C in Table I), in particular the porosity. Furthermore, the hot modulus of rupture, indicative of hot erosion resistance, is increased in ANKERTAP HMC269X and ANKERTAP HMC287X. In both grades the carbon-bonding system provides sufficient residual flexibility and good oxidation resistance.

The developmental focus for EAF applications involved tailoring the metallic-ceramic bonding system and resulted in ANKERTAP TB077.

Field Trial Results of Segmented Taphole Sleeves

The new ANKERTAP HMC269X and ANKERTAP HMC287X BOF brands were evaluated in several field trials at selected customers. A summary of the results is shown in Figure 7.

The flow rate increase for each heat (tonnes/minute) provided a measure of inner sleeve wear. Both ANKERTAP HMC269X and ANKERTAP HMC287X demonstrated a performance increase in all the trials, ranging from 2–46%. As a consequence of the positive trial results, these brands are now established on the market. Currently, ANKERTAP TB077 is being trialled in EAF shops.

Isostatically Pressed Taphole Sleeve Grade Advances

Following the merger with Orient Refractories Ltd., in Bhiwadi (India), RHI now has the opportunity for dense isostatic pressing. This has enabled the taphole range to be extended and RHI has focused on evaluating existing isostatically pressed grades in field trials, modifying benchmark recipes, and developing new grades.

Field Trial Results of Isostatically Pressed Taphole Sleeves

ANKERTAP WX10 was developed for producing isostatically pressed taphole sleeves using slightly higher pressing pressures than typically used for isostatically pressed flow control products while ANKERTAP IMR802 was a grade advance for pressing sleeves at higher pressures. The physical properties and chemical composition of the two grades are shown in Table II.

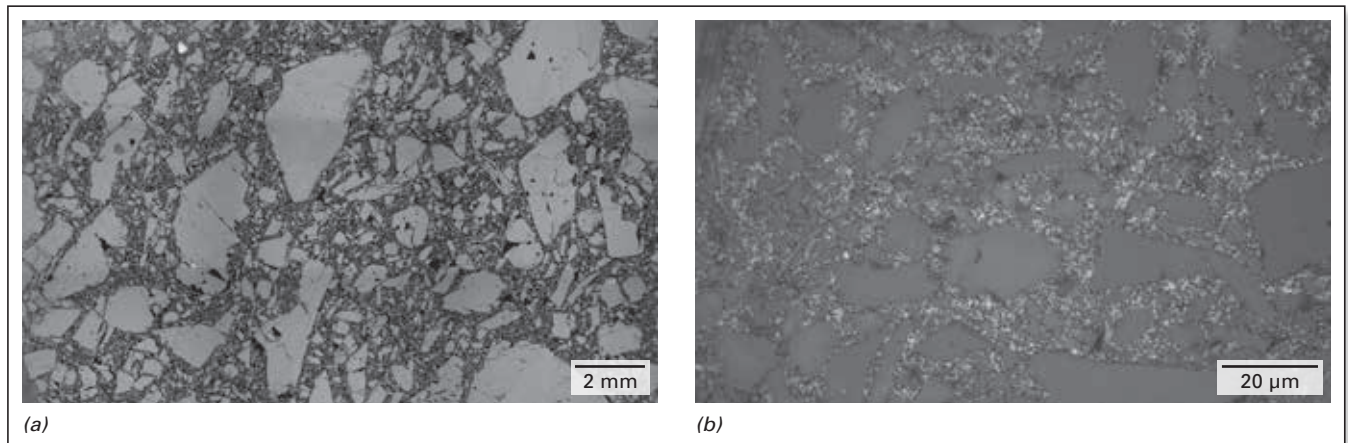


Figure 6. ANKERTAP HMC269X. (a) overview of the dense microstructure and (b) detail of the homogeneously distributed fine and ultrafine magnesia as well as the carbon-containing components.

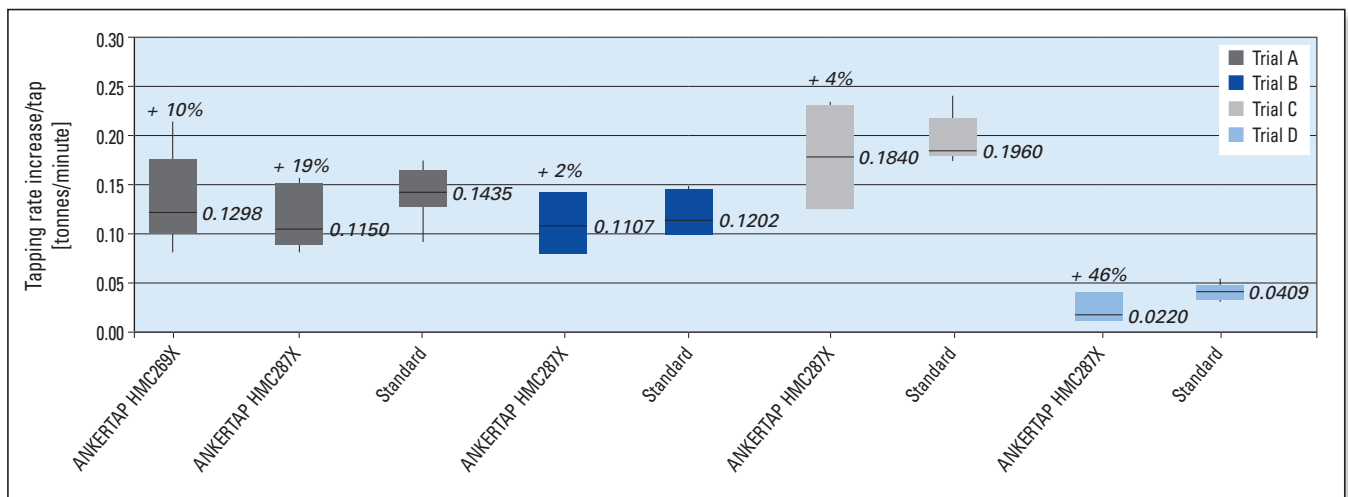


Figure 7. Box and whisker plots showing the field trial results of segmented taphole sleeve grades. Mean values are indicated by a line within the box and the average is included numerically. The performance increase was determined from the average flow rate values.

Service trials were conducted at a US steel shop to compare the two grades. The dense isostatically pressed taphole grade ANKERTAP IMR802 showed a > 50% higher performance, in terms of a lower wear rate, compared to the ANKERTAP WX10 under the same converter conditions and taphole design. The results of this trial are summarized in Figure 8 regarding the tapping rate increase for each heat.

A postmortem investigation of the well-performing ANKERTAP IMR802 showed a slag layer at the hot face, a reduced layer containing magnesiowustite and iron droplets, and a reduced layer with secondary phases (Figure 9).

	ANKERTAP WX10	ANKERTAP IMR802
Physical properties		
BD (g/cm ³)	2.86	3.02
AP (vol.%)	4.0	2.1
CCS (N/mm ²)	44.0	65.6
MOR (N/mm ²)	18.0	15.1
HMOR at 1400 °C (reduced conditions) (N/mm ²)	18.0	13.3
After coking at 1000 °C		
BD (g/cm ³)	2.88	2.97
AP (vol. %)	9.0	9.7
CCS °C (N/mm ²)	42.0	36.2
MOR (N/mm ²)	6.0	3.1
After coking at 1500 °C		
BD (g/cm ³)	2.81	2.94
AP (vol. %)	12.1	11.2
CCS (N/mm ²)	29.5	27.3
MOR (N/mm ²)	4.8	n.a.
Chemical composition		
MgO (wt.%)	85	95
C (wt.%)	17	9

Table II. Physical properties and chemical composition of two grades for isostatically pressed BOF sleeves. Abbreviations include bulk density (BD), apparent porosity (AP), cold crushing strength (CCS), modulus of rupture (MOR), hot modulus of rupture (HMOR), and not available (n.a.).

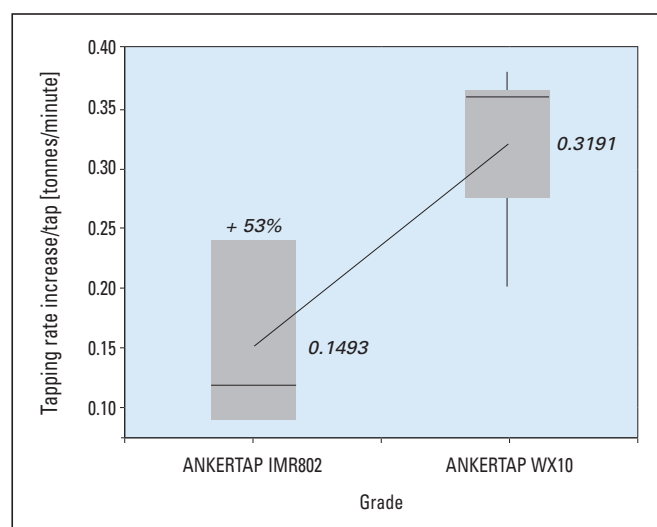


Figure 8. Box and whisker plots showing the field trial results of ANKERTAP IMR802 isostatically pressed tapholes compared to ANKERTAP WX10. Mean values are indicated by a line within the box and the average is included numerically. The performance increase was determined from the average values.

The magnesiowustite-containing layer protected the graphite below against oxidation. Furthermore, the sleeve material showed no steel infiltration. The metal powder additives had formed carbides that provided strength. Surface cracks were observed that were very likely due to mechanical stresses occurring during operation.

Isostatically Pressed Taphole Sleeve Grade Developments

The development of new grades for isostatically pressed BOF and EAF sleeves involved an in-depth analysis of RHI benchmark grades and a comprehensive literature study. The careful selection of matrix materials was essential for creating high-performance products, and as described for the segmented sleeves the primary raw materials used in the new grades are RHI's high-purity Normag fused magnesia (FMN98 TOP fused) (see Figure 4) with very large periclase crystals as well as high-purity graphite (see Figure 5) to provide more oxidation and corrosion resistance. In addition, optimizing the ratio of metal additives and the carbon content resulted in very good physical properties (Table III) as well as improved slag and oxidation resistance compared to the well-performing ANKERTAP IMR802. As oxidation resistance is an essential requirement for BOF sleeves, this property was examined at 1000 °C in an oxidizing atmosphere (Figure 10).

During operation the inner sleeve is subject to erosion. Therefore, abrasion testing was performed at room temperature in order to compare this material property of the different grades (see Table III). The test measures the volume of material (cm³) abraded from a flat surface positioned at 90° to a nozzle through which 1 kg of size-graded silicon carbide grain is blasted by air at a defined pressure.

As a result of carefully balancing the metal additives a grade was developed for customers requiring fired sleeves, which provides longer lifetimes and better thermal shock resistance (ANKERTAP IMR814BX). By achieving the optimum ratio between the metal powders, Al₄C₃ hydration can be avoided.

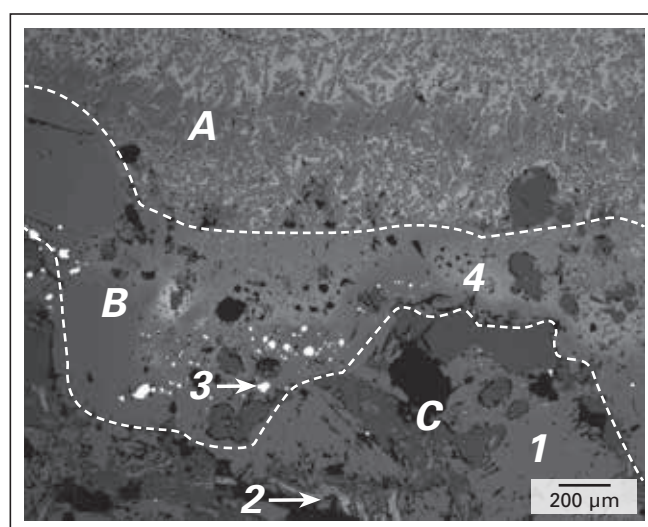


Figure 9. Microstructure of a used isostatically pressed ANKERTAP IMR802 sleeve. A slag layer at the hot face (A), a reduced layer containing magnesiowustite (B), and a reduced layer with secondary phases (C) are visible. Periclase grains (1), graphite (2), iron droplets (3), and magnesiowustite (4) are indicated.

In several steel plants, steady cracking in the sleeves is observed due to cooling during maintenance followed by a sudden increase to the tapping temperature. This results in steel penetration into the sleeve and spalling. Therefore a special additive was incorporated to produce a more flexible structure. This brand was trialled under laboratory conditions and no thermal fracturing was observed.

To evaluate the performance, several service trials are either in progress or planned for the near future with a selection of the new grade developments.

Simulation of Slag Carryover With Different Taphole Channel Geometries

Towards the end of tapping when the steel level is significantly reduced, a certain amount of slag will be entrained into the taphole. CFD was used to investigate this process and characterize various taphole geometries in terms of their ability to reduce the amount of residual steel and slag carryover.

Slag entrainment occurs when vortex formation is established as a result of the interface between the slag and steel

	BOF grade	New BOF grades		New BOF and EAF grade	New EAF grades	
	ANKERTAP IMR802	ANKERTAP IMR815X	ANKERTAP IMR825X	ANKERTAP IMR801X	ANKERTAP IMR814BX	ANKERTAP IAR849X
Physical properties						
BD (g/cm ³)	3.02	2.93	2.94	2.86	2.94	3.14
AP (vol.%)	2.1	0.4	0.6	1.2	3.1	0.4
CCS (N/mm ²)	65.6	80.4	50.0	47.0	80.7	146.0
MOR (N/mm ²)	15.1	20.3	14.0	11.9	17.7	33.3
HMOR at 1400 °C (reduced conditions) (N/mm ²)	13.3	22.0	14.0	16.1	15.0	11.0
After coking at 1000 °C						
BD (g/cm ³)	2.97	2.82	2.65	2.74	2.82	3.04
AP (vol.%)	9.7	13.6	18.6	13.5	11.6	13.2
CCS (N/mm ²)	36.2	29.1	24.0	15.6	33.7	68.1
MOR (N/mm ²)	3.1	2.7	4.0	0.9	2.9	7.7
Oxidation test at 1000 °C	+	+++	+++	++	++	+
Abrasion (cm ³)	13.0	11.4	12.6	16.2	10.2	5.7
Chemical composition						
MgO (wt.%)	94	93	90	90	91	
Al ₂ O ₃ (wt.%)						81
C (wt.%)	9	11	12	13	11	9

Table III. Physical properties and chemical composition of new grades for isostatically pressed BOF and EAF sleeves. All the new grades are not dense pressed. Abbreviations include bulk density (BD), apparent porosity (AP), cold crushing strength (CCS), hot modulus of rupture (HMOR), and not available (n.a.).

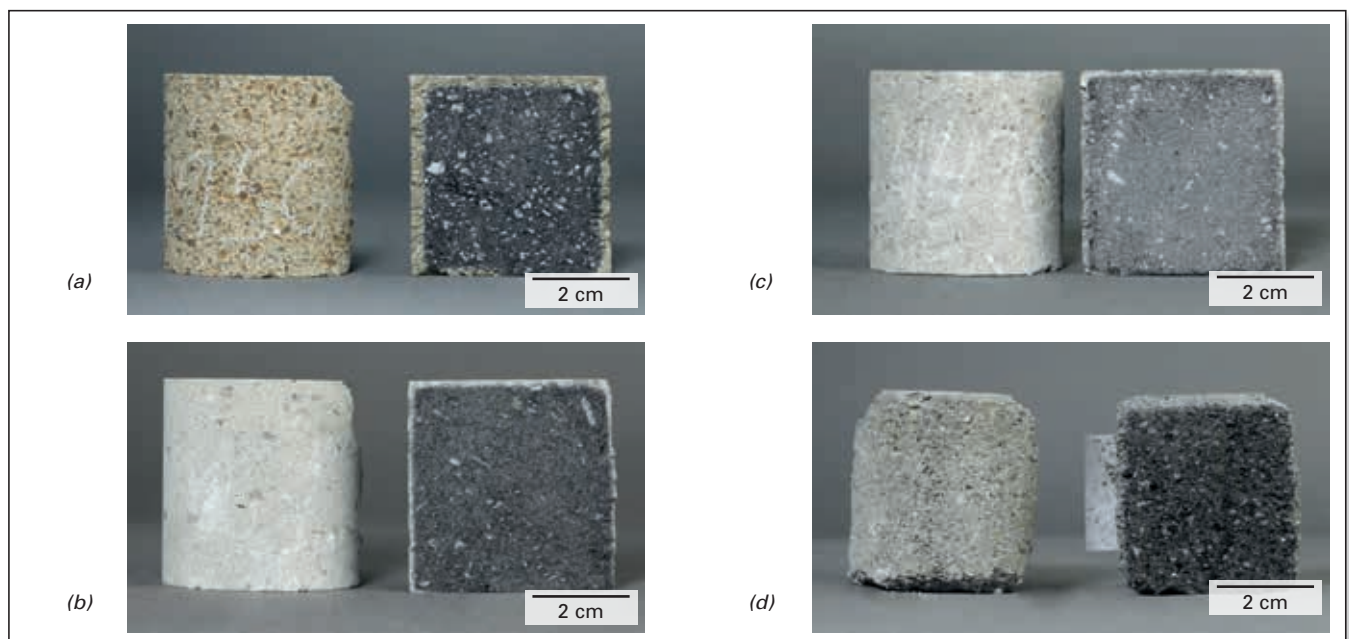


Figure 10. Oxidation resistance results after 2 hours at 1000 °C in an oxidizing atmosphere. (a) ANKERTAP IMR802, (b) ANKERTAP IMR815X, (c) ANKERTAP IMR825X, and (d) ANKERTAP IMR801X.

collapsing. This process can be examined using two theoretical approaches: The Rankine vortex and the hollow vortex. The Rankine vortex can be used to describe flow through an orifice for lower bath levels, since at this stage the flow is strongly whirling [4]. It describes a swirling flow resulting from a forced vortex at the central core surrounded by potential flow. The second approach—the hollow vortex—can be used to describe a vortex in a system comprising two fluids, where initially the lighter fluid is on top of a heavier fluid. Once the vortex has formed the inner lighter fluid is at rest, while the surrounding fluid is moving. This has an effect on vortex stability [5].

The following study focused on BOF tapholes; however the results are also valid for EAF applications. The three inner sleeve geometries investigated were a 140-mm diameter cylinder (CYL), a CFD-optimized HYFLO design with a transition from an inlet diameter of 170 mm to an outlet diameter of 110 mm, and a 120-mm cylinder with a conical entrance area decreasing from an inlet diameter of 180 mm to 120 mm (Figure 11). All three designs have the same start tapping times during actual operation. Only a section of the BOF immediately surrounding the taphole was included in the simulation.

At the start of the simulation the steel in the BOF was 1 m high with a 0.3-m thick slag layer. When the numerical model was exposed to gravity the steel and slag flowed out until the BOF was empty. The slag carryover and residual steel levels were measured as the amount of slag entrained in a cross-sectional area 10 cm from the taphole outlet increased from 0 up to 100% (Figure 12). The CYL geometry resulted in the highest level of residual steel and the highest slag carryover, while with the HYFLO design minimized both the amount of residual steel and slag carryover. To compare the three geometries more precisely, the residual steel and slag carryover were examined when the cross-sectional area 10 cm from the

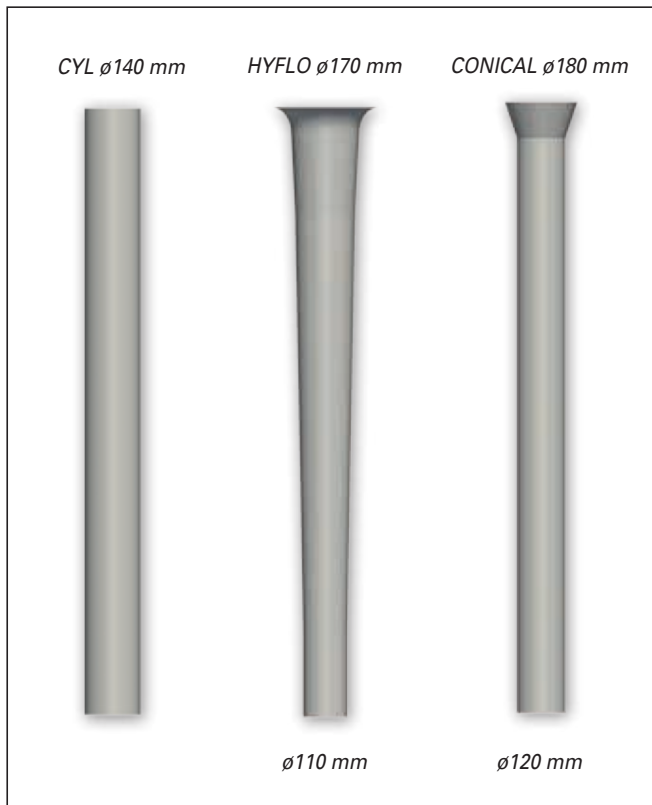


Figure 11. Simulated taphole geometries. (a) cylindrical (CYL) with a diameter of 140 mm, (b) HYFLO with a transition from an inlet diameter of 170 mm to an outlet diameter of 110 mm, and (c) cylindrical with a conical entrance area (CONICAL) decreasing from an inlet diameter of 180 mm to 120 mm.

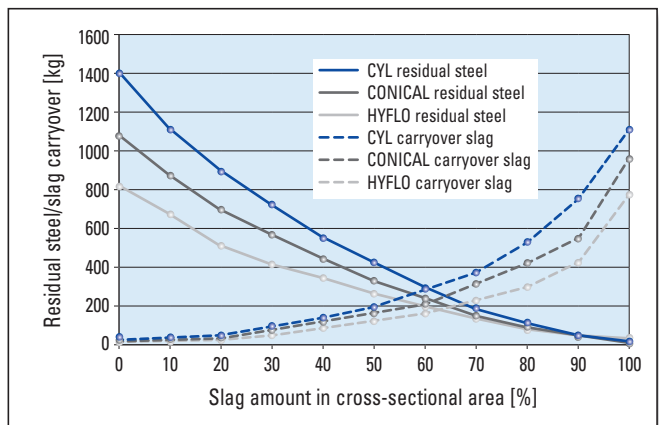


Figure 12. Residual steel and the slag carryover using the CYL, HYFLO, and CONICAL taphole geometries as slag entrainment in a cross sectional area 10 cm from the taphole outlet increased from 0–100%.

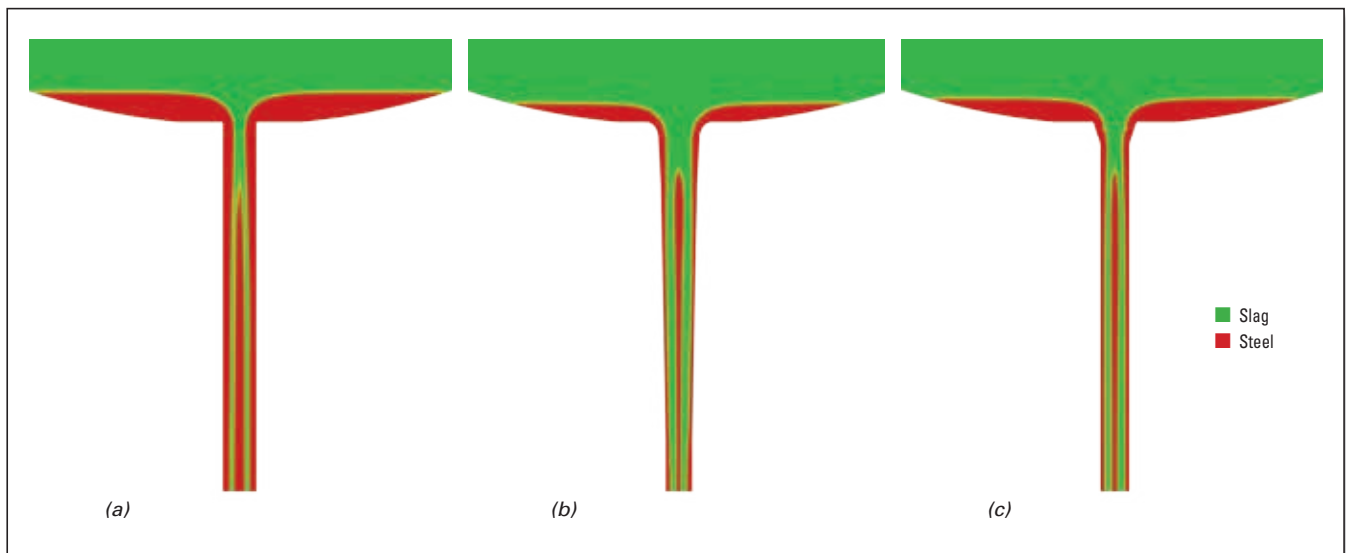


Figure 13. Comparison of the residual steel in the BOF when 20% of the cross-sectional area 10 cm from the taphole outlet contained entrained slag. (a) CYL, (b) HYFLO, and (c) CONICAL.

taphole outlet contained 20% entrained slag (Figure 13). At this point there was a measurable difference between slag carryover and residual steel with the different geometries. The conical inflow area on a cylindrical taphole reduced the residual steel by approximately 0.7% compared to the cylindrical taphole without the modified inlet area and had no impact on the amount of carryover slag (Figure 14). With the HYFLO channel design the residual steel was reduced by 53% compared to the cylindrical taphole and the carryover slag was decreased by 43%. This is equivalent to an

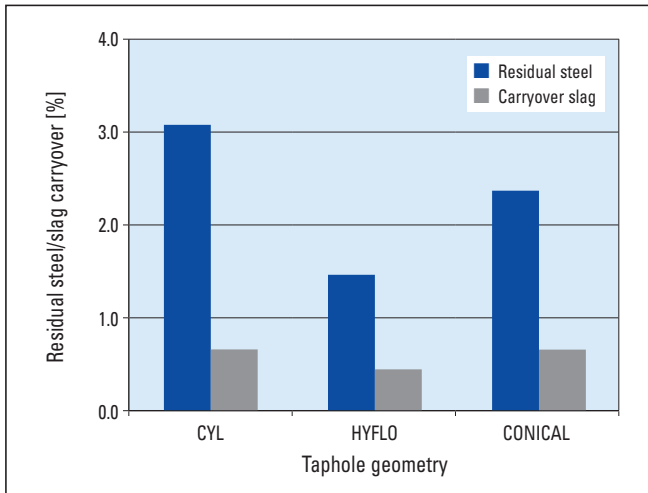


Figure 14. Comparison of residual steel and slag carryover with the CYL, HYFLO, and CONICAL taphole geometries when 20% of the cross-sectional area 10 cm from the taphole outlet contained entrained slag.

increased steel yield of > 3 tonnes per heat for a 200-tonne converter. This is a direct result of the CFD-optimized design, which reduces turbulence close to the inlet area. Decreasing the diameter of a cylindrical taphole led to minimal reduction of the residual steel level and had no effect on reducing slag carryover.

Conclusion

In summary, three high-performance brands are now available on the market for BOF taphole sleeves. The newly developed ANKERTAP HMC269X and ANKERTAP HMC287X are top level grades for segmented BOF tapholes, while ANKERTAP IMR802 marks a new standard for isostatically pressed BOF tapholes. Based on the service trial results, additional material advances have been realized that are tailored for specific applications and additional performance benefits are expected. The EAF trials with the newly developed grades will also enable high-performance taphole sleeves to be established and launched on the market for this application.

CFD simulations have clearly demonstrated the relationship between taphole geometry and slag carryover. The results show the CFD-optimized HYFLO channel geometry provides significant advantages regarding the level of residual steel and slag carryover compared to standard cylindrical and conical channel designs. Currently the simulations are being extended to examine tapping with entire BOF and EAF models and the results will provide precise figures regarding the benefits that can be achieved with customized taphole geometries. In addition, water modelling is planned to support and visualize the findings.

References

- [1] Bachmayer, J. and Sorger, R. Electric Arc Furnace Taphole Changing Systems. *RHI Bulletin*. 2006, No. 2, 34–37.
- [2] Jeitler, J., Pungerssek, R. and Sauer, G. i-TAP BOF: The New Converter Taphole System. *RHI Bulletin*. 2007, No. 1, 20–23.
- [3] Pungerssek, R., Schantl, W., Pagger, J. and Weiss, R. Twenty Years of ISOJET Converter Tapholes and the TBD Changing Device. *RHI Bulletin*. 2010, No. 2, 23–29.
- [4] Siekmann, H.E. and Thamsen, P.U. *Strömungslehre: Grundlagen*; Springer: Berlin, Heidelberg, New York, 2007.
- [5] Llewellyn Smith, S.G. and Crowdy, D.G. Structure and Stability of Hollow Vortex Equilibria. *J. Fluid Mech.* 2012, 691, 178–200.

Authors

Birgit Bellgardt, RHI AG, Technology Center, Leoben, Austria.
 Sarah Köhler, RHI AG, Technology Center, Leoben, Austria.
 Bernd Neubauer, RHI AG, Technology Center, Leoben, Austria.
 Roland Pungerssek, RHI AG, Steel Division, Vienna, Austria.

Corresponding author: Roland Pungerssek, roland.pungerssek@rhi-ag.com

Thomas Kollmann, Philip Bundschuh, Volker Samm, Johannes Schenk and Marcus Kirschen

Gas Purging Benefits in the BOF: A Focus on Material Efficiency and CO₂ Emission Reduction

In highly competitive steel markets worldwide, an economical and climate-friendly steelmaking process is required to ensure profitable crude steel production in the future. Considering the tightening global CO₂ emission requirements, which result in rising energy prices and the purchase of carbon credits, raw material and energy efficiency have to be continuously optimized. One option to increase resource efficiency in the steelmaking process chain is the use of bottom inert gas purging in the BOF. Gas purging increases mass and energy transfer in the molten metal, the mixing energy, and bath kinetics, promoting improved decarburization and dephosphorization reaction rates. Further essential benefits include higher thermal and chemical homogeneity of the liquid metal bath, better process control, and increased yield from raw materials due to the reduced consumption of various fluxes, alloys, and oxygen.

Introduction

Global annual crude steel production has significantly increased over the last decades, from 200 million tonnes in the 1950s to 1662 million tonnes in 2014 [1]. The annual growth trend of global crude steel production, subdivided into China and the rest of the world, over the last 8 years is shown in Figure 1 [1]. In 2014 the annual crude steel production increased by 1.2% compared to 2013. In 2014, the Middle East, the smallest region for crude steel production, had the most robust growth. Crude steel production in the EU28, North America, and Asia grew modestly in 2014 compared to 2013, while in the Commonwealth of Independent States (CIS) and South America it decreased [1].

The iron and steelmaking industry is one of the most energy-intensive industries, with an annual energy consumption of about 26×10^9 GJ, namely 5% of the world's total energy consumption. The steel industry accounts for 7% of the total global greenhouse gas emissions [2]. Furthermore, 30% of the total CO₂ emissions from industrial processes are caused by the iron and steel industry.

To realize a significant CO₂ emission reduction, the currently implemented iron and steelmaking technologies and raw material concepts have to be optimized from the process point of view.

BOF Steelmaking Route

A range of diverse process routes are used for iron and steelmaking, depending on raw material availability and energy resources. Crude steel production can be divided into two main distinct routes: The integrated blast furnace/BOF process based on iron ore and the EAF route using scrap and/or direct-reduced iron as the main iron source. Steel production at an integrated iron and steel mill is accomplished using several interrelated processes such as coke, lime, sinter, iron, and steel production. The global integrated production route is characterized by energy consumption levels in the range of 15–25 GJ/t_{crude steel} and CO₂ emission levels of 1600–2500 kg_{CO₂}/t_{crude steel}, depending on the calculation method and boundary conditions [2,3]. For the European steel production sector, total average values of 1800 kg_{CO₂}/t_{crude steel} have been obtained. A breakdown of the average CO₂ emissions generated by the integrated

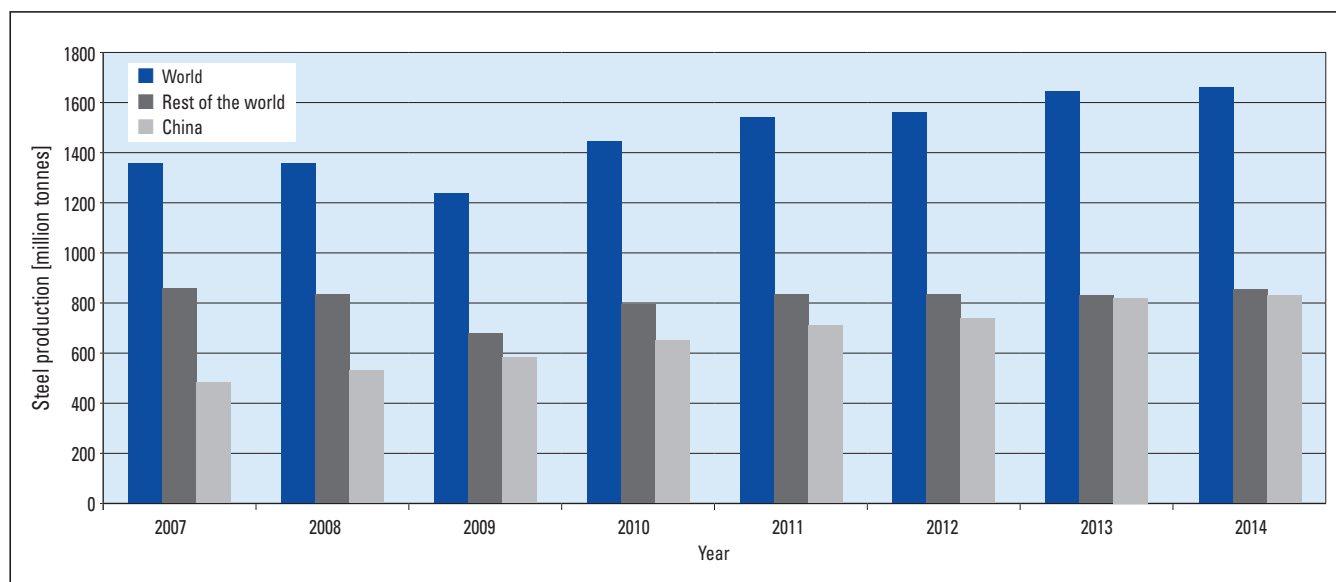


Figure 1. Annual global crude steel production from 2007–2014 [1].

blast furnace/BOF route are detailed in Table I and Figure 2, showing that the CO₂ emissions are primarily caused by the sinter and coking plants, blast furnace, and power plant that supplies the required energy to maintain and guarantee steel production [3–5].

In steelmaking, the main percentage of total energy consumption, namely 80–90%, relates to liquid steel production, while the remaining 10–20% is for casting and shaping applications. Hot metal is produced by reducing iron oxide ores in the blast furnace. Hot blast is injected through tuyeres and oxygen reacts with coke, petroleum coke, or coal, creating a reducing atmosphere (i.e., formation of CO₂ and CO) in which the iron oxides are reduced and melted to hot metal as a result of exothermic reactions. Gas in the top of the blast furnace has an average composition of 22 vol.% CO, 22 vol.% CO₂, 5 vol.% H₂, and 51 vol.% N₂, which corresponds to CO₂ emissions ranging from 380–400 kg/t_{crude steel}. CO₂ emissions also result from calcining carbonate fluxes. Limestone (CaCO₃) and magnesium carbonate (MgCO₃) form lime (CaO), magnesium oxide (MgO), and CO₂ during the burning process in the shaft furnace. The process-related emissions of these calcination process are 785 kg_{CO₂}/t_{lime}, while the energy-related emissions are only 200 kg_{CO₂}/t_{lime}. The CaO and MgO carriers are required to balance the acidic coke and iron ore in the blast furnace.

Application	CO ₂ emissions (kg/t _{crude steel})
Sinter plant	218–250
Coking plant	180–210
Blast furnace	380–400
BOF	70–95
Rolling mill	100–120
Finishing	60–85
Power plant	600–850
Total	1608–2010

Table I. CO₂ emissions for various process steps in the integrated blast furnace/BOF route [6].

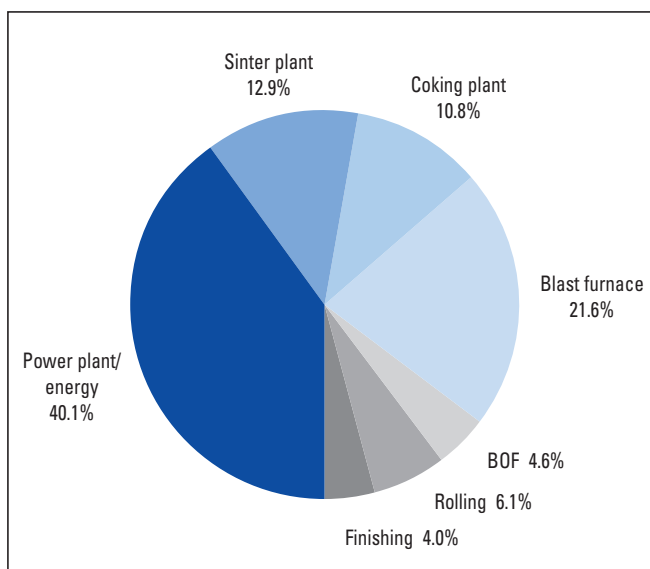


Figure 2. Relative CO₂ emissions per tonne of crude steel produced using the blast furnace/BOF route [6].

In the BOF, lime addition is influenced by the [Si] input from the hot metal and the targeted slag basicity, while focusing on the [P] level at the end of blowing. For efficient dephosphorization, rapid slag formation with a high reaction potential and lime activity has to be realized. To minimize the refractory wear rate during the initial stage of slag formation, it is necessary to charge or provide a MgO carrier in the form of fluxes and avoid <MgO> dissolution from the lining. However, rising (MgO) levels in the slag result in increased viscosity and a lower metallurgical reaction potential during refining, although this does have the advantage that it promotes better slag adherence on the lining when using slag splashing or coating.

The primary aim of the BOF process is oxidation of undesired elements (e.g., [P], [S], [Mn], [C], and [Si]), to achieve the lowest levels in the hot metal, as well as stable, highly reproducible temperatures, and [C] and [O] levels at the end of blowing, with the lowest level of reblowing. The BOF is more efficient for decarburization and dephosphorization than desulphurization. This is due to the oxidizing atmosphere during refining, where pure oxygen is blown through the top-blown lance onto the liquid metal bath. A heating effect is generated by the exothermic reactions that melt the fluxes and scrap. On average, refining requires 15–20 minutes. The BOF off-gas is characterized by an average composition of 60 vol.% CO, 15 vol.% CO₂, and 25 vol.% N₂, leading to CO₂ emissions of between 70–95 kg/t_{crude steel} [6–12].

Benefits of Gas Bottom Purging in the BOF

Gas purging patterns, especially the number, arrangement, and type of plugs, as well as the flow rates and the type, quality, and shifting points of the inert gases have a significant influence on the BOF process and the metallurgical results. These parameters must be strictly coordinated, otherwise the process is difficult to effectively control and targeted metallurgical results cannot be achieved. Bottom gas purging (Figure 3) enables the system to approach equilibrium at the end of blowing. In addition, the bath kinetics and mixing energy are increased, resulting in lower [C] at lower oxygen levels (i.e., without steel bath over-oxidation) at the end of blowing [13,14].



Figure 3. Improved mixing of the steel bath in a BOF due to bottom gas purging.

A typical indicator of efficient bottom purging performance is the product of the dissolved [C] and [O], which compared to a top-blown converter is much lower as well as more stable and controllable depending on the steel grades produced. An efficient bottom purging system is characterized by [C] x [O] levels between 20–25 x 10⁻⁴ and is also reflected in a less turbulent refining, reduced slopping potential, and lower reblow numbers. In addition, higher yields and lower slag volumes are obtained and chemically aggressive and too liquid slag is minimized. Furthermore, the total oxygen consumption is approximately 2% and the tapping temperature is on average 10 °C lower compared to the original LD process without bottom purging. The charged flux amount is reduced by 5–10% due to the improved bath kinetics via bottom purging. The bath kinetics can be verified by calculating the mixing energy. The relationship between the calculated mixing energy, which

is related to the equation of Nakanishi et al., [14], on the distribution of the [C] x [O] levels for a vessel with and without bottom purging at the end of blowing is shown in Figure 4. The nonpurging mode shows a very high deviation of the [C] x [O] levels ranging between 26–45 x 10⁻⁴ while bottom gas purging increases the mixing energy and simultaneously leads to a considerable decrease in the [C] x [O] levels and their fluctuation at the end of blowing. Furthermore, the process is more flexible and the adjustment of targeted [C] x [O] or p_{CO} levels can be better controlled. Figure 5 shows the behaviour of the [C] x [O] levels after bottom purging was commissioned compared to a parallel vessel in operation without bottom purging. As a result the [C] x [O] levels decreased by 8–10 x 10⁻⁴ including an average reduction of the [C] levels by 0.015% and a 200 ppm lower [O] content in the liquid steel bath at the end of blowing (Figure 6) [13,14].

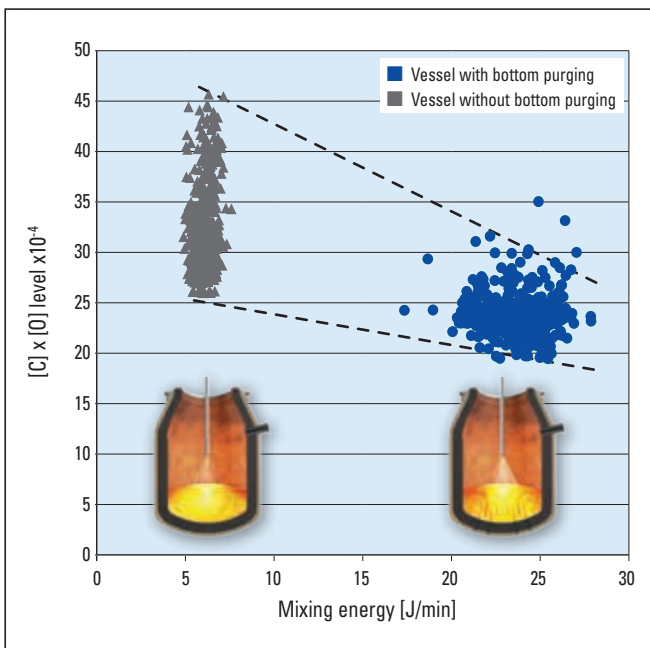


Figure 4. The relationship between [C] x [O] levels and the mixing energy with and without bottom gas purging [13].

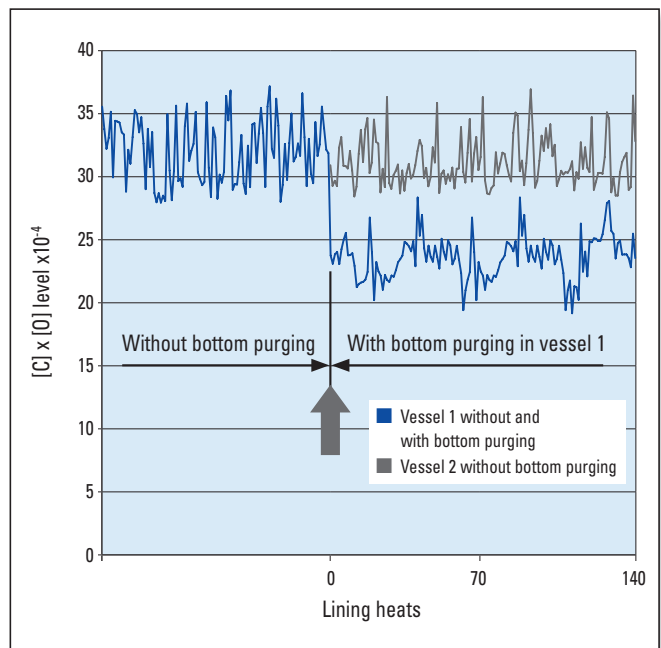


Figure 5. [C] x [O] levels with and without bottom purging [13].

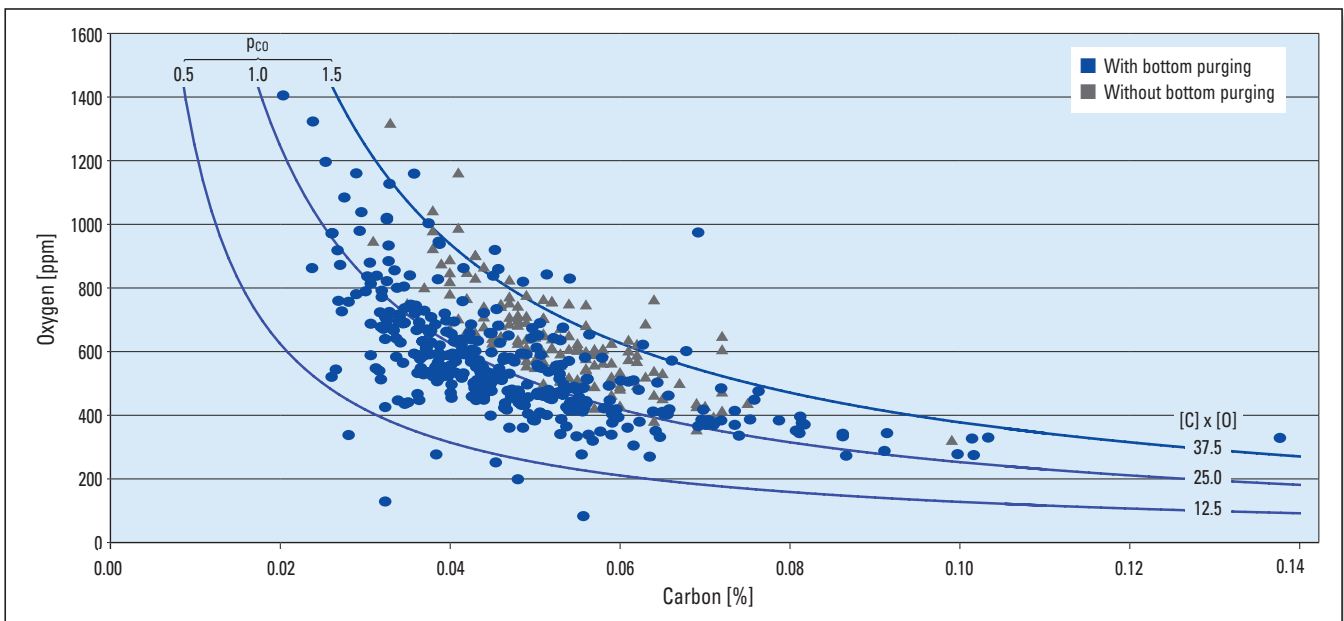


Figure 6. Comparison of [C] and [O] levels at the end of blowing with and without gas purging [13].

Calculation of CO₂ Emissions Generated by the BOF Process

The various types of greenhouse gas emissions associated with industrial processes can be clustered into three main scopes (Figure 7). In terms of the BOF, the first scope includes emissions that are produced directly during the blowing process, the second covers the purchased electricity, and the third comprises emissions that are related to the production and consumption of flux agents and raw materials as well as transport. In the following study only CO₂ emissions from the BOF were considered for the calculations. The calculations were based on data obtained from a plant where two converters are operating: One equipped with bottom gas purging and the other without purging. The calculations included the charged materials, namely hot metal, scrap, Hi-Cal lime, dolomite, dolostone, briquetted dust, FeSi75, and coke. The calculations were performed using a dynamic converter model developed by the Chair of Ferrous Metallurgy at the Montanuniversität Leoben (Austria). The calculations were performed for three different [C] levels at the end of blowing (i.e., 350, 500, and 800 ppm). Based on each of these outcomes, the necessary amount of oxygen (Nm³) was used to calculate the kg of CO₂ per tonne of crude steel produced by the electric power generation for the oxygen production. The purchased electricity was based on an assumed value (10 kWh/t_{crude steel}) that was multiplied by the CO₂ emission factor (0.279 kgCO₂/kWh) [15]. This factor is a country-specific value for electric supply in Austria. The third emission scope was calculated with certain

assumptions for the kg CO₂ emissions per tonne of produced material (e.g., pellets and coke). Values for the emissions generated due to lime and dolomite production were based on the work of Ecofys Netherlands and the Fraunhofer Institute [16]. The amount of CO₂ emitted in relation to the FeSi was taken from the BAT reference document for the nonferrous metals industries [17]. A wide range of values for CO₂ emissions derived from secondary aluminium production were reported in a study by the Austrian Umweltbundesamt [18] and a value of 1500 kgCO₂/t_{aluminium} was used for the calculations.

Focusing on the three different emission scopes, the largest CO₂ share is due to indirect emissions. For these cases bottom purging is essential to ensure and guarantee an optimized BOF process that decreases flux addition, oxygen and energy consumption, and operates with higher yield, lower slag volumes, and lower reblow numbers. Slag maintenance, such as slag splashing, reduces the vessel availability and also the reaction volume, causing problems regarding yield, decarburization, and dephosphorization. It has to be considered that for an efficient slag splashing operation, a (MgO) saturated slag is commonly targeted, otherwise the splashed slag does not adhere properly to the lining. This results in higher (MgO) carrier consumption, rising slag viscosity, and limited metallurgical slag activity and is why an optimized maintenance strategy has to be adapted to the regional BOF production philosophy to meet the expected vessel lifetime and metallurgical requirements from an economic and environmental point of view [13,14,20,21].

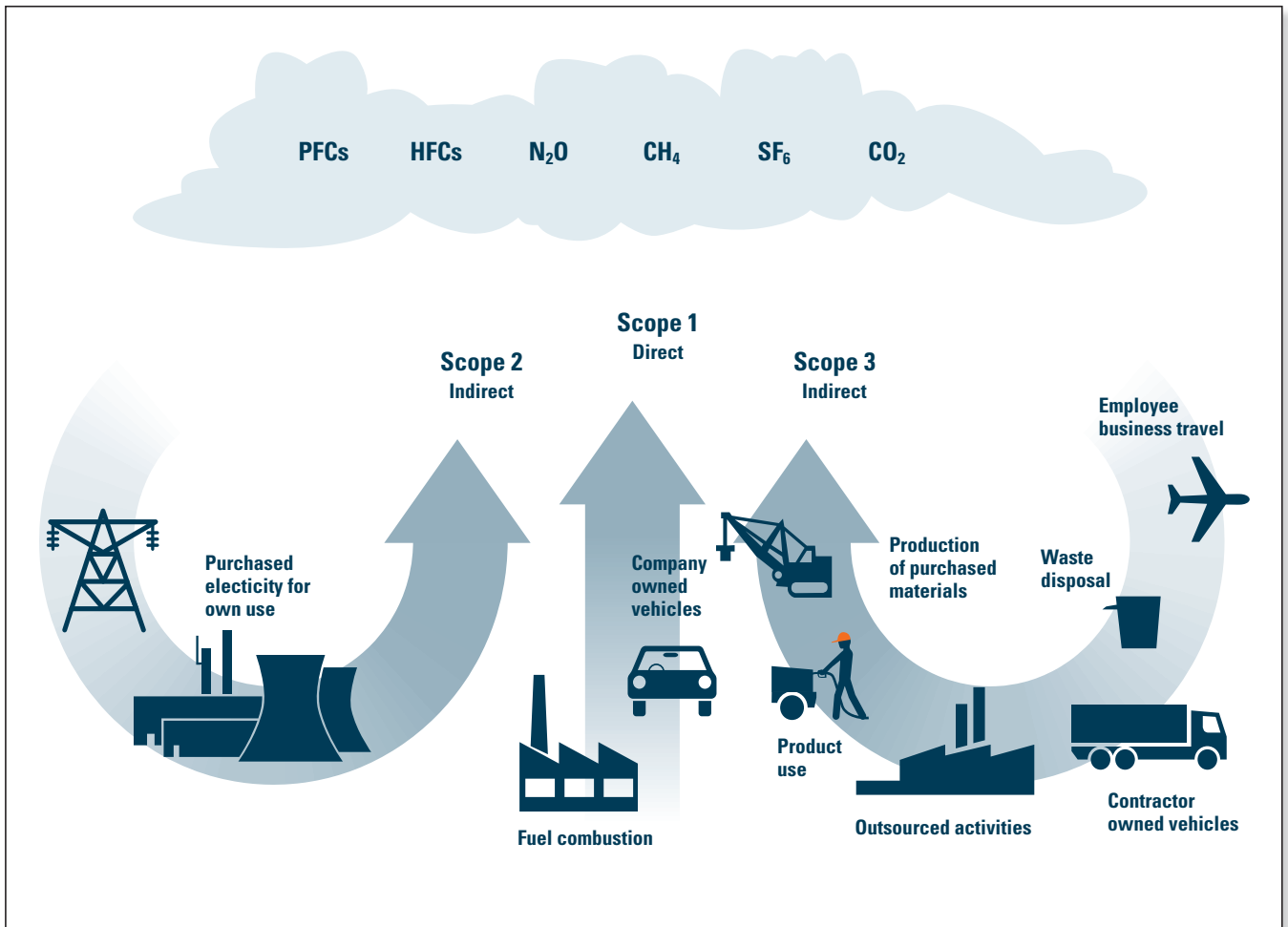


Figure 7. Greenhouse gas emissions associated with industrial processes [19].

The results of the CO₂ calculations for the BOF process with and without bottom purging are shown in Table II.

The CO₂ emissions based on alloying during converter tapping were also calculated (Table III). For this step the amount of dissolved oxygen and carryover slag play a very important role. The results of different simulations enabled a good estimation of the amount of alloying materials that are necessary for a defined ladle furnace slag volume and wire without silicon. Aluminium for deoxidation, Hi-Cal lime, and dolomite were considered for the alloying step during converter tapping. The results of the CO₂ calculations are provided in Table III.

Both sets of calculations show a positive influence of bottom gas purging on the CO₂ emissions from the BOF process. The highest savings were obtained for the case of a [C] level of 350 ppm at the end of blowing, with nearly 16 kgCO₂/t_{crude steel} (including alloying at tapping). In comparison the savings for a [C] level of 800 ppm were about 8 kgCO₂/t_{crude steel}. All the CO₂ emission saving results are summarized in Figure 8.

Conclusion

Increasing concerns over global climate change have made minimizing CO₂ emissions and increasing energy efficiency crucial to ensure future competitiveness and a lower environmental impact. In order to reduce the CO₂ emissions from an integrated steel plant it is necessary to analyse and quantify the optimization potential regarding the process, raw materials, maintenance philosophy, and energy management. With respect to the BOF vessel, implementing bottom inert gas purging correlates with a significant increase in process efficiency in comparison to operating using only a top-blowing oxygen lance. In addition, the process is more stable and controllable, resulting in higher yields and improved metallurgical key parameters with lower flux and oxygen consumption per heat.

The CO₂ saving potential (e.g., direct emissions; emissions from electricity, heat, and steam; and indirect emissions) from gas purging systems in a BOF is in the order of 10 kgCO₂/t_{crude steel} for a typical European steel plant.

[C] at end of blowing (ppm)	Sum CO ₂ emission	With bottom purging (kgCO ₂ /t _{crude steel})	Without bottom purging (kgCO ₂ /t _{crude steel})	Δ (kgCO ₂ /t _{crude steel})
350	Total	12.80	17.74	-4.94
500	Total	9.45	12.68	-3.23
800	Total	6.50	8.52	-2.02

Table III. Total CO₂ emissions based on alloying during converter tapping with and without bottom gas purging for three final carbon contents.

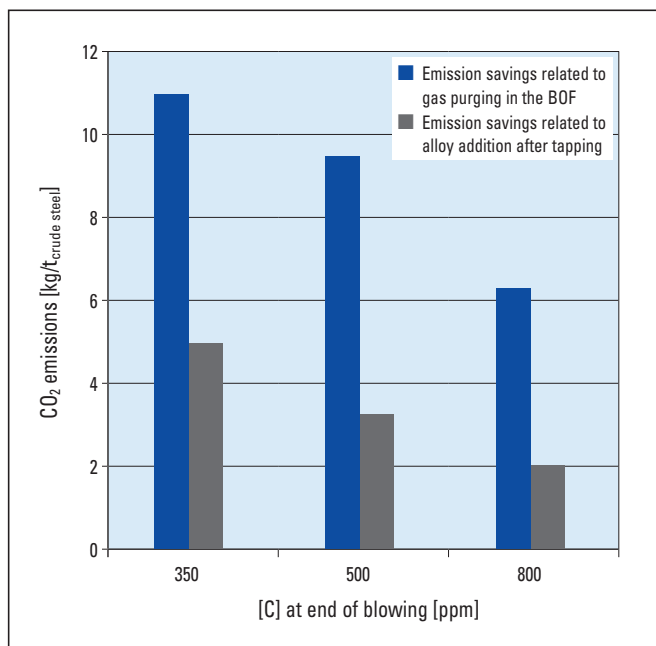


Figure 8. CO₂ emission savings.

[C] at end of blowing (ppm)	CO ₂ emission type	With bottom purging (kgCO ₂ /t _{crude steel})	Without bottom purging (kgCO ₂ /t _{crude steel})	Δ (kgCO ₂ /t _{crude steel})
350	Direct emissions	40.71	41.96	-1.25
500	Direct emissions	39.89	41.12	-1.23
800	Direct emissions	38.49	39.63	-1.14
350	Emissions from electricity, heat, and steam	10.66	10.76	-0.10
500	Emissions from electricity, heat, and steam	10.41	10.49	-0.08
800	Emissions from electricity, heat, and steam	10.07	10.14	-0.07
350	Indirect emissions	1352.04	1361.66	-9.62
500	Indirect emissions	1343.40	1351.54	-8.14
800	Indirect emissions	1327.55	1332.62	-5.07
Combined emission types (total)				
350	Total emissions	1403.42	1414.38	-10.96
500	Total emissions	1393.69	1403.15	-9.46
800	Total emissions	1376.12	1382.39	-6.27

Table II. BOF-specific CO₂ emissions with and without bottom gas purging for three final carbon contents.

In summary it should be emphasized that:

- >> Gas purging systems are an available and proven technological option for steelmaking.
- >> Gas purging systems are considered to be the most cost-effective available technology for increasing energy efficiency in steelmaking.

>> Besides the CO₂ emission reduction potential, further cost savings from gas purging systems include increased process safety and control, decreased electric energy costs, and decreased consumption of flux additives.

References

- [1] <http://www.worldsteel.org/media-centre/press-releases/2015/World-crude-steel-output-increases-by-1.2-in-2014.html>
- [2] Laplace Conseil. Impacts of Energy Market Developments on the Steel Industry. Presented at 74th Session of the OECD Steel Committee, Paris, France, July 1–2, 2013. <http://www.oecd.org/sti/ind/Item%209.%20Laplace%20-%20Steel%20Energy.pdf>
- [3] Gerspacher A., Arens, M. and Eichhammer, W. Zukunftsmarkt Energieeffiziente Stahlherstellung, Fraunhofer Institut für System- und Innovationsforschung, Karlsruhe, 2011. http://www.isi.fraunhofer.de/isi-media/docs/e/de/publikationen/Fallstudie_Eisen-Stahl.pdf
- [4] Scholz, R., Pluschkell, W., Spitzer K.-H. and Steffen, R. Steigerung der Stoff- und Energieeffizienz sowie Minderung von CO₂ Emissionen in der Stahlindustrie. *Chemie Ingenieur Technik*. 2004, 76, 1318.
- [5] "Available and Emerging Technologies for Reducing Greenhouse Gas Emissions From the Iron and Steel Industry". Prepared by U.S. Environmental Protection Agency, Office of Air Quality Planning and Standards, Sector Policies and Programs Division, North Carolina, Sept., 2012.
- [6] Margolis, N. and Brindle, R. Energy and Environmental Profile of the U.S. Iron and Steel Industry, Report for U.S. Department of Energy, Office of Industrial Technologies, Energetics Inc., Columbia, 2000.
- [7] Müller, A., Redl, C., Haas, R., Türk, A., Liebmann, L., Steininger, K., Brezina, T., Mayerthaler, A., Schopf, J., Werner, A., Kreuzer, D., Steiner, A., Mollay, U. and Neugebauer, W. Energy Investment Strategies And Long Term Emission Reduction Needs. EISERN Project Report, Vienna, Nov., 2012. http://www.ivv.tuwien.ac.at/fileadmin/mediapool-verkehrsplanung/News/EISERN/m%C3%BCller-2012_EISERN-Endbericht.pdf
- [8] Kirschen, M., Badr, K., Cappel, J. and Drescher A. Intelligent Refractory Systems: A Cost Effective Method to Reduce Energy Consumption and CO₂ Emissions in Steelmaking. *RHI Bulletin*. 2010, No. 2, 43–48.
- [9] Mathiesen, L. and Maestad, O. Climate Policy and the Steel Industry. Achieving Global Emission Reductions by an Incomplete Climate Agreement. *Energy Journal*. 2004, 25, 91–114.
- [10] Hasanbeigi, A., Price, L., Aden N., Chunxia, Z., Xiuping, L. and Fangqin, S. A. Comparison of Iron and Steel Production Energy Use and Energy Intensity in China and the U.S. Ernest Orlando Lawrence Berkeley National Laboratory, Berkley, June, 2011. <http://china.lbl.gov/sites/all/files/lbl-4836e-us-china-steeljune-2011.pdf>
- [11] Larsson, M. and Dahl, J. Reduction of the Specific Energy Use in an Integrated Steel Plant – The Effect of an Optimization Model. *ISIJ International*. 2003, 43, No. 10, 1664–1673.
- [12] Neelis, M. and Patel, M. Long-Term Production, Energy Consumption and CO₂ Emission Scenarios for the Worldwide Iron and Steel Industry. Copernicus Institute, Utrecht University, Utrecht, Nov., 2006.
- [13] Kollmann, T. *Influence of Bottom Purging on the Metallurgical Results*, Master's Thesis, Montanuniversität Leoben, Austria, 2010.
- [14] Nakanishi, K., Nozaki, T., Kato, Y. and Suzuki, K. Physical and Metallurgical Characteristics of Combined Blowing Processes. *65th Steelmaking Conference Proceedings*, Pittsburgh, USA, March 28–31, 1982; pp. 101–108.
- [15] Wenzel, P., Wenzel, B. and Wagner, H.-J. Länderspezifische Strombereitstellungsfaktoren- und CO₂-Emissionsfaktoren. *Energiewirtschaftliche Tagesfragen*. 1999, 49, 432–437.
- [16] Neelis, M., Worrell, E., Mueller, N., Angelini, T., Cremer, C., Schleich, J. and Eichhammer, W. Developing Benchmarking Criteria for CO₂ Emissions. Ecofys Netherlands and Fraunhofer Institute for Systems and Innovation Research, Feb., 2009. http://ec.europa.eu/clima/policies/ets/cap/allocation/docs/benchm_co2emiss_en.pdf
- [17] Best Available Techniques (BAT) Reference Document for the Non-Ferrous Metals Industries. Joint research Centre: Institute for Prospective Technological Studies, Sustainable Production and Consumption Unit, and European IPPC Bureau. GC/EIPPCB/NFM_Final Draft, Oct., 2014. http://eippcb.jrc.ec.europa.eu/reference/BREF/NFM_Final_Draft_10_2014.pdf
- [18] Frischenschlager, H., Karigl, B., Lampert, C., Pölz, W., Schindler, I., Tesar, M., Wiesenberger, H. and Winter, B. Klimarelevanz ausgewählter Recycling-Prozesse in Österreich. Umweltbundesamt, REP-0303, Vienna, 2010. <http://www.umweltbundesamt.at/fileadmin/site/publikationen/REP0303.pdf>
- [19] Daviet, F. Designing a Customized Greenhouse Gas Calculation Tool. World Resources Institute, Washington, June 2006. <http://pdf.wri.org/GHGProtocol-Tools.pdf>
- [20] Choudhary, S. and Ajmani, S. Evaluation of Bottom Stirring System in BOF Steelmaking Vessel Using Cold Model Study and Thermodynamic Analysis. *ISIJ International*. 2006, 46, 1171–1176.
- [21] Messina, C. Slag Splashing in the BOF - Worldwide Status, Practise and Results. *Iron and Steel Engineer*. 1996, 73, 17–19.

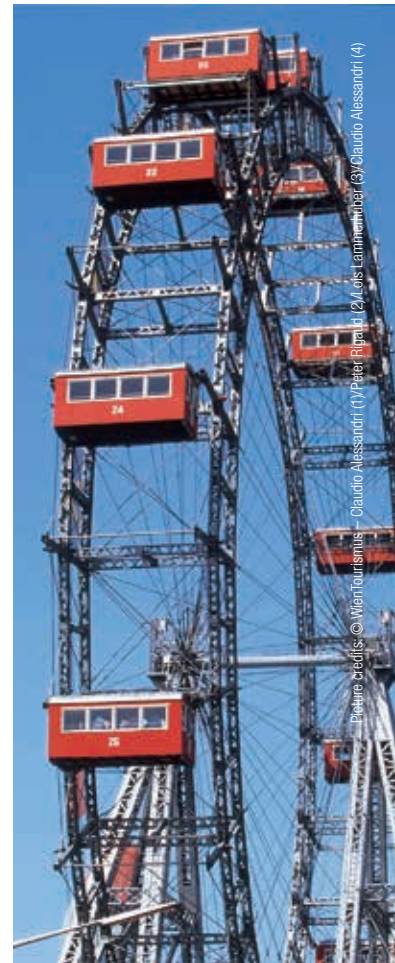
Originally presented at AISTech 2015 and published in the AISTech 2015 Conference Proceedings. Reprinted with permission from the Association for Iron and Steel Technology (AIST).

Authors

Thomas Kollmann, RHI AG, Steel Division, Vienna, Austria.
 Philip Bundschuh, Chair of Ferrous Metallurgy, Montanuniversität Leoben, Austria.
 Volker Samm, RHI AG, Steel Division, Vienna, Austria.
 Johannes Schenk, Chair of Ferrous Metallurgy, Montanuniversität Leoben, Austria.
 Marcus Kirschen, RHI AG, Steel Division, Vienna, Austria.

Corresponding author: Thomas Kollmann, thomas.kollmann@rhi-ag.com

PARTNERSHIP IN MATERIALS AND TECHNOLOGY



14th Biennial Worldwide Congress

UNITECR 2015

Unified International Technical
Conference on Refractories

VIENNA · AUSTRIA
SEPTEMBER 15–18

www.unitecr2015.org

**REGISTRATION
NOW OPEN**

Topics

- Industrial Refractory Applications
- Raw Materials and Recycling
- Advances in Manufacturing, Control and Installation
- Tests, Testing Equipment and Standardization
- Innovation in Materials and Technology
- Basic Science in Refractories
- Refractory Engineering – Design, Modeling and Simulation
- Environment and Sustainability
- Education
- Economic and Political Challenges



Thomas Drnek

Is the Current European Emissions Trading System a Suitable Means for Achieving Climate Protection Goals?

Introduction

In the last years, the threat posed by greenhouse gases and global warming has drawn tremendous media attention. However, climate change is only one of a series of global crises that have been covered extensively by the media in recent decades. Others include forest dieback in Europe, the ozone hole, HIV/AIDS, avian flu, SARS, and most recently Ebola [1–6]. In the case of all these latter examples the outcomes have been positive; they have either been resolved or effectively managed. This is an aspect not emphasized nearly enough in the media's coverage because negative headlines sell better than positive ones. However, the fact that these crises were overcome is certainly due in no small part to media involvement, as many of the measures that were taken may not have been implemented or not until much later if it hadn't been for the coverage and opinions reported by the media. It is also important once measures have been introduced to continue monitoring and reporting on both their positive and negative impacts, thereby maximizing the chance of a successful outcome.

To develop future legislation regarding global climate change it is essential to examine what has been achieved to date as well as aspects that require reform. This paper focuses on greenhouse gas emissions, initially presenting facts regarding climate change and CO₂ levels, as well as the global distribution of greenhouse gas emissions. It also describes the energy and emission targets adopted by the European Union (EU) and the emissions trading scheme that was introduced to decrease emission levels. Certain negative aspects of the trading scheme have come to light since its implementation, such as the drop in CO₂ certificate price as well as the potential impact on value creation and employment figures. Using the knowledge that has been gained in the last years, suitable reforms to the legislation need to be considered and these are discussed in this article.

Facts Regarding Climate Change and Greenhouse Gases

A rise in the concentration of carbon dioxide in the Earth's atmosphere has been observed for quite some time. The atmospheric CO₂ measured at Mauna Loa Observatory in Hawaii has increased from roughly 320 ppm in 1958 to approximately 400 ppm in 2014 (Figure 1) [7]. One noticeable aspect of this trend is the annual fluctuation in the CO₂ levels, which is demonstrated by a very regular, jagged curve. These fluctuations are seasonal, as plant dormancy takes hold during winter in the Northern Hemisphere, which means that plants convert much less CO₂ into oxygen through photosynthesis than during the summer, causing levels to rise. These levels fall again in the summer when plants come out of dormancy. Over the same period, namely just over 50 years, the average temperature has increased by approximately 0.5 °C, as shown in Figure 1.

Greenhouse Gas Emissions

Globally, CO₂ makes up the largest proportion of greenhouse gases. There are other greenhouse gases, for example methane, which are measured in CO₂ equivalents. An overview of greenhouse gas emissions worldwide from 1990–2012 is shown in Figure 2, including levels only resulting from CO₂ emissions. In addition, the total world CO₂ emissions subdivided into China and the rest of the world from 1990–2012 are depicted in Figure 3. In 2012, global CO₂ emissions totalled approximately 32.5 billion tonnes, with China accounting for 26%, the USA 16.6%, and the EU 11%. By comparison, Europe's share was 20% in 1990. The EU's greenhouse gas emissions in CO₂ equivalents fell from 5748 million tonnes in 1990 to 4488 million tonnes in 2012, which represents a 22% decrease (see Figure 2). For the sake of comparison, the EU's climate target for 2020 is a reduction of 20%, which corresponds to 4598 million tonnes of CO₂. This means that the climate target was already met in 2012 if it is assumed that emissions will not increase further [8].

The "Climate Change 2014: Synthesis Report" published by the International Panel on Climate Change (IPCC) lists total greenhouse gas emissions at 49.5 +/- 4.5 billion tonnes [9]. Therefore, it can be assumed that another 17 billion tonnes of CO₂ equivalents are emitted in the form of other greenhouse gases each year in addition to the 32.5 billion tonnes of CO₂. It must be noted that the energy intensity of European industry declined by nearly 19% between 2001 and 2011, which has contributed significantly to fulfilling European climate targets [10]. From a global perspective, Europe's share of global emissions is low, and the impact of the EU's CO₂ reduction measures is negligible.

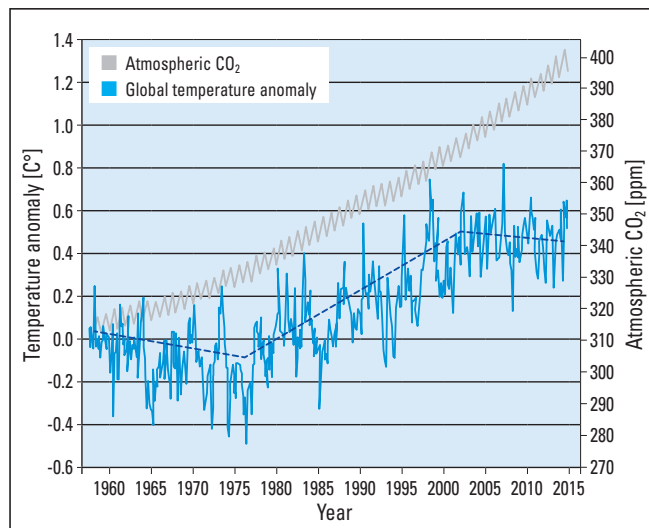


Figure 1. Atmospheric CO₂ levels at the Mauna Loa Observatory (Hawaii) and global temperature change from 1958–2014 [7].

The United Nations (UN) has been trying to negotiate a global climate treaty for many years, but these efforts have repeatedly failed due to differing viewpoints of the member states. The most recent UN climate conferences have been held in the following locations:

- >> 2014: New York City, USA, and Lima, Peru.
- >> 2013: Warsaw, Poland.
- >> 2012: Doha, Qatar.
- >> 2011: Durban, South Africa.
- >> 2010: Cancun, Mexico.
- >> 2009: Copenhagen, Denmark.

All the conferences listed above failed because it seems to be impossible to reach a global consensus regarding

climate protection. This is due to the fact that the viewpoints about this topic and the significance of energy use differ considerably among the various economic regions (e.g., EU, USA, China, India, and the CIS). The next UN climate conference will be held in 2015 in Paris, and the long-awaited breakthrough is expected to come here. The fact that the international community cannot agree to a mutual treaty is a dilemma.

If actual emissions are compared with the forecasts for the last several decades, it becomes evident that the forecasts have been relatively accurate. For example, the US Department of Energy projected global CO₂ emissions of approximately 32 billion tonnes in 2012 based on 2007 levels (Figure 4) [11].

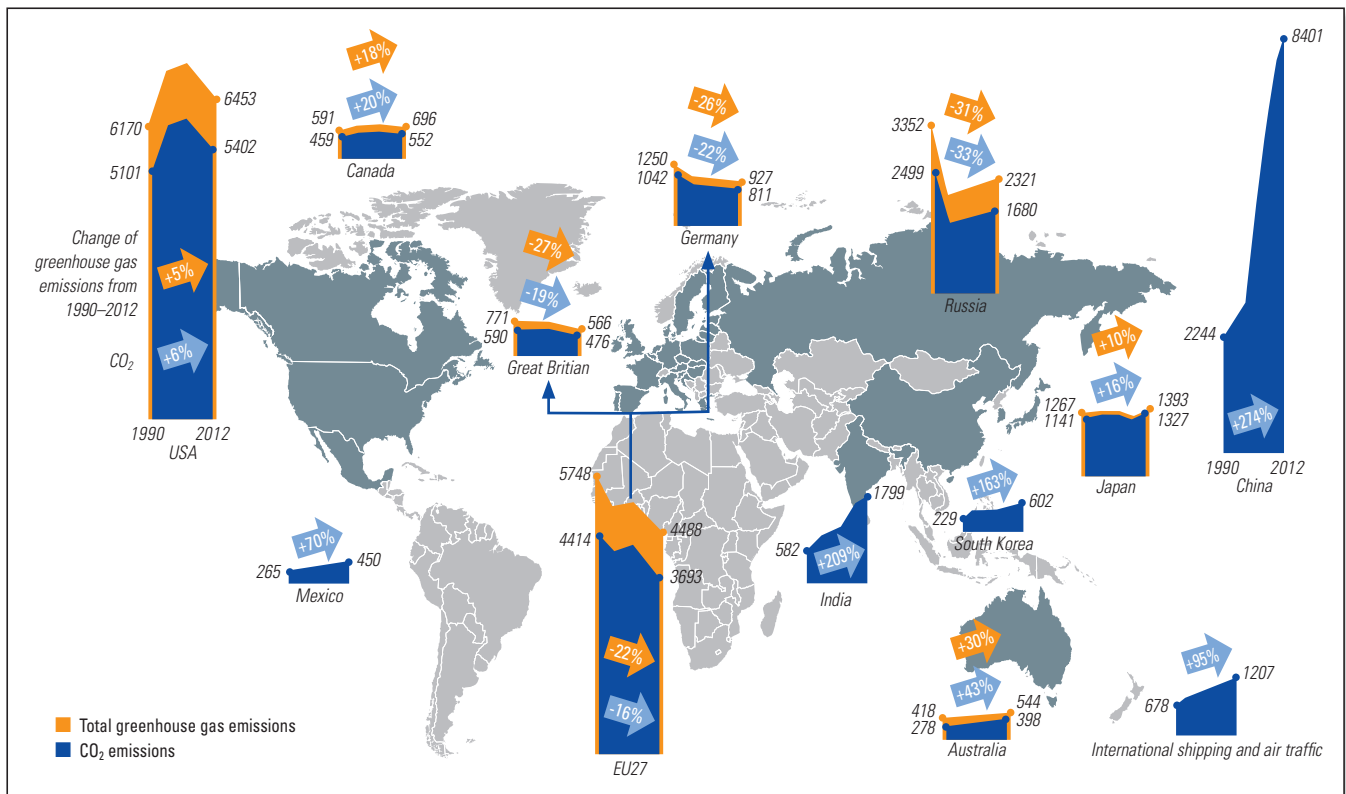


Figure 2. Greenhouse gas emissions in different countries from 1990–2012. The annual values are millions of tonnes of CO₂ equivalents [8].

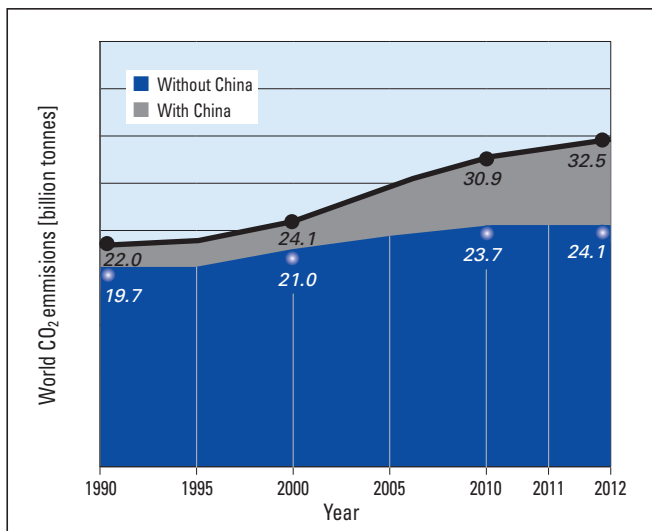


Figure 3. Global CO₂ emissions from 1990–2012, subdivided into China and the rest of the world. The annual values are billions of tonnes of CO₂ [8].

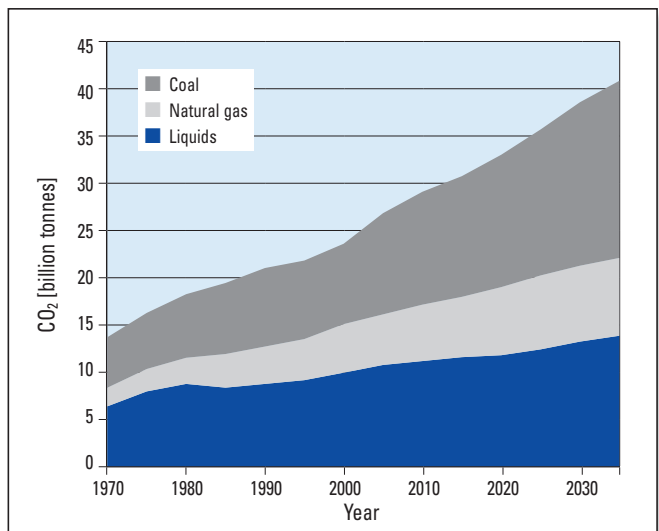


Figure 4. Global CO₂ emissions by energy source, with projected values from 2007 [11].

The Situation in the European Union and Austria

The EU has adopted the following climate and energy goals, termed the 20-20-20 targets, which are to be met by 2020:

- >> A 20% reduction in EU greenhouse gas emissions compared to 1990 levels.
- >> An increase in the share of renewable resources for primary energy generation in the EU to 20%.
- >> A 20% increase in energy efficiency (although it is unclear how this is to be measured).

The target of reducing greenhouse gases by 20% has already been achieved if it is assumed that emissions will not increase again. The question of what has caused this reduction is difficult to answer. It is most likely a result of an increase in energy efficiency and the generally weak economy in the EU. However, the impact of renewable energy—particularly in Germany—must also be taken into account [12].

The situation in Austria has remained relatively unchanged over the years. Greenhouse gas emissions are approximately 80 million tonnes a year (Figure 5). Starting at approximately 80 million tonnes in 1995, emissions rose to just over 90 million tonnes up to 2005 and have subsequently shown a downward trend, reaching 80.1 million tonnes in 2012. This means that emissions are now at roughly the same level as they were in 1995. One noteworthy aspect is the fact that emissions have fallen by approximately 5 million tonnes of CO₂ equivalents to 28.4 million tonnes in the sectors subject to emissions trading over the past 10 years or so. Nevertheless, Austria's Kyoto target of 68.8 million tonnes is still a long way off (see Figure 5) [13].

Emissions Trading in the European Union

The EU was the first major economic region in the world to introduce a greenhouse gas emissions trading system. The current emissions trading period runs from 2013–2020 and will then be extended until 2027. In essence, the emissions trading system applies to industrial installations, which must have the appropriate number of CO₂ certificates to cover their CO₂ emissions. The following principles for the allocation and purchase of these certificates are the cornerstones for emissions trading in the period from 2013–2020:

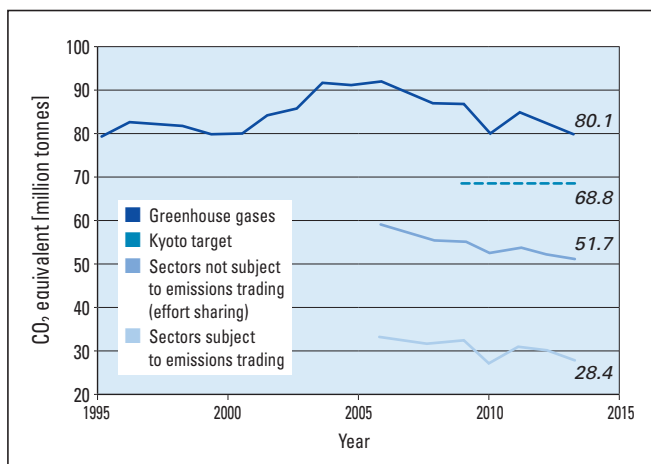


Figure 5. Greenhouse gas emissions in Austria from 1995–2012 [13].

- >> Auctioning and trading of allowances by the power sector (group I).
- >> Transitional rules for the manufacturing industry: Free allocation of 80% in 2013, which will decrease to 30% in 2020 and then to 0% in 2027 (group II).
- >> Free allocation of up to 100% for sectors that fall under carbon leakage, namely sectors that would move out of Europe if they were fully subject to emissions trading (group III). These sectors are identified according to Nomenclature of Economic Activities (NACE) codes [14].

The group III sectors that fall under carbon leakage are further subdivided based on the following criteria [15]:

- >> The sum of direct and indirect costs resulting from implementing the emissions trading system would lead to at least a 5% increase in production costs, calculated as a proportion of the gross value added.
- >> The trade intensity of the sector with countries outside the EU is above 10%. Namely:

$$(M + X)/(P + M) \tag{1}$$

Where *M* is imports, *X* is exports, and *P* is the production in the EU.

- >> The sum of direct and indirect additional costs is at least 30%.
- >> The non-EU trade intensity is above 30%.

Figure 6, which depicts Europe's industrial sectors defined by NACE, provides an overview of the carbon leakage sectors in European industry [16]. The industries above the blue line are all group III sectors, according to the European Commission carbon leakage criteria. It is evident that approximately half the industrial sectors fall into the area of carbon leakage, which means that there is certainly a risk of a general relocation of industry due to emissions trading. Furthermore, the defined 30% cost increase boundary is too high because what company would be able to withstand such a substantial cost increase? It must also be noted that the allocations within the carbon leakage sectors have not reached 100% (with regard to the CO₂ emissions of the relevant companies), but have remained significantly lower in many cases. In addition, the annual allocations are not constant, but are lowered each year by a reduction factor of 1.8%.

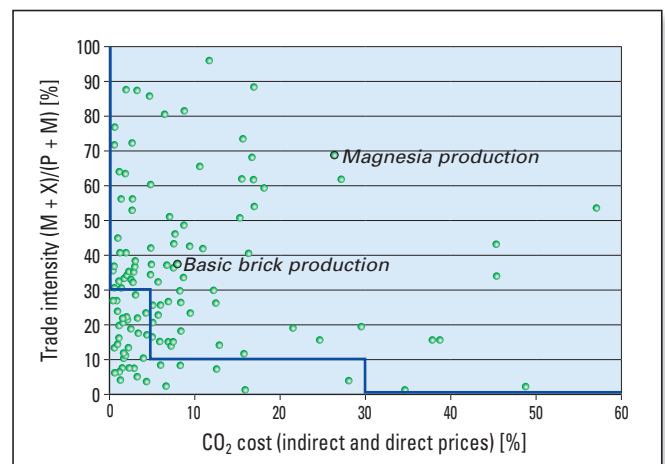


Figure 6. EU industrial sectors and their relative position with regard to the defined area of carbon leakage (above the blue line) [16]. Abbreviations include imports (*M*), exports (*X*), and production in the EU (*P*).

The EU introduced a system for trading CO₂ certificates (i.e., European Union Allowances (EUAs) and Certified Emission Reductions (CERs), which functions according to the following principles: One certificate represents an allowance for the emission of 1 tonne of CO₂, and only a fixed quantity of certificates are issued. This ensures that CO₂ emissions are limited so that the emissions target can be reached. If CO₂ emissions are low enough—as is currently the case—then a relatively low number of CO₂ certificates are required and the price of the certificates fall. However, if more CO₂ certificates were needed than are available, the supply would become scarce and the price would rise accordingly.

The development of certificate prices is shown in Figure 7 [17]. It is clear to see that certificate prices have fallen dramatically since 2011. The price for EUAs has decreased from just under €20 to €5, while CERs have gone from approximately €14 to less than €1 [17]. The reason for the decrease in prices relates to the power utilities: These companies dominate the market and due to economic conditions in Europe and the rapid expansion of renewable energy sources, they currently need fewer certificates than was originally expected.

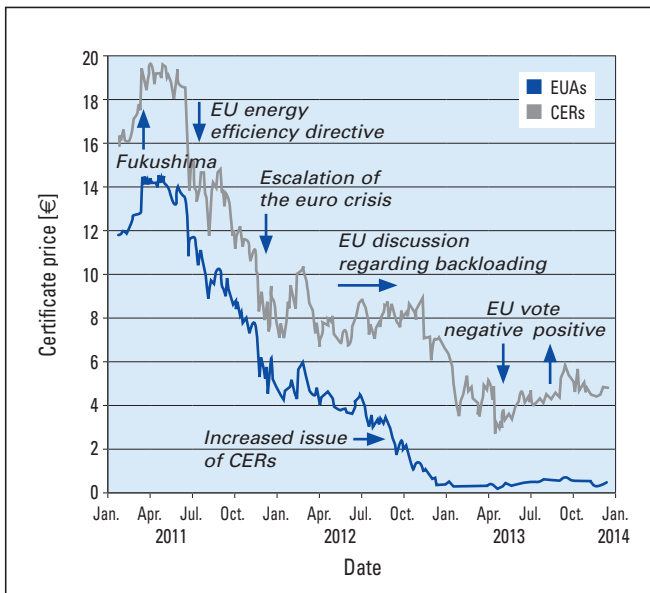


Figure 7. Development of EUA and CER prices from 2011–2014 [17].

According to the initial targets and plans, the certificate price should range from €20–€30. In order to counteract the drop in prices, the EU adopted so-called backloading legislation, in which 900 million tonnes of emissions allowances were removed from trading, with their sale being postponed until a later date [18]. The corresponding certificates will be rereleased to the market towards the end of the current trading period (i.e., 2019–2020). However, this measure has had no effect on certificate prices.

The argument in favour of €20–€30 per certificate lies in the notion that such a price would encourage emitters to invest in alternatives. However, the power utilities say that the price of emissions allowances would have to be between €80–€100 per tonne in order to get emitters to invest in other energy sources. The question raised by this situation is: What would happen if certificate prices were this high in the EU? There would be a mass exodus of industry away from Europe and households would face significantly higher energy costs. It is quite clear what this would mean for employment and prosperity in Europe.

In order to analyse the decline in prices more closely, the emissions allowance market must be examined in detail. If the number of installations are compared with their actual emissions, it becomes evident that just over 10% of installations are responsible for approximately 85% of CO₂ emissions (Figure 8) [19]. If the industrial sectors are analysed based on their emissions, it is clear that the majority of CO₂ emissions in Europe are related to energy and heat generation (Figure 9) [19,20].

The analysis by sector shows that energy and heat producers cause approximately 73% of CO₂ emissions [19]. This is followed by the cement and lime industries with a share of 8% and then the iron/steel industries and refineries, which each have a 7% share. The other sectors combined, excluding air transport, account for only approximately 2% of emissions. This 2% share of emissions represents a wide range of industrial sectors, all of which can be defined as energy-intensive industries. Generally, however, this segment consists of a myriad of small and medium-sized industrial companies. The cost structure of a typical energy-intensive company is shown

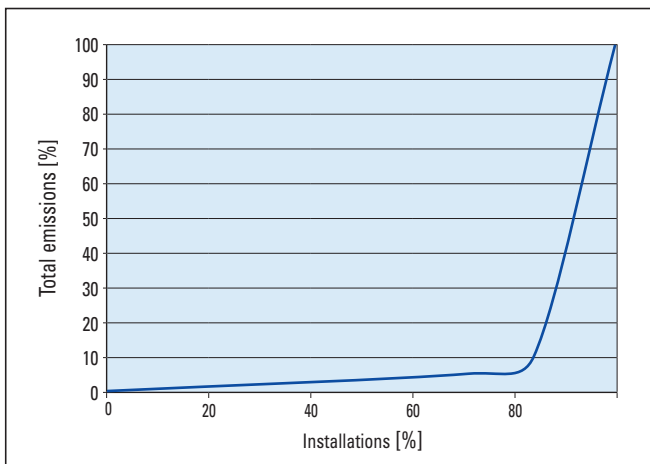


Figure 8. Relationship between the total CO₂ emissions and number of installations [19].

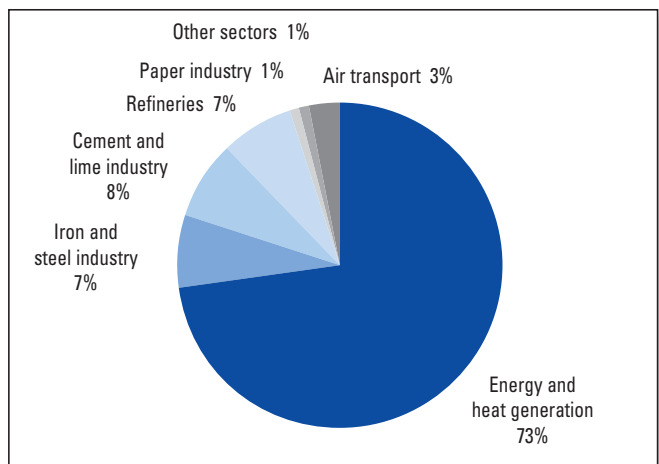


Figure 9. CO₂ emissions according to sector from 2008–2012 [19].

in Figure 10. It is clear where the economic focus will be for the company depicted in Figure 10, namely energy consumption and energy costs. It can also be assumed that the potential savings in terms of specific energy use will be very low. Essentially, a company such as this can only reduce its emissions by scaling back production. Therefore, the company's only choice in this case is to transfer production elsewhere, which means that the conditions for carbon leakage are satisfied. This clearly shows that the EU's carbon leakage policy makes a great deal of sense.

With regard to the risk of carbon leakage, it is important to consider not only the fact that value creation and jobs will be lost in Europe, but also what will happen in terms of CO₂ emissions after a potential relocation. This scenario is clearly illustrated in Figure 11 using the example of magnesite and sintered magnesia [21]. CO₂ emissions are produced when natural, iron-rich magnesite (MgCO₃) is sintered to produce magnesia using direct firing at RHI's Breitenau plant (Austria). Process emissions from the carbonate amount to approximately 1 tonne of CO₂ per tonne of MgO and CO₂ emissions from natural gas combustion are approximately 0.3 tonnes of CO₂ per tonne of MgO. For comparison, the production of sintered magnesia at the RHI's Turkish plant in Eskisehir (MAS) also results in around 1 tonne of CO₂ per tonne of MgO from the carbonate; however, because the firing intensity is higher due to the low-iron content, natural gas combustion emits approximately 0.6 tonnes of CO₂ per tonne of MgO in this process. Magnesia can also be produced synthetically. In this case, the total process and fuel-related CO₂ emissions are higher, at nearly 2 tonnes of CO₂ per tonne of MgO. If these emissions are compared with production in China, the process emissions are the same, because magnesite is also fired in this case. However, coal is used as the fuel, which has much lower energy efficiency than in the cases presented above. As a result, the emissions resulting from firing magnesite in China are around 2.5 tonnes of CO₂ per tonne of MgO. This shows that the transfer of production out of Europe would lead to significantly higher emissions. Therefore, it is important to once again emphasize how necessary appropriate carbon leakage rules are in order to prevent global CO₂ emissions from increasing further as well as preserving value creation and jobs in Europe.

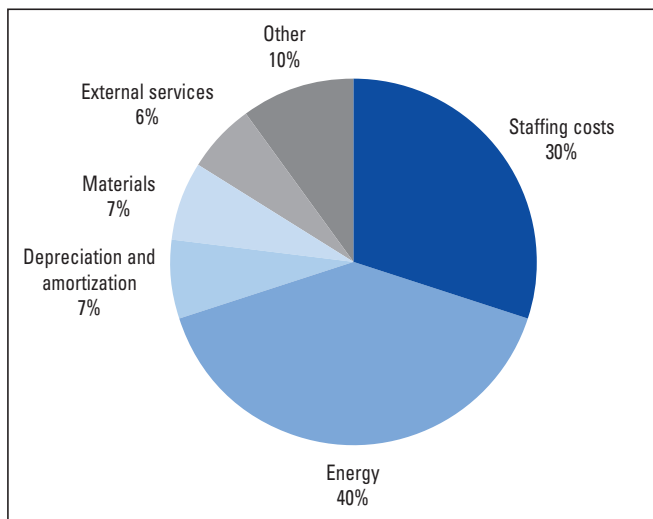


Figure 10. Cost structure of an energy-intensive company.

Suggestions for a Reform of the Emissions Trading System

What options make sense for a reform of the emissions trading system in order to further reduce greenhouse gas emissions while also ensuring that value creation remains in Europe? The system is certainly in need of a major reform and the main areas of reform are listed below:

- >> A radical reduction of the market participants, namely limiting the system to the approximately 10% of installations that cause around 85% of the emissions. This would also curtail the uncontrolled growth in the amount of bureaucracy that applies to CO₂ monitoring. As a result small industrial installations would no longer be included in the system and this would also eliminate the impact on the production of material goods. Instead, the system would be limited to the energy sector.
- >> Additionally, process emissions should be exempt from trading because they are generated all over the world and the purchase of certificates for these emissions only leads to the distortion of competition.

As no one at the EU level is satisfied with the current system and the "reform" introduced through backloading did not have any effect, there are widespread discussions regarding a complete overhaul of the system. It can only be hoped that such a reform is aimed in the right direction.

New European Union Climate Targets

The EU has already adopted new, more far-reaching climate targets, for example the climate and energy figures for 2030 are:

- >> CO₂ (greenhouse gas) reduction 40%
- >> Energy efficiency 27%
- >> Share of renewable energies 27%

It is still unclear how these targets can be achieved. It also remains to be seen how energy efficiency will be measured. In addition, there is the question of how realistic these targets are. As it took three decades to reduce emissions in the EU by approximately 20% (Figure 12), it seems unrealistic to expect the same amount of CO₂ to be eliminated in only a single decade. The decrease over three decades was aimed

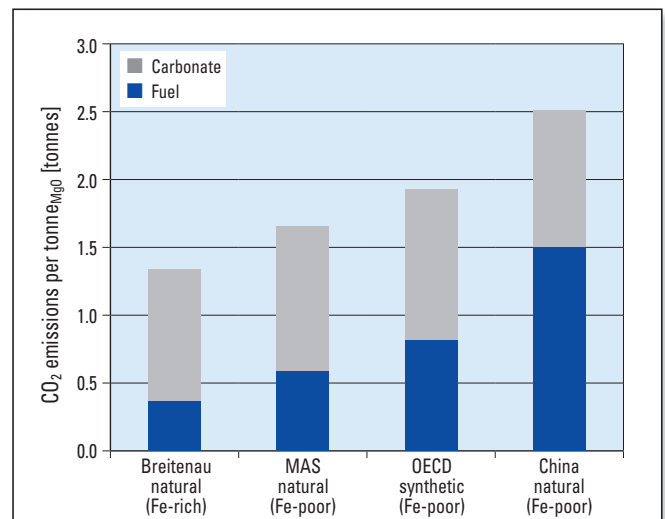


Figure 11. Comparison of CO₂ emission levels resulting from the production of sintered magnesia using different production methods [21].

at achieving a 20% reduction (and this target will presumably be reached; the reduction totalled approximately 40 million tonnes per year). For the next decade, a further reduction of 20% (based on 1990 levels) would mean a reduction of approximately 120 million tonnes per year. As previously stated, it is still unclear how this will be achieved [22]. Often breakthrough technologies are discussed in this context. However, these technologies are not yet on the horizon and it will take longer than a single decade to adopt new technologies on a widespread basis.

Impact of Climate Targets on Austria

Simulation models have been developed to investigate the effects of these new climate targets, but unfortunately these models are not yet available on an EU-wide basis. However, the simulation for Austria has been completed and published indicating a further, significant reduction of emissions (i.e., a 40% reduction as planned by the EU) would have the following results:

- >> Increased costs for companies (additional greenhouse gas prevention measures and the purchase of additional CO₂ certificates).
- >> A reduction in private energy consumption, but an increase in nonenergy consumption as a result of modernization measures for heating systems, building renovations, and new vehicle technologies.

However, the effects are much more far-reaching because “The decline in economic output will also have a negative impact on the labour production factor, resulting in job losses. A lower employment level will lead to lower consumption, and these secondary effects, in turn, will weaken the economy” [23].

The simulation results show that if the free allocation of CO₂ certificates continues, it will lead to a lower cost burden for the companies covered by the EU’s emissions trading system, and higher value creation by these sectors will generate a higher gross domestic product and lower unemployment. This would result in approximately 3000 additional jobs per year and a €400 million increase in value creation. In the event of energy-intensive industry relocating due to

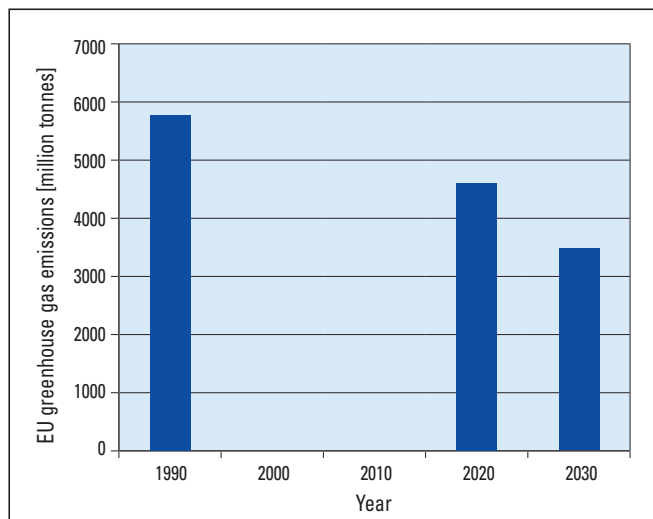


Figure 12. The EU’s CO₂ reduction path: Defined targets [22]. No targets were set for 2000 and 2010.

increases in costs (due to a 40% reduction of greenhouse gases at the EU level), the general negative developments would be drastically intensified. In 2030, the gross domestic product would decrease by approximately €11 billion, while unemployment would increase by around 61600 people [23].

Summary

Based on the undisputed fact that the level of CO₂ in the atmosphere is constantly rising and the assertions put forward in the IPCC’s climate reports that climate change has already started, the question arose as to how this issue should be dealt with. Over a decade ago, the EU began counteracting these changes with the introduction of the emissions trading system. The subsequent developments have raised the question of how energy-intensive industries in Europe are dealing with this system, what impact emissions trading has had, and what direction climate protection will take in the future.

In order to reduce emissions among major industrial companies in Europe, the EU introduced an emissions trading system. Under this system, there are three groups that are treated differently. The first group (power producers) must acquire 100% of their emissions allowances by auctioning and trading, while the second group (all other installations with the exception of group III) received a free allocation of allowances for 80% of their emissions in 2013, which will be reduced to 30% in 2020 and then to 0% by 2027. This means that there will no longer be any difference between groups I and II starting in 2027. The third group consists of emitters that are exposed to a risk of carbon leakage, namely industrial companies that face intense international competition and/or would be impacted by an extreme increase in costs due to emissions trading. The third group receives a free allocation of allowances of up to 100% because it has been recognized that these industries would otherwise relocate, which would result in a significant loss of value creation and jobs.

If the impact of emissions trading is examined, it becomes apparent that the certificate prices are relatively low (in the range of a few euros per tonne) and the market is far removed from the targeted price of €20–€30. The reason for this is that power producers dominate the entire emissions trading system, as 73% of the CO₂ emissions (covered by emissions trading) are caused by the generation of energy and heat.

In addition, analysis has shown that approximately 85% of emissions come from just 10% of installations. This means that relatively small emitters are at a disadvantage because the level of bureaucracy involved is tremendous and their influence on the overall system (with regard to both emissions trading and CO₂ emissions) is minimal to nonexistent. Therefore, it is clear that the emissions trading system must be reformed. The European Commission has already tried to reform the system with backloading legislation, which had no apparent success. A better approach would likely be to only include very large emitters in the system and give small installations more leeway, because the majority of the actual value creation takes place in the so-called energy-intensive industry sectors, which are only responsible for a relatively small share of the emissions. Furthermore, process emissions should be excluded from the system because they are generated globally.

The new targets for 2030 that have been proposed by the EU, including a 40% reduction of greenhouse gases, have not been sufficiently thought out and would lead to a significant loss of value creation and a tremendous number of jobs under the current emissions trading system. A study of Austria shows that unemployment would increase by about

60000 people and value creation would decline by approximately €11 billion. Unfortunately, no figures are available for the EU as a whole at this point. These predicted outcomes also indicate that a reform of the emissions trading system is urgently needed. Aside from this, an international treaty regarding climate protection is imperative.

References

- [1] Die Waldbestände erholen sich in vielen Teilen der Welt. Frankfurter Allgemeine Zeitung, Feb., 25, 2011.
<http://www.faz.net/aktuell/wirtschaft/unternehmen/die-waldbestaende-erholen-sich-in-vielen-teilen-der-welt-1593942.html>
- [2] State of the World's Forests 2011. Food and Agriculture Organization (FAO) of the United Nations, Rome, 2011.
<http://www.fao.org/docrep/013/i2000e/i2000e.pdf>
- [3] Abschied vom Ozonloch. Frankfurter Allgemeine Zeitung, Aug., 13, 2014.
<http://www.faz.net/aktuell/wirtschaft/menschen-wirtschaft/vergangenheit-abschied-vom-ozonloch-13094502.html>
- [4] UNO: Welt kann Aids bis 2030 in den Griff bekommen. Kurier, Nov., 19, 2014.
<http://kurier.at/lebensart/gesundheit/uno-welt-kann-aids-bis-2030-in-den-griff-bekommen/97.974.099>
- [5] Bertisch, B. Kleine Influenza-Historie. Division of Infectious Diseases, Cantonal Hospital St. Gallen, May 26, 2009.
<http://infekt.ch/2009/05/Kleine-Influenza-Historie/>
- [6] Müller warnt nach Ebola-Impfstoff-Test vor zu großen Erwartungen. Frankfurter Allgemeine Zeitung, Nov., 28, 2014.
<http://www.faz.net/agenturmeldungen/unternehmensnachrichten/mueller-warnt-nach-ebola-impfstoff-test-vor-zu-grossen-erwartungen-13291072.html>
- [7] <http://www.climate4you.com/GreenhouseGasses.htm>
- [8] Die Welt-Klimakarawane hält in Warschau. Frankfurter Allgemeine Zeitung, Nov., 9, 2013.
<http://www.genios.de/presse-archiv/artikel/FAZ/20131109/die-welt-klimakarawane-haelt-in-war/fd1201311094084103.html>
- [9] Climate Change 2014: Synthesis Report. Approved Summary for Policymakers on the 1st November 2014. Intergovernmental Panel on Climate Change (IPCC), Copenhagen, Oct., 27–31, 2014. http://www.ipcc.ch/pdf/assessment-report/ar5/syr/SYR_AR5_LONGERREPORT_Final.pdf
- [10] Europäische Kommission schlägt höheres und realistisches Energieeinsparungsziel für 2030 vor. European Commission, Brussels. July 23, 2014.
http://europa.eu/rapid/press-release_IP-14-856_de.htm
- [11] International Energy Outlook 2010. US Department of Energy, Washington. July 2010.
<http://large.stanford.edu/courses/2010/ph240/riley2/docs/EIA-0484-2010.pdf>
- [12] Berliner Klimapolitik macht Emissionshandel witzlos. EU-Energiekommissar Cañete besorgt über Zertifikatpreisverfall/“South Stream hatte für die EU nie Priorität. Frankfurter Allgemeine Zeitung, Dec., 6, 2014.
<http://www.genios.de/presse-archiv/artikel/FAZ/20141206/berliner-klimapolitik-macht-emissio/FR1201412064443033.html>
- [13] Klimawandel, Emissionen. Environment Agency Austria, Vienna. Statistics Austria.
http://www.statistik.at/web_de/statistiken/wie_gehts_oesterreich/umweltorientierte_nachhaltigkeit/17/index.html
- [14] <http://siccode.com/en/pages/what-is-a-nace-code>
- [15] http://ec.europa.eu/clima/policies/ets/cap/leakage/index_en.htm
- [16] www.asser.nl/upload/eel-webroot/.../81121b.xls
- [17] Emissionshandel. Carbon-Scout 2013.
<http://www.carbon-scout.com/cms/wp-content/uploads/2014/10/CO2-Preisentwicklung-und-Handelsinstrumente-Carbon-Scout.pdf>
- [18] Europe Strengthens its Carbon Market for a Competitive Low-Carbon Economy. European Commission, Brussels. Jan., 8, 2014.
http://europa.eu/rapid/press-release_MEMO-14-4_en.htm
- [19] Schleicher, S: Optionen für die Zukunft des EU Emissionshandelssystems. IV-Konsultationsgruppe EU Emissionshandel. Wegener Center for Climate and Global Change, University of Graz, Austria. May 7, 2014.
- [20] Schleicher, S. Steht das EU-Emissionshandelssystem vor seinem Ende? Umweltschutz der Wirtschaft. WKO, Austrian Federal Economic Chamber. 2014, No. S/14, 2014, p. 50–51.
- [21] Drnek, T. and Maier, F. Die Kohlendioxid-Problematik am Beispiel von Magnesit und der RHI-AG. BHM. 2003, 148, Issue 8, 325–333.
- [22] Hartung, M. and Milojevic, G. Outlook for the German Lignite industry 2014. World of Mining – Surface and Underground. 2014, 66, 205–218.
- [23] Schneider, F., Steinmüller, H., Goers, S., Baresch, M. and Priewasser, R. Wirtschaftliche und finanzielle Auswirkungen eines neuen THG-Ziels für 2030 in Österreich und Betroffenheit der österreichischen Volkswirtschaft, Energieinstitut an der Johannes Kepler Universität Linz and Johannes Kepler Universität Linz. Aug., 2014.

Article reprinted by courtesy of Springer-Verlag Vienna.

Author

Thomas Drnek, RHI AG, Raw Materials Division, Breitenau, Austria.

Corresponding author: Thomas Drnek, thomas.drnek@rhi-ag.com

Matthias Höck, Sarah Köhler, Kerry Servos and Bernhard Spieß

IBOS—Improved Bottom Optimized Solution for Enhanced High-Quality Steel Yields

In the steelmaking process, transfer of steel from the ladle to the tundish is an important step that significantly influences steel quality and steel plant profitability. This tapping process must be stopped by the slide gate at an appropriate time to avoid slag carryover into the tundish, while also minimizing the amount of residual steel in the ladle. As a result of modelling studies, RHI recently developed a new ladle bottom concept called Improved Bottom Optimized Solution (IBOS), which enables maximum steel yield and minimum slag entrainment. It can be implemented as a prefabricated solution for both the wear and permanent lining in steel ladles. During an initial customer trial, IBOS was found to outperform competitor products in terms of increased steel yield. In addition, the ladle bottom lifetime exceeded the average number of heats typically achieved at the steel plant.

Introduction

With the increasing demands on steel quality and profitability, every production step must be considered as a source for improvement. In the case of tapping the ladle into the tundish, many new technologies have been developed in recent years to maximize steel yield and minimize slag carryover. To optimize this process, RHI has been investigating the flow of steel and slag in a nearly empty ladle at the end of the tapping process using modelling approaches.

From the metallurgical view point, if ladle slag is transferred to the tundish several negative effects occur. Not only does carryover slag generally decrease the steel cleanliness, but depending on the specific slag type various additional effects can occur. For example, silicon-containing slags in combination with a high CaO containing wear lining also lead to an increased sintering of the tundish wear lining. This can overheat the tundish permanent lining and make descaling much more difficult. Furthermore, alumina-containing slags in the tundish are not only very aggressive but increase the risk of clogging occurring downstream in the casting nozzle. Finally, high-FeO containing slags are linked to a higher oxygen activity in the steel that also directly affects inclusion formation, potentially influencing steel castability from the tundish to the mould.

The composition of the RHI tundish wear lining and cover powder should be tailored to each other in order to prevent steel reoxidation, protect the refractory material, and increase casting performance. However, any carryover slag will contaminate the cover powder, leading to a higher tendency of wear lining infiltration and subsequent higher wear. In addition, not only is there a negative influence on the tundish wear lining, but the stopper and ladle shroud body material is affected. This worsens over time as more heats are cast during a tundish sequence. Therefore, slag detection systems are now state of the art.

On the other hand, if the slide gate is closed too early in the tapping process significant amounts of steel remain in the ladle that have to be removed and returned to the scrap cycle. Depending on the ladle size this can be between 1–5 tonnes per heat. Especially in the case of high-grade

steel production, these yield losses have a considerable financial impact over time. Therefore, steel plants are very interested in different ways to improve tapping. For example, a steel plant with a heat size of 165 tonnes and a production level of 1.8 million tonnes per annum can produce approximately 11000 tonnes more steel if the residual steel is reduced by an average of 1 tonne per heat.

Vortex Formation and Slag Entrainment

In order to optimize the yield, the fluid flow phenomena occurring during the final stages of ladle draining must be understood. Therefore, both computational fluid dynamics (CFD) and water modelling have been used to examine the process [1,2]. Using these approaches it was found that as draining proceeds, three phenomena occur:

- >> Early low-strength intermittent vortices.
- >> Full vortexing resulting in breakup of the slag-steel interface.
- >> Formation of a slag-entraining funnel.

In the past, many approaches have been taken to solve these issues. The eccentric placement of the taphole and inclined bottom construction are regularly used in steel plants, while solutions to stop vortexes, such as bricks extending out of the wall and inert gas purging in the well block have been less successful. Recently, a closer look at the geometry of the ladle bottom was performed resulting in several solutions [3,4] that are now on the market with varying degrees of success.

An innovative approach by RHI has led to significant improvements compared to the current bottom solutions. Not only is the yield improved but also the complexity and costs are decreased and it is compatible with all standard ladle bottom designs (Figure 1). Patent applications covering features of this Improved Bottom Optimized Solution (IBOS) have been filed in several countries around the world [5,6].

Ladle Draining Simulations

CFD provides the opportunity to gain detailed information about the flow behaviour during the draining process in a steel ladle and a multiphase approach can be used.

With the appropriate material properties for steel, slag, and air (Table I), it is possible to simulate steel ladle draining, vortexing, and subsequent surface collapse.

To develop a new ladle bottom that increases steel yield, the flow during ladle tapping was simulated for various ladle bottom geometries. For all cases the ladle had the

Properties	Steel	Slag	Air
Density (kg/m ³)	7000	3500	1.225
Viscosity (kg/ms)	0.005	0.05	1.789 x 10 ⁻⁵

Table I. Material properties of steel, slag, and air.

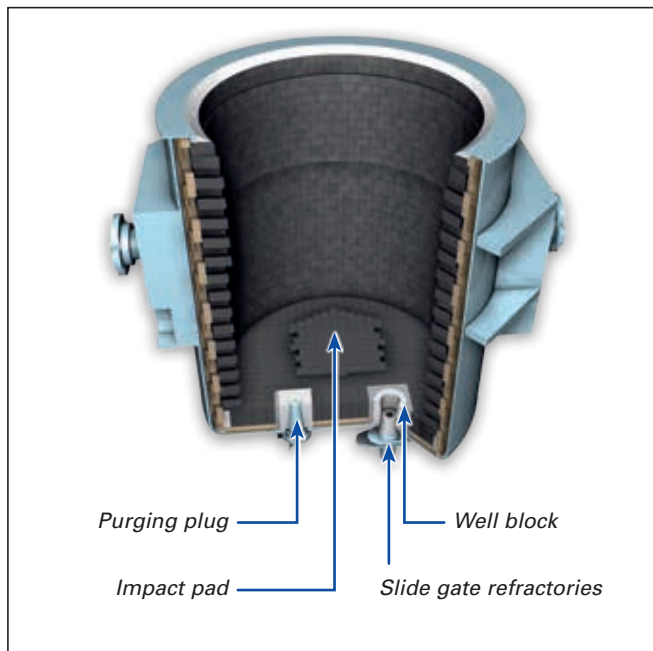


Figure 1. Ladle with an impact pad, well block, slide gate refractories, and purging plug located in the bottom.

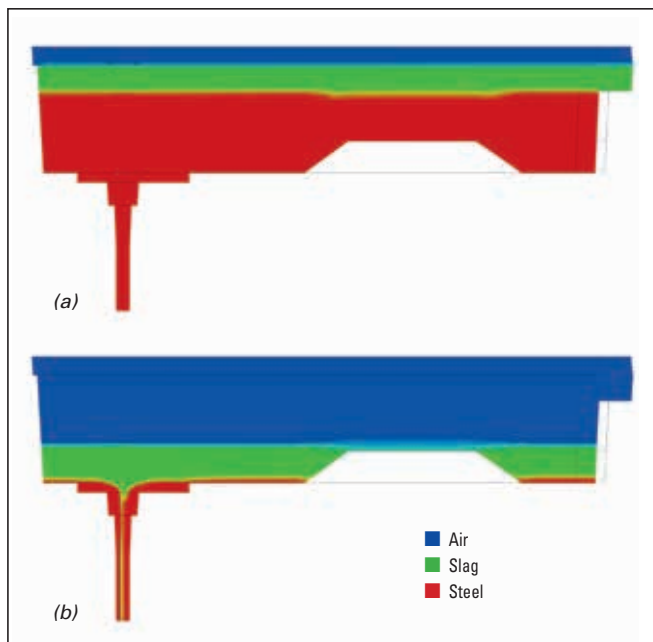


Figure 2. CFD models of the start and end of the tapping process. (a) filled ladle with a 10 cm slag layer and (b) slag entrainment.

same starting bath level and was drained until slag entrainment was observed (Figure 2). Two main influences were examined—the inclination angle of the bottom and the geometry of the recessed area surrounding the well block.

In an earlier investigation, the situation at the start of ladle tapping was simulated to evaluate the forces exerted on the well block filler sand by the steel flow. A recessed area around the well block was found to modify steel flow, which would reduce washing out the well block filler sand and thereby increase the slide gate opening rate. In the current study, to evaluate the influence of a recessed box around the well block area on steel yield as well as the benefit of an inclined bottom, four geometries were compared (Figure 3):

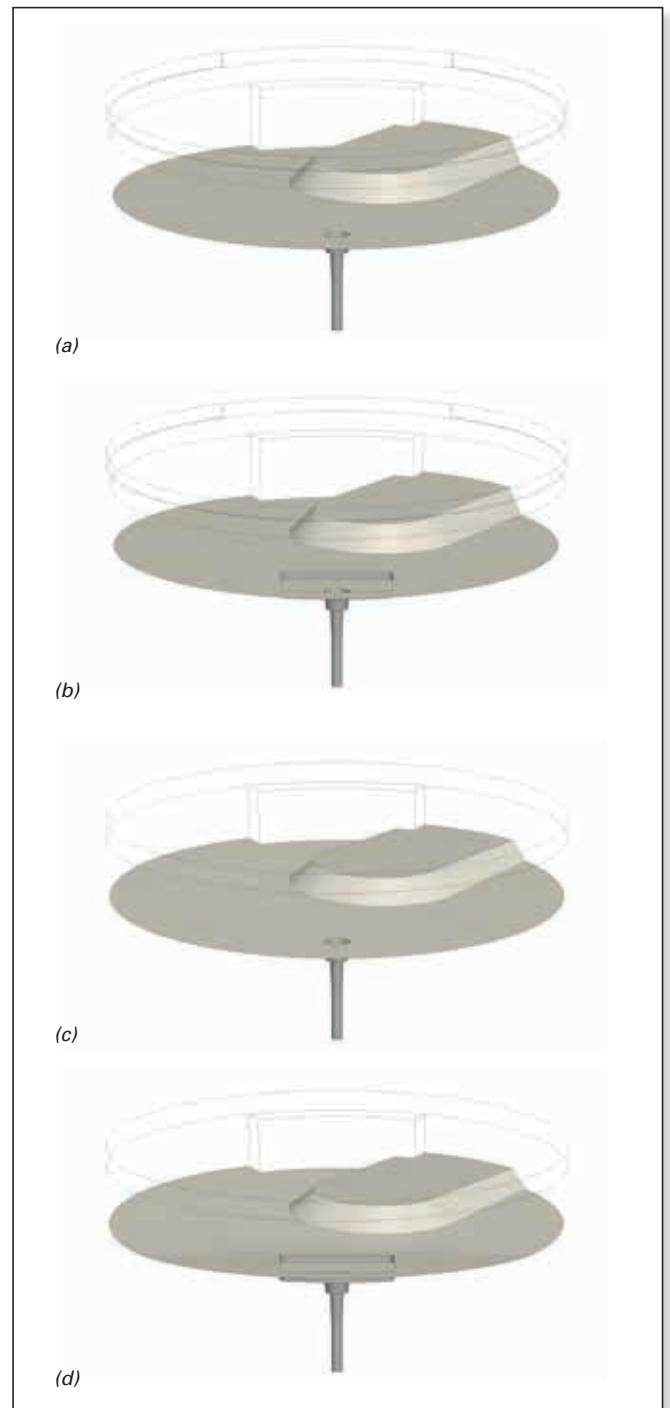


Figure 3. Modelled ladle geometries. (a) straight bottom, (b) straight bottom with a recessed box around the well block, (c) inclined bottom, and (d) inclined bottom with a recessed box around the well block.

- >> Straight bottom.
- >> Straight bottom with a recessed box around the well block.
- >> Inclined bottom.
- >> Inclined bottom with a recessed box around the well block.

The onset of vortex formation during the tapping process, as a result of the interface between the slag and steel collapsing, is shown for the various bottom geometries in Figure 4. With a straight bottom, incorporating a recessed box around the well block led to a significant reduction in residual steel at the point of slag entrainment (Figure 5). Inclining the bottom also decreased the amount of residual steel. However, the most effective design was a combination of a recessed box and inclined bottom, which reduced the residual steel by approximately 70% compared to the standard straight ladle bottom.

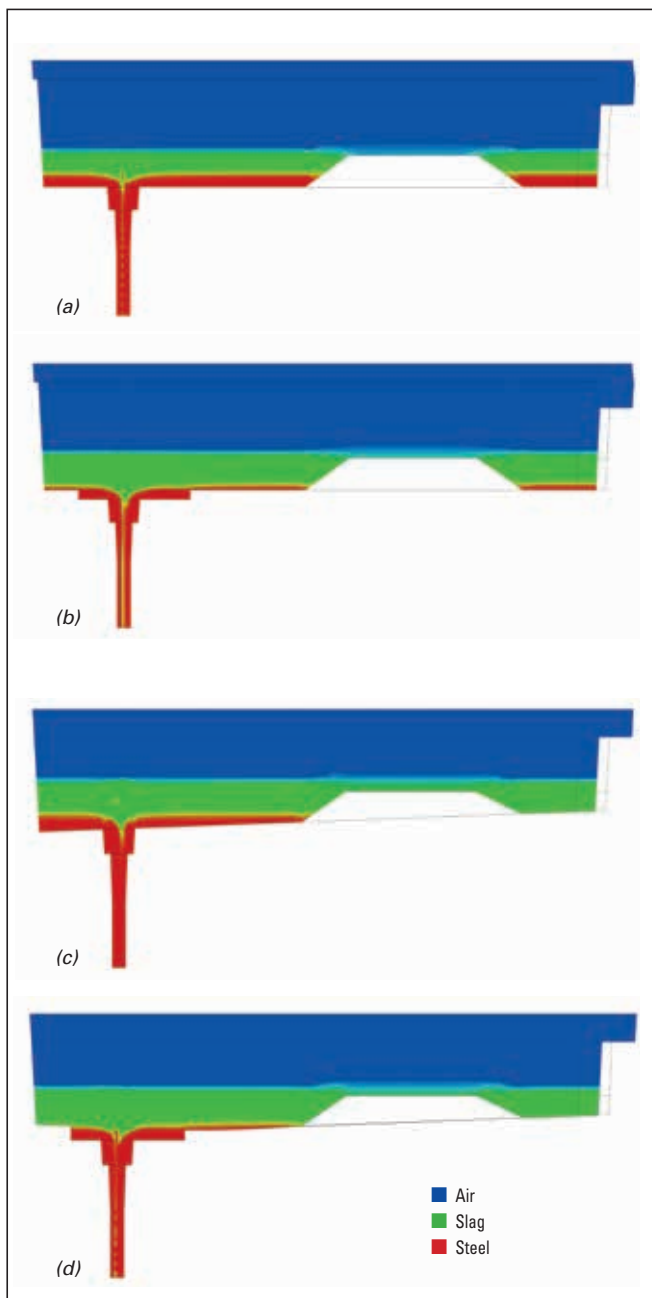


Figure 4. Modelling results of slag entrainment with various ladle bottom geometries. (a) straight bottom, (b) straight bottom with a recessed box around the well block, (c) inclined bottom, and (d) inclined bottom with a recessed box around the well block.

IBOS is available for both the wear and permanent lining and provides benefits through a combination of different design features. The prefabricated ladle bottom comprises steps and inclinations to generate a specific bottom surface. The number and angles of the inclinations, in addition to the number and height of the steps, are optimized for the general ladle design and customer demands. Each IBOS is a tailor-made solution for the particular customer requirements, taking into account the ladle size, entire refractory lining, position and design of the slide gate and purging ceramics, and impact pad.

Wear Lining IBOS Options

For the special high-yield IBOS design that is realized by the wear lining, a prefabricated ladle bottom (Figure 6) is placed on a standard permanent lining comprising bricks or monolithics. The following advantages can be achieved with this approach:

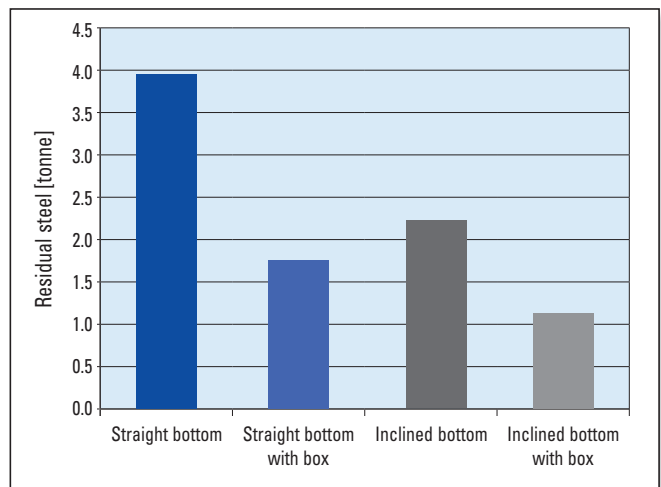


Figure 5. Residual steel in the ladle with the various bottom designs shown in Figure 3.

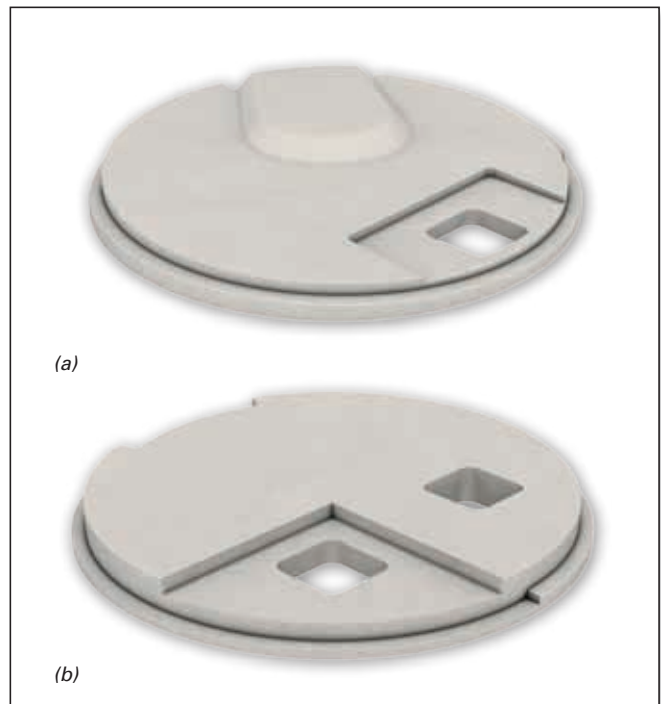


Figure 6. Tailored wear lining bottom designs. (a) sidewall bearing and recessed region around well block and (b) recess for reinforced area in the sidewall and special dimensional shapes.

- >> Higher yield—decreased residual steel.
- >> Timesaving installation—prefabricated shape for the wear lining.
- >> Decreased work force—no individual bricklaying required for the wear lining.
- >> Minimized joints in the lining—no gaps between the bricks.
- >> Use of monolithic bottoms without additional equipment.
- >> Easy installation of the starter ramp—especially for semi-universal (SU) shapes.

In addition to the precast IBOS design, RHI provides bottoms made of preassembled bricks (Figure 7) or a combination of monolithic and brick refractories. The latter design is characterized by using bricks in the impact pad of a precast shape.

The tailor-made options include:

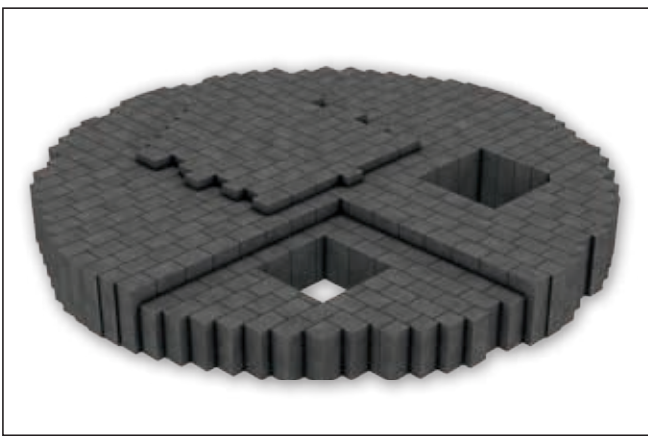


Figure 7. Preassembled brick design for the wear lining.

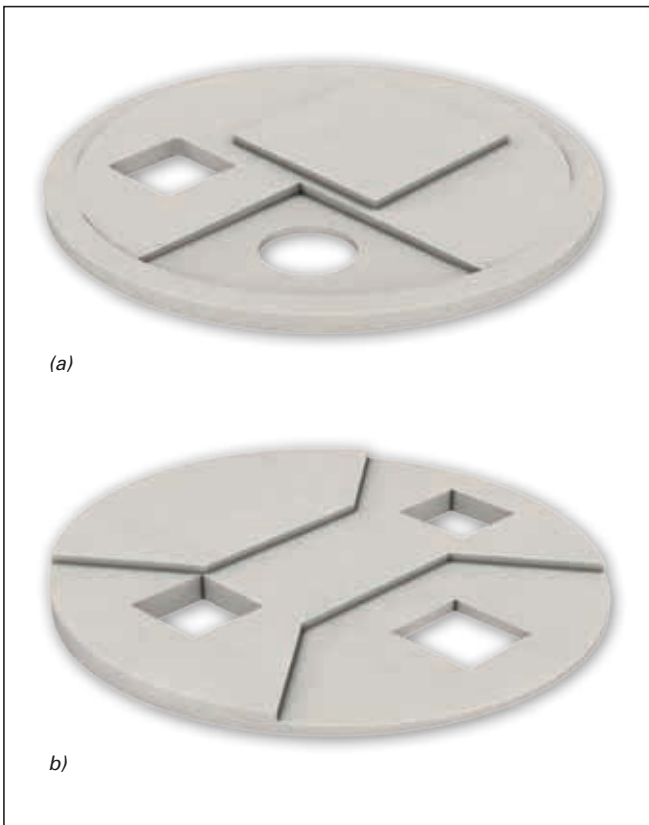


Figure 8. Prefabricated permanent lining solutions. (a) bearing for the sidewall wear lining and (b) extended impact pad.

- >> Design with or without a sidewall bearing.
- >> Impact pads of different heights.
- >> Recesses for reinforced areas in the sidewall.
- >> Special dimensional shapes.
- >> Spiral for SU shapes.

Permanent Lining IBOS Options

The special high-yield IBOS permanent lining design is achieved through a prefabricated shape used for the permanent lining (Figure 8). The prefab is installed on a levelled ladle bottom. The usual wear lining bricks are placed on the IBOS to generate the high-yield design. Various advantages can be achieved with this approach:

- >> Higher yield—decreased residual steel.
- >> Reproducible contour for several campaigns.
- >> Timesaving installation—prefabricated shape for the permanent lining.
- >> Decreased work force—no individual bricklaying required for the permanent lining.
- >> Minimized joints in the lining—no gaps between the bricks.
- >> No special shapes required to line special bottom designs—one wear lining brick size for all areas.

Lifting and Fixing the IBOS in the Ladle

Each IBOS shape is equipped with suitable lifting connections to enable it to be manipulated by crane and easily lifted into the ladle (Figure 9).

When a wear or permanent lining IBOS is installed, correct securing in the ladle is essential to ensure the bottom does not become loose. This can be achieved by incorporating a bearing at the edge so the heavy weight of the entire



Figure 9. Installation of an IBOS shape into a ladle using lifting connections.

sidewall holds the bottom shape in place. If the IBOS comprises a multipiece design (Figure 10), appropriate fixing is much more critical. In this case it is necessary to include special fixing joints in the prefabricated bottoms. These joints are then rammed or cast after the bottom shape has been secured. The IBOS permanent lining has a reduced thickness especially in the well block region. Therefore, RHI performs finite element analysis to check the yield stresses in the prefab and ensure the construction is safe.

Wear Lining Installation on an IBOS Permanent Lining

It is necessary to fill all the gaps that are present when the wear lining bricks are placed on a stepped and/or inclined permanent lining (Figure 11), using for example a small



Figure 10. Special fixing joints in an IBOS.

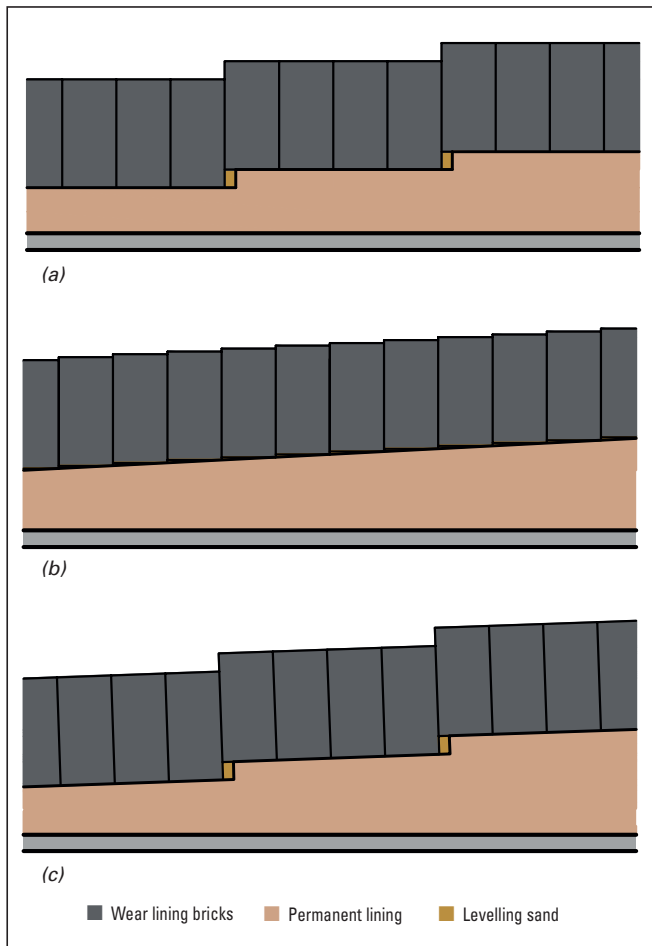


Figure 11. (a) stepped design, (b) inclined design for a straight wear lining, and (c) combined inclined and stepped design.

amount of levelling sand. The sand provides a stable installation base for the wear lining bricks. In the case of an inclined design, the wear lining bricks can either be placed parallel to the inclination (Figure 11b) or horizontally (Figure 11c).

In-Service Experiences

The first IBOS customer application was at an integrated BOF steel plant in North America, producing approximately 2.5 million tonnes of low carbon and ultra low carbon steel strip annually. The production process uses 250-tonne ladles that are routed through the RH-OB degasser or ladle metallurgy furnace for the secondary metallurgy.

The ladle bottom design is a synergy of RHI high-alumina spinel-forming castable technology and alumina-magnesia-carbon (AMC) bricks. Although previous ladle bottom experiences at this steel plant had shown very high impact pad wear in the ladle bottom due to high tapping stream erosion, RHI has achieved superior results with the combined castable and brick design. The tailor-made IBOS design consists of 6.2 tonnes of mix and 68 individual bricks. A layer of cast mix lies above and below the AMC brick pad. The pad is preassembled and glued at the RHI Dalian plant (China) using a special tongue and groove interlocking system. The tongue and groove design is important because it ensures the bricks remain locked into place during use and as the bricks become worn at the end of the ladle bottom campaign it prevents the thin residual brick lining from floating up and exposing the bottom castable mix.

The ladle bottom shape had to be cast in an inverted position in order to incorporate the tailored IBOS shape in the design. The ladle bottom was 3.5 m in diameter with a 381-mm thick impact pad. The bottom wear surface had an inclination of 83 mm from the outside diameter, adjacent to the raised impact area, sloping downwards to the IBOS recessed ledge (Figure 12).

The target RHI set for this IBOS bottom was 100 heats and to match or exceed the steel yield results of the current bottom suppliers. The steel plant has a weighing scale incorporated in the mill crane used to pick up the ladles from the caster so it was possible to obtain immediate and accurate data regarding the dump weight in the ladle and compare the performance of the IBOS bottoms with that of the competitor designs. When this article was written, RHI had completed three ladle bottom campaigns and the fourth ladle



Figure 12. Customer-specific tailored IBOS design.

bottom was in service. The results of the first three bottoms showed that the IBOS outperformed the competitor high-yield ladle bottoms: The average dump weight after tapping with the first IBOS bottom compared to competitor bottom designs is shown in Figure 13. Typically, the average ladle bottom life in this steel plant is around 85 heats; therefore, it was also very positive that the IBOS bottoms came out of service at 90, 100, and 103 heats.

Creating a Customized IBOS

As conditions and ladle designs vary considerably at each steel plant, it is necessary to provide a tailor-made solution for each customer. To achieve this, RHI has established a standard procedure for the assessment and design:

- >> Check actual situation at customer's site.
- >> Create a tailor-made solution.
- >> Show improvements with CFD modelling.

Conclusion

RHI's Improved Bottom Optimized Solution—IBOS—is a new system for ladle bottoms that provides tailor-made refractory prefabs for the wear and permanent lining. The main advantage for steel plants is the improved yield of high-quality steel. Additional benefits of the prefabricated bottom parts, such as timesaving during installation and avoiding gaps between bricks are combined with an innovative design that minimizes faults and provides a support layer for the side-wall. The advantages of IBOS are summarized in Figure 14.

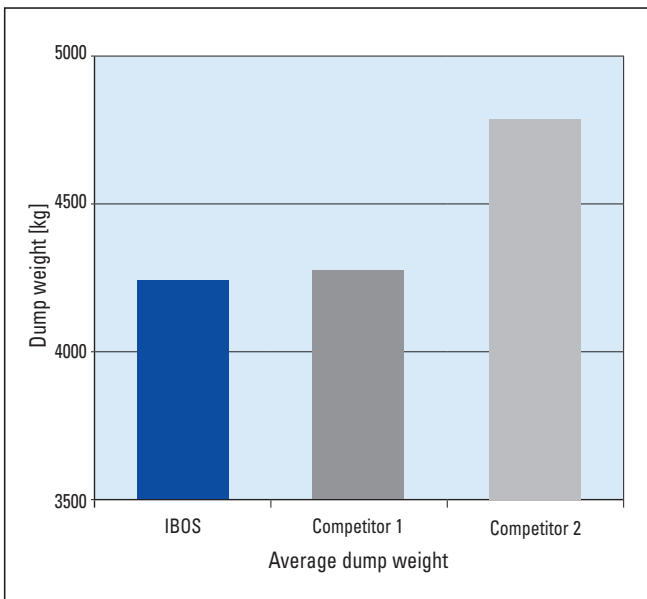


Figure 13. The average dump weight after tapping with IBOS compared to competitor bottom designs.

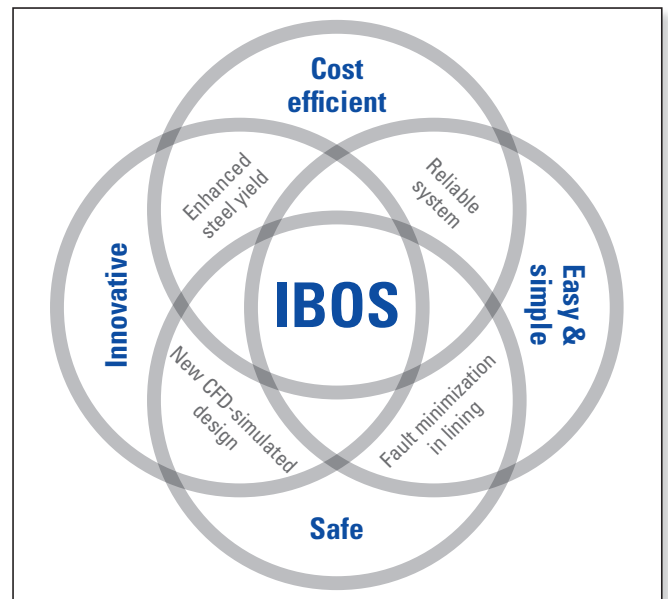


Figure 14. Advantages of the IBOS.

References

- [1] Davila, O., Ferro, L., Morales, R.D., Demedices, G.L. and Ramirez-Perez, P. Physical Model and Mathematical Simulations of Ladle Draining Operations. Presented at AISTech 2005, Charlotte, USA, May 8–12, 2005.
- [2] Mazzaferro, G.M., Piva, M., Ferro, S.P., Bissio, P., Iglesias, M., Calvo, A. and Goldschmit, M.B. Experimental and Numerical Analysis of Ladle Teeming Process. *Ironmaking and Steelmaking*. 2004, 3, No. 6, 503–508.
- [3] Heaslip, L.J., Dorricott, J.D. and Richaud, J. Caster Steel Yield Improvement by Enhanced Ladle Bottom Design. Presented at AISTech 2007, Pittsburgh, USA, May 7–10, 2007.
- [4] Richaud, J., Chung, W. and Rogler, J. Enhanced Ladle Draining by Ladle Bottom Design Optimization. Presented at METEC InSteelCon 2011, Düsseldorf, Germany, June 27–July 1, 2011.
- [5] Maranitsch, A., Höck, M. and Kirschen, M. Fireproof Ceramic Bottom. Patent application WO2014106553 A1, 2014.
- [6] Köhler, S., Maranitsch, A. and Servos, K. Ladle bottom and Ladle. Patent application WO2014173583 A1, 2014.

Authors

Matthias Höck, RHI AG, Steel Division, Vienna, Austria.
 Sarah Köhler, RHI AG, Technology Center, Leoben, Austria.
 Kerry Servos, RHI Canada Inc., Steel Division, Burlington, Canada.
 Bernhard Spieß, RHI AG, Steel Division, Vienna, Austria.
Corresponding author: Matthias Höck, matthias.hoeck@rhi-ag.com

Harald Taferner, Rainer Neuböck and Ferdinand Schüssler

Slag Corrosion of Doloma Refractories

Introduction

Doloma, comprising approximately 60 wt.% CaO and 40 wt.% MgO, is thermodynamically stable when in contact with various slag compositions and liquid metal, making it an excellent refractory material for steelmaking applications [1]. However, as is the case for other refractory types, several corrosion mechanisms, acting synergistically in most instances, lead to degeneration of the refractory lining during operation. Understanding the wear mechanisms of solid oxides in doloma refractories when in contact with specific slag chemistries contributes to improving the durability of these linings. This article provides an overview of the main corrosion processes that occur when doloma refractories are in contact with slags used in steelmaking units, using examples from postmortem microstructural analyses.

Types and Application Areas of Doloma Refractories

Doloma refractories are used for wear and safety linings in a wide range of applications such as lime shaft kilns, cement and dolomite rotary kilns, and various vessels used in the steelmaking process. However, the steel industry is the main consumer of this material.

The use of dolomite as a lining material for Thomas converters first started in 1878 after it was discovered that dephosphorization and desulphurization in basic steel refining was far more effective with a basic lining compared to an acidic lining [2]. The removal of phosphorous in a dolomite-lined Bessemer converter enabled the use of phosphorus-rich iron ore. This was an important step that accelerated the development of doloma-based products for steel refining. Initially crushed dolomite was bonded with sodium silicate binder, formed into tiles, and calcined in situ in the converter [1]. However, due to an increase in basic steel refining for the production of high-quality steel, which requires precise metallurgical control, there has been considerable growth in the use of high-purity doloma refractories for steelmaking applications over the last decades.

Direct-bonded (fired) and carbon-bonded (pitch- or resin-bonded) doloma bricks are applied in steel ladles, various furnaces, as well as for argon oxygen decarburization (AOD), vacuum oxygen degassing (VOD), and vacuum arc degassing (VAD) vessels used in stainless steelmaking. Doloma-based monolithic materials are used to line tundishes and electric arc furnace hearths and in conjunction with doloma- and magnesia-based bricks for ladles, AODs, and other steelmaking vessels, as well as for maintenance applications. However, more commonly doloma refractories are pressed shapes. The type of doloma raw material (sintered or fused) and amounts of other raw materials added, for example magnesia (mag-dol refractories) or carbon, vary depending on the required refractory material performance.

The advantages of a doloma refractory lining in steelmaking units result from a low oxygen resupply to the steel

melt, relatively high stability under vacuum and reducing atmospheres, and a high resistance to basic process slags [3,4]. Doloma is also a highly cost-effective lining solution. The main disadvantages are susceptibility to hydration in humid environments and, primarily in the case of fired bricks, spalling of brick areas heavily infiltrated by slag when there are temperature changes during operation.

Corrosion Mechanisms of Refractories in Contact With Slag

Refractory corrosion in steelmaking units is a complex phenomenon involving chemical and physical wear processes that may act independently or, as in most cases, synergistically. Slag corrosion can be defined as any type of gradual destruction of a solid phase (e.g., CaO and MgO in the case of doloma) through chemical reactions with a slag and can be subdivided into the following major processes:

- >> Penetration: Permeation of liquid slag into the refractory via open porosity.
- >> Diffusion: Caused by thermally activated random motion of atomic-scale particles.
- >> Dissolution: A chemical process by which refractory components continuously dissolve in the liquid slag.
- >> Erosion: Abrasion of refractory material components (original as well as newly formed phases) due to slag movement.

Commonly these processes do not occur individually, in most cases a combination of factors result in corrosion. Furthermore, resistance of a material to slag depends on the chemical (e.g., basicity) and physical (e.g., density, porosity, and permeability) nature of the refractory, slag chemical composition, and temperature.

Corrosion can be subdivided into active and passive corrosion [5]. Active corrosion is when phases, formed due to the reaction of slag and refractory, are soluble or dissociate directly into liquid slag, which may lead to destruction of the refractory material. In contrast, passive corrosion occurs if the reaction product is not soluble or only partly dissolves in liquid slag and in addition may form a protective layer to prevent further corrosion.

Chemical Interactions Between Slag and Doloma Refractories

Doloma refractory wear strongly depends on the refractory's quality, location in the metallurgical vessel, and the metallurgical process. Therefore, the corrosion behaviour is often complex due to a combination of these factors. However, the three major doloma refractory wear mechanisms can be summarized as follows:

- >> Degeneration of the microstructure due to burnout of the binder phase (in the case of carbon-bonding).
- >> Mechanical overload.
- >> Heat-induced chemical reactions between the refractory and slag [6].

In the latter case, solid refractory oxide components start to react with liquid slag during operation resulting in the formation of thermodynamically stable phases. In general doloma grains comprising CaO and MgO dissolve in the slag until chemical equilibrium is achieved.

The presence of free lime provides doloma refractories with a significant advantage in terms of slag resistance when in contact with slags not fully saturated with lime [1] because further slag penetration is limited due to the formation of a dense layer of recrystallized lime and calcium silicates (particularly $3\text{CaO}\cdot\text{SiO}_2$) at the refractory hot face (phases have melting points significantly $> 1600\text{ }^\circ\text{C}$). However, slags deficient in lime but high in sesquioxides (e.g., Al_2O_3) may promote the corrosion of doloma components mainly due to the formation of calcium aluminates and calcium ferrites with melting points of $1600\text{ }^\circ\text{C}$ or significantly lower (Table I). These newly formed phases are liquid during steel refining, soften the infiltrated area at temperatures $> 1600\text{ }^\circ\text{C}$, and slag movement causes enhanced wear of the refractory by hot erosion. The phases that form mainly depend on the amounts of sesquioxides, the SiO_2 content, and the CaO/SiO_2 (C/S) ratio of the slag. Moreover, the slag chemistry changes during operation according to the operational steps during steel refining and can have a varying influence on the corrosion behaviour of the refractory material over time.

Phase	Formula	Melting point ($^\circ\text{C}$)
Tricalcium silicate	$3\text{CaO}\cdot\text{SiO}_2$ (C_3S)	[1800]
Monocalcium aluminate	$\text{CaO}\cdot\text{Al}_2\text{O}_3$ (CA)	1600
Tricalcium aluminate	$3\text{CaO}\cdot\text{SiO}_2$ (C_3A)	[1540]
Mayenite	$12\text{CaO}\cdot 7\text{Al}_2\text{O}_3$ (C_{12}A_7)	1420
Dicalcium ferrite	$2\text{CaO}\cdot\text{Fe}_2\text{O}_3$ (C_2F)	1448

Table I. Most common products of doloma corrosion. The transformation or decomposition points are indicated by square brackets.

Wear Phenomena Observed in Postmortem Studies

The following wear phenomena have been observed in post-mortem studies of direct-bonded and carbon-bonded doloma refractories.

The corrosion process of direct-bonded doloma and mag-dol refractories starts when slag directly permeates the refractory during operation via the open porosity. The rate of slag penetration depends on various factors like the permeability of the refractory microstructure, slag viscosity, and temperature. As the dissolution rate of CaO is higher than MgO, initially lime is corroded due to its reaction with metal oxides (e.g., Fe_2O_3 and Al_2O_3), mainly resulting in the formation of dicalcium ferrite and Ca-Al oxides (calcium aluminate, tricalcium aluminate, and mayenite) at the hot face (Figures 1 and 2). These newly formed phases are able to infiltrate deeply into the matrix due to their low melting points. In several cases chromium-containing compounds with high melting points may be present (e.g., chromium spinel from the slag or calcium chromite as a reaction product between the slag and refractory). Calcium silicate from the slag is usually the main phase in the infiltrated zone (in most cases filling the pores). With ongoing corrosion, dicalcium silicate reacts with lime and transforms to alite ($3\text{CaO}\cdot\text{SiO}_2$ in Figure 3).

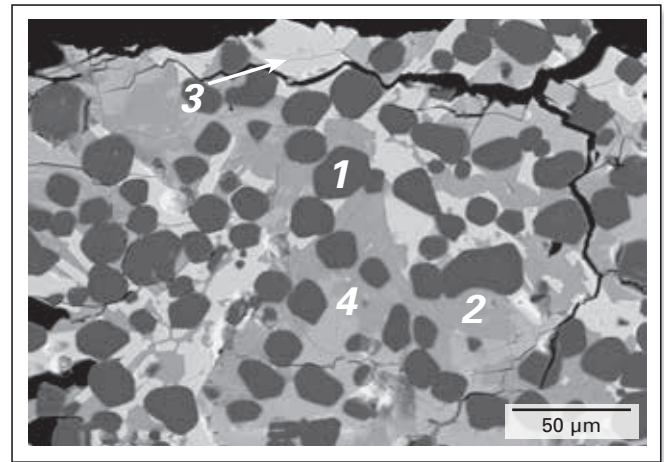


Figure 1. Microstructural detail of the immediate hot face of a used direct-bonded doloma brick. Sesquioxides from the slag caused the corrosion of lime (in the brick) resulting in the formation of low melting calcium ferrites and calcium aluminates. Microcracks at the immediate hot face indicate degeneration of dicalcium silicate. Periclase (1), dicalcium silicate (2), chromium-containing dicalcium ferrite (3), and calcium chromite (4) are indicated.

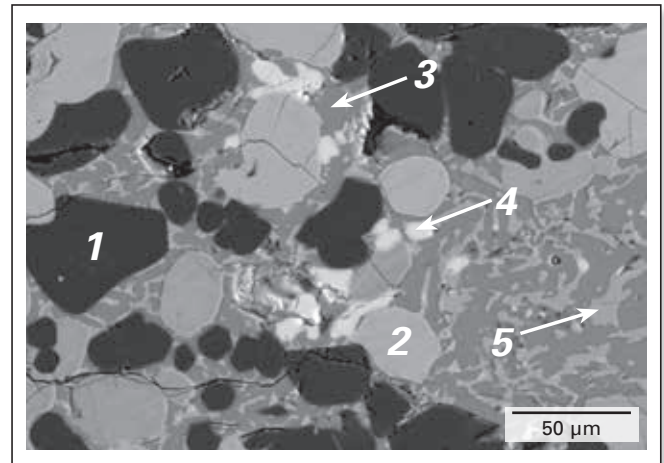


Figure 2. Microstructural detail of a used direct-bonded doloma brick 1 mm from the hot face. Reaction of alumina (in the slag) and lime (in the brick) formed low melting mayenite (melting point: $1420\text{ }^\circ\text{C}$). Periclase (1), lime (2), fluorine-containing mayenite (3), calcium sulphide (4), and fluorine-containing calcium silicate (5) are indicated.

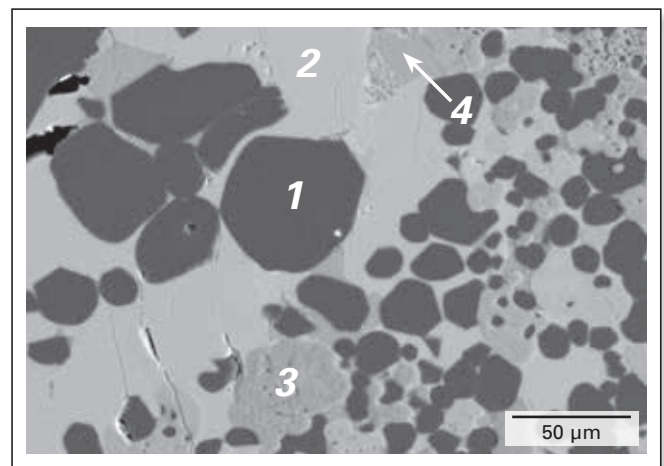


Figure 3. Microstructural detail of a used direct-bonded doloma brick approximately 5 mm from the hot face. Tricalcium silicate formed due to the reaction of dicalcium silicate (precipitated from the infiltrated slag) with lime from the brick. Periclase (1), tricalcium silicate (2), lime (3), and fluorine-containing calcium aluminate (4) are indicated.

The ratio of the newly formed higher and lower melting point phases (depending on the slag chemistry) regulates the infiltration depth and slag resistance of the doloma refractory. As a result, MgO remains isolated in a matrix of primarily tricalcium silicate, dicalcium ferrite, and Ca-Al oxides and is partly dissolved as a function of the slag chemistry. In areas close to the hot face, lamellar segregations in periclase may occur due to the reaction of iron oxide with MgO.

Dicalcium silicate and tricalcium silicate may contain fluoride, stemming from CaF_2 (fluorspar) added to increase the desulphurizing potential. The consequence is a decreased melting point of these phases. Therefore, CaF_2 addition causes deeper infiltration, stronger corrosion, and increased wear by hot erosion. The combination of CaF_2 addition, low basicity, and SiO_2 may lead to the formation of cuspidine ($\text{Ca}_4(\text{Si}_2\text{O}_7)(\text{F},\text{OH})_2$), a fluorine-bearing calcium silicate mineral with a low melting point ($\sim 1400^\circ\text{C}$) and the potential for deep infiltration. In addition, sulphide-containing melts exhibit low solidification points and may deeply infiltrate the brick structure.

Slag coating, when observed at the immediate hot face, is mainly composed of dicalcium silicate that undergoes multiple phase transformations when the lining cools down. Transformation of the monoclinic to orthorhombic polymorph is accompanied by a volume expansion of more than 10 vol.%, resulting in disintegration of the solidified slag.

Cracks can occur parallel to the hot face in the transition area between slag infiltrated and noninfiltrated refractory zones. These types of cracks are caused by changed physical properties in the infiltrated zone and are an indication that spalling and discontinuous wear may occur. The lining life of steelmaking units can be significantly improved by keeping the lining at the highest possible temperature during operational stops.

In contrast to direct-bonded (fired) doloma and mag-dol refractories, carbon-bonded grades are penetrated by slag when the bonding phase is decarburized. The reaction zone, where liquid slag and solid refractory components are able to interact chemically, is relatively thin compared to direct-bonded doloma and mag-dol refractories (Figures 4 and 5). Postmortem samples show continuous wear due to carbon burnout, slag penetration, the reaction of slag and CaO to form high-lime (low melting) compounds, and washout of various compounds (including MgO) due to slag movement.

Influence of the Refining Slag Composition on Corrosion

Several studies have shown that the refining slag composition significantly influences refractory wear. Especially the slag basicity as well as iron oxide and MgO contents exert considerable influence on the lining wear rate.

The corrosion behaviour of various bricks used in converters and secondary steel refining furnaces, including a fired doloma brick, in the presence of a commonly used $\text{CaO-SiO}_2\text{-Fe}_2\text{O}_3\text{-MgO}$ steelmaking slag under static conditions was examined and the results showed that the wear rate generally decreased with increasing slag basicity (Figure 6) [7]. The effect of Fe_2O_3 on the wear was clearly seen in slags

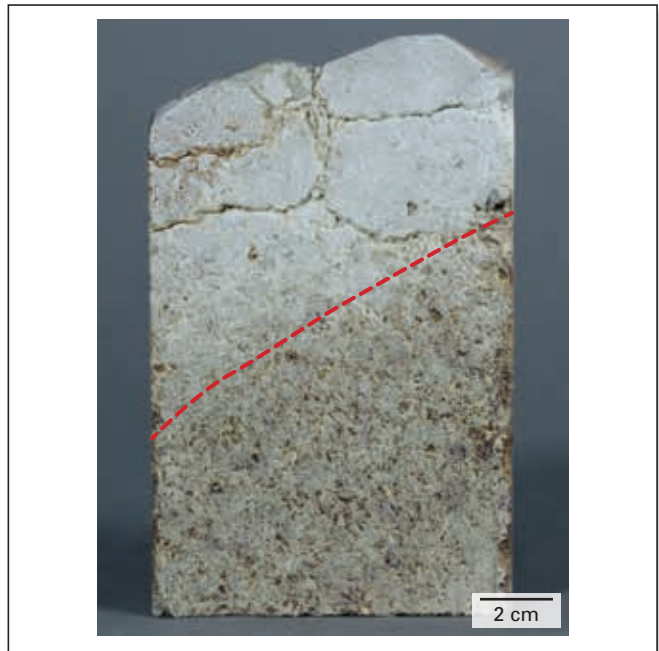


Figure 4. Used direct-bonded doloma brick showing deep infiltration of the refining slag. Cracks are mainly parallel to the hot face and located in the infiltrated zone. Hot erosion causes continuous wear and when cracked areas of the brick spall off discontinuous wear starts. The transition between infiltrated and noninfiltrated brick areas is indicated by the dashed red line.

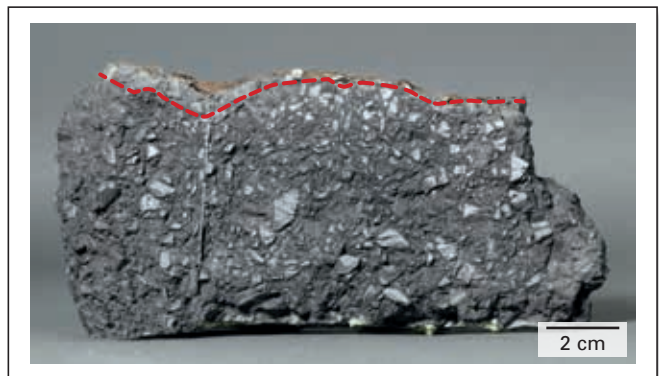


Figure 5. Used carbon-bonded doloma brick showing continuous wear. Slag infiltration and reaction with refractory components resulted in the formation of high-lime (low melting) phases occurring at the immediate brick hot face. Transition from the infiltrated and decarburized area at the hot face to the carbon-containing noninfiltrated area is indicated by the dashed red line.

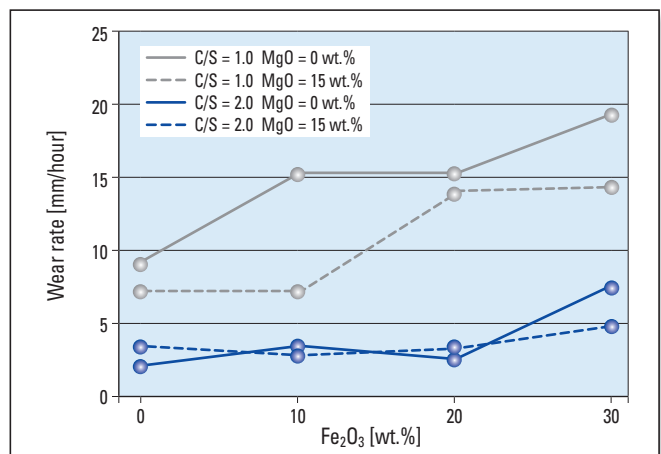


Figure 6. Influence of the refining slag composition on the wear rate of doloma refractories. Slags with a high basicity and low Fe_2O_3 content are less corrosive to fired doloma bricks [7].

exhibiting a low basicity ($C/S = 1.0$), where increased Fe_2O_3 levels caused elevated wear. However, amounts of up to approximately 20 wt.% Fe_2O_3 had no substantial influence on the corrosion rate of the bricks at higher slag basicity ($C/S = 2.0$). The addition of MgO to the slag generally decreased the brick wear rate.

The presence of Al_2O_3 in refining slags causes an increased wear rate of doloma refractories. The influence of Al_2O_3 on the dissolution of CaO is similar to that of the fluxing agent CaF_2 . The main difference is that the fluxing potential of CaF_2 is higher.

Summary

Doloma is a highly-cost effective lining solution, providing long service life at low specific refractory cost. Furthermore, it has a low oxidation potential and facilitates desulphurization. The chemical and physical properties of doloma make it compatible with metallurgical practices employing basic slag chemistry. However, slags deficient in lime but high in sesquioxides may promote the corrosion of doloma components mainly due to the formation of compounds with melting points of 1600 °C or significantly lower. By understanding the precise corrosion mechanisms through postmortem studies, slag chemistry and operating practices can be optimized to maximize the refractory lifetime.

References

- [1] Schacht, C. (Ed). *Refractories Handbook*; Marcel Dekker Inc: New York, 2004.
- [2] Thomas, S.G. Verfahren zur Herstellung von feuerfesten basischen Ziegeln durch Mischen von magnesiahaltigem Kalkstein mit geringen Mengen von Kieselsäure, Thonerde und Eisenoxyd, Formen der Masse zu Ziegeln und Brennen derselben bei Weissglühhitze. German Patent 5869, 1879.
- [3] Routschka, G. and Wuthnow, H. (Eds). *Praxishandbuch Feuerfeste Werkstoffe (5th Edition)*; Vulkan-Verlag: Essen, 2011.
- [4] Driscoll, M. Refractory Dolomite: Stainless Reputation. *Industrial Minerals*. 1998, 369, No. 6, 35–43.
- [5] Lee, W. and Zhang, S. Direct and Indirect Slag Corrosion of Oxide and Oxide-c Refractories. Presented at VII International Conference on Molten Slags Fluxes and Salts, Cape Town, South Africa, Jan., 25–28, 2004; pp 309–320.
- [6] Hartenstein, J. Einsatz von Dolomit als feuerfester Baustoff in der Stahlindustrie. Presented at Stahlinstituts VDEh Seminar Feuerfeste Stoffe und Schlacken in der Metallurgie, Bad Neuenahr, Germany, Dec., 2–5, 2012; p. 22.
- [7] Hiragushi, K., Fukuoka, H., Asano, K. and Hayashi, K. Corrosion of Various Basic Bricks by $CaO-SiO_2-Fe_2O_3-MgO$ Slag. *Taikabutsu Overseas*. 1985, 5, No. 1, 12–20.

Authors

Harald Taferner, RHI AG, Technology Center, Leoben, Austria.
 Rainer Neuböck, RHI AG, Technology Center, Leoben, Austria.
 Ferdinand Schüssler, Dolomite Franchi, Steel Division, Brescia, Italy.
Corresponding author: Harald Taferner, harald.taferner@rhi-ag.com

Reinhard Ehrenguber and Roland Bühlmann

INTERSTOP Ladle Gate Type S—A New Milestone in Ladle Gate Technology

Development of the new INTERSTOP Ladle Gate Type S series focused on solving three main issues relayed by customers. Firstly, steel plants are facing high pressure to reduce production costs; secondly, continuous system improvements are necessary to meet the demands of modern clean steel production; and thirdly, personnel and equipment safety are playing a very important role in every steel plant. The new INTERSTOP Ladle Gate Type S sets a new standard as it fulfils all three of these requirements.

Introduction

The new INTERSTOP Ladle Gate Type S (Figure 1) is a high-performance ladle gate system focused on optimizing total cost of ownership (TCO) as well as safe and easy operation. The advanced refractory concept is able to cover a range of casting diameters with the same mechanical system, leading to higher efficiency. The smart handling characteristics enable easy and safe operation and they are incorporated within a maintenance-friendly design. The new development has a positive impact on the overall operating costs and increases the safety standard during handling and operation. This paper outlines the advantages of the new INTERSTOP Ladle Gate Type S and demonstrates the advantages for customers with regards to the aforementioned main points.

System Highlights

The new INTERSTOP Ladle Gate Type S features improved refractory utilization by using ideal refractory sizes and designs tailored to the required mass flow of the continuous casting machine. The new concept enables optimization of refractory efficiency, resulting in lower ladle gate system operating costs. It is possible to cover a larger range of

mass flows with the same mechanical system by installing different refractory sizes (Table I). This allows optimization of the bore diameter and positively influences the necessary throttling for steel flow control, resulting in less refractory wear and reduction of negative pressure caused by throttling. The ideal refractory plate overlap was defined according to the required mass flow. The refractory plate geometry and stroke of the mechanical system, together with the optimized plate size, ensure safe operation of the system.

Type	Size	Working stroke (mm)	Nominal diameter (mm)
S0	S0-S	100	35
S1	S1-S	100	40
	S1-E	130	50
S2	S2-S	140	60
	S2-E	170	70
S3	S3-S	180	80
	S3-E	210	90
S4	S4-S	230	100

Table I. INTERSTOP Ladle Gate Type S sizes.

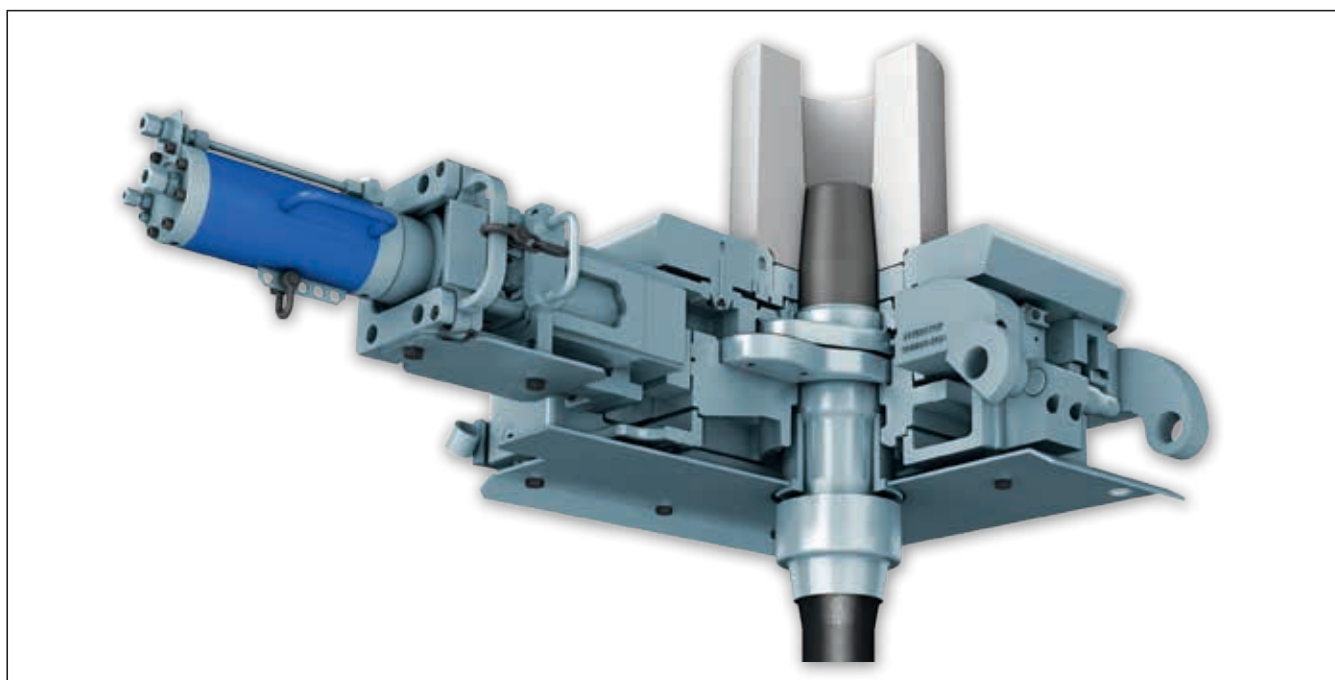


Figure 1. INTERSTOP Ladle Gate Type S.

Automatic System Tensioning and Self-Clamping of the Plates

Technical advances in the new ladle gate system design lie in the system tensioning that is applied automatically and self-clamping of the refractory plates inside the system. The user-friendly ladle gate design reduces the weight and complexity of the gate handling components to improve personnel safety and reduce human error during the service and preparation of the ladle gate at the ladle preparation area in the steel plant (Figure 2).

The automatic system tensioning and self-clamping of the plates ensure the plates are positioned correctly within the mechanical system at all times. As a result of these advances many possible sources for human mounting errors have been eliminated. The centring with a mechanical stop, together with the directional forces, have a positive influence on performance in the wear zone area (Figure 3).

The self-clamping is automatically activated by a single device (Figure 4) when the ladle gate slider strokes the lower plate into the ready-for-operation position. The clamping is maintained in combination with the three lugs positioned around each plate. No additional devices are required and no manual handling to clamp the refractory plates within the ladle gate system is necessary.

Advanced Mechanical Design

The impact of varying temperatures on the ladle gate mechanical system results in plastic deformation, leading to multiaxial stresses. The material expands when it is exposed to heat and shrinks during cooling. The alternating stresses, occurring repeatedly during gate operation, also affect the refractory behaviour within the system.

Finite element analysis enabled an optimized design of the INTERSTOP Ladle Gate Type S housing and slider.

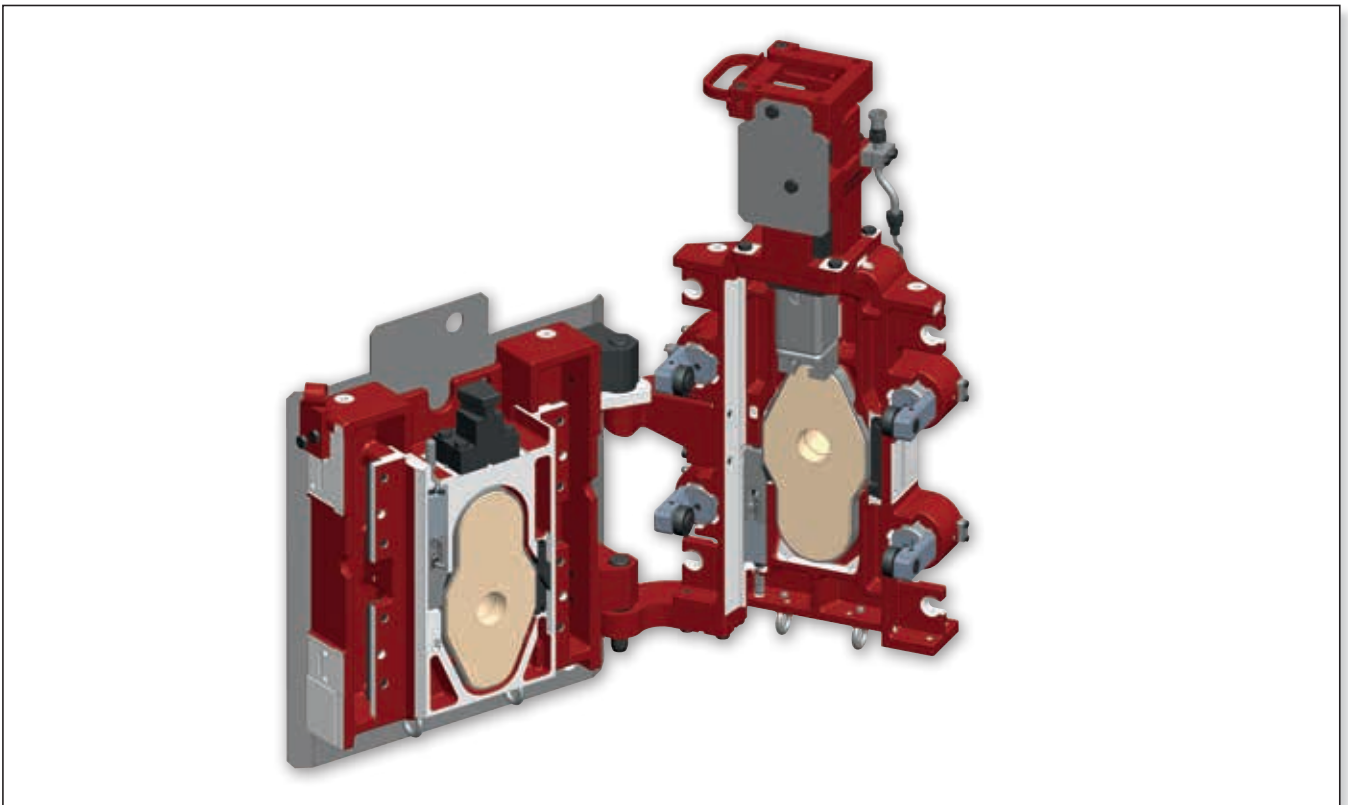


Figure 2. User-friendly ladle gate design.

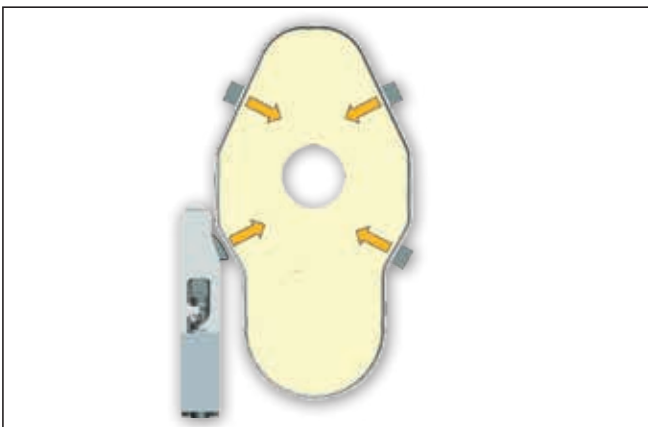


Figure 3. Clamping and centring of the new INTERSTOP Ladle Gate Type S refractory plates.

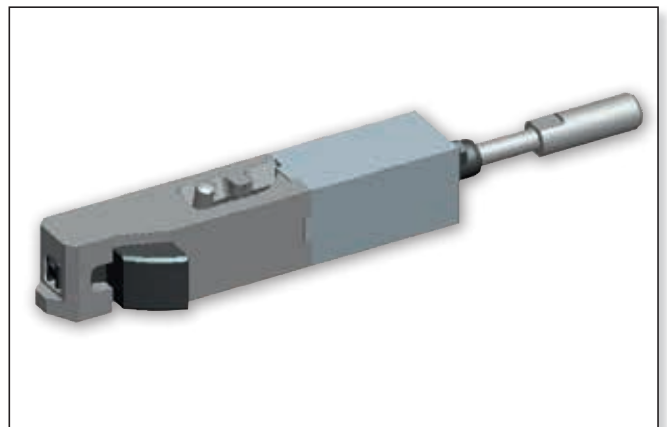


Figure 4. Self-clamping device for the refractory plates.

The improved thermal behaviour is based on a two-piece slider design, providing thermal separation and ensuring maximum stiffness over a long lifetime. Concurrently, negative influences on the behaviour of refractory parts within the system are minimized (Figure 5).

Mounting Flexibility

The INTERSTOP Ladle Gate Type S series can be mounted in either a horizontal or vertical position (Figure 6). As a result, especially customers where the steel plant layout at the casting platform requires horizontal mounting of the INTERSTOP Ladle Gate Type S can now benefit from a two-part slide gate (e.g., no extra heat shield handling is required).

Improved Mounting Cylinder Handling at the Preparation Area

The INTERSTOP Ladle Gate Type S always guarantees easy handling and coupling of the mounting cylinder at the preparation area, independent of the drive configuration. For a standard application (Figure 7a), coupling of the mounting cylinder remains sideways into the cylinder bracket where the casting cylinder is also coupled at the casting platform. For all special drives (e.g., extended drive and bell crank), the mounting cylinder is coupled from the front side towards the cylinder bracket (Figure 7b), independent of the casting cylinder coupling position. This guarantees, besides a new lightweight cylinder, ergonomic and easy coupling of the mounting cylinder.

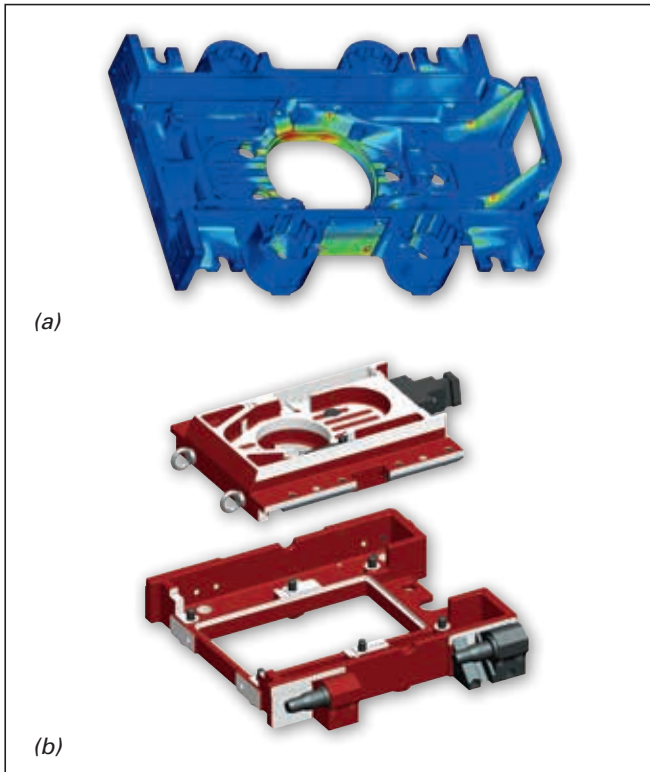


Figure 5. Advanced mechanical design. (a) principal stress pattern in the housing and (b) two-piece slider design of the INTERSTOP Ladle Gate Type S.

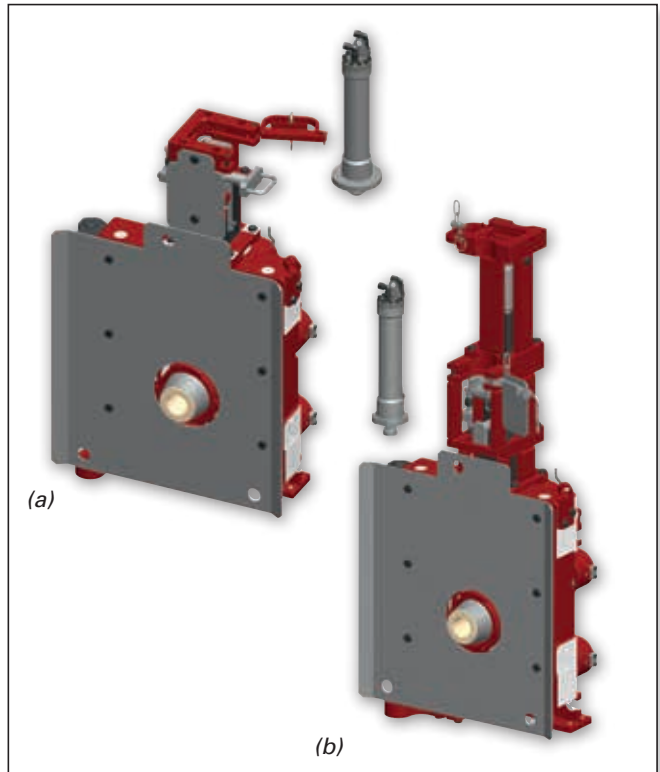


Figure 7. Coupling of the mounting cylinder (a) sideways with a standard drive or (b) from the front in the case of an extended drive configuration.

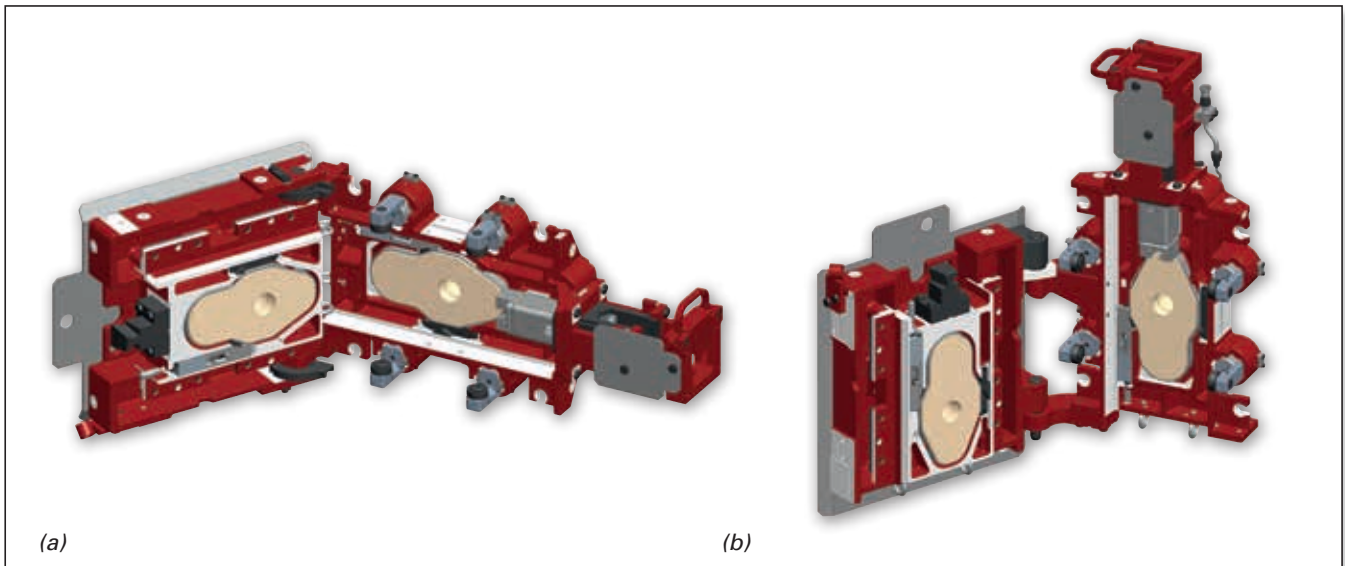


Figure 6. Mounting flexibility of the INTERSTOP Ladle Gate Type S. (a) horizontal and (b) vertical mounting position.

Superior Tensioning System

The INTERSTOP Ladle Gate Type S series features an automatic tensioning system to ensure optimal surface contact between the plates. At its core are four independent tensioning modules (Figure 8). Each tensioning module can be easily and quickly removed and attached to the housing. The spring elements are designed for highest durability to provide reliable tensioning also during operations where the system is exposed to high temperatures (e.g., vacuum tank degassing). The system tensioning can be checked either offline or online when the INTERSTOP Ladle Gate Type S is mounted to the ladle.

The transfer of tension via rollers minimizes wear during system operation, which also has a positive impact on the system reliability, maintenance requirements, and costs. The tensioning system does not require lubricants.

Maintenance-Friendly Design

The INTERSTOP Ladle Gate Type S consists of only a few parts (Figure 9), and the design enables easy and quick access to all parts for cleaning, inspection, and maintenance. The parts are designed for a long lifetime to minimize effort and costs and to guarantee long inspection intervals and short inspection times.

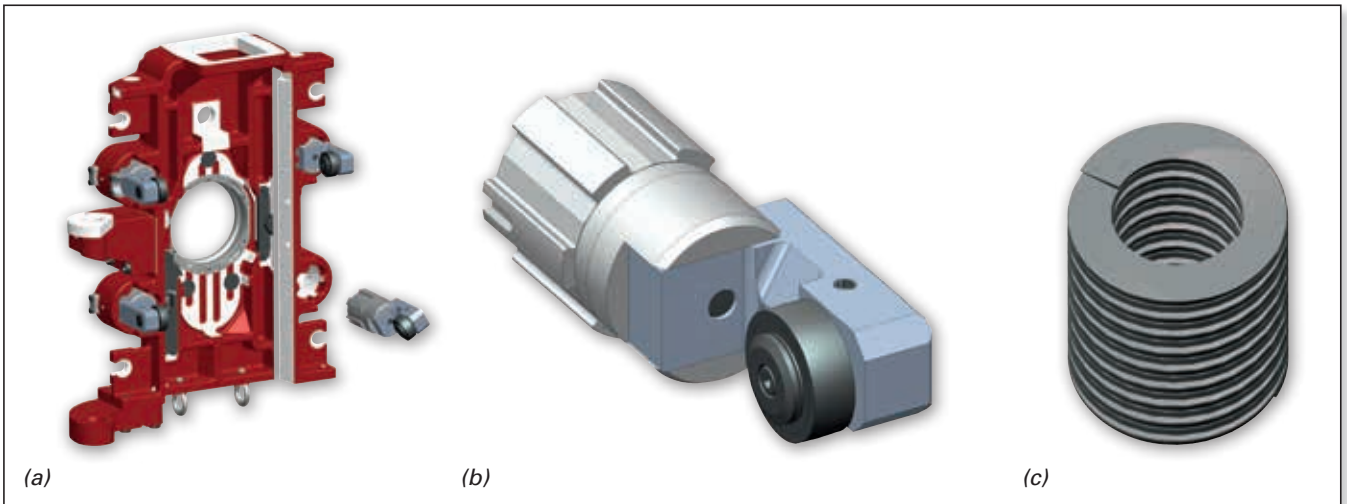


Figure 8. Ladle Gate Type S tensioning system. (a) tensioning modules positioned within the housing, (b) tensioning module, and (c) spring element.

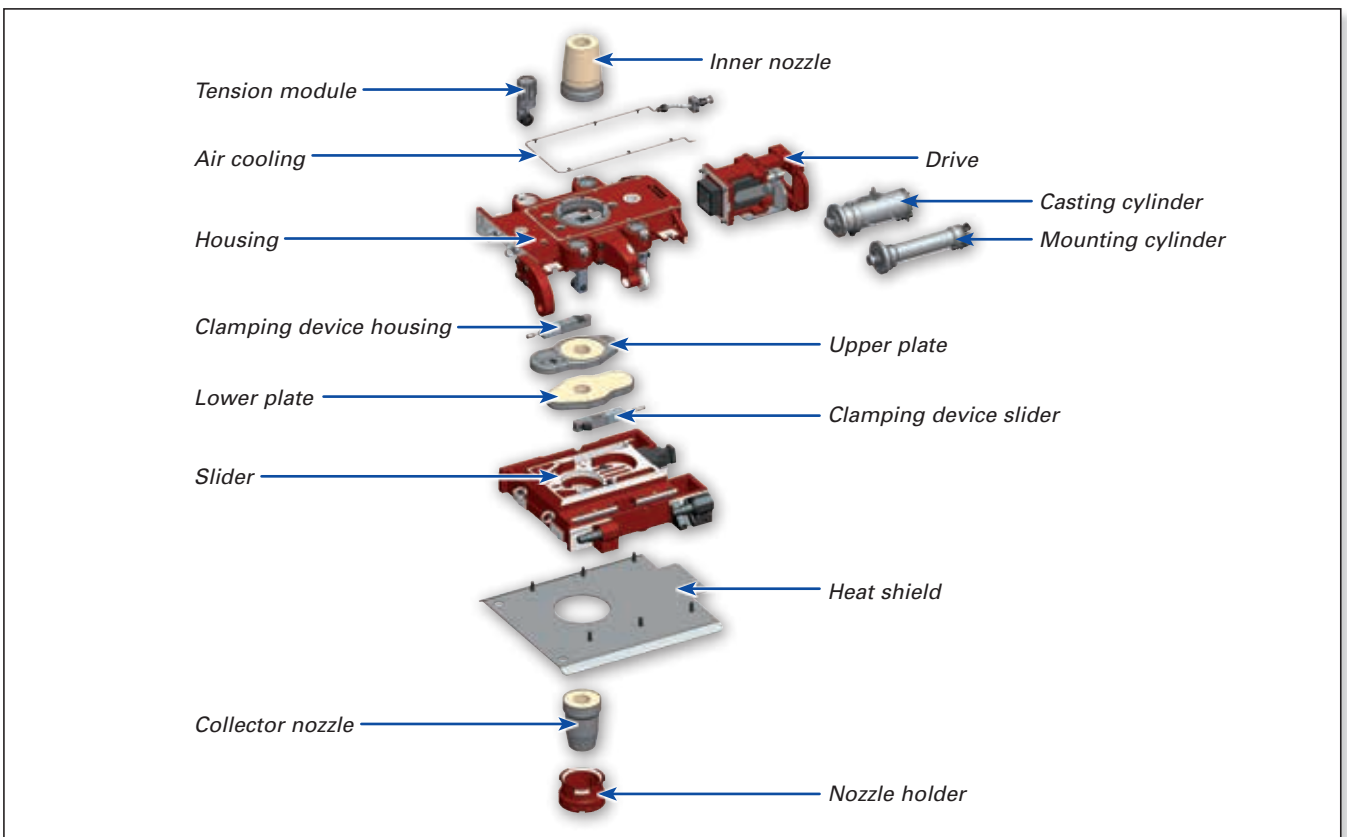


Figure 9. Main parts of the INTERSTOP Ladle Gate Type S.

Quick Operation at the Preparation Area

Due to the superior handling characteristics, less actions have to be performed by personnel to exchange the refractory parts. For example:

- >> Due to the automatic tensioning system, no tools and devices are required to load or unload the tension, and no parts need to be screwed or removed.
- >> The refractory plates are self-clamping.
- >> The refractory plates are easily removable and easy to install; no screws have to be manipulated.

As a result the time demand for the ladle at the preparation area is decreased. Furthermore, the critical manual handling activities in the harsh working environment beside the hot ladle are minimized for personnel. This leads to substantial time savings and the following advantages:

- >> Personnel are less exposed to heat and radiation.
- >> Quick ladle availability.
- >> Increased crane availability.

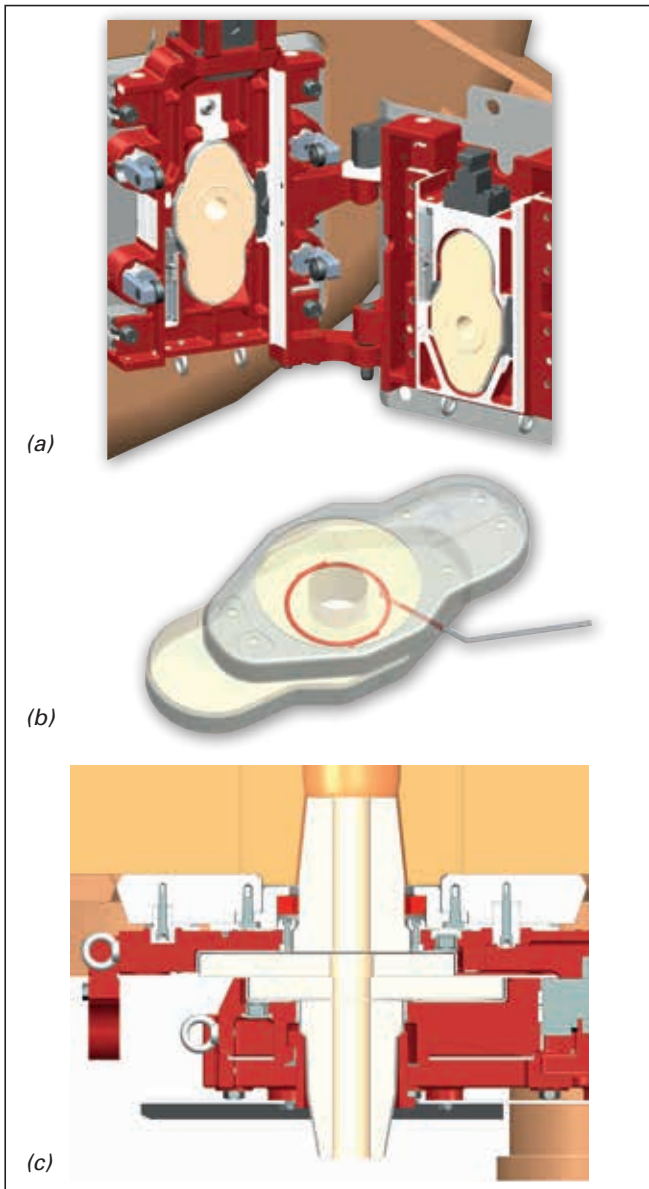


Figure 10. Ladle Gate Type S design features to counteract the introduction of impurities. (a) option for argon purging between the plates, (b) large plate overlap in the casting position, and (c) installation of a slag detection system.

Clean Steel Readiness

Throttling the steel flow naturally creates an under pressure that INTERSTOP counteracts by special design features in the Ladle Gate Type S in combination with INTERSTOP inert gas purging solutions (Figures 10a and 10b) (see page 13). As a result, all external influences causing the formation of Al_2O_3 inclusions can be eliminated.

A significant source of nonmetallic inclusions is due to slag carryover from the ladle into the tundish and the most effective measure to control this is the installation of an effective slag detection system. The Ladle Gate Type S series enables easy integration of such a system, providing effective support for all clean steel orientated customers (Figure 10c).

Innovative Refractories

The principal layout of the inner nozzle, plates, and collector nozzle is shown in Figure 11. The well-proven inner nozzle design from other INTERSTOP ladle gate systems, comprising a mechanical stop, ensures a controlled thickness of the mortar joint between the nozzle and upper plate. The exchangeable nozzle follows the zero-joint concept based on positive experiences with previous INTERSTOP ladle gate systems.

The opportunity for flexible use of two refractory plate sizes within the same sized mechanical system leads to lower operational costs due to the optimized plate geometry.

The INTERSTOP Ladle Gate Type S plates are optimized with regards to:

- >> Maximized overlap in the open, closed, and throttling position provided by the plate geometry.
- >> Minimized size through the unique automatic plate self-clamping feature.

The results are decreased operating costs without increased risk of a system failure. Hence, the improvement of refractory utilization is achieved without restrictions concerning safety and clean steel production.

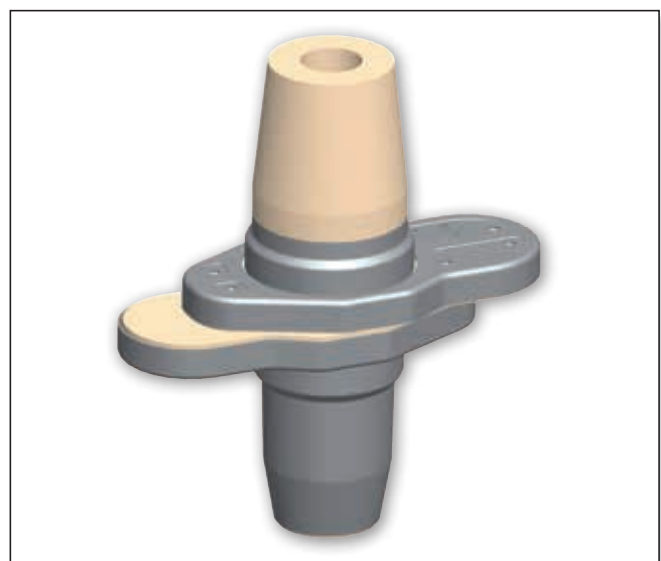


Figure 11. Refractory layout of the INTERSTOP Ladle Gate Type S.

The self-clamping enables an optimized plate design and new plate shape. The refractory plate is flat, without grooves or recesses, and the compact design supports a wider refractory grade portfolio. In addition, the directional forces resulting from the specific mounting configuration provide a large area of compressive stress, especially to the critical regions of the slide gate plate (Figure 12). These forces, together with the geometric plate design, lead to a defined plate cracking pattern, resulting in the fact that cracks are directed to non-critical areas. Besides operational safety, another positive effect is an increase in refractory performance.

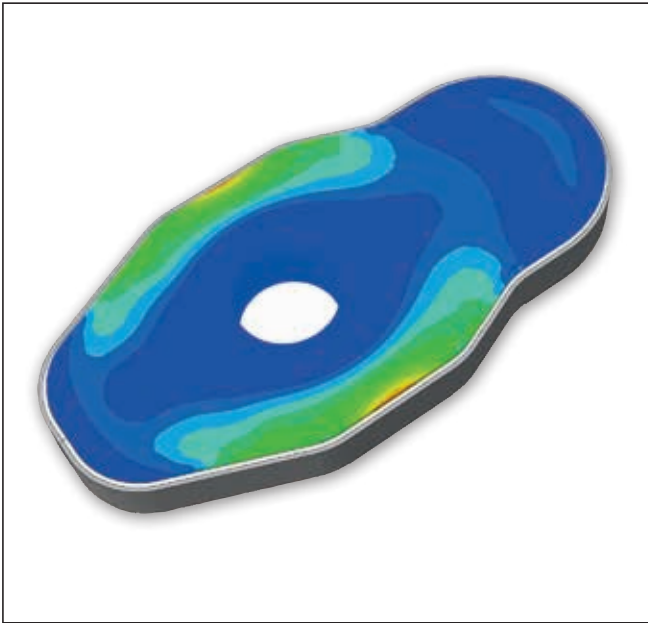


Figure 12. Principal stresses on a refractory INTERSTOP Ladle Gate Type S plate.

INTERSTOP Ladle Gate Type S is an Integral Part of the System Package

The new INTERSTOP Ladle Gate Type S is an integral part of RHI's system approach, to enable outstanding operational results with regards to system reliability, safety for personnel and the process, as well as minimal operational costs (calculated in terms of TCO). The total package consists of:

- >> Automated Tundish Level Control (TLC) system.
- >> Advanced hydraulic/electronic process control system.
- >> Simulation of optimized casting diameter and flow geometry.
- >> Full refractory package comprising a highly developed brand portfolio including inner nozzles, plates, collector nozzles, well filler sands, and mortars to provide clear ownership and optimization opportunities.
- >> Intensive training and after-sales service.
- >> Long-term reliable supply and spare part availability.

Summary

The new INTERSTOP Ladle Gate Type S series is proven to be a high-performance ladle gate in terms of mechanical lifetimes, refractory performance, and system reliability. The Ladle Gate Type S series features outstanding designs and functions like those described above, and is the gate offering superior handling and maintenance characteristics for operator personnel.

As an integral part of the RHI and INTERSTOP system package approach, the Ladle Gate Type S is the best available slide gate system for customers demanding low TCO impact, support of clean steel production, and highest system reliability in terms of operator and process safety.

Authors

Reinhard Ehrenguber, Stopinc AG, Hünenberg, Switzerland.

Roland Bühlmann, Stopinc AG, Hünenberg, Switzerland.

Corresponding author: Reinhard Ehrenguber, reinhard.ehrenguber@rhi-ag.com

GYRO Nozzle—The Innovative Solution for High-Performance Bloom and Billet Casting



The newly developed GYRO Nozzle from RHI reduces the jet penetration depth in billet and bloom moulds and generates soft stirring. As a result, this nozzle design promotes the flotation of nonmetallic inclusions and slightly activates the meniscus surface resulting in enhanced particle absorption by the mould flux.

The helix-type slotted ports can be designed for specific customer requirements, tailored to the individual casting conditions. A further benefit is the even velocity distribution leads to a longer slag band lifetime and reduced corrosion.

The innovative GYRO Nozzle is targeted to clean steel production, providing a competitive advantage for our highly valued customers.

Bianca Agnes Secklehner, Marcos Tomás Casado, Andreas Viertauer, David Wappel and Bianca Brosz

Tundish Technology and Processes: A New Roadmap

During the last few years, steel plants have been changing the way they address the steel market. In a very competitive, global environment the search for differentiation is needed and can be attained through a wide steel grade portfolio, extending from commodity to high-end clean steel grades. For the first case, the focus is on optimizing total running costs mainly through longer sequences at the caster, namely endless casting. For the latter area, differentiation can be achieved through technological advances, casting special grades, and/or creating and casting new qualities that can fulfil existing or new steel applications: This can be summarized as meeting high metallurgical targets to produce clean steel. From the tundish perspective this situation generates segmentation on the market, as the targets and product requirements are very different: Open casting technology, shrouded casting technology, as well as the general processes. However, although the product requirements are different, cost efficiency is a huge driver for both. This article provides a short overview about existing tundish technology and processes and the diverse influencing parameters in this context. It is the first in a series of publications on this topic, each focusing in detail on different aspects. This paper introduces RHI's New Tundish Roadmap and describes the sources and influence of hydrogen, nitrogen, and carbon pick-up in the tundish, presenting recent conclusions and accumulated experiences to improve these typically undesired pick-ups.

Introduction

Over many years, the tundish has progressively extended its function from a single, initial role of distributing steel to the moulds to a multifunctional vessel with increasing quality implications [1]. While optimal distribution is essential to assure caster productivity and low production costs, the impact of different tundish operations on the required final product performance has become more and more evident. Computational fluid dynamics (CFD) simulation and water modelling, as well as know-how generated on site are amplifying an understanding of the continuous casting process and driving new developments in this field.

Tundish technology and processes involve multiple factors that have to be considered and have different weight and/or impact depending on the desired final steel grade and properties. These topics can be subdivided into the three groups concerning metallurgy and design, and are summarized in Table I.

	Topic
Group I	>> Hydrogen and nitrogen pick-up >> Carbon pick-up
Group II	>> Nonmetallic inclusions and defects in semi-finished products originating from the tundish >> Slag entrainment >> Clogging/castability >> Ladle and tundish slag (e.g., tundish cover powder influences) >> Temperature and heat losses >> Open eye formation
Group III	>> Tundish shape and size >> Tundish bath level and maximum yield >> Flow pattern: Residence time distribution analysis, compensating ladle shroud misalignment effects, minimizing steel losses during grade changes >> Safety and environment

Table I. Topics relating to metallurgical and design issues in the tundish.

RHI's New Tundish Roadmap

The clustering of topics in Table I provides a structured approach to address the diverse tundish-related issues. It is the basis for RHI's New Tundish Roadmap, which comprises tundish technology and processes (Figure 1), tundish refractories (Figure 2), tundish reactions (Figure 3), and tundish simulation methods (Figure 4). Developed to systematically provide a range of interrelated services, the New Tundish Roadmap shares RHI's know-how and findings, thereby supporting steel producers. It constitutes a novel and future-orientated way of looking at all the variables involved in the tundish during the continuous casting of steel. Every topic has greater or less relevance depending on the steel grade and property requirements, which also determine the type of casting process. There are also multiple interconnections between certain topics.

The Tundish Technology and Processes

A summary of tundish technology and processes is shown in Figure 1. It includes open casting on the left-hand side, which is represented by a metering nozzle changer (INTERSTOP MNC-RSP). The alternative shrouded casting option is depicted on the right-hand side with isostatically pressed products (i.e., mono-block stopper and submerged entry nozzle), a weir, purging beam, and tundish lid. The general requirements that are beneficial for both open and shrouded casting include a TUNFLOW antiturbulence box for the impact area, pictured in the middle.

All these diverse requirements in continuous casting are very challenging for steel producers, as well as refractory and flow control suppliers. Frequently, there are conflicts of objectives to overcome when looking for the best concept on site. As a global partner for the steel industry, RHI's goal is to offer extraordinary customer solutions based on individual conditions and demands. Apart from unique material concepts and innovative designs, technological partnerships are provided by taking an in-depth look at the customer's metallurgical requirements.

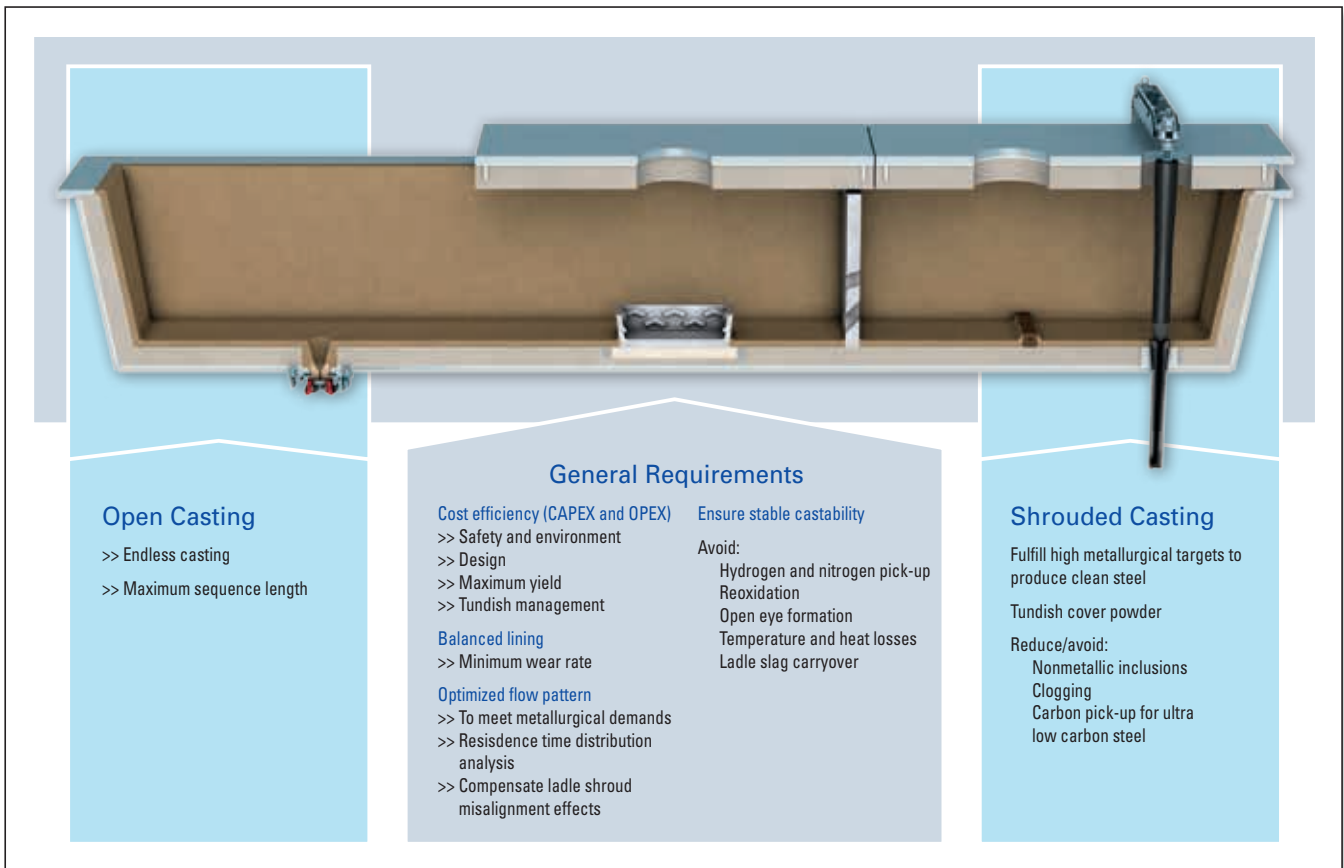


Figure 1. Tundish technology and processes.



Figure 2. Tundish refractories.

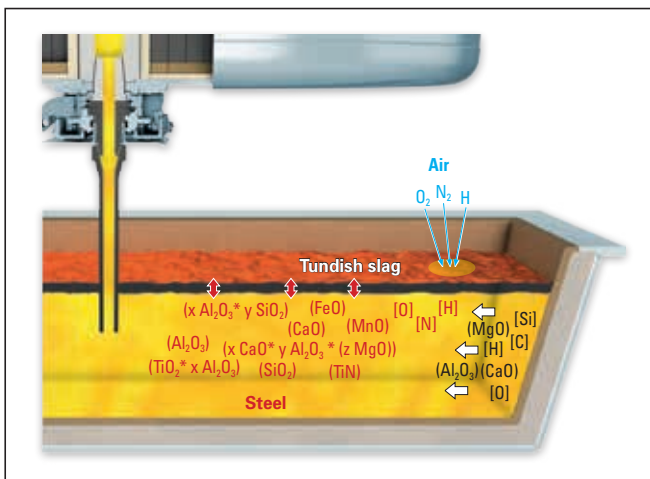


Figure 3. Tundish refractions.

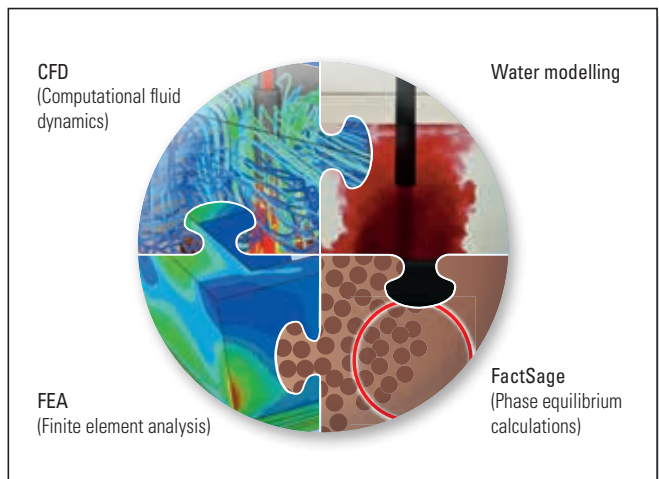


Figure 4. Tundish simulation methods.

The following sections in this paper focus on the Group I topics summarized in Table I: Hydrogen and nitrogen pick-up as well as carbon pick-up.

Hydrogen and Nitrogen Pick-Up

Hydrogen causes a number of steel defects and failures. These defects result from internal pressures that develop when hydrogen atoms pair to form the stable higher volume H₂ molecule [2]. Just a few parts per million of hydrogen dissolved in steel can cause hairline cracks (i.e., flakes), especially in the case of increasing manganese content in the steel (Figure 5); hydrogen induced cracks (HIC), especially for API steel grades (sour gas tubes) where sulphur and phosphorus are present at very low levels (Table II); hydrogen embrittlement; as well as hydrogen blistering and loss of tensile ductility, particularly in large ingots, blooms, and slabs [3]. In combination with nitrogen, hydrogen can lead to pinholes and blowholes (Figure 6).

Hydrogen and nitrogen are inevitable components in all commercial steels. Nitrogen can be considered an impurity or a desired alloying additive, being present interstitially in steel or as a nitride of aluminium, titanium, and/or other nitride-forming elements. Dissolved nitrogen in the steel can increase yield and tensile strengths, decrease ductility, and adversely affect the formability of ultra low carbon (ULC)

cold rolled steel (Table III). A summary of the maximum hydrogen, nitrogen, and carbon impurity levels, among other elements, for various steel products is provided in Table II.

Sources of Hydrogen Pick-Up From the Ladle to the Tundish

Hydrogen pick-up by liquid steel during casting is a very complex process. The standard industrial method to correctly measure hydrogen uses the Hydris sensor system from Heraeus Electro-Nite [2]. Monitoring has shown that in reality the total hydrogen pick-up results from various sources, which are described in the following sections.

Elements	Form	Mechanical properties affected
Nitrogen and carbon	Solid solution	>> Solid solubility (enhanced), hardenability
	Settled dislocation	>> Strain aging (enhanced), ductility and toughness (lowered)
	Pearlite and cementite	>> Dispersion (enhanced), ductility and toughness (lowered)
	Carbide and nitride precipitates	>> Precipitation, grain refining (enhanced), toughness (enhanced) >> Embrittlement by intergranular precipitation

Table III. Influence of nitrogen and carbon levels on mechanical properties [6].

Steel product	Maximum impurity fraction	Maximum inclusion size
IF steel Automotive and deep-drawing sheet	[C] ≤ 30 ppm, [N] ≤ 40 ppm, T.O ≤ 40 ppm, [C] ≤ 10 ppm, [N] ≤ 50 ppm [C] ≤ 30 ppm, [N] ≤ 30 ppm	100 µm
Drawn and ironed cans	[C] ≤ 30 ppm, [N] ≤ 30 ppm, T.O ≤ 20 ppm	20 µm
Alloy steel for pressure vessels	[P] ≤ 70 ppm	
Alloy steel bars	[H] ≤ 2 ppm, [N] ≤ 10–20 ppm, T.O ≤ 10 ppm	
HIC resistant steel (sour gas tubes)	[P] ≤ 50 ppm, [S] ≤ 10 ppm	
Line pipe	[S] ≤ 30 ppm, [N] ≤ 35 ppm, T.O ≤ 30 ppm, [N] ≤ 50 ppm	100 µm
Sheet for continuous annealing	[N] ≤ 20 ppm	
Plate for welding	[H] ≤ 1.5 ppm	
Bearing	T.O ≤ 10 ppm	15 µm
Tyre cord	[H] ≤ 2 ppm, [N] ≤ 40 ppm, T.O ≤ 15 ppm	10 µm
Nongrain-orientated magnetic sheet	[N] ≤ 30 ppm	
Heavy plate steel	[H] ≤ 2 ppm, [N] ≤ 30–40 ppm, T.O ≤ 20 ppm	Single inclusion 13 µm Cluster 200 µm
Wire	[N] ≤ 60 ppm, T.O ≤ 30 ppm	20 µm

Table II. Steel cleanliness requirements for various steel products [7,8]. Abbreviations include total oxygen content (T.O).

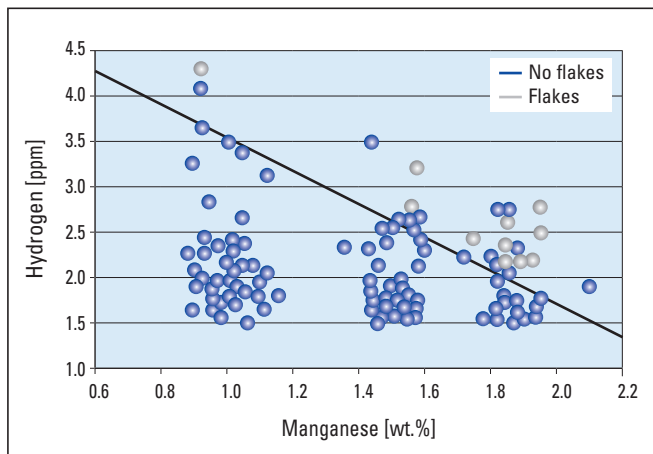


Figure 5. Relationship between hydrogen and manganese levels and the formation of flakes [4].

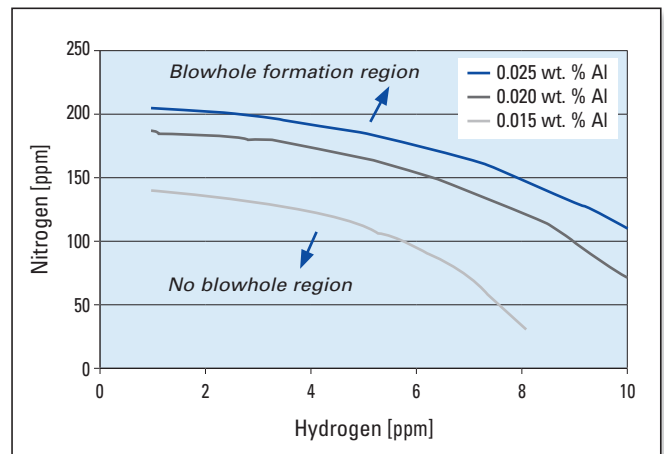


Figure 6. Influence of hydrogen and nitrogen levels on the formation of blowholes [5].

Tundish Wear Lining

If the tundish wear lining contains significant amounts of water (e.g., slurry gunning mixes) and the drying process is not sufficient for total water evaporation, the residual water can result in hydrogen pick-up during the first and second ladle of a sequence. This phenomenon is shown in Figure 7 [9] where it is clear that hydrogen pick-up from the tundish lining decreases significantly with longer casting times and an increased sintered layer thickness.

For the first ladle of a casting sequence, some of the hydrogen pick-up may possibly come from the tundish lining. With longer casting times, the impact from the tundish lining decreases significantly because all the remaining water after preheating is fully released during the first two ladles. Consequently, a significant increased hydrogen pick-up after the first ladle is unlikely to come from the tundish lining and can only be explained by a wet cover powder, high turbulences, and/or an insufficiently dried tundish [9].

Tundish Mortars and Castables

Mortars and castables are used during tundish preparation, for example to fix nozzles and isostatically pressed products and for permanent lining repair. Typically cements containing nonbasic or basic materials are used for this type of repair or fixation. To activate the binding reaction a certain amount of water is added. Insufficient drying of these mixes is a critical aspect that can lead to increased hydrogen pick-up in the steel.

Different Sources of Air Ingress

Air is always humid and consequently a source of potential hydrogen pick-up, although it is important to note air has a greater influence on nitrogen pick-up than hydrogen. Air can enter the steel bath through the various routes described below:

- >> During a ladle change caused by a reduction of the bath level.
- >> High turbulences leading to an open eye (an area that is not covered by tundish cover powder) during the casting process.
- >> Suction through ladle slide gates.
- >> Suction into the ladle shroud or ingress during a ladle shroud change.

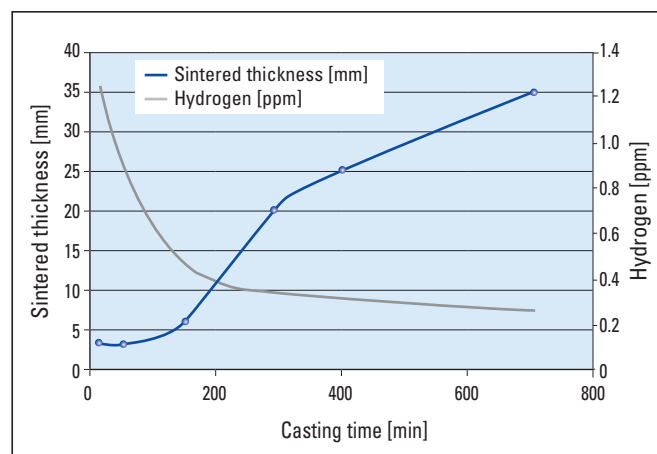


Figure 7. Relationship between hydrogen pick-up in the tundish and thickness of the sintered lining layer [9].

- >> Contact in the case of a non self-opening ladle (i.e., O₂ lancing).

Furthermore, increased air humidity levels can result in higher hydrogen pick-up, as was observed at a U.S. Steel plant (Figure 8) [10]. The measurements taken at the caster over a 17-month period indicated that atmospheric conditions can have an impact on hydrogen pick-up.

Moisture or Chemically Bonded Hydrogen in Tundish Cover Powder

An external source that has a significant influence on hydrogen pick-up in the tundish is the moisture or chemically bonded water from different additives that are applied during casting, for example the tundish cover powder. This aspect is discussed in detail in a later section using a case study.

Water Vapour or Hydrogen Adsorption from Preheating Gas

Depending on the chemical composition of the burned gas and adjustment at the preheating station, adsorption of water vapour and/or hydrogen by the tundish wear lining can be possible. This is due to the fact that the open porosity of the wear lining ranges from 30–45 vol.%, which enables infiltration over the entire wear lining thickness. For example, the combustion reaction for methane gas is:



This can be a problem especially if high hydrogen-containing gases are used for preheating, such as BOF gas and/or coke oven gas.

Minimizing Hydrogen Pick-Up

The following options are available to avoid or minimize hydrogen pick-up in the tundish:

- >> Change the wear lining method to a lower water content material.

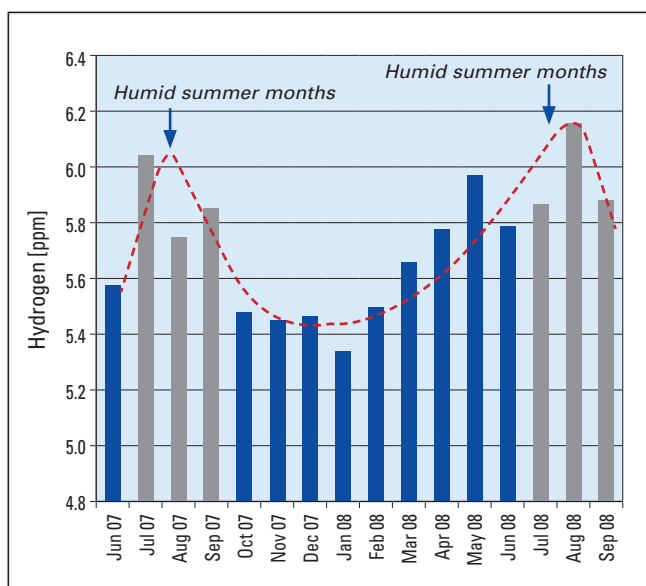


Figure 8. Average monthly hydrogen levels in all nondegassed heats over a 17-month period at a U.S. Steel plant [10].

- >> Seal the tundish with inert gas to displace and/or avoid any air and thereby moisture contact. A protective tundish lid with carefully sealed edges also helps to avoid contact with moisture-containing air.
- >> Measure and control the water content of the tundish cover powder before application and avoid the presence of hydrated phases (e.g., Ca(OH)₂).
- >> Evaluate the steel flow via CFD or water modelling to reducing the bath surface turbulence in the impact area at all times during casting and avoid direct contact between the steel melt and moisture in the air.

Regarding the wear lining method, the total amount of water in the mix after lining with different lining technologies is shown in Table IV. Compared to a slurry gunning mix, where the water content exceeds 25 wt.%, a dry setting mix contains significantly lower levels of chemically bonded water in the binder.

By definition all organic substances contain carbon and hydrogen atoms that can be oxidized at a certain temperature resulting in the release of carbon dioxide and water. The thermogravimetric analysis of a pure organic binder used in the cold setting mix technology is shown in Figure 9. Water vapour from oxidation of the organic binder is mainly formed in the temperature range between 170–300 °C. Carbon dioxide formation starts at a temperature of 200 °C, with two characteristic peaks at 230 °C and 480 °C. After 600 °C no CO₂ and H₂O are formed because the entire volatile fraction of the organic binder has reacted (mass reduction nearly 100%). In conclusion, the results indicate that all volatile components are removed below 600 °C and water is nearly completely removed at < 300 °C.

Another important factor for hydrogen pick-up that has to be considered is how water release actually happens in the

mix. This differs between slurry gunning mixes, and dry setting and cold setting mixes, as described in the following sections.

Slurry Gunning Mixes

After lining is finished and the hardening process has taken place at ambient temperature, the water added to the slurry mix is physically bonded. In theory, this physical water will evaporate at 100 °C during the drying process and migrate towards the permanent lining. Due to the strong interaction of the wear and permanent lining caused by the slurry gunning process, there is no gap between the two. Furthermore, the amount of water that has to be removed from the wear lining is very high compared to the other lining technologies (see Table IV). Therefore, high amounts of water will evaporate and migrate through the wear lining towards

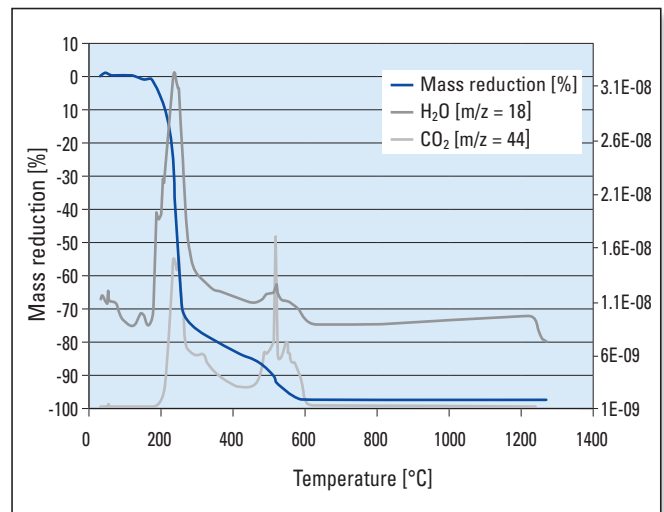


Figure 9. Thermogravimetric and differential thermal analysis of a RHI organic binder in the self-hardening mixes in air.

	Slurry gunning	Dry setting	Cold setting, liquid binder	Cold setting, self hardening
Necessary equipment	ANKERTUN machine	Curing equipment and template	ANKERTUN CS machine and template	ANKERTUN CS machine and template
Mix	Slurry gunning mixes	Dry setting mixes	ANKERTUN liquid binder mixes	ANKERTUN self hardening mixes
Curing	3–6 hours from RT up to 550 °C (depending on wear lining thickness)	1.5 hours from RT up to 250 °C	30 minutes setting at RT	30 minutes setting at RT
Curing equipment	Gas burner	Hot air generator/electric heating/gas burner	Not necessary	Not necessary
Cold start	Not possible	Possible	Possible	Possible
Preheating	Up to 1250 °C	Up to 1250 °C	Special preheating curve required (RT to 1000 °C within 1 hour)	Special preheating curve required (RT to 1000 °C within 1 hour)
Heating equipment	Gas burner	Gas burner	Gas burner	Gas burner
Lining and curing	5–9 hours	2–4 hours	45–90 minutes	45–90 minutes
Chemically bonded water in binder	0.5 wt. %	1.5–2.5 wt. %	2.0–2.5 wt. %	1.8–2.0 wt. %
Added fresh water during lining	25–30 wt. %	0 wt. %	0 wt. %	1.2–1.5 wt. %
Total amount of water after lining	25–30 wt. %	1.5–2.5 wt. %	2.0–2.5 wt. %	3.0–3.5 wt. %
Hydrogen pick-up potential	Water addition necessary for spraying the mix	Water coming from binding agents. Depending on the binding system different water content	Water coming from the liquid binder and hardener	Water coming from the binding agents and water addition
Carbon pick-up potential (total carbon content)	0.7–1.0 wt. %	0.0–2.3 wt. %	0.3 wt. %	~1.9 wt. %

Table IV. Characteristics of different tundish wear lining technologies. Abbreviations include room temperature (RT).

the permanent lining (Figure 10). In most cases the permanent lining temperature is below 100 °C, which causes condensation of the evaporated water in either the back of the wear lining or the permanent lining. Consequently, a high amount of energy and quite high temperatures are required on the inner side of the tundish to fully remove water from the wear and permanent lining.

This migration phenomenon was examined by installing resistors at different heights in the tundish, as the drier the lining becomes the higher its resistance. The measurements clearly showed that there was a water vapour stream into the permanent lining and not towards the top of the tundish (see Figure 10). Due to the high amount of water, lengthy evaporation period, and strong interaction between the permanent and wear lining, the potential for residual water in the tundish is higher than with dry setting and cold setting linings.

Dry Setting and Cold Setting Mixes

Due to the different lining concept of dry setting and cold setting mixes, the mechanism of water removal is different. The tundish mix is filled into the tundish (with or without vibration) and not sprayed, which reduces the binding strength between the wear lining and the permanent lining. It is common that there is a small gap in between, which leads to much easier water release at the interface. For the same drying or preheating conditions used for slurry gunning mixes, water is released into this gap at a much earlier stage. Using the same experimental setup as described above (i.e., installation of resistors at different heights between the wear and permanent lining), the water release into this gap was clearly detectable. There was a clear water stream from the bottom to the top of the tundish, which could be measured from the decreased resistance due to water vapour increase (see Figure 10).

In comparison to the slurry gunning mix, the experiment also showed that the removal of water was much faster and easier. Furthermore, the total amount of water (physically and chemically bonded) in the dry setting and cold setting mixes is approximately 90% less than in slurry gunning mixes, which generally indicates that the potential for hydrogen pick-up coming from the water in the wear lining is much higher for slurry gunning mixes.

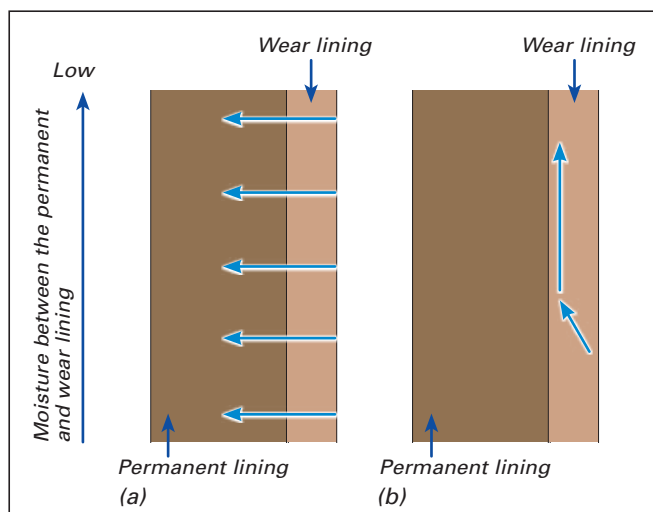


Figure 10. Water release for different tundish lining technologies. (a) slurry gunning mixes and (b) dry and cold setting mixes.

This behavioural difference also has an impact on the permanent lining performance, namely it normally increases when dry or cold setting mixes are installed as a wear lining. To reduce the potential influence of the hydrogen coming from the wear lining a change from slurry gunning mixes to dry setting or cold setting mixes is recommended. If for whatever reason a change of wear lining technology is not an option, an optimized drying/preheating curve—both temperature and time—can lead to a reduction of hydrogen pick-up coming from the tundish lining.

Another important factor for slurry mixes is the use of an appropriate tundish steel shell design (i.e., with holes). It should enable condensation on the outer part of tundish steel surface, facilitating water extraction, otherwise there is a potential for hydrogen pick-up due to the lack of water diffusion through the permanent lining during drying and preheating.

Hydrogen Pick-Up From Tundish Cover Powder—Case Study

A short case study was performed to examine the potential for hydrogen pick-up from water/hydrogen-containing cover powders using a calcium aluminate tundish cover powder with the composition and mineral phases detailed in Table V. It had a high CaO content and a high loss on ignition due to thermal decomposition of the prior formed CaCO_3 and Ca(OH)_2 , both of which were detected by X-ray diffraction. When the chemically bonded water was analysed it was found that the total water content of the tundish cover powder was approximately 4.6 wt.%, mainly derived from Ca(OH)_2 .

In the literature it has been proven that tundish cover powder can have a significant influence on hydrogen pick-up if hydrated phases are present, for example Ca(OH)_2 [11,12].

Chemical analysis	Wt. %
Loss on ignition	13
Determination by XRF ⁽¹⁾	
Na_2O	0
MgO	0.5
Al_2O_3	23.77
SiO_2	1.99
K_2O	0
CaO	73.49
TiO_2	0
Cr_2O_3	0
MnO	0
Fe_2O_3	0.15
Phase analysis by X-ray diffraction ⁽²⁾	
Mineral phase	Formula
Lime	CaO
Calcite	CaO_3
Portlandite	Ca(OH)_2
Fluorite	CaF_2

Table V. Chemical analysis and X-ray diffraction of a tundish cover powder sample. Ignited original sample (1) and original sample (2).

Figure 11 shows that the hydrogen pick-up is proportional to the amount of $\text{Ca}(\text{OH})_2$ added (e.g., from the tundish cover powder). Therefore, it is possible that the hydrogen pick-up can increase after the first ladle if fresh cover powder is added.

The theoretical hydrogen pick-up from the calcium aluminate tundish cover powder was calculated as follows. If it is assumed there is 28 tonnes of steel in the tundish and 200 kg of tundish cover powder was added containing 4.6 wt.% water, as mentioned above, this would lead to a maximum water release of 9.2 kg from the cover powder. If the total hydrogen pick-up from the cover powder by the steel is considered to be approximately 2% of the total bonded water [12], assuming that all the hydrogen is picked up within the first tundish, it would result in a total hydrogen increase in the steel of around 6 ppm. These approximate and theoretical calculations demonstrate that even if the $\text{Ca}(\text{OH})_2$ content of the tundish cover powder is only a few percent, the potential for hydrogen pick-up is very high. In this case the solution would be to use a tundish cover powder with comparable chemical composition, which is based on calcium aluminate, but is water free (both moisture and chemically bonded water) so no $\text{Ca}(\text{OH})_2$ can form.

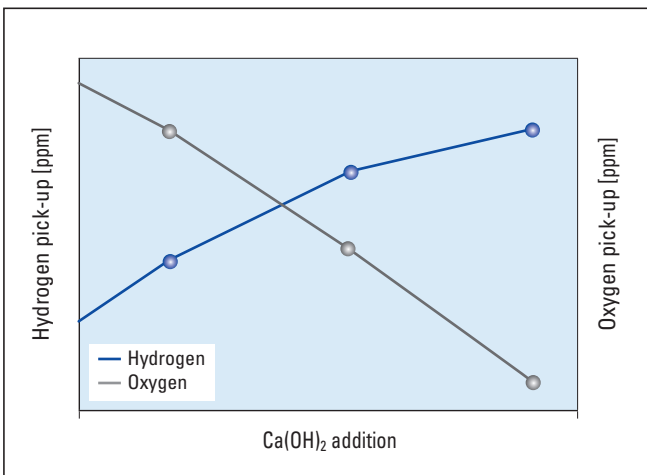


Figure 11. Correlation between hydrogen pick-up and $\text{Ca}(\text{OH})_2$ addition [11,12].

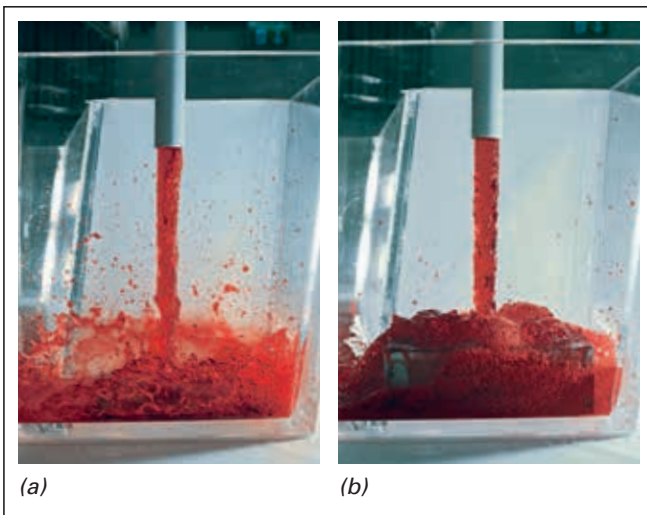


Figure 12. Water modelling of ladle opening (a) without and (b) with TUNFLOW [13].

Avoiding Open Eye Formation

The use of an appropriate TUNFLOW in the impact area of the tundish can significantly reduce surface turbulences and thereby avoid open eye formation. By this means a source of hydrogen and nitrogen pick-up can be minimized (Figure 12).

The turbulent kinetic energy at the tundish surface during steady casting conditions is shown in Figure 13 for a throughput of 2 tonne/minute, a tundish bath level of 1060 mm, and a ladle shroud immersion depth of 300 mm. Using the correct set up in the tundish impact area can reduce a potential source of hydrogen and nitrogen pick-up.

Sources of Nitrogen Pick-Up

The difference between nitrogen content at the end of secondary steelmaking and in the tundish or mould is an indicator of air entrainment during casting. After deoxidation, the low dissolved oxygen content in the steel and pressure distribution at the ladle slide gate system enables rapid air absorption. Nitrogen pick-up therefore serves as a crude indirect measure of total oxygen content, as well as an indication of steel cleanliness and quality problems from reoxidation inclusions, as indicated in Figure 14 [15].

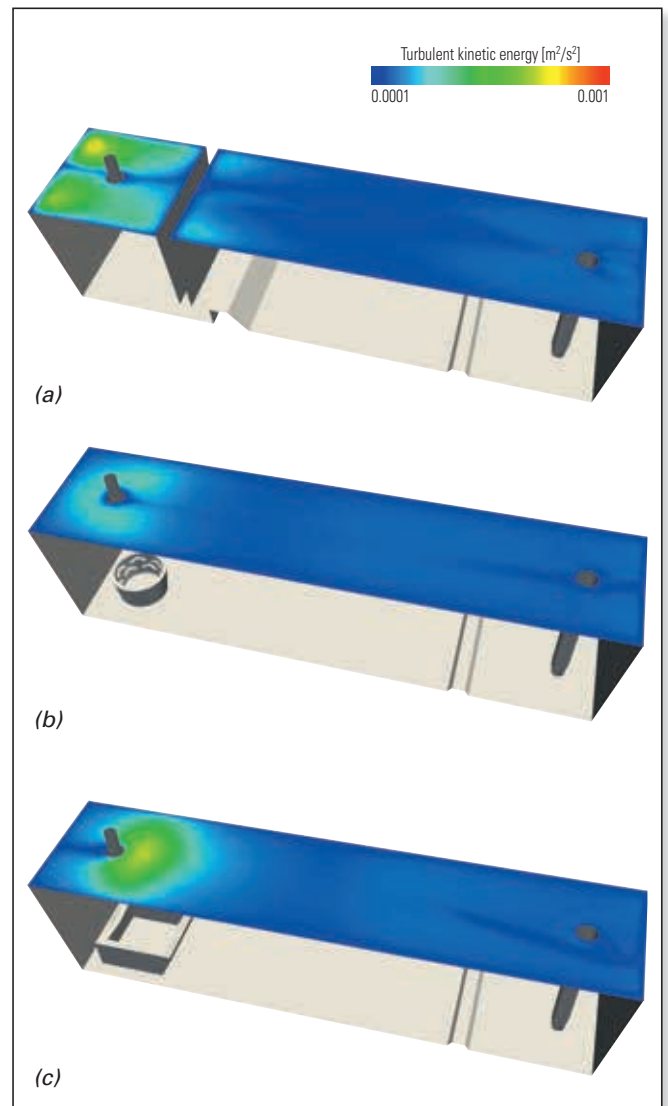


Figure 13. Turbulent kinetic energy at the tundish surface for (a) dam and weir configuration, (b) TUNFLOW CHE impact pot, and (c) normal impact pot [14].

There are several sources of open eye formation and thereby air contact including:

- >> Argon flow too intensive at the shroud.
- >> Off-centre ladle shroud.
- >> Ladle shroud breakage at the slag line.
- >> Too little tundish cover powder.

A high argon flow rate in the shroud can cause an open eye by disturbing the tundish cover powder. This, in addition to leaks in the shrouding system, can expose the liquid metal to the atmosphere and cause oxidation of dissolved aluminium and liquid iron. Such exposure also causes nitrogen absorption [10]. Additionally, a high bath surface turbulence in the

impact area can also expose the liquid metal to the atmosphere and cause nitrogen absorption (Figure 15).

Special consideration regarding nitrogen pick-up needs to be paid during unsteady casting conditions, such as a ladle change and ladle gate opening operations, where slag entrainment and air absorption into the molten steel are possible. Considerable research has been performed in the past few years and published regarding this topic comparing unsteady versus steady casting conditions [17]. Another important factor during ladle opening operations is ladle shroud misalignment (Figure 16), which can lead to air exposure (higher turbulence) if the TUNFLOW for the tundish impact area is not carefully selected.

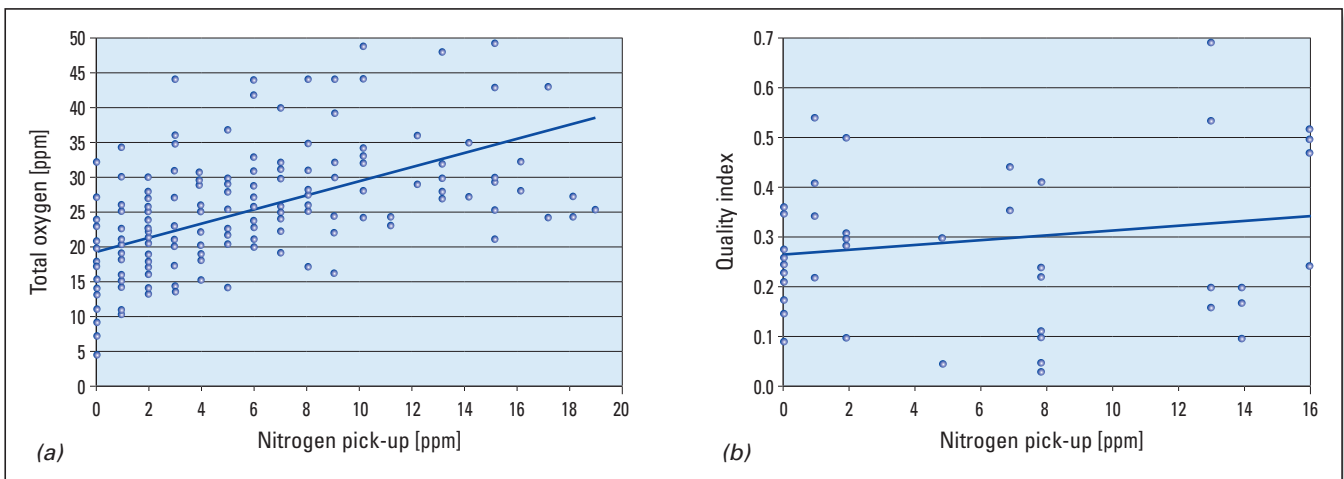


Figure 14. Relationship between (a) total oxygen levels in the steel and nitrogen pick-up and (b) steel quality and nitrogen pick-up [15].

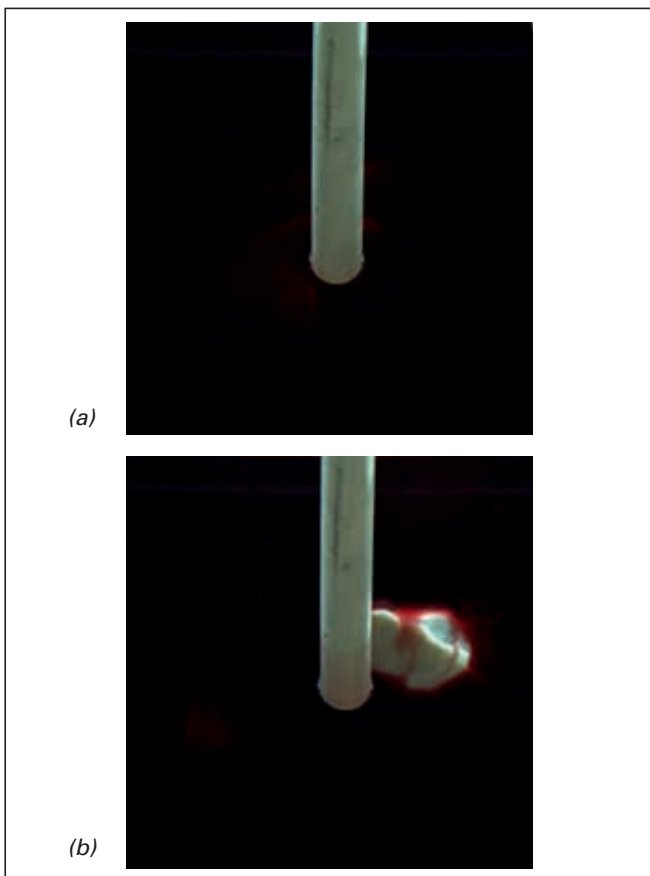


Figure 15. Water modelling simulation showing (a) bath coverage by the tundish cover powder and (b) open eye formation during steady casting conditions [16].

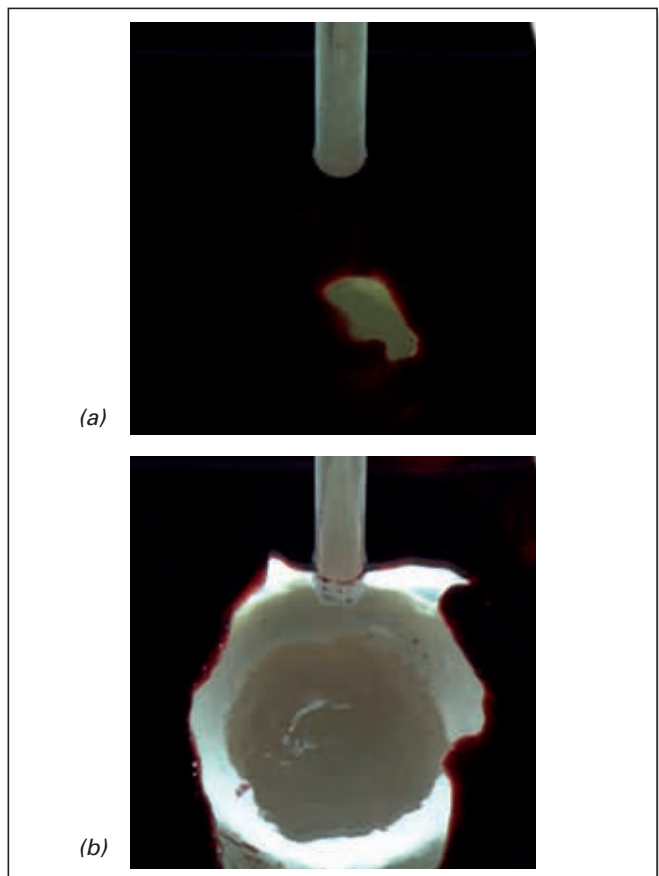


Figure 16. Effect of ladle shroud misalignment (3.2°) during steady casting on the tundish surface. (a) TUNFLOW CHE impact pot and (b) normal impact pot [16].

Minimizing Nitrogen Pick-Up

Generally, nitrogen pick-up can be controlled at 1–3 ppm by optimizing conditions from the ladle to the mould. Inert gas can protect the steel from air contact in many ways. Tundish cover powder is added after the steel is already flowing, in order to prevent nitrogen entrapment into the steel. Combined with the turbulence caused by ladle opening, air entrainment is a problem for up to 15 minutes at the beginning of casting [18]. To combat this problem, the tundish can be purged with inert gas (to displace the air) prior to ladle opening, which lowers both the total oxygen and nitrogen pick-up during start up [19]. The most effective way to prevent air entrainment is shrouded casting. This starts with sealing the slide gate plates and the connection between collector nozzle and the ladle shroud using argon. The nitrogen content development during production of a hydrogen induced crack resistant (HIC) steel (sour gas pipe) is shown in Figure 17. The nitrogen content in the tundish is typically around 45 ppm.

An optimal connection between the sealing rings, argon-shrouded ladle nozzle, and ladle shroud has been shown to lower nitrogen pick-up from 8 to < 1 ppm [6]. In addition, improving the submerged entry nozzle connection and increasing maintenance lowered initial nitrogen pick-up from 1.8 to 0.3 ppm.

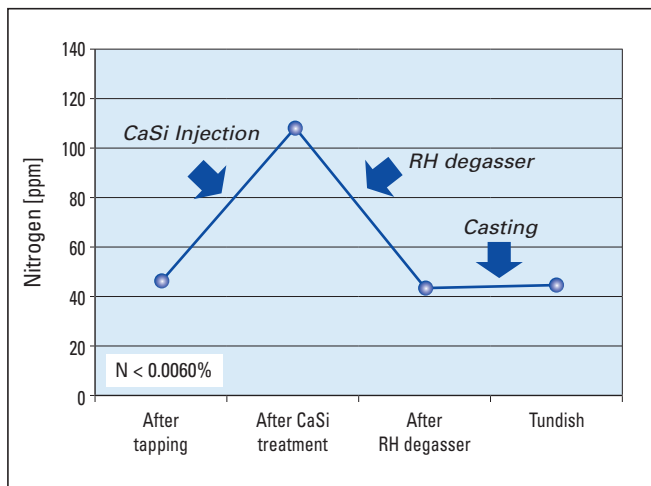


Figure 17. Average nitrogen content development during HIC steel production [20].

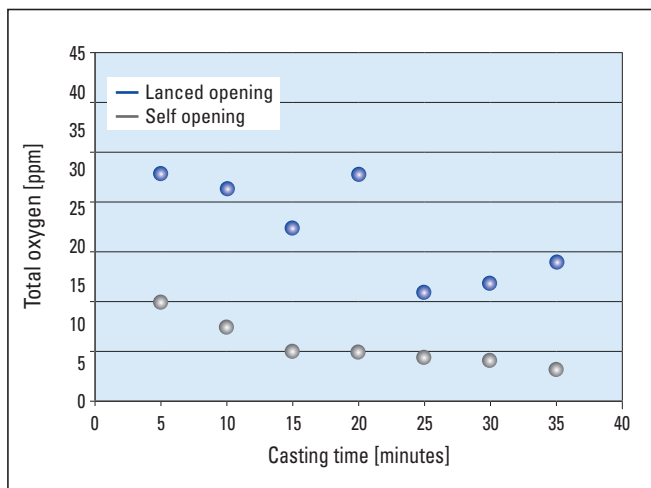


Figure 18. Total oxygen levels resulting from self-opening and lance-opened ladles [18].

A self-opening ladle, which opens without having to lance the nozzle, prevents nitrogen pick-up, as lancing requires removing the shroud. When oxygen lancing is performed it increases the oxygen pick-up in the steel (Figure 18). The use of a reversed taper ladle shroud and submerged ladle opening can have a positive effect on minimizing nitrogen pick-up during unsteady casting conditions.

The tundish cover powder provides several functions. Firstly, it insulates the molten steel both thermally (to prevent excessive heat loss) and chemically (to prevent air entrainment and reoxidation). For example, at IMEXA Steel (Mexico), by changing the tundish cover powder, nitrogen pick-up from the ladle to the mould decreased from 16 to 5 ppm [21]. Therefore a good tundish cover powder practice is highly recommended to avoid this potential source of nitrogen (and hydrogen) pick-up.

Influence and Sources of Carbon Pick-Up

Since molten steel reacts with refractory lining materials, ladle shrouds, monoblock stoppers, submerged entry nozzles, insulating material, tundish cover powder, and mould flux, they can all result in some degree of carbon pick-up during the steelmaking process. Especially for ultra low carbon interstitial-free (ULC-IF) grades with carbon requirements below 20 ppm in the final product and bake-hardenable (BH) steels with a narrow carbon range, a zero pick-up target is challenging. Wherever possible, it is important to use refractory materials with low or carbon-free levels. For example, carbon pick-up can be reduced by 5 ppm when a 1 wt.% carbon-containing tundish insulating material is used compared to a 4.4 wt.% carbon-containing material [22]. The variation in steel carbon content from the BOF to the tundish is shown in Figure 19. It illustrates most of the parameters influencing an increased carbon content during the process are prior to the tundish.

Minimizing Carbon Pick-Up From the Refractory Lining

The different technologies for tundish wear lining and their main parameters are shown in Table IV. While the majority of wear lining mix technologies have a potential for carbon pick-up due to the carbon content in the binding system, a specially developed binding system for dry setting mixes leads to a total carbon content of nearly zero. This binding

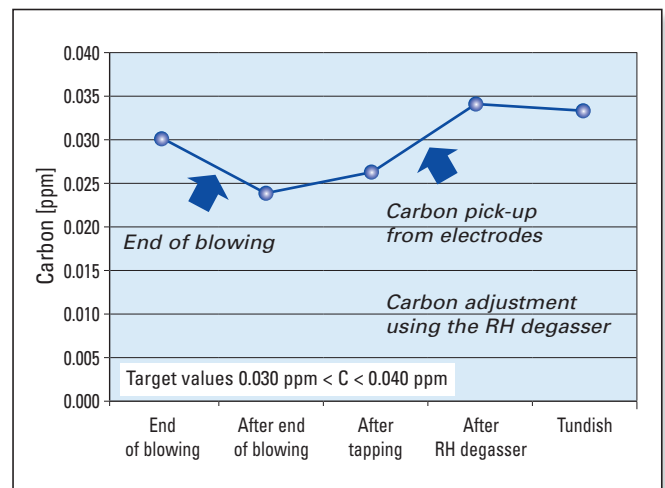


Figure 19. Average carbon content development during steel production [19].

system is available for different raw material concepts and is specially used for ULC-IF steel grades, where a significant reduction of the carbon pick-up has been observed.

Conclusions and Outlook

This article introduces RHI's New Tundish Roadmap, presenting the complexity of diverse requirements that come into play during the continuous casting of steel using both open and shrouded casting techniques. Various metallurgical as well as design aspects have to be considered for the

tundish, to achieve a holistic ladle to mould approach at the customer. In this context the sources and influences of hydrogen, nitrogen, and carbon pick-up in the tundish need to be examined in detail and the various ways to minimize these undesired pick-ups such as avoiding air ingress at all possible inlets, the correct choice of wear lining, furniture, cover powder, preheating, and an optimized steel flow in the tundish should be adopted. Apart from excellent refractory solutions, RHI provides technological partnerships to support the customer's casting process by carefully considering all the complex requirements.

References

- [1] Marique, C. *IISI Study on Clean Steel: State of the Art and Process Technology in Clean Steelmaking*; International Iron and Steel Institute: Brussels, 2004; p 16–17
- [2] Vergauwens, Ir.M. *Hydri Applications in Modern Steel Making*. Heraeus Electro-Nite International N.V: Houthalen, Belgium, 1996; pp. 30–32.
- [3] Hurst, C.R. and Verhauwens, Ir. M. Heraeus Electro-Nite: Gas Analysis in Steel: Identifying, Quantifying and Managing Hydrogen Pick Up in Steel. Heraeus Electro-Nite Australia and Heraeus Electro-Nite International N.V.
- [4] Haumann, W., Heller, W., Jungblut, H-A., Pircher, H., Poepperling, R. and Schwenk, W. Der Einfluss von Wasserstoff auf die Gebrauchseigenschaften von unlegierten und legierten Stählen. *Stahl und Eisen*. 1987, 12, 585–594.
- [5] Huang, K. and Liu, Q. Blowhole Formation During Solidification of Steel. *Steel Research*. 1996, 67, No. 7, 268–272.
- [6] Zhang, L., Thomas, B.G. and Wang, X. Evaluation and Control of Steel Cleanliness-Review. Proceedings 85th Steelmaking Conference, Iron and Steel Society, Nashville, USA, March 10–13, 2002, pp. 431–452.
- [7] Zhang, L., and Thomas, B.G. State of the Art in Evaluation and Control of Steel Cleanliness. *ISIJ International*. 2003, 43, 271–291.
- [8] Lifeng, Z. and Thomas, B.G. Inclusions in Continuous Casting of Steel. Proceedings XXIV National Steelmaking Symposium, Morelia, Mexico, Nov., 26–28, 2003, pp. 2–9.
- [9] Buoro, S. and Romanell. Use of Dry Refractory Liners in Continuous Caster Tundishes: Characterization and Quality Aspects. Presented at AISTech 2012, Atlanta, USA, May 7–10, 2012.
- [10] Misra, S., Li, Y. and Sohn, I. Hydrogen and Nitrogen Control in Steelmaking at U.S. Steel. Presented at AISTech 2009, St. Louis, USA, May 4–7, 2009.
- [11] Braganca, S.R., Hohemberger, J.M., Vicenzi, J., Marques, C. M., Basegio, T., Lima, A.N.C. and Bergmann, C. P. Reduction of the Hydrogen Content in the Continuous Casting of Steel. Laboratório de Cerâmicos da Universidade Federal do Rio Grande do Sul–LACER/UFRGS, Brazil. www.researchgate.net
- [12] Fruehan, R.J. and Misra, S. Hydrogen and Nitrogen Control in Ladle and Casting Operations, Materials Science and Engineering Department, Carnegie Mellon University Pittsburgh, Jan., 15, 2005. http://energy.gov/sites/prod/files/2013/11/f4/casting_ops.pdf
- [13] Hackl, G., Fellner, W. and Petritz, B. RHI's New Tundish Water Modelling Facility. *RHI Bulletin*. 2013, No. 1, 54–57.
- [14] Tang, Y. 2014. Unpublished data. RHI AG, Technology Center, Leoben, Austria.
- [15] Melville S.D. and Brinkmeyer, L. Evaluating Steelmaking and Casting Practices Which Affect Quality. Proceedings 78th Steelmaking Conference, Iron and Steel Society, Nashville, USA, April 2–5, 1995, pp. 563–569.
- [16] Lukesch, G. 2013. Unpublished data. RHI AG, Technology Center, Leoben, Austria.
- [17] Hackl, G., Wappel, D., Meurer, D., Casado, M.T. and Komanecky, R. Product Development and Flow Optimization in the Tundish by Modelling and Simulation. Presented at AISTech 2014, Indianapolis, USA, 5–8 May, 2014.
- [18] Hughes, K.P., Schade, C.T. and Shepherd, M.A. Improvement in the Internal Quality of Continuously Cast Slabs at Lukens Steel. *Iron and Steelmaker*. 1995, 22, No. 6, 35–41.
- [19] Bannenber, N. and Harste, K. *Rev. Métall. Cah. Inf. Tech.* 1993, 90, 71–76.
- [20] Jungreithmeier, A. and Grill, R. Metallurgie und Walztechnik zur Erzeugung sauergasständiger Röhrenbleche bei Voestalpine Stahl GmbH in Linz. *BHM*. 2003, 148, Heft 11, 440–449.
- [21] Tapia, V.H., Morales, D., Camacho, J. and Lugo, G. The Influence of the Tundish Powder on Steel Cleanliness and Nozzle Clogging. Proceedings 79th Steelmaking Conference, Iron and Steel Society, Pittsburgh, USA, March 24–27, 1996, pp. 539–547.
- [22] Tassot, P., Reichert, N., Willoughby, C. and Turrel, C. The Tundish as a Metallurgical Reactor. *Stahl und Eisen*. 2012, 132, 31–36.

Acknowledgement

The authors wish to thank Uxia Diéguez-Salgado, Patricia Polatschek, and Adrian Diaz for their contribution to the paper.

Authors

Bianca Agnes Secklehner, RHI AG, Steel Division, Vienna, Austria.

Marcos Tomás Casado, RHI AG, Steel Division, Leoben, Austria.

Andreas Viertauer, RHI AG, Steel Division, Vienna, Austria.

David Wappel, RHI AG, Technology Center, Leoben, Austria.

Bianca Brosz, RHI AG, Steel Division, Vienna, Austria.

Corresponding author: Marcos Tomás Casado, marcos.tomas@rhi-ag.com

Gernot Hackl, Gerald Nitzl, Yong Tang, Christoph Eglsäer and Georg Krumpel

Novel Isostatically Pressed Products for the Continuous Casting Process

Introduction

In the steelmaking continuous casting process, isostatically pressed products such as submerged entry nozzles/shrouds (SEN/SES), exchangeable submerged nozzles (MT), and monoblock stoppers play an important role in controlling liquid steel flow from the ladle down to the mould. One major function of this product group is protecting the liquid steel from reoxidation when it is transferred from one steel-making unit to another. As the requirements for clean steel and productivity are continuously increasing, in the last years many novel design concepts for isostatically pressed products have appeared for the steelmaking industry. These new technologies not only include material innovations for higher wear resistance, but they also provide functionalities that can significantly improve the continuous casting process. Examples of these improvements include stabilizing the mould level and thereby avoiding mould powder entrapment, promoting nonmetallic inclusion removal, and optimized argon gas purging at the stopper tip.

RHI is continually engaged in further improving the functionality of refractory products for the continuous casting process and developing new concepts for these flow control products to meet the growing demands from the steel industry. In the following sections, the latest developments regarding continuous casting refractories for billet/bloom and slab casting are introduced and will be discussed.

Novel Stopper Technology

Monoblock stoppers are used to precisely control liquid steel flow when it is transferred from the tundish to the mould. Depending on the application, argon can be injected into the liquid steel, traditionally through the stopper tip, which increases the pressure below the throttling point and reduces alumina build up in the casting nozzle (i.e., clogging). When using argon stoppers in slab casting, it is a well-known phenomenon that the argon backpressure is unstable and/or keeps increasing during the sequence. A consequence of

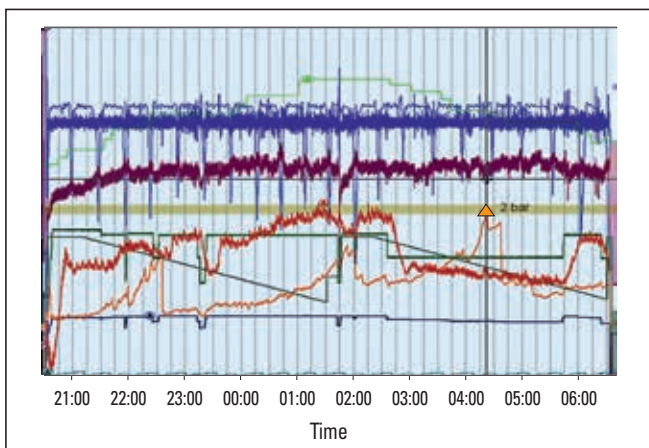


Figure 1. Argon pressure (orange curve) increase during casting.

variations in the argon flow rate injected into the mould can be an increased tendency for surface defects on the final product, resulting in extra costs for rework and inspection. In the worst-case scenario the cast product is downgraded or even scrapped. A casting graph, indicating multiple pressure increases during a sequence is shown in Figure 1 (orange curve). The maximum, indicated by the triangle, exceeded a value of 2 bar in this specific case.

One of the possible reasons for the argon pressure increase is a blockage in the argon purging channel of the stopper. The blockage can result from different sources, such as ingress of liquid steel into the argon channel caused by pressure fluctuations at the stopper tip. In the case of aluminium-killed steel, carbon principally originating from the refractory acts as a reducing agent that carries oxygen from the refractory to the steel and results in precipitation of alumina [1]. In addition, analysis of deposits found in the gas channel has shown they also consist of reaction products originating from contaminated argon gas, as well as from refractory components and lubricant, which can create volatiles at high temperature, as shown in Figure 2.

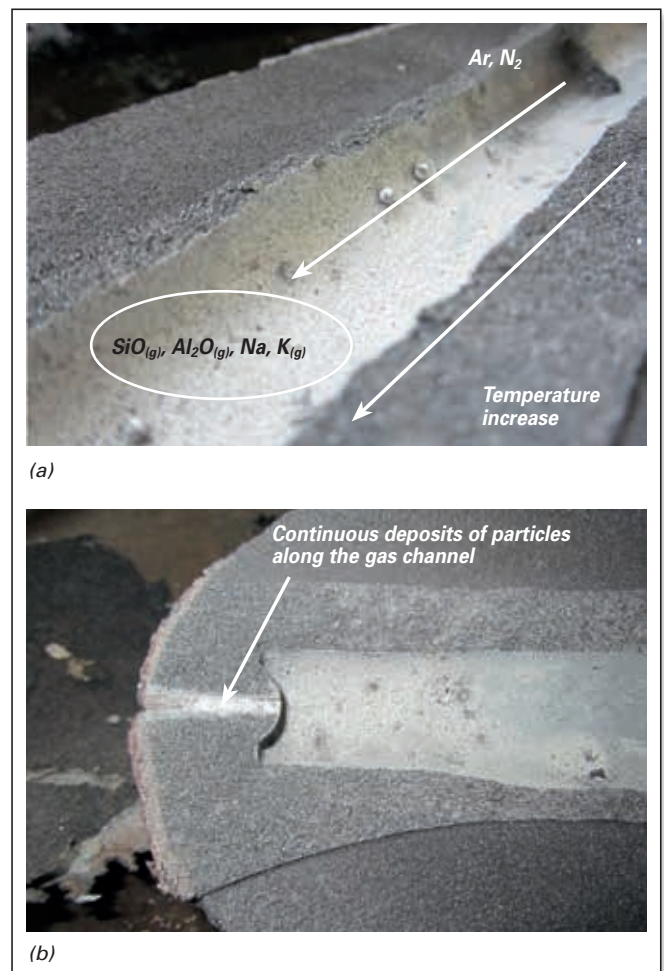


Figure 2. (a) particle deposition and (b) blockage of the argon channel.

In order to avoid the described disadvantages of conventional argon stoppers, RHI has developed a new technology to ensure consistent gas flow throughout the entire sequence, which is called the Clean Stream Cartridge (CSC). The CSC is installed inside the stopper and it adsorbs sub-micron species and volatiles, thereby avoiding gaseous reactive species condensing in the small argon channel.

Experience has shown that significant mould level fluctuations (MLF) can contribute to surface defects and breakouts of the cast steel. Several mechanisms are known to contribute to these fluctuations. One important factor is the multiphase flow regime resulting from argon injection. A non-homogeneous injection of argon bubbles as well as the transition from bubbly to slug flow has been shown to result in severe MLF [2]. Transient submeniscus velocity measurements in the continuous casting mould, as described in the literature [3], have indicated that strong perturbations in the mould can be connected with argon injection from a standard stopper. This led to a new stopper nose design with a circular slot-type argon injector, called the Slot Hole Plug (SHP). Details of the SHP design are shown in Figure 3 and compared to a conventional argon-supply system.

Comparative water modelling experiments were conducted to examine the argon distribution at the stopper tip of different stopper types. Figure 4a shows the gas distribution from a standard single hole stopper nose with a 5 mm argon channel diameter. It is evident that nonuniform gas injection had taken place. The gas exiting the hole was sucked in the direction of the throttling gap, which is the region of lowest pressure in the system. Pressure and

velocity fluctuations in the gap and at the tip triggered the nonuniform gas distribution. In contrast, the SHP stopper generated a homogeneous argon bubble distribution in the casting channel (Figure 4b). This was achieved by changing the type of injection. Instead of gas injection through a single point, the argon exits the stopper via a several hundred micron thick annular gap. This geometric configuration is not as susceptible to pressure instabilities and therefore the argon distribution is much more homogeneous.

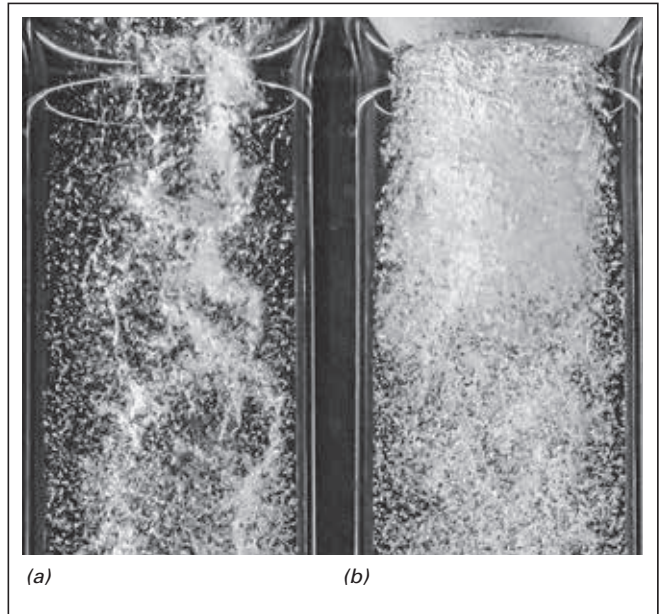


Figure 4. Water modelling results of the gas distribution achieved with (a) standard stopper and (b) SHP stopper.

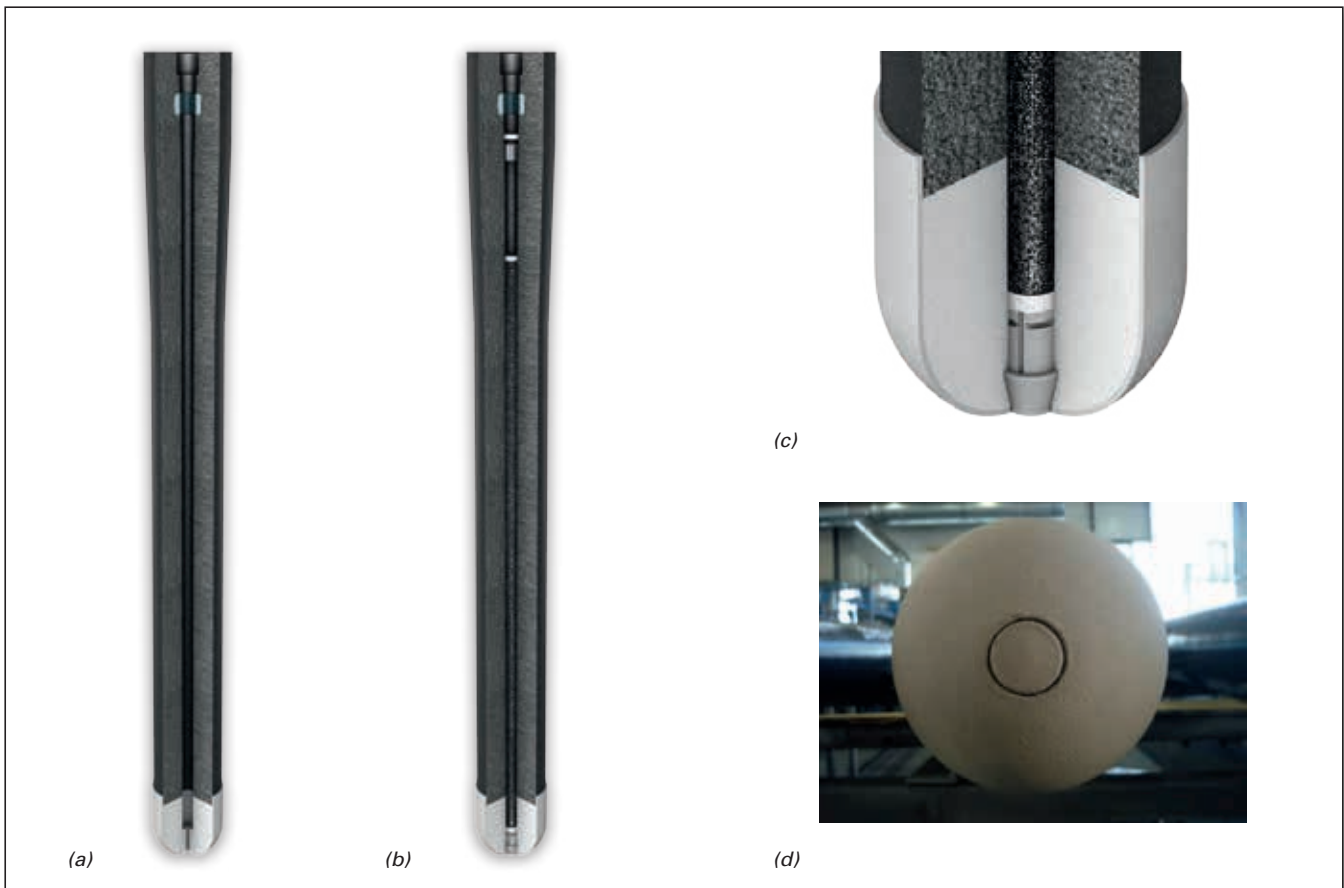


Figure 3. (a) conventional stopper with a single hole in the nose, (b) SHP stopper design, (c) section through the SHP stopper nose, and (d) circular slot at the SHP stopper tip.

Novel GYRO Nozzle for Billet and Bloom Casting

Fluid flow in the mould is known to have a significant impact on the quality of continuously cast products. The mould represents the last step in the process where nonmetallic inclusions can be removed before they can become entrapped in the solidifying steel. Since flow in the mould is strongly influenced by the SEN design, it can be modified to enhance inclusion removal. For billet and bloom casting, single-port SEN types are traditionally used because of their simplicity. However, as demand for steel cleanliness increases, research has indicated that this type of SEN may not be suitable to meet all the requirements. Due to the considerable penetration depth of the jet into the liquid pool, floating up of nonmetallic inclusions towards the mould surface where they are absorbed by the slag is prevented. Instead, they are transported deep down into the strand where they can be entrapped by the solidifying steel. A further consequence of the deep jet penetration is that heat transport towards the meniscus is relatively low [4], which may result in insufficient mould powder melting. Agitated steel flow, for example using mould electromagnetic stirrers (M-EMS), is an additional requirement to break the dendrites during solidification and enhance an equiaxed crystal growth structure over columnar. The latter structure is associated with a high degree of segregation and porosity in the cast product. Especially when superheat is high, which may be beneficial for melting the mould powder, the percentage of equiaxed crystals further decreases resulting in increased centreline segregation and porosity [5].

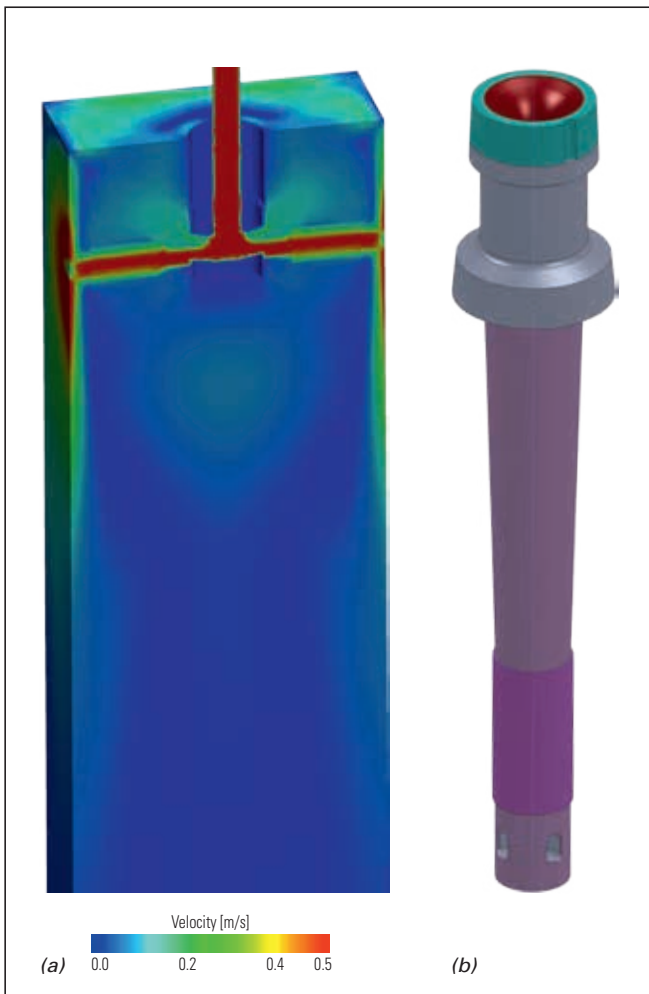


Figure 5. (a) calculated velocity profile in a rectangular bloom mould using a four-port SEN and (b) the four-port SEN design.

In recent years, there has been a trend to use multi-port SENs in bloom casting for high-grade steel, such as bearing and rail steels. It is considered that the multi-port SEN has a better ability to remove nonmetallic inclusions in the mould than a single-port SEN. However, one critical aspect is the considerable jet impingement velocity on the thin solidified shell, which may lead to detrimental shell thinning caused by remelting. An example of this situation is indicated by the results of a computational fluid dynamics (CFD) study (Figure 5). In this case, the four SEN ports were directed perpendicular to the centre of each wall in a rectangular mould. With this configuration a considerably high flow velocity occurs in the impingement regions.

Since 2000, many researchers have remarked that a swirling motion generated by the casting nozzle can effectively control the flow pattern in the mould. A very uniform velocity distribution in the mould is established downstream from the SEN outlet and the depth of inclusion penetration is decreased [6]. Different approaches to create swirling flow in the mould using concepts similar to conventional multi-port designs have been proposed [5,7]. In the last years RHI has invested significant effort to develop a nozzle that enhances swirling flow in the mould, which can be manufactured using a simple adaptation of conventional tooling. The new development for bloom/billet casting, called GYRO Nozzle, is shown in Figure 6. Several benefits are associated with this new concept:

- >> Deep jet penetration is avoided, resulting in efficient nonmetallic inclusion removal.
- >> Rotational flow in the mould is achieved to support or reduce the need for electromagnetic flow actuators.
- >> Efficient mixing in the upper mould region occurs, which results in a better mould powder melting rate to improve strand lubrication and reduce freezing.
- >> Reduced steel jet impingement on the solidifying shell is achieved when compared to conventional multi-port designs.



Figure 6: Example of a GYRO Nozzle

Numerical and physical modelling approaches using CFD and water modelling on a 1:2 scale model, fulfilling Froude similarity, were applied to investigate the aforementioned advantages. The CFD simulation was performed with the OpenFOAM software package. Incompressible, isothermal flow was solved in the domain by applying the RANS approach. Turbulence was considered by using the realizable $k-\epsilon$ model. A comparative study of a single-port SEN and the GYRO Nozzle used in a rectangular mould is depicted in Figure 7, showing the positive effects of the new concept: A fundamental alteration of the flow pattern in the mould was achieved in terms of jet penetration depth and generation of a rotational flow pattern.

In a second CFD simulation, the effect of mould size, using a round cross section, on the formation of a rotational flow structure was evaluated. Figure 8 indicates the velocity profile and flow direction at the meniscus for different mould sizes, ranging from 180 to 360 mm in diameter, considering a throughput of 0.45 tonnes/min without using a M-EMS. The CFD simulation revealed a rotational flow structure at the meniscus. The velocity profile appeared to be very stable and homogenous and the velocity magnitude was in the desired range below 0.3 m/s for all configurations.

Additional water modelling experiments were performed to investigate the behaviour of particle movement in the

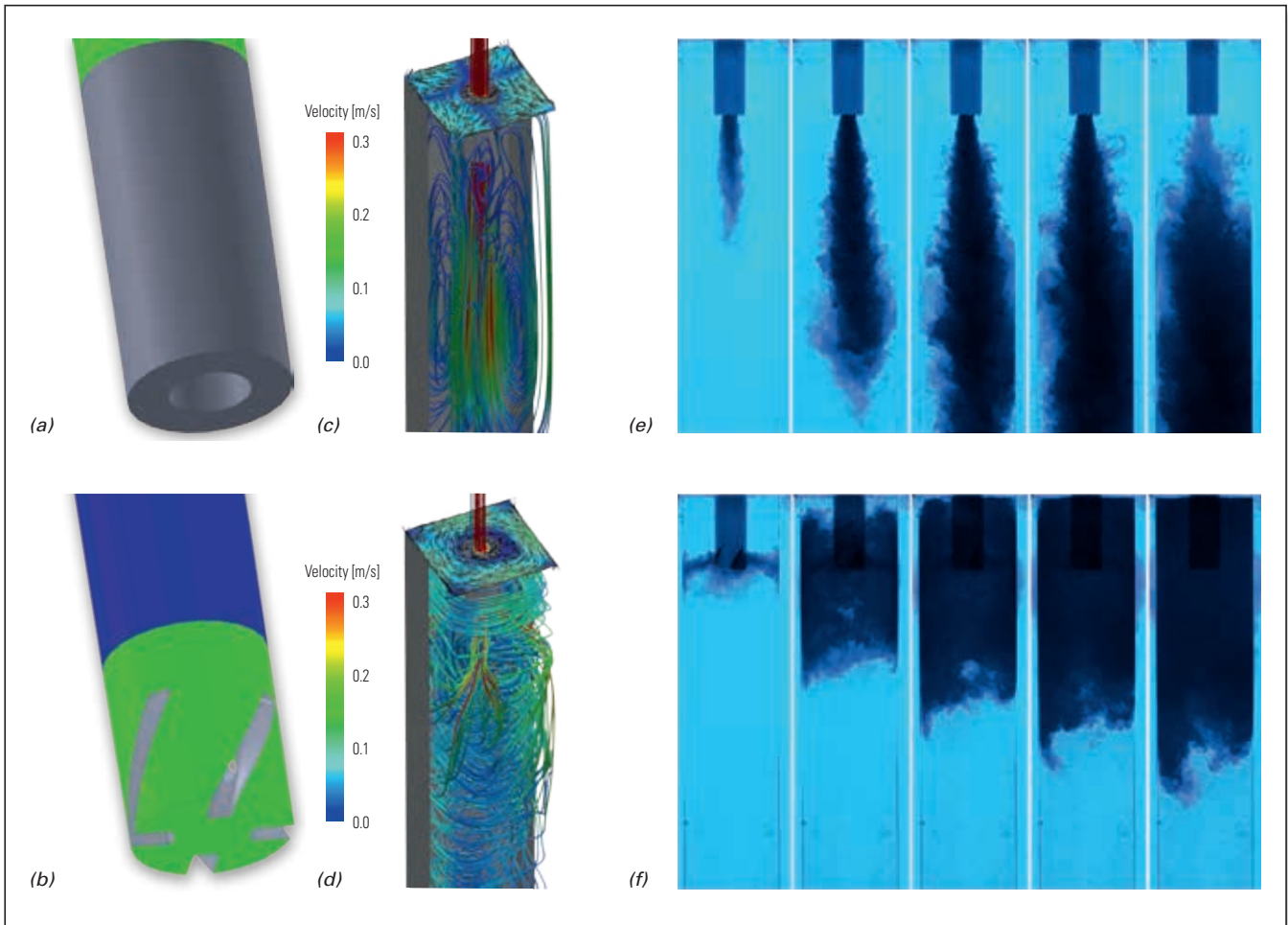


Figure 7. (a) conventional and (b) GYRO Nozzle SEN port geometry; stream tracer obtained by CFD for the (c) conventional and (d) GYRO Nozzle; and dye injection experiment with (e) conventional single-port SEN and (f) GYRO Nozzle.

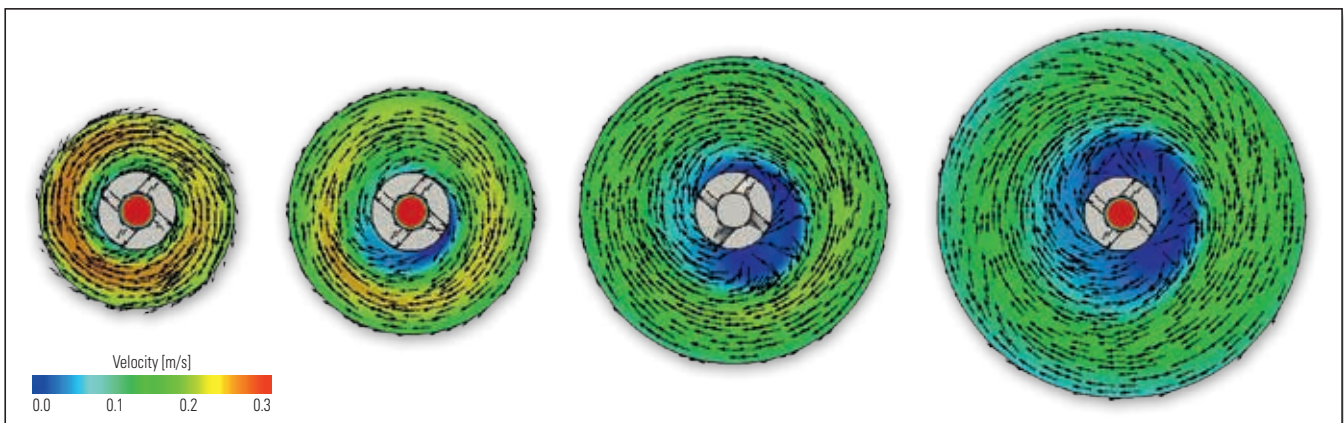


Figure 8. Meniscus velocity profile using the GYRO Nozzle in different mould sizes.

mould for both designs. The tests confirmed the favourable function of the GYRO Nozzle. In Figure 9 a snap shot is shown, indicating the trajectory of injected particles. Due to the deep penetration depth of the vertical jet from the single-port SEN, particles were transported deep down into the strand, thereby increasing the risk of entrapment in the solidifying steel. In contrast, due to the flow modification provided by the GYRO Nozzle, most particles remained in the upper mould region and continuously floated up. If the mould flux has a strong absorption effect, the rising particles would be easily incorporated into the mould flux, increasing the final steel product cleanliness.

The first industrial trials with the GYRO Nozzle have been successfully performed. The photograph of a piece after service is shown in Figure 10. All the ports were clear, without any sign of clogged areas. Temperature measurements were conducted during the trial that indicated a higher meniscus temperature profile compared to the strand equipped with a conventional single-port SEN. The measurements are an indirect verification of the simulation results, which predicted more active meniscus conditions.

In addition, it was reported that porosity of the cast product could be reduced when compared to the standard single-port SEN. This is an indication of the superior performance achieved with the GYRO Nozzle.

Conclusion

Novel concepts for flow control refractory products used in the continuous casting process are presented and discussed in this paper. With the aid of numerical and physical modelling the functionality of various concepts was investigated and compared against standard solutions.

The new generation of monoblock stopper designs incorporating the CSC and SHP technology provide several benefits over conventional designs. These include eliminating pressure increase at the start of casting, maintaining stable back pressure and argon flow in the argon line during long-sequence casting, and enhancing an even gas distribution to the mould, leading to improved flux melting and lubrication as well as reduced mould level fluctuations.

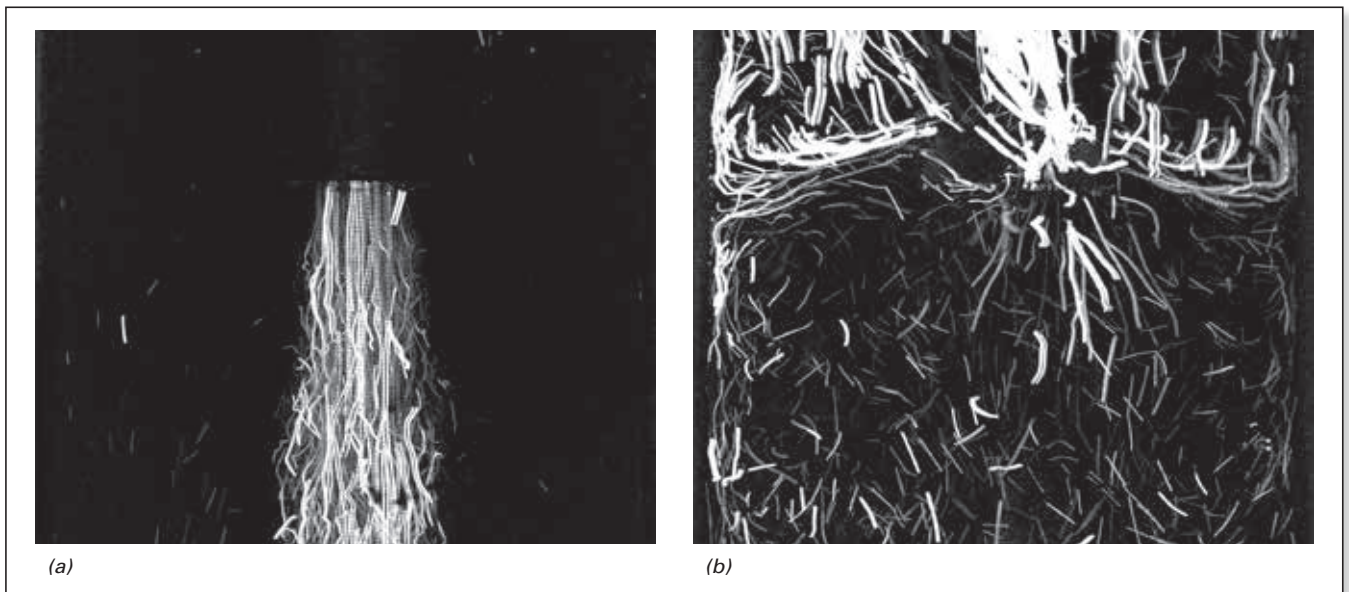


Figure 9. Comparison of particle movement in the water model with (a) single-port SEN and (b) GYRO Nozzle.



Figure 10. (a) schematic showing the original GYRO Nozzle geometry and (b) appearance of a GYRO Nozzle after use.

The GYRO Nozzle design for billet and bloom casting has a remarkable influence on fluid flow in the mould. As a result of its helical slot-type port configuration a rotational flow is established in the mould, which is known to improve the crystal structure by minimizing the volume of columnar crystals. When compared to a single-port nozzle, deep jet penetration is avoided, thus leading to a better flotation potential for nonmetallic inclusions and improved heat transport towards the meniscus. In contrast to conventional multi-port designs, the impinging velocity on the solidifying shell is reduced, which minimizes the risk of local shell remelting.

References

- [1] Nadif, M., Burty, M., Soulard, H., Boher, M., Pusse, C., Lehmann, J., Ruby-Meyer, F. and Guiban, M.A. *IISI Study on Clean Steel: State of the Art and Process Technology in Clean Steelmaking*; International Iron and Steel Institute: Brussels, 2004; p 126.
- [2] Higson, S.R., Drake, P., Lyons, A., Peyton, P. and Lionheart, B. Visualisation of Steel Flow in the Continuous Casting Nozzle Using an Electromagnetic Technique. Presented at 4th ECCO, Birmingham, UK, Oct., 14–16, 2002.
- [3] Hackl, G., Tang, Y., Nitzl, G., Chalmers, D., Dorricott, J. and Heaslip, L. Design Optimization of Submerged Entry Nozzles Using Simulation Technology. *RHI Bulletin*. 2014, No. 1, 47–53.
- [4] Capurro, C., Copola, J., Ferro, S. and Cicutti, C. Effect of Submerged Entry Nozzle Design on the Distribution of Inclusions in Cast Products. Presented at AISTech 2013, Pittsburgh, USA, May 6–9, 2013.
- [5] Choudhary, S.K. and Ganguly, S. Morphology and Segregation in Continuously Cast High Carbon Steel Billets. *ISIJ International*. 2007, 47, 1759–1766.
- [6] Yokoya, S., Takagi, S., Iguchi, M., Marukawa, K. and Yasugaira, W. Development of Swirling Flow Generator in Immersion Nozzle. *ISIJ International*. 2000, 40, 584–588.
- [7] Sun, H., Li, Y., Zhang, J., He, Q. and Fan, L. Morphology, Soundness and Segregation Improvement of Bloom Castings by Using Swirling Flow Nozzle. Presented at AISTech 2013, Pittsburgh, USA, May 6–9, 2013.

Originally presented at AISTech 2015 and published in the AISTech 2015 Conference Proceedings. Reprinted with permission from the Association for Iron and Steel Technology (AIST).

Authors

Gernot Hackl, RHI AG, Technology Center, Leoben, Austria.

Gerald Nitzl, RHI AG, Steel Division, Vienna, Austria.

Yong Tang, RHI AG, Technology Center, Leoben, Austria.

Christoph Eglsäer, RHI AG, Steel Division, Vienna, Austria.

Georg Krumpel, RHI AG, Steel Division, Vienna, Austria.

Corresponding author: Gernot Hackl, gernot.hackl@rhi-ag.com

Helmut Dösinger, Clare McFarlane, Gerald Nitzl, Yong Tang and Gernot Hackl

Anticlogging Solutions for Isostatically Pressed Submerged Nozzles

Introduction

Continuous casting accounted for more than 95% of global crude steel production in 2013 [1]. Before it is continuously cast, the steel should be fully deoxidized or killed by adding metals such as aluminium or silicon, which have the propensity to consume free oxygen at very low partial pressures. This is performed to minimize gas evolution during the solidification process and avoid blowholes or pinholes in the final product. A negative consequence of this process is the formation of indigenous nonmetallic inclusions in the liquid steel (e.g., alumina), which if not captured by the slag are detrimental to the casting process and negatively influence mechanical properties of the cast product.

In the continuous casting process, isostatically pressed submerged nozzles provide shrouded molten steel transfer from the tundish to the mould. This product group includes submerged entry nozzles, shrouds, and in-cast exchangeable monotubes of varying dimensions (Figure 1). Typically, submerged shrouds are manufactured from alumina-graphite refractory grades with a zirconia-graphite insert positioned in the region where the nozzle dips below the steel meniscus and comes into contact with corrosive mould powder. Additional materials can be incorporated into the design, such as magnesia-graphite in the seat area. The steel flow pattern within the mould is controlled by the submerged nozzle port geometry and is tailored to the specific mould configuration and casting conditions.

A serious productivity and quality problem associated with continuous casting results from clogging, due to adherence

of nonmetallic inclusions, such as alumina, on the inner refractory surfaces. This deposition can occur at various positions from the tundish to the mould, including on the tundish slide gate plates, in the submerged nozzle seat area, as well as in the submerged nozzle bore and at the ports (Figures 2 and 3). It can alter steel flow through the submerged nozzle and in the worst-case scenario interrupts the casting process. Furthermore, clogging is detrimental to steel cleanliness for many reasons including [2]:

- >> Dislodged clogs become trapped in the solidifying steel or alter the mould flux composition.
- >> Clogs change the nozzle flow pattern and jet characteristics exiting the nozzle, disrupting flow in the mould and causing an abnormal temperature distribution.
- >> Clogging interferes with mould level control as the flow regulation device tries to compensate for clogging.

Main Factors Influencing Submerged Nozzle Clogging

Clogging is a very complex phenomenon and multiple mechanisms have been discussed in the literature to explain the process [2]. In addition to the formation of indigenous nonmetallic inclusions as a result of steel deoxidation, there are additional downstream factors that have been reported to contribute to the level of submerged nozzle clogging; they are either additional sources of inclusion formation or enhance adhesion of inclusions to the refractory surface. A number of these factors are described in the following sections to provide a background to the various

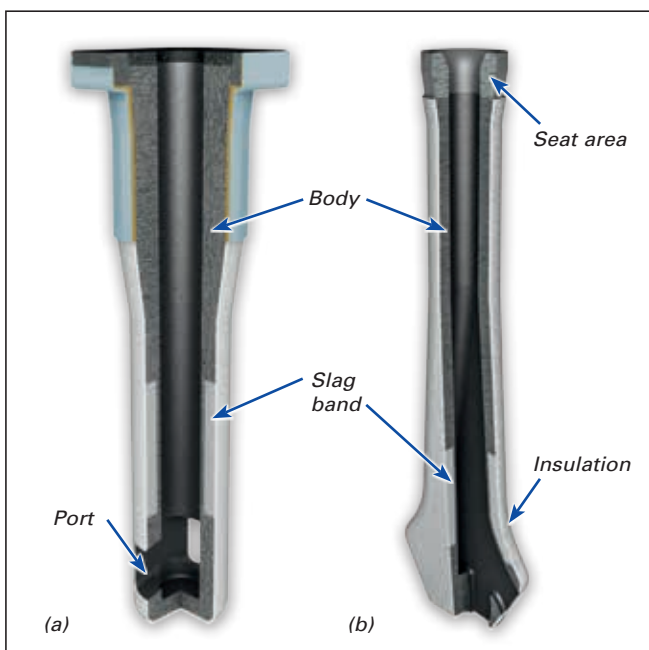


Figure 1. (a) monotube and (b) thin slab submerged entry nozzle.

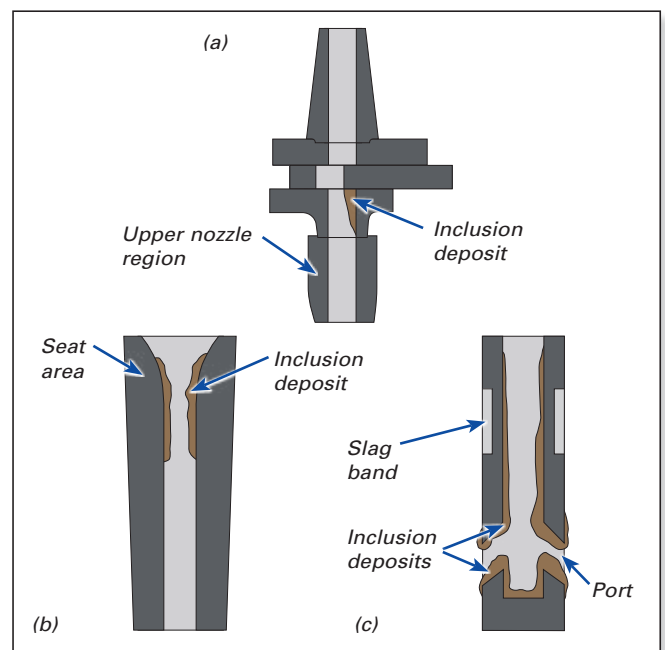


Figure 2. Deposition of nonmetallic inclusions (a) around the tundish slide gate plates, (b) in the upper submerged nozzle, and (c) in the bore and port regions [3].

anticlogging solutions RHI has developed to minimize inclusion build up in submerged nozzles.

Air Ingress Through Refractory Joints and Pores

Steel flow is regulated between the tundish and mould using a slide gate system or monoblock stopper. Both mechanisms are a potential source of air ingress through any gaps that are present due to under pressure forming inside the refractory parts as a result of steel flow. The air reacts with various components in the steel, for example aluminium and silicon, to form nonmetallic inclusions. Low pressure in the submerged nozzle bore has also been postulated to drive air ingress across the wall as a result of the inherent refractory permeability [2]; this results in the formation of oxidic nonmetallic inclusions either directly or through the intermediate formation of carbon monoxide [4].

Thermally Induced Inclusions at the Refractory Wall

Oxygen solubility decreases in steel as it cools. Therefore, as the steel temperature drops during flow through the submerged nozzle it results in decreased oxygen solubility in the melt. It has been proposed that this drives the Al–O₂–Al₂O₃ equilibrium towards the formation of alumina directly at the steel-refractory interface [5].

Thermochemical Reactions in the Refractory Material

Thermochemical reactions within the submerged nozzle refractory material produce suboxide gases and carbon monoxide that are transported to the refractory-steel interface where they can reoxidize metals present in the steel, causing oxidic precipitates on the inner nozzle wall [6]. These reactions are mediated by the inherent refractory permeability and carbon in the matrix.

Additional thermochemical mechanisms have been proposed involving reactions between the molten steel and nozzle refractory material [2]. For example, dissolution of carbon from the refractory into steel provides an additional source of carbon monoxide via the direct reaction with oxygen in the steel or by the reduction of oxide species [6].

Once formed, any nonmetallic oxides at the refractory-steel interface provide a site for the adhesion of inclusions already present in the steel.

Flow-Mediated Nozzle Clogging and Inclusion Adherence

There are several theories regarding the mechanism of nozzle clogging; however, one of the most widely accepted is that it results from transport of inclusions to the surface of the nozzle bore, followed by their adhesion to the refractory material or other already deposited inclusions, and subsequent sintering [7]. Therefore, the flow characteristics of the steel stream are considered to have an important influence on clogging, and in particular regions of biased or stagnant flow at the wall and ports enhance the build up of nonmetallic inclusions. Additionally, the high wetting angle between steel and alumina is a strong driving force for alumina particles to adhere to materials with a similar surface energy, for example other alumina particles or the refractory surface [2].

Anticlogging Solutions

Due to the complex nature of clogging, RHI has developed multiple approaches to minimize inclusion build up. They comprise material as well as design advances, and can be incorporated individually or combined in submerged nozzles to reduce the deposition of inclusions. They also involve upstream flow control products.

Argon Purging

Argon purging is commonly used in the steel industry to reduce clogging (see page 14). Especially during the continuous casting process it plays an important role in eliminating air ingress via joints, as well as to prevent inclusion attachment or dislodge any clogs that have formed. Furthermore, the inert atmosphere decreases the propensity for redox reactions to occur and interferes with the sintering of inclusions. Depending on the operating practice, argon can be injected through the monoblock stopper, via the tundish nozzle, at the slide gate system, and directly into the submerged nozzle. A recent argon purging advance from RHI is the SHP monoblock stopper (see page 79), which generates homogeneous argon bubble distribution in the casting channel.

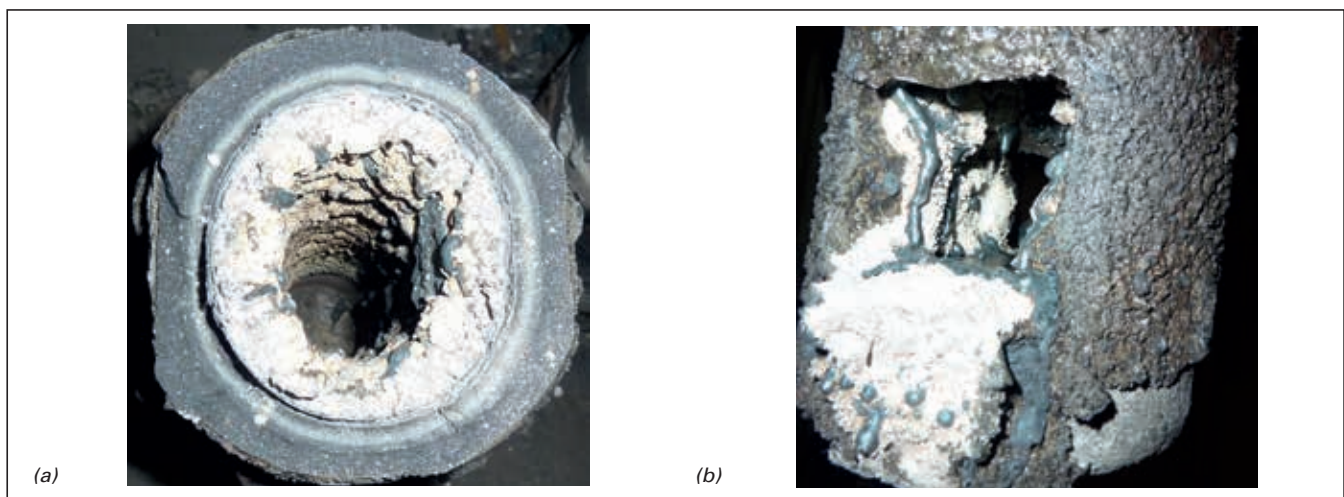


Figure 3. Submerged nozzle clogging in the (a) bore and (b) at the port region.

Decreasing Refractory Permeability—FREEFLOW^{PLUS}

It is well established that refractory materials used to produce submerged nozzles have an inherent permeability. Despite glaze protection, which not only minimizes decarburization but also helps to prevent air permeation through the wall material, there is still residual permeability that enables gaseous migration (e.g., carbon monoxide) towards the bore. In order to reduce this potential source of inclusion formation, extensive work has been conducted to develop a material called FREEFLOW^{PLUS}, which significantly reduces refractory permeability. The benefits of this advance on reducing relative permeability are shown in Figure 4. The permeability is further decreased with FREEFLOW^{PLUS} after the submerged nozzle is preheated.

In addition to decreasing permeability of the refractory material with FREEFLOW^{PLUS}, a decarburized layer is integrated into the submerged nozzle. It reduces carbon monoxide formation and also provides an insulating layer, decreasing temperature loss of the liquid steel at the refractory surface. This minimizes any reduction in oxygen solubility in the liquid steel, which can lead to alumina deposition on the refractory surface.

In summary, the anticlogging FREEFLOW^{PLUS} material development provides the following advantages:

- >> Reduced refractory permeability.
- >> Minimal carbon source near the bore.
- >> Decreased thermal conductivity.

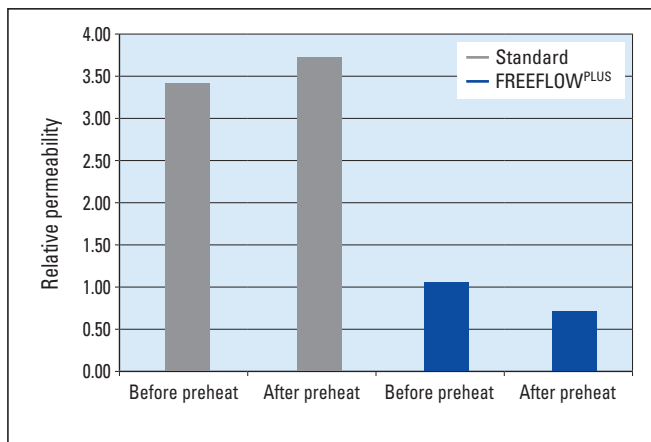


Figure 4. Relative permeability of standard alumina-graphite material and FREEFLOW^{PLUS} before and after preheating.

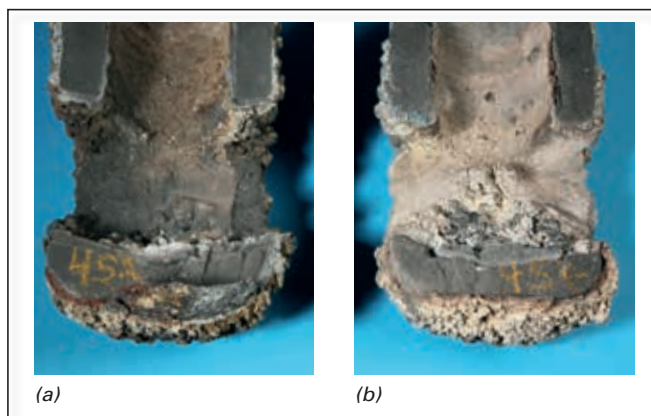


Figure 5. Clogging at the bore of a submerged nozzle comprising (a) FREEFLOW^{PLUS} and (b) standard alumina-graphite material.

Since FREEFLOW^{PLUS} was introduced on the market it has been shown to significantly reduce clogging, especially in the bore area, compared to standard alumina-graphite submerged nozzle grades (Figure 5).

Decreased Refractory Reactivity and Wettability to Molten Steel

Reactions occurring between molten steel and the refractory material are considered to be important for clogging because they result in the formation of oxide species on the refractory surface that can provide an attachment point for inclusions present within the steel. In addition, the interfacial properties between steel and refractory materials may influence clogging. Therefore, sessile drop tests were performed at 1600 °C in an inert gas atmosphere to examine the wetting angle and reactivity of steel on various refractory surfaces [8]. The results showed that certain refractory materials caused a change

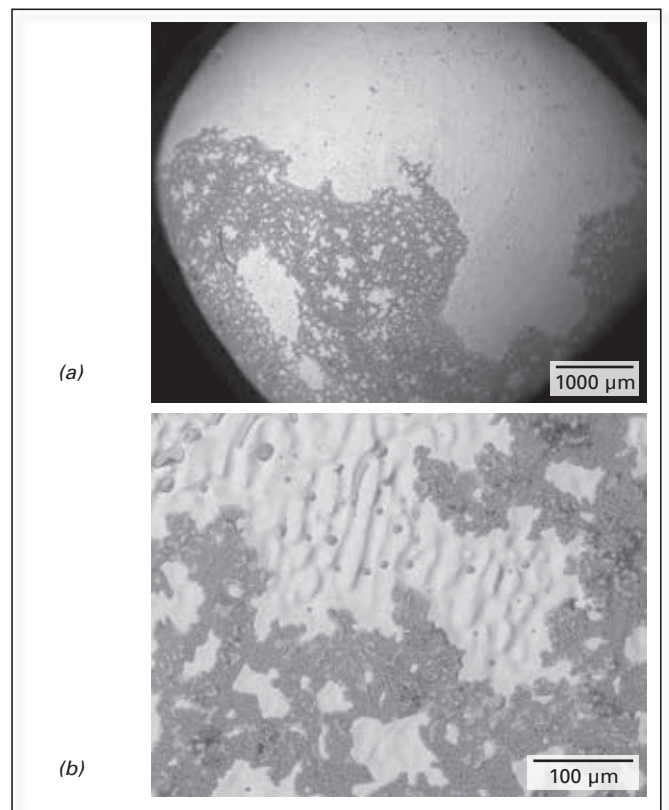


Figure 6. (a) sessile drop test results examining the wetting angle and reactivity of steel on a refractory material at 1600 °C and (b) surface of the steel drop covered in various oxides [8].



Figure 7. Seat insert manufactured from DELTEK S682.

in the wetting angle and/or reacted with the steel, resulting in oxide species detectable on the steel drop surface (Figure 6). With other materials only a minimal change in the steel contact angle occurred and/or no oxidic layer was formed.

On the basis of this analysis, seat insert materials for submerged nozzles were developed that reduce clogging in this region. The inserts comprise various high-quality raw materials and provide high wear resistance and reduced wettability. In addition they are carbon-free, as well as glaze and coating-free. One of these seat insert grades is DELTEK S682 (Figure 7).

Flow Modification in the Bore— COUNTER HELIX

Steel entering the submerged nozzle is highly turbulent. The transport of nonmetallic inclusions from this turbulent steel flow to the nozzle inner surface wall is intimately related to the flow behaviour, which is determined by the inner nozzle design. Clogging preferentially takes place at locations where stagnant flow occurs within the nozzle because the very low liquid steel velocity enables inclusions to remain near the refractory wall for a longer duration, thereby aiding adhesion. Owing to the low velocities present in these zones, minimal shear stresses are present to remove the inclusions. RHI used computational fluid dynamics (CFD) and water modelling technologies to optimize the inner submerged nozzle geometry and reduce steel flow stagnation at the nozzle wall. The resulting COUNTER HELIX bore design creates perturbation on the bore wall, reducing stagnant zones in the liquid flow, as well as maximizing turbulence in the bore and at the ports. Consequently the probability of shear stresses washing away adhered inclusions on the nozzle walls are high and clogging is minimized. The CFD modelling results of turbulent kinetic energy distribution near the lower part of submerged nozzle wall for a standard inner nozzle geometry compared to the COUNTER HELIX modification are shown in Figure 8. Due to a novel tooling development, the COUNTER HELIX design can be incorporated as part of the established manufacturing processes.

References

- [1] <http://www.worldsteel.org/dms/internetDocumentList/bookshop/World-Steel-in-Figures-2014/document/World%20Steel%20in%20Figures%202014%20Final.pdf>
- [2] Michelic, S. and Karasangabo, A. *SEN-Clogging During Continuous Casting – Mechanisms and Related Influencing Parameters*, Literature Study, Montanuniversität Leoben, Austria, 2011.
- [3] Ogibayashi, S. Mechanism and Countermeasure of Alumina Buildup on Submerged Nozzle in Continuous Casting. *Taikabutsu Overseas*. 1995, 15, No. 1, 3–14.
- [4] Poirier, J., Thillou, B., Guiban, M.A. and Provost, G. Mechanisms and Countermeasures of Alumina Clogging in Submerged Nozzles. *78th Steelmaking Conference Proceedings*, Nashville, USA, April 2–5, 1995; pp. 451–456.
- [5] Tehovnik, F., Burja, J., Arh, B. and Knap, M. Submerged Entry Nozzle Clogging During Continuous Casting of Al-Killed Steel. *METALURGIJA*. 2015, 54, 371–374.
- [6] Nadif, M., Burty, M., Soulard, H., Boher, M., Pusse, C., Lehmann, J., Ruby-Meyer, F. and Guiban, M.A. *IISI Study on Clean Steel: State of the Art and Process Technology in Clean Steelmaking*; International Iron and Steel Institute: Brussels, 2004.
- [7] Andersson, M. Some Aspects of Oxygen and Sulphur Reactions Towards Clean Steel Production, PhD Thesis, Royal Institute of Technology, Sweden, 2000.
- [8] Arth, G. 2013. Unpublished data. Chair of Metallurgy, Montanuniversität Leoben, Austria.

Authors

Helmut Dösinger, RHI AG, Technology Center, Leoben, Austria.

Clare McFarlane, RHI AG, Technology Center, Leoben, Austria.

Gerald Nitzl, RHI AG, Steel Division, Vienna, Austria.

Yong Tang, RHI AG, Technology Center, Leoben, Austria.

Gernot Hackl, RHI AG, Technology Center, Leoben, Austria.

Corresponding author: Helmut Dösinger, helmut.doesinger@rhi-ag.com

Summary

Submerged nozzle clogging can cause significant quality and production issues during the continuous casting of steel. The principal aspects influencing the build up of nonmetallic inclusions are numerous and involve metallurgical, thermodynamic, refractory-related, and hydrodynamic factors. Therefore, RHI has taken a multifaceted approach regarding the development of anticlogging solutions. Argon purging can be introduced at various stages in the continuous casting process to reduce the formation and adherence of detrimental inclusions and excellent inert gas purging systems are available from RHI/INTERSTOP. Submerged nozzle seat inserts and FREEFLOW^{PLUS} are material developments designed to counteract various inherent refractory properties that can mediate clogging at steelmaking temperatures. An additional approach to diminish clogging in the bore and port region can be realized by incorporating the COUNTER HELIX inner nozzle geometry into standard designs. These various anti-clogging solutions are available individually or can be combined into the different submerged nozzle products.

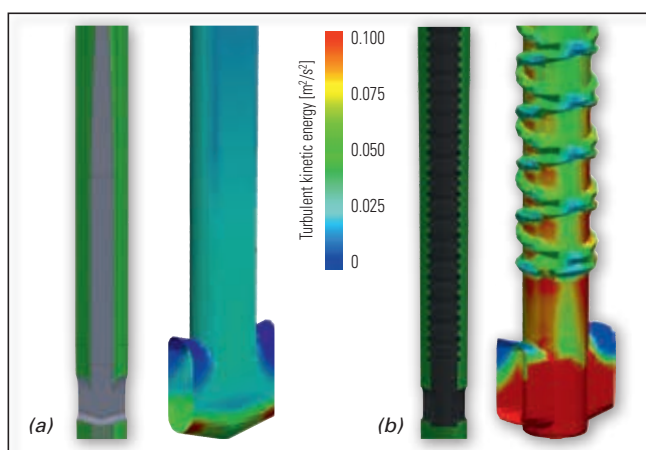


Figure 8. Turbulent kinetic energy distribution on the submerged nozzle inner walls. (a) standard inner geometry and (b) COUNTER HELIX design.

RHI Bulletin >1> 2015

The Journal of Refractory Innovations

